ASNC IMAGING GUIDELINES FOR NUCLEAR CARDIOLOGY PROCEDURES

Introduction

Edward P. Ficaro, PhD, ASNC Quality Assurance Committee Chair
Christopher L. Hansen, MD, ASNC Imaging Guidelines Subcommittee Chair

The *Imaging Guidelines for Nuclear Cardiology Procedures* are a set of state-of-the-art applications and protocols developed for the nuclear cardiology community. All chapters are comprehensively reviewed and approved by writing group participants, the ASNC Imaging Guidelines Subcommittee, an expert External Review Panel, the ASNC Executive Council, and the ASNC Board of Directors.

Within the document protocol items judged to be *required* are indicated as such. *Standard* means that the parameter value listed represents methodology judged to be standard by the consensus of the committee; its utilization is recommended, but other techniques may also be valid. *Preferred* means that the parameter value listed is expected to provide the best results and its selection is strongly recommended. Techniques termed *optional* indicate that the parameter value listed may be employed or another acceptable parameter may be substituted. Techniques still considered primarily research applications and those not published in peer-reviewed journals usually have not been included.

The *Imaging Guidelines* are designed to provide imaging guidelines for those physicians and technologists who are qualified in the practice of nuclear cardiology. Although care has been taken to ensure that information supplied is accurate, representing the consensus of experts, it should not be considered as medical advice or a professional service. The imaging guidelines described in this manual should not be utilized in clinical studies at any institution until they have been reviewed and approved by qualified physicians from that institution.

ASNC IMAGING GUIDELINES FOR NUCLEAR CARDIOLOGY PROCEDURES

Instrumentation quality assurance and performance

Kenneth J. Nichols, PhD,[a] Stephen L. Bacharach, PhD,[b] Steven R. Bergmann, MD, PhD,[b] Ji Chen, PhD,[b] S. James Cullom, PhD,[b] Sharmila Dorbala, MD,[b] Edward P. Ficaro, PhD,[b] James R. Galt, PhD,[b] Darcy L. Green Conaway, MD,[b] Gary V. Heller, MD, PhD,[b] Mark C. Hyun, CNMT, NCT, RT(N)(R),[b] Jonathan Links, PhD,[b] and Josef Machac, MD[b]

INTRODUCTION

The proper choice of equipment to acquire clinical data for specific purposes and a well-designed quality assurance (QA) program are both essential requirements for optimizing diagnostic accuracy. The following guidelines are intended to provide appropriate means of assessing equipment function in conjunction with nuclear cardiology imaging. Because equipment manufacturers can vary considerably with the optimal manner in which to perform specific tests, this document should be used as guidelines only and is not intended to replace the recommendations by manufacturers of specific models of imaging equipment. A thorough and rigorous QA program is essential to ensure consistent high-quality imaging.

EQUIPMENT

Planar imaging. The small–field-of-view (FOV) scintillation camera is ideal for cardiac imaging. The 10-inch FOV covers the heart and shows enough surrounding area to evaluate lung uptake and to sample extracardiac background activity. A 128 × 128 matrix over this FOV results in pixel spacing of about 2 mm. A camera with a 15-inch FOV should be zoomed using a magnification factor of 1.2 to 1.5 so that the pixel size is less than 3 mm and approximately equal to 2.5 or 2.0 mm.

Energy windows should be symmetric about the photopeak. A window of 20% is standard for technetium 99m. With the improved energy resolution of many modern cameras, a 15% window can be used with little loss of primary gamma rays, with some improvement in contrast. The low energy and greater width of the thallium 201 photopeak require a wider window. An energy window setting of 30% is appropriate for the 70-keV peak of Tl-201 and a 15% energy window for the 167-keV peak. The absolute energy calibration can be unreliable at the low energy of Tl-201 falling at slightly different energy positions in the spectrum of different cameras. Thus energy peak and window settings should be established for each individual camera based on the energy spectrum display.[1]

Parallel-hole collimation is standard. The low-energy, high-resolution collimator is usually best for Tc-99m, although some "all-purpose" collimators give excellent results. Imaging with Tl-201 is usually best with the low-energy, medium-resolution (all-purpose) collimators because count statistics become limiting when using high-resolution collimators. The difference in medium- and high-resolution collimators is usually that the collimator depth (length of the collimator hole) is greater in high-resolution collimators. They have similar near-field resolution. The "high-resolution" collimator maintains good resolution at a greater distance from the collimator face. The difference is more important in single photon emission computed tomography (SPECT) imaging, where the distance from patient to collimator is greater.[2]

Collimators. The selection of which collimator to use is important to resultant image quality. A confounding aspect of this selection is that collimators with the same name (eg, "general purpose") vary in performance from one manufacturer to another. Table 1 gives approximate values for collimator specifications. Refer to specific imaging protocols for appropriate collimator selection. It is important to perform periodic assessment of collimator integrity, as failure to detect and correct for localized reduced sensitivity can generate uniformity-related artifacts, including reconstruction artifacts.[3,4]

SPECT imaging. SPECT detectors are scintillation cameras mounted on a gantry. Many variables dictate the performance of a SPECT imaging system, including the number of detectors for a given device. Single-head cameras have been used widely for cardiac imaging. Adding more detectors is beneficial, since doubling the number of detectors doubles acquired counts, if all other variables remain fixed. For cardiac SPECT studies in

From the Chair.[a] Member.[b]
J Nucl Cardiol 2007;14:e61-78.
1071-3581/$32.00

doi:10.1016/j.nuclcard.2007.09.024

Table 1. Performance parameters for low energy (<150 keV collimators)

Collimator type	Resolution (FWHM at 10 cm)	Relative sensitivity
Ultra-high resolution	6 mm	0.3
High resolution	7.8 mm	0.6
All/general purpose	9.3 mm	1*
High sensitivity	13.2 mm	2.1

*A relative sensitivity of 1 corresponds approximately to a collimator efficiency of 2.7×10^{-4}, whereas efficiency is defined as the fraction of gamma rays and x-rays passing through the collimator per gamma ray and x-ray emitted by the source.

which a 180° orbit is recommended, the preferred configuration is to have two detectors separated by 90° as they rotate around the heart. For studies in which a 360° orbit is preferred, three detectors separated by 120° from each other are preferred.

The trend is to trade off some of the additional counts that would be obtained with multiple detectors equipped with general-purpose collimators for higher-resolution imaging by using higher-resolution collimators. Fan beam collimators are available but are not now commonly employed in cardiac imaging. These collimators allow more of the crystal area to be used in imaging the heart, magnifying the image and increasing sensitivity.[2] In large patients or when using a converging geometry with a steep angle, there is a potential for cutting off, or truncating, portions of the heart and/or chest. This truncation may generate artifacts.

Another variable in SPECT systems is detector orbit. The traditional orbit used for SPECT acquisition has been circular, with a rotational range of 180° or 360° and with step-and-shoot motion. Most systems today allow elliptical detector motion to follow the body contour, reducing the distance from the camera to the body, thereby improving spatial resolution. For single-head cameras, the 180° angular range from the 45° right anterior oblique to the 135° left posterior oblique orientation has become the preferred orbit, because the detector is closer to the heart in these views, resulting in higher spatial resolution and image contrast. There is also less scatter and attenuation over this angular range. The 360° orbit usually results in better uniformity of normal myocardium.[5,6] Some double- and triple-head systems acquire the entire 360° orbit because of the fixed separation of the detectors. In these systems the entire 360° orbit can be used. One concern in using 360° acquisitions is that reconstructed images can have a different "normal distribution" compared to those from 180° orbits. This could cause a misdiagnosis if interpreted as a 180°-acquired study, since the inferior wall usually has lower activity in normal subjects acquired with a 180° orbit than when acquired with a 360° orbit.[5,6]

Most SPECT systems use the step-and-shoot mode of acquisition in which the detector does not acquire data as it moves from one angle to the next. Some systems offer either continuous or continuous step-and-shoot acquisition modes such that detectors do acquire data as they move. Studies using both computerized and phantom simulations have shown that image quality is essentially the same whether data are collected continuously or in a step-and-shoot fashion.[7]

SPECT/transmission computed tomography imaging. Currently, there are two types of transmission tomographic imaging systems for acquiring patient-specific attenuation maps that can be used to correct SPECT images for photon attenuation. The first type, referred to in these guidelines as transmission computed tomography (TCT), uses a sealed source (eg, gadolinium 153) with the standard collimated scintillation detectors used for SPECT imaging. The second type of transmission imaging system uses an x-ray tube in conjunction with a computed tomography (CT) detector. The primary difference between these classes of transmission imaging systems is the photon emission rate that dictates the quality-control (QC) protocols that are required. Because x-ray tubes can produce photon currents which can be counted with CT detectors at significantly higher rates than conventional sealed sources and scintillation detectors, CT-acquired images can be acquired on the order of seconds to a few minutes depending on the tube strength. As a result, x-ray CT projection data are not contaminated by scatter emission photons. The number of photons used to form the transmission image is much lower for TCT than for CT, resulting in transmission of higher noise content so the emission scatter or cross-talk into the transmission window cannot be ignored for TCT. Due to the lower number of photons making up the transmission image and the non-negligible cross-talk scatter component from the injected radiotracer, the TCT QC procedure is slightly more involved and will be outlined separately from the QC for systems using x-ray tubes.

SPECT x-ray CT imaging. Consistent with trends in positron emission tomography (PET)/CT systems, hybrid SPECT systems have evolved, combining SPECT and CT systems. While PET systems are generally complete rings or a partial-ring system, the SPECT components are typically large-FOV variable-angle dual-detector systems. These combined systems, in practice, demonstrate a range of capability and integration. CT components range from non-diagnostic units suitable for use in anatomical localization and attenuation correction

to multislice (16 slices or more) systems capable of CT angiography. The SPECT detectors in SPECT/CT systems do not differ in any significant way from those of stand-alone SPECT systems. These systems may be viewed from a protocol perspective as stand-alone systems where an emission study is followed or preceded by a CT scan for attenuation correction. Depending upon the number of CT slices acquired, the CT scanner may be used, as with stand-alone CT scanners, for CT angiography and calcium scoring. The CT and SPECT components may then be analyzed independently or in 3-dimensional (3D) image registration, depending on the type of study.

PET imaging—2-dimensional versus 3D scanners. The majority of dedicated PET cameras consist of rings of small detectors (typically a few millimeters on a side, several tens of millimeters deep). Coincidences between detectors in a single ring produce one tomographic slice of data. Usually one or more adjacent rings may also contribute to counts in that slice. In a so-called 2-dimensional (2D) PET scanner, there is a lead or tungsten septum (a 1-dimensional collimator) between adjacent rings. This septum partially shields coincidences from occurring between detectors in one ring and detectors in a non-adjacent ring. By minimizing coincidences between a ring and its more distant neighboring rings, the septum greatly reduces scattered events. Many manufacturers have tried to increase the sensitivity of their scanners by removing the septa between adjacent rings. This permits coincidences between all possible pairs of detectors, greatly increasing sensitivity but also greatly increasing scatter. A scanner with no septa in place is referred to as a "3D" or "septa-out" scanner. The increased sensitivity is greatest for the central slice and falls rapidly (and usually linearly) for slices more distant from the central slice. The edge slices have a sensitivity about the same as in a 2D scanner but with greater scatter. Scatter as measured by the National Electrical Manufacturers Association (NEMA) is typically on the order of 10% to 15% for 2D scanners and 30% to 40% or more for 3D scanners. In chest slices encompassing the heart (as opposed to the relatively small NEMA phantom), there is an even larger increase in scattered counts for 3D imaging. For cardiac applications, scatter tends to increase the counts in cold areas surrounded by higher-activity regions (eg, a defect surrounded by normal uptake). Some manufacturers have scanners that have retractable septa, permitting the user to choose between 2D or 3D operation. Many (but not all) PET/CT manufacturers have opted for scanners that operate only in 3D mode (which many companies feel is optimum for oncology studies due to patient throughput concerns).

Situations in which 3D mode may be advantageous include those in which (1) whole-body patient throughput is important (eg, a busy oncology practice); (2) radiation exposure is critical, so reductions in injected activity are desired; and (3) special (usually research) radiopharmaceuticals are being used, which can only be produced in sub-millicurie quantities.

PET imaging—crystal types. Three different crystal types are commonly employed—BGO (bismuth germanate), GSO (gadolinium oxyorthosilicate), and LSO (lutetium oxyorthosilicate)—although there are also other crystal types in use. Each can be used successfully for cardiac imaging. BGO has the highest stopping power, but it has the poorest energy resolution (useful for scatter reduction) and timing resolution (useful for minimizing random events). GSO and LSO both have better timing resolution and, in theory, better energy resolution. If 2D imaging is being contemplated, it is possible that GSO and LSO may not offer much advantage over BGO. For 3D imaging, GSO and LSO can better minimize random events, although some BGO machines can in part compensate for this with better dead-time performance. The better energy resolution of GSO or LSO and consequent reduction of scatter in 3D mode make these detector types advantageous. At present, the theoretical energy resolution for these detectors does not seem to have been realized in practice, leaving all three crystal types with similar energy-based scatter rejection and making 2D imaging still the method of choice if scatter rejection is critical.

PET imaging—attenuation correction. In most previous models of PET scanners, rotating rod sources of germanium 68/gallium 68 were used to perform a transmission scan prior to or immediately after emission imaging. Current commercially available PET scanners are PET/CT scanners, which rely on CT scans for attenuation correction. In 2D scanners, rotating rod sources work well for cardiac imaging, although it adds 3 to 8 minutes to scan time. For scanners that can only operate in 3D mode, a rotating rod source can be problematic, due to excessive count rates in the detectors. Sometimes, a non–positron-emitting source such as cesium 137 (shielded from the closest detectors) is used to reduce count rate problems, although this methodology has some difficulties, especially with scatter. The CT scanner in hybrid systems is usually used for the attenuation correction transmission scan, though this can cause problems if the CT and PET scans are not precisely aligned.

PET/CT imaging. The latest trend in emission computed tomography (ECT), including both SPECT and PET, is the addition of a CT system to the ECT scanner. These combined systems, in practice, demonstrate a range of integration. At one end of the spectrum, the hardware and software of the CT system are completely integrated within the PET scanner. In this approach, a common, unified gantry is used, and a single, unified software system with an integrated ECT/CT

interface is provided. At the other end of the spectrum, the hardware and software of the CT system stand alone. In this approach, a separate CT gantry is carefully placed in front of or behind the ECT gantry, and a separate workstation is used to control the CT system.

The commercially available PET/CT systems demonstrate this range of integration. In all cases, the manufacturer starts with a state-of-the-art PET scanner, whose characteristics have been described in the section above. The manufacturer then adds a CT system, consisting of a 2-, 4-, 6-, 8-, 16-, 32-, or 64-slice scanner. In all cases, the combined PET/CT scanner appears to have a unified gantry (because of the covers), although separate gantries for the PET and CT portions may actually be used. Depending on the degree of system integration, separate workstations may be used to control the PET and CT portions of the combined system, or a single, unified workstation may be present.

ACCREDITATION ISSUES RELATED TO EQUIPMENT AND QA

A well-designed, regularly followed QA plan for imaging devices ensures the best possible diagnostic service to the patient population. Agencies that accredit facilities for medical use take QA programs seriously. For instance, the Joint Committee on the Accreditation of Hospital Organization's guidelines address the use of medical isotopes and associated radiation measuring and imaging equipment.

Over the past few years, there has been a growing trend among medical insurance companies to require that a facility be accredited by an external agency as a prerequisite for reimbursement of medical imaging procedures.[8]

Agencies that accredit nuclear cardiology facilities, specifically, include the American College of Radiology (ACR) and the Intersocietal Commission for the Accreditation of Nuclear Medicine Laboratories (ICANL).[9] The ACR equipment guidelines require proof of a QA program specific to gamma cameras, SPECT cameras, and PET cameras (as appropriate to a given facility), including the submission of images of flood fields, bar phantoms, multipurpose Plexiglas SPECT phantoms, multipurpose Plexiglas PET phantoms, and equipment acceptance testing reports.[8,10] An annual physicist's report also must be submitted, which includes all of the imaging examples just described, along with the results of additional annual camera tests and the results of tests of non-imaging equipment used to measure radiation (survey meters, dose calibrators, and so on). For QC procedures for non-imaging radiation equipment, and the frequency with which those procedures should be performed, please refer to the ACR and ICANL accreditation documents,[11,12] which discuss these at length. An acceptable proof of proper credentialing of all physicians, technologists, and physicists must be submitted. Representative clinical images also must be submitted. Panels of physicists review phantom images and physicists' reports, and panels of physicians review clinical images, all of which must be judged to be of an acceptable quality in order for a facility to be eligible for accreditation.

Laboratories applying for ICANL accreditation have the options of accreditation for nuclear cardiology, general nuclear medicine, or PET or a comprehensive accreditation that includes two or more modalities. The ICANL equipment guidelines also require proof via written documentation of ongoing camera and non-imaging equipment QC that is reviewed during the site visit. In addition to the camera-specific QC program that must include daily energy peaking and intrinsic or extrinsic uniformity, weekly resolution and linearity, monthly high count floods, and center of rotation (COR), the laboratory must also submit camera- and computer-specific acquisition and processing protocols.[9] Many other written protocols and documentation of their adherence are reviewed during the site visit and include but are not limited to radiation safety and radioactive materials handling, clinical and general protocol guidelines, and administrative protocols. In addition to the protocols, all medical and technical personnel interpreting and performing imaging services within the laboratory are required to be appropriately trained, experienced, and credentialed and/or licensed. A typical application submission for accreditation consists of a compilation of documentation, including the professional credentials of medical and technical staff, a list of imaging and non-imaging equipment, and written imaging and stress procedure protocols. Additionally, the laboratories are required to submit selected patient studies in digital format as well as copies of the final reports sent to referring physicians. For nuclear cardiology, a minimum of five myocardial perfusion studies is required, and all nuclear cardiology case studies must be randomly selected using the guidelines outlined in the application.

QC PROCEDURES

Planar imaging QC. Appropriate QC procedures are necessary to ensure images of the highest possible technical quality for the equipment used and thus allow the best possible diagnostic service to the patient population (Tables 2 and 3).[13]

Table 2. Planar QC procedures

Test	Frequency	For information, see paragraph
Energy peaking	Daily	1
Uniformity test	Daily	2
Resolution and linearity	Weekly	3
Sensitivity test	Weekly or daily	4

1. **Energy peaking.** Energy peaking is performed to verify that the camera is counting photons having the correct energy. This test consists of either manually or automatically placing the correct pulse height analyzer's energy window over the photopeak energy to be used. Care must be taken that the technologist verifies the correct placement of the window and that a radioactive point source is used at a distance away of greater than 5 useful FOV (UFOV) diameters from the uncollimated camera; a sheet source is typically used in front of a collimated camera.[14] In either case, the full UFOV of the camera should be illuminated by the source. Window verification should be done even on automated systems where there are single buttons or computer protocols to select for each energy; even in these automated systems, the energy windows tend to drift. These systems allow for window offsets to correct for these drifts. This peaking test should indicate for each camera head whether the camera's automatic peaking circuitry is working properly, whether the peak appears at the correct energy, and whether the shape of the spectrum is correct. If cost, time, and the equipment permit, photographs of the spectra with the superimposed energy window should be taken and stored.
2. **Uniformity test.** Uniformity testing is performed to verify that the camera's sensitivity response is uniform across the detector's face. Some manufacturers recommend that this test be performed intrinsically (using a point source without collimators), while others recommend that this test be performed extrinsically (with the collimator in place in conjunction with a sheet source, usually of cobalt 57). This test consists of exposing the camera with a uniform source of radioactivity, a process commonly referred to as "flooding" the detector. If performed intrinsically, a radioactive point source is positioned at a distance at least five times the crystal's UFOV from the center of the detector. This test is usually performed immediately following peaking of the detector. The point source should consist of a small volume (approximately 0.5 mL) of fluid and low activity (7-11 MBq). For large rectangular cameras (such that the point should be 7-8 feet away), 20 to 25 MBq is appropriate. In some cameras, obtaining intrinsic flood fields can be difficult. Some manufacturers provide software to correct for non-uniformities due to the necessity of having a point source closer than 5 UFOV diameters. Because of these difficulties, it may be more practical to perform this test extrinsically using radioactive sheet flood sources. To ensure a true response during acquisition, count rates should be kept between 10 and 25 kcps. For some older systems, a lead ring should be used to shield the outermost tubes from the radiation to prevent edge packing. Flood images that will be inspected visually should be acquired as 256 × 256 matrices for 3 M counts (5 M for larger rectangular detectors). Photographs of the flood field should be recorded and stored, both physically and digitally. Flood images used for calculations of uniformity require two to three times more counts to reduce statistical noise. The recommended number of counts is at least 4,500 counts/cm^2 (eg, 5.7 M counts for a 400-mm circular detector). NEMA recommends acquiring a minimum of 10,000 counts for the center (6.4 mm) pixel of the flood image.[14]

   The flood images should be examined each day for each detector prior to use to verify that the detectors are properly peaked and that the floods are uniform. In addition, several parameters are quantified from the flood images, which should be computed and the results recorded as part of the usual QA procedures. In the event of power shortages and power outages, the process of peaking and flooding the detectors should be performed again to ensure proper function before resuming patient imaging. Two uniformity parameters are computed—integral uniformity and differential uniformity. If the flood images are acquired in a larger matrix size, the pixel matrix should be reduced to 64 × 64 by summing or averaging pixels prior to uniformity calculation. Integral uniformity is a global parameter measuring uniformity over an extended area of the detector, expressed as follows:

$$\text{Integral uniformity} = 100\% \times (\text{Max} - \text{Min})/(\text{Max} + \text{Min})$$

where *Max* is the maximum count and *Min* is the minimum count found in any pixel within the specified area. Differential uniformity is a regional parameter that measures contrast over a small neighborhood. This measurement is performed using all 5 × 1–pixel areas in both the X and Y directions, expressed as follows:

Table 3. Performance parameters for detectors

Parameter	Standard	Preferred	For information, see paragraph
Integral uniformity	<5%	<3%	2
Differential uniformity	<5%	<3%	2
Intrinsic resolution full width at half maximum	<6 mm	<4 mm	3

Table 4. SPECT QC procedures

Test	Requirement	Frequency	For information, see paragraph
COR	Mandatory	Weekly	1
Uniformity correction	Mandatory	Weekly	2
Multipurpose Plexiglas phantoms	Strongly recommended	Quarterly-annually	3

Differential uniformity = 100%
× Largest deviation (Max − Min)/(Max + Min)

It should be noted that manufacturers vary considerably as to their recommendations regarding the ability of a particular camera to use a flood field collected at one energy (eg, 140 keV for Tc-99m) to correct the field of data acquired at a different energy (eg, 70 keV for Tl-201).[15] For some Anger cameras, it may be essential to acquire flood fields separately for Tl-201, iodine 123, I-131, and so on. In that case, most users will perform these corrections intrinsically, not extrinsically. Failure to apply an adequate overall flood-field correction is seen most strikingly on the uniform section of a multipurpose Plexiglas SPECT phantom.[13]

3. **Resolution and linearity test.** For systems based on Anger camera technology (ie, NaI sheet crystals with photomultiplier tubes), this test is performed to document spatial resolution and its change over time as well as the detector's ability to image straight lines. The test consists of imaging a flood source intrinsically through a spatial resolution test phantom. The flood source should be acquired as described in the "Uniformity test" section. Most commercially available bar phantoms are suitable for this test. These include the parallel-line equal-space bar phantoms and orthogonal hole or 4-quadrant phantoms. If the 4-quadrant phantom is used, each time the test is conducted, the phantom should be rotated 90° so that every fifth time the test is done, the pattern position repeats. Bar phantom images should be recorded and stored. These images should be assessed for how straight the lines imaged are and for intrinsic spatial resolution. Change in resolution is assessed by documenting the smallest bars that are discerned. Spatial resolution as measured by the full width at half maximum may be approximated by multiplying 1.7 times the smallest bar size seen.[13] For other systems not based on the Anger camera technology (eg, solid state detectors), the manufacturer should provide a QC procedure to ensure that the resolution and linearity stability are maintained by the system.
4. **Sensitivity test.** This test is performed to document the sensitivity of the detector and, more importantly, the change of sensitivity over time. The test consists of calculating detector sensitivity (expressed in terms of counts per minute per megabecquerel) of a known source, calibrated with a dose calibrator. The point source should always be located at exactly the same distance in front of the camera for repeat measurements. A convenient means of measuring sensitivity changes is by recording the time that it takes to acquire the preset counts for an intrinsic (or extrinsic, if more practicable) flood source.

SPECT imaging QC. All of the QC procedures required of planar imaging instruments are also required for SPECT imaging, since tomography depends on acquiring accurate planar projections (Table 4). In addition, procedures specific to SPECT imaging systems are discussed below.

1. **COR.** An alignment error between the electronic matrix of the detector and the mechanical COR can potentially result in a characteristic "doughnut" (if a 360° orbit and a point source are used) or "tuning fork" artifact (if a 180° orbit is used) in the transverse

images.[16] The effects are most evident when the error is greater than two pixels in a 64 × 64 matrix. Errors less than this reduce spatial resolution and image contrast through blurring of the image and cause significant artifacts (particularly at the apex).[17] The accuracy of COR alignment should be checked weekly for each camera head, unless indicated otherwise by the manufacturer. In some systems this means that two separate acquisitions are required: one for each detector (with the other detector disabled). Many manufacturers require that a specific protocol be followed for the determination and recalibration of the COR. While some manufacturers limit the COR calibration to service engineers, all systems may be checked for correct COR calibration. If no specific COR acquisition protocol is recommended by the manufacturer, the COR may be determined through the acquisition of a point source of activity (18-37 MBq) on the patient table 4 to 8 inches away from the axis of rotation. SPECT data are acquired over 360° with equally spaced projections with a circular orbit. The same angular orientation, collimation, zoom, matrix size, and energy window employed for the patient study should be employed for the COR acquisition. Five to ten seconds per frame for 64 views over 360° is sufficient. COR correction values for each orbit are then computed, stored in the computer, and used to realign the projection data before reconstruction. It is essential that COR errors be checked for each collimator that is to be used clinically.[18] It is recommended that these measurements be performed weekly. New COR calibrations should be performed after servicing of the camera, after power surges or outages, and for the computer after software upgrades.

2. **High-count extrinsic flood-field uniformity corrections.** Manufacturers vary considerably as to their recommended schedule and means of acquiring these high-count corrections. It has recently been noted that some cameras may not require the acquisition of extrinsic floods more often than annually to verify collimator integrity and that all uniformity corrections should be acquired intrinsically, so long as the camera is correctly tuned.[15] For many systems, collimators are sufficiently well designed and manufactured that they do not degrade SPECT uniformity. Therefore, as with any of the procedures discussed in these guidelines, it is always important to follow the manufacturers' recommended QA protocols.

   In SPECT, it is implicitly assumed that the efficiency of photon detection is constant across the surface of the collimated detector. Flood-field uniformity errors result when the variation in efficiency is significant as compared to the performance parameters in the above table. Anger cameras utilize stored flood-field correction maps to correct for variations in sensitivity across the FOV before reconstruction. Deficiencies can lead to characteristic "ring" artifacts, most easily seen on the uniform sections of multipurpose Plexiglas SPECT phantoms[13] and myocardial perfusion artifacts. Daily checks of flood-field extrinsic (with collimator) uniformity are performed with a 3 million–count flood for a typical FOV 128 × 128 or 256 × 256 matrix. To correct for sensitivity variations due to the collimator, 30 to 100 million–count images are acquired for each detector (128 × 128 or 256 × 256 matrix) and stored for uniformity correction. It is essential to perform uniformity measurements for each collimator and that the same collimator that was used to acquire the flood and generate the correction matrix be used to acquire the patient study. It is important that energy values similar to those being used for clinical studies also be used for the flood source. Co-57 solid sheet sources (122 keV) are commonly used and, more rarely, Tc-99m fillable sources for Tl-201 and Tc-99m imaging. A solid sheet source is less problematic for daily use. Using the lower-energy correction floods for higher-energy radionuclides can result in incorrect compensation and therefore is not recommended.

3. **Multipurpose Plexiglas phantoms.** It is strongly recommended by NEMA that acquisition and reconstruction of a multipurpose Plexiglas phantom should be performed quarterly.[19] For facilities intending to pursue laboratory ACR accreditation, performing these tests is mandatory. In particular, it should be noted that if accreditation is sought from the ACR, it is required to submit acceptable SPECT phantom images for both Tc-99m and Tl-201 simulations. These SPECT phantoms are cylindrical or elliptical water baths into which radioactivity is injected and contain regions with solid spheres of different sizes, regions with solid rods or bars of different sizes alternating with radioactive water, and regions containing only radioactive water.[20] These phantoms are used to determine the 3D contrast, resolution, and uniformity of the scanner, for which high activities (740-925 MBq) and "fine" sampling (128 × 128 matrices and 128 projections over 360°) generally are employed.[13] Acquisitions are performed using typical Tc-99m energy settings, with detectors positioned as close to the phantom as is feasible throughout a 360° acquisition, so as to optimize spatial resolution.[2] At least 30 million counts should be acquired, and data then are reconstructed for sections of the phantom to enable assessment of contrast through the center of spheres, 3D resolution through sections of rods, and uniformity through "blank" sections. Systemic prob-

Table 5. QC procedures for sealed-source SPECT/TCT systems

Test	Frequency	For information, see paragraph
Energy peaking	Daily	1
Transmission source mechanics	Daily	2
Source strength	Monthly	3

lems that can be revealed in this fashion include suboptimal energy resolution through failure to display adequate contrast, potential COR problems through loss of resolution through solid rod sections, and inappropriate or inadequate flood-field corrections through the appearance of anomalous concentric rings in uniform sections. These tests should be performed quarterly, as well as following major equipment repairs and installation of new software, to verify the overall ability of the hardware and software to correctly perform tomographic reconstructions. When used in conjunction with standards established during acceptance testing, these quarterly tests can be helpful in signaling the point at which the manufacturer's service representatives should be called to further diagnose the causes of significant degradation of 3D system performance and to remedy these problems.[15]

QC procedures for sealed-source SPECT/TCT systems. SPECT parameters outlined in the SPECT imaging QC section of these imaging guidelines should be used to ensure the quality of the emission tomographic data. In addition to those parameters, QC guidelines need to be followed to ensure that the transmission system using a sealed radioactive source is operating as designed (Table 5).

1. **Energy peaking.** This test is performed to verify that the camera is counting photons in the proper energy windows. Using a pulse height energy (z) analyzer, which is available on all acquisition stations, the operator should verify that the emission, transmission, and scatter (if applicable) windows are properly set and that photons are being counted in each window. For some systems, this may necessitate manually opening the shutter to the transmission source. If this is not possible, a quick "blank" scan (see next paragraph) can be acquired to verify that transmission photons are being properly counted.

   NOTE: Consult the vendor's recommendation for energy peaking. Some vendors do not permit or require the peaking of all energy windows simultaneously.
2. **Transmission source mechanics.** When patients are not being imaged, the transmission source is shielded and, on systems where the source translates across the FOV, left in the "parked" position. When a patient is imaged, the shutter used to shield the source is opened, allowing transmission photons to be directed toward and through the patient. In some systems, the source will then translate axially along the axis of the body for each projection. To verify the operation of the source shutter and translating mechanics, a reference "blank" transmission scan should be acquired. This scan is required for all TCT protocols and is recommended to be acquired weekly and possibly daily prior to the first use of the system for that day. The frequency of this test will depend on the half-life of the isotope of the transmission source and the stability of the TCT system. Follow the manufacturer's recommended acquisition protocol for acquiring a transmission blank scan. When complete, visually inspect planar images and check for artifacts (ie, focal cold spots, bands of missing data, axial discontinuities). A common misconception is that the blank scan should be uniform, similar to uniformity floods. Stringent uniformity indices of $\pm$ 10% are not reasonable for the blank scan. Rather, the blank scan should be inspected to ensure that there are no gross non-uniformity artifacts (ie, holes or bands of pixels with no counts). For scanning-source systems, the blank scans should not show discontinuities or abrupt changes in pixel intensity in the axial direction of the scanning source. The presence of these artifacts is consistent with improper scanning-detection alignment and should be checked by a service engineer.
3. **Source strength.** For systems using a Gd-153 transmission source, photons collected in the transmission window consist of primary transmission photons and scattered photons (cross-talk) from the emission radiotracer. The ratio of these components, transmission and cross-talk, is referred to as the transmission–to–cross-talk ratio (TCR). This TCR value depends on the transmission source strength, the injected radiopharmaceutical, the injected activity, and the body habitus. Transmission source decay, higher injected activities, and larger body sizes all tend to decrease the TCR value. Lower TCR values result in reconstructed attenuation maps with increased bias and noise. Since the TCR value will decrease as the source decays, its behavior should be trended over the life of the source, which can guide the user as to when the sources should be replaced. This QC protocol should be performed at least monthly, with the baseline scan being performed when the TCT-ECT system

is installed or the transmission sources have been replaced. If the user suspects problems with the TCT-ECT system, a test should be performed immediately prior to using the system for patient imaging. Two protocols are provided, one using a cylinder phantom and the other using an anthropomorphic chest phantom. The chest phantom provides the more comprehensive check of the TCT-ECT system for cardiac imaging compared to the cylinder for obvious reasons. For those sites that may not have access to a chest phantom, the cylinder protocol is provided which is capable of identifying potential problems with a TCT-ECT system.

SPECT/TCT Protocol 1: Cylinder Phantom

Required Equipment

18- to 20-cm-diameter fillable cylinder
111 to 185 MBq (3-5 mCi) Tc-99m or 37 MBq (1 mCi) Tl-201

Acquisition Protocol

1. The cylinder is positioned with the long axis of the cylinder parallel to the table bed. Since processing will involve summing slices, any tilt in the cylinder should be minimized, as seen by the detector.
2. The vendor-recommended TCT-ECT acquisition protocol should be used.

   NOTE: The total acquisition time should not be less than 12 minutes.

Processing Protocol

1. Emission cross-talk is removed from transmission data (for most systems, this is done automatically and does not need to be initiated by the user).
2. Attenuation maps are reconstructed from the transmission projection data. If a filter is applied to the reconstructed image data, the vendor-recommended filter should be used.
3. Map slices from the center of the cylinder to provide a single 5-cm-thick slice are summed.
4. A circular region of interest (ROI) is drawn centered in the cylinder image that is approximately 90% of the diameter of the cylinder.
5. The mean attenuation coefficient (μ) value in the ROI is recorded. Table 6 provides the expected range of μ values for the transmission isotope energy.

   NOTE: Units for the attenuation coefficient (μ) may depend on the system and vendor.
6. Non-corrected (NC) and attenuation-corrected (AC) emission data are reconstructed. Slices are summed from the center of the cylinder to provide a 5-cm-thick slice.

Table 6. Expected measured attenuation coefficient ranges

Isotope	Energy (keV)	μ Expected range
Gd-153	100	0.160/cm-0.176/cm
Co-57	122	0.152/cm-0.168/cm
Tc-99m	140	0.145/cm-0.161/cm
Barium 133	360	0.106/cm-0.117/cm

The NC and AC images should be inspected together. The AC image should be more uniform than the uncorrected image. Due to the low activity levels injected into the phantom, it is difficult to provide an acceptable quantitative range for an ROI.

SPECT/TCT Protocol 1: Troubleshooting

If the ROI value from step 5 falls outside of the expected range, the system can potentially yield erroneous data. Possible sources of error are as follows:

1. Transmission sources are too weak. The acquisition should be repeated with longer scan duration (ie, double the scan time). The processing steps should be repeated and a new ROI value recorded for the attenuation map. If the value improves, then the sources are weak, and it is recommended that either the imaging times should be increased for the clinical protocols or the transmission sources should be replaced.
2. Cross-talk correction is incorrect. While this correction is typically done automatically without user interaction, it does have the potential for failure. To investigate if improper cross-talk correction is the source of error, the measurement should be repeated with no activity injected in the cylinder. This will necessitate refilling the tank with water (no activity) and repeating the protocol. If the new ROI value for the attenuation map without activity is within the tabulated range, the service representative should be contacted to have the TCT-ECT system checked. The cross-talk estimate used to correct the transmission data is likely the problem, as the uncontaminated data are within the acceptable range and the cross-talk "compensated" values are not.
3. Bad blank scan: A new blank scan and a new cylinder phantom filled only with water should be acquired (no activity injected into cylinder). If the new ROI value is not within the tabulated range and your sources have not expired, call the service representative. In this case, there is likely a serious inconsistency

problem between the transmission and blank scan data. If the new ROI value is within the acceptable range, inject activity into the phantom and reacquire the phantom.

SPECT/TCT Protocol 2: Chest Phantom

Required Equipment

An anthropomorphic chest phantom with a heart insert (no defects in heart).

Injected Activity Concentrations

A simulated 1,110 MBq (30 mCi) sestamibi stress study.

Heart: 250 kBq/mL (6.8 μCi/mL)
Tissue: 25 kBq/mL (0.7 μCi/mL)
Liver: 150 kBq/mL (4.0 μCi/mL)
Lungs: 0 kBq/mL (0.0 μCi/mL)

Acquisition Protocol

1. The phantom is positioned on the imaging bed.
2. The vendor-recommended TCT-ECT cardiac acquisition protocol is used.

   NOTE: The total acquisition time should not be less than 12 minutes.

Processing Protocol

1. Emission cross-talk is removed from transmission data (for most systems, this is done automatically and does not need to be initiated by the user).
2. The attenuation maps are reconstructed from the transmission projection data.
3. The transmission maps are visually inspected. Possible artifacts and their sources are identified. Obvious artifacts include image truncation (ring artifact on periphery of imaging FOV) and cross-talk correction errors (depressed pixel intensities in region of heart or liver). If the truncation artifact involves a significant area of the imaging FOV, the phantom is repositioned and data are reacquired. If cross-talk errors are present, the troubleshooting section below should be consulted.
4. Two small circular ROIs are drawn in the region of the heart and the liver. The mean μ values are recorded for the heart and liver ROIs. The expected ranges of μ values for the transmission isotope energy are presented above.

   NOTE: Units for the attenuation coefficient (μ) may depend on the system and vendor.
5. NC and AC emission data are reconstructed. NC and AC polar maps are computed from the image data.
6. NC and AC short-axis and horizontal and vertical long-axis images are reviewed in a comparative display. Visually, the AC images should be more uniform than the NC images. No region of the heart should be noticeably hotter than the rest. The apex of some phantom hearts may be cooler than the rest of the phantom as the wall thickness of some phantom hearts does vary and can fall below the imaging resolution. In this case, the partial-volume effect can be attributed to the lower activity values.
7. The AC intensity values in the anterior, lateral, posterior, and septal regions should be derived, using the ROI tool with either the polar maps or a mid–short-axis image, and the results recorded. The anterior-posterior and septal-lateral ratios should be 1.0 ± 10%.

SPECT/TCT Protocol 2: Troubleshooting

If the ROI value from the above steps falls outside of the accepted range, the system can potentially yield erroneous data. Possible sources of error are as follows:

1. Transmission sources are too weak. The acquisition should be repeated with a longer scan duration (ie, double the scan time). The processing steps should be repeated and results recorded for a new ROI value for the attenuation map. If the value improves, then the transmission sources are weak, and it is recommended that either the imaging times for clinical protocols should be increased or new transmission sources should be installed.
2. Cross-talk correction is incorrect. While this correction is typically done automatically without user interaction, it does have the potential for failure. To investigate if improper cross-talk correction is the source of error, the measurement should be repeated with no activity. This will necessitate refilling the tank with water (no activity) and repeating the protocol. Alternatively, the cylinder protocol could be performed, as this protocol is ideally suited to determine cross-talk of blank scan problems. See troubleshooting comments 2 and 3 for the cylinder protocol.

If the ROI ratio values from step 7 fall outside of the accepted range, the system can potentially yield erroneous data. Possible sources of error are as follows:

1. Transmission sources are too weak. The acquisition should be repeated with longer scan duration (ie, double the scan time). The processing steps should be repeated and results recorded with a new ROI value for the attenuation map. If the value improves, the sources are weak, and it is recommended that either the clinical imaging time be increased or new transmission sources be installed.

Table 7. CT QC procedures

Test	Requirement	For information, see paragraph
Calibration	Mandatory	1
Field uniformity	Mandatory	2

2. Cross-talk correction is incorrect. While this correction is typically done automatically without user interaction, it does have the potential for failure. To investigate if improper cross-talk correction is the source of error, repeat the measurement with no activity. This will necessitate refilling the tank with water (no activity) and repeating the protocol. If the new ROI value for the attenuation map without activity is within the tabulated range, the service representative should be contacted to have the TCT-ECT system checked. If the new value is not within the tabulated range and your sources have not expired, the service representative should be called. If the sources are near their expiration date, the sources should be replaced.

QC procedures for X-ray–based SPECT/CT systems. All of the QC procedures required of SPECT imaging are required for SPECT/CT imaging. Additionally, procedures specific to CT imaging are required and are listed below. In the current state of hybrid SPECT/CT and PET/CT development, the CT equipment is very similar or identical for these two modalities. The tables in this section list the critical requirements (Table 7).

1. **Calibration.** The reconstructed CT image must exhibit accurate, absolute CT numbers (in Hounsfield units). This is critical for the use of CT images for SPECT attenuation correction, because the quantitative CT values are transformed (usually via a bilinear or trilinear function with one hinge at or near the CT value for water) to attenuation coefficients at 511 keV. Any errors in CT numbers will be propagated as errors in estimated radionuclide attenuation coefficients, which in turn will adversely affect the AC SPECT values. CT system calibration is performed with a special calibration phantom that includes inserts of known CT numbers. This calibration is done by the manufacturer's field service engineers. The CT calibration is then checked daily with a water-filled cylinder (usually 24 cm in diameter; usually provided by the manufacturer). In practice, if the error is greater than 5 Hounsfield units (ie, different than the anticipated value of 0 Hounsfield units), the CT system is considered out of calibration. The technologist will usually then do an air calibration, to determine if this corrects the overall calibration (ie, brings the CT number for water back to within 5 Hounsfield units of 0). If it does not, the manufacturer's field service engineer must be called. On an annual basis, or after any major repair or calibration, calibration is checked by the manufacturer's field service engineer with a special phantom that includes plastic inserts that simulate bone, muscle, fat, and water.
2. **Field uniformity.** The reconstructed CT image must exhibit uniform response throughout the FOV. In practice, this means that a reconstructed image of a uniform water-filled cylinder must itself demonstrate low variation in CT number throughout this image. In practice, small circular ROIs are placed at the four corners of the cylinder image, and the mean CT number is compared to that from a region in the center of the phantom; the difference in mean region CT number should not exceed 5 Hounsfield units. Nonuniformities greater than this may produce sufficient quantitative inaccuracies as to affect SPECT attenuation correction based on the CT image.
3. **QC schedules for CT used for SPECT/CT.** Users should consult the manufacturer regarding the specific manner and frequency with which tests should be performed for the CT component of their SPECT/CT device. The frequency and details of test procedures vary somewhat depending on whether the CT unit is a diagnostic-quality CT (usually regarded as units of 8 slices or more) or is instead a CT unit intended for feature localization and attenuation correction (usually regarded as units with 4 slices or less). Two typical schedules are provided in Tables 8 and 9, one for a non-diagnostic CT unit and one for a diagnostic CT. For more information as to reasonable requirements for the frequency and details of performing QC on CT equipment, please refer to the ACR Web site (www.acr.org).

Table 8. Schedule of non-diagnostic-quality CT QC for SPECT/CT units

Test	Frequency
Air table creation	Daily
Scout scan	Daily
CT of water phantom	Daily

Combined SPECT/CT QC procedures. The SPECT portion of the combined system should be assessed as described above. The CT portion should likewise be assessed via standard CT QC procedures. With respect to its use in a combined SPECT/CT system,

Table 9. Schedule of diagnostic-quality CT QC for SPECT/CT units

Test	Frequency
Water phantom QC	Daily
Tube warm-up	Daily
Air calibration ("fast QC")	Daily
Water phantom checks	Monthly
Slice thickness	
Accuracy	
Positioning	

Table 10. Combined SPECT/CT QC procedures

Test	Requirement	For information, see paragraph
Registration	Mandatory	1
Attenuation correction accuracy	Mandatory	2

the CT portion should undergo the following tests (Table 10).

1. **Registration.** The reconstructed SPECT and CT images must accurately reflect the same 3D locations (ie, the two images must be in registration). Such registration is not easily achieved, because the SPECT and CT portions of commercial combined SPECT/CT systems may not be coincident (ie, the SPECT and CT "slices" are not in the same plane) and because SPECT and CT gantries may be contiguous. In practice, this means that the SPECT and CT acquisitions may not simultaneously image the same slice. For contiguous gantries, the bed must travel different distances into the gantry to image the same slice in the patient for SPECT versus CT, providing ample opportunity for misregistration, via x, y, z misalignment of bed motion or (of perhaps even greater concern) because of differential "bed sag" for the SPECT and CT portions. In addition, electronic drift can influence the "position" of each image so that calibrations for mechanical registration can become inaccurate over time. Thus it is imperative to check SPECT-to-CT registration on an ongoing basis. This can be performed with a specific phantom or jig containing an array of point sources visible in both SPECT and CT. Errors in co-location in the fused SPECT-CT images are assessed, such as by means of count profiles generated across transaxial slices. Such errors (after software registration corrections) should be not greater than the spatial resolution of the SPECT scan. It is important to image this registration jig in a number of positions along the bed. It may also be helpful to place a weight on the end of the bed (to simulate some sagging of the imaging bed) and repeat the assessment.
2. **Attenuation correction accuracy.** The use of the CT image for SPECT attenuation correction requires a transformation of the observed CT numbers (in Hounsfield units) to attenuation coefficients at the energies of the radionuclides. This transformation is usually accomplished with a bilinear calibration curve, "hinged" at a CT value of 0 (ie, hinged at the CT value for water). At a minimum, it is important to image a water-filled cylinder to assess SPECT field uniformity and SPECT activity concentrations after CT-based SPECT attenuation correction. Errors in CT-to-SPECT attenuation transformations are usually manifested as a corrected SPECT image without a "flat" profile from edge to center (ie, the activity at the edge is either too high or too low relative to that at the center of the phantom) and with resulting AC absolute SPECT values that are incorrect (although these values depend on absolute SPECT scanner calibration as well as accurate CT-based SPECT attenuation correction). Moreover, if available, more sophisticated phantoms with variable attenuation (and variable activity distributions) can be used to more comprehensively assess any errors in CT-based SPECT attenuation correction.
3. **Misregistration consequences.** With the proliferation of SPECT/CT systems, experience has begun to accumulate regarding the appearance of CT artifacts, the prevalence of misregistration between SPECT and CT transaxial tomographic sections, and the influence of all of these on perfusion quantitation. Recent publications suggest that an incidence in excess of 40% of misregistration judged to be "moderate to severe" occurs routinely.[21] Misregistration by only 1 pixel may create perfusion artifacts.[22] Consequently, methods are being developed to enable manual registration between SPECT and CT scans.[23] The QC procedures listed above are specific to guaranteeing the integrity of equipment used to acquire and combine the data under ideal circumstances.

PET imaging QC. Table 11 lists recommended PET imaging QC schedules. Note that, unlike planar and SPECT imaging, there are no widely accepted, published QC procedures for PET. Some additional procedures may be required by particular manufacturers (see paragraph 6 below). The procedures below should be suitable for ensuring overall proper basic operation of a PET scanner.

Table 11. Suggested QC procedures: Dedicated PET imaging devices

Procedure	Frequency	For information, see paragraph
Acceptance testing as per NEMA NU 2-2001	Once upon delivery and upon major hardware upgrades	1
Sensitivity and overall system performance	Daily (or at least weekly)	2
Transverse resolution	Annually	3
Accuracy (corrections for count losses and randoms)	Annually	4
Scatter fraction	Annually	4
Accuracy of attenuation correction	Annually	5
Image quality	Annually	5
Measurements specified by manufacturer	As per manufacturer	6

Suggested QC procedures: Dedicated PET imaging devices.

1. **Acceptance testing.** It is recommended that the NEMA performance measurements (NU 2-2001) be made before accepting the PET scanner.[24] Many of these tests can be performed by the company supplying the PET scanner. If so, it is recommended that the purchaser's representative work with the manufacturer's representatives during these tests, as the manufacturer may not perform them as specified by NEMA recommendations. These recommendations have been evolving in recent years, and the more recent recommendations (NU 2-2001) have superseded older recommendations (NU 2-1994),[25] primarily to accommodate PET scanners that are operated in 3D mode.[26] However, these newer recommendations also better reflect imaging of objects of the size of a typical adult thorax region by incorporating measurements of the International Electrotechnical Commission (IEC) body phantoms.[27] Aside from this phantom, however, if a facility intends to operate the PET scanner only in 2D mode, the older measurements in the 1994 standard, which are somewhat easier to perform, may be satisfactory. There are some differences between these NEMA standards (both 1994 and 2001) and the IEC standards.

   There are two reasons for performing these measurements: (1) to ensure that the new PET scanner meets specifications published by the manufacturer and (2) to provide a standard set of measurements that allow the user to document the limitations of the scanner, providing a standard against which to track changes that may occur over time.
2. **Sensitivity.** Subtle changes in PET system sensitivity may occur slowly over time. More dramatic changes in sensitivity may occur that are associated with hardware or software malfunction. There are simple tests designed to monitor such changes in sensitivity, as well as to check proper machine operation prior to each day's patient scans. Ideally, these tests should be performed daily, but not less frequently than weekly. One recommended procedure to measure system sensitivity is the following:
   a. A 20-cm-diameter × 20-cm-long (or longer) water-filled phantom can be used with a uniform concentration of a water-soluble fluorine 18 compound (eg, F-18 fluorodeoxyglucose) (eg, 1-2 mCi for a 2D scanner or a factor of 5 less for a 3D scanner). Alternatively, a uniform cylindrical phantom of approximately the same size can be used containing Ge-68/Ga-68 (available as a solid). The phantom is placed on the imaging table with the long axis of the cylinder parallel to the long axis of the scanning bed, centered in the transaxial field of the scanner. The phantom should be aligned as well as possible, with the assistance of a laser-positioning device if available.
   b. Data are acquired for at least 15 minutes, which should be sufficient for a 2D or 3D mode scanner with the activities specified above, with attenuation correction, using whichever mode of attenuation correction is being used clinically in the facility (eg, CT, rotating Ge-68 rod, or rotating Cs-137 rod attenuation corrections).
   c. Phantom images should be reconstructed using a typical clinical protocol.
   d. A circular ROI should be drawn on the central part of the transaxial slice, of a diameter on the order of 15 cm. For each slice, the mean measured concentration (in units of meqabecquerels per milliliter) should be computed and divided by input concentration, which is known from the measured activity and phantom volume for an F-18 phantom or from the specification sheet for a Ge-68 phantom. Values across slices should be within approximately 5% to 10% of each other. The mean sensitivity

value should be computed over all slices (but excluding the first and last 2-3 slices). These values should be within 10% of unity and should change only slowly over time.

e. Each slice, as well as the sum of all slices but excluding the first and last 2 to 3 slices, should be inspected for artifacts. The count profile across the summed slice should be generated and examined, which should be uniform to within the tolerance established during the initial acceptance testing of the PET scanner.

f. Note that if F-18 is used rather than Ge-68/Ga-68, the variation in measured mean values (meqabecquerels per milliliter/known meqabecquerels per milliliter) will depend on both variations in the scanner and variations in the device used to measure the injected activity.

3. **Transverse resolution.** This is measured using either the NEMA NU 2-2001 recommendations for a point source or NEMA NU 2-1994 recommendations for a rod source.
4. **Scatter fraction.** This typically is measured according to either NEMA NU 2-2001 (section 6) or NEMA NU 2-1994 specifications, although it is recommended that if the scanner is to be used in 3D mode, NU 2-2001 is preferred.
5. **Accuracy of attenuation correction and overall clinical image quality.** Attenuation correction should be assessed using the IEC phantom, as specified in the NU 2-2001 recommendations.[24] If this phantom is not readily available, it is suggested that similar measurements can be performed with a phantom approximating a typical human body shape and size (eg, a 20 × 30−cm elliptical phantom or anthropomorphic phantom) with at least one cold sphere or cylinder and one hot sphere or cylinder, as well as at least some material simulating lung tissue, to ensure proper performance in the presence of non-uniform attenuating substances.
6. **Variations among manufacturers.** The above recommendations regarding PET scanner QA are general guidelines. Each manufacturer has its own periodic QC recommendations for parameters such as "singles" sensitivity, coincidence timing, energy calibration, and overall system performance. These, by necessity, require very different measurement protocols that may vary even between models for the same manufacturer. These measurements must be performed as detailed by the manufacturer. However, the measurements specified above are not intended to replace these basic system-specific QC measurements.

Table 12. CT QC procedures

Test	Requirement	For information, see paragraph
Calibration	Mandatory	1
Field uniformity	Mandatory	2

PET/CT imaging QC. The PET portion of the combined system should be assessed as described above. The CT portion should likewise be assessed via standard CT QC procedures. With respect to its use in a combined PET/CT system, the CT portion should undergo the following tests (Table 12):

1. **Calibration.** The reconstructed CT image must exhibit accurate, absolute CT numbers (in Hounsfield units). This is critical for the use of CT images for PET attenuation correction, because the quantitative CT values are transformed (usually via a bilinear or trilinear function with one hinge at or near the CT value for water) to attenuation coefficients at 511 keV. Any errors in CT numbers will be propagated as errors in estimated 511-keV attenuation coefficients, which in turn will adversely affect the AC PET values. CT system calibration is performed with a special calibration phantom that includes inserts of known CT numbers. This calibration is done by the manufacturer's field service engineers. The CT calibration is then checked daily with a water-filled cylinder (usually 24 cm in diameter; usually provided by the manufacturer). In practice, if the error is greater than 5 Hounsfield units (ie, different than the anticipated value of 0 Hounsfield units), the CT system is considered out of calibration. The technologist will usually then do an air calibration, to determine if this corrects the overall calibration (ie, brings the CT number for water back to within 5 Hounsfield units of 0). If it does not, the manufacturer's field service engineer must be called. On an annual basis, or after any major repair or calibration, calibration is checked by the manufacturer's field service engineer with a special phantom that includes plastic inserts that simulate bone, muscle, fat, and water.
2. **Field uniformity.** The reconstructed CT image must exhibit uniform response throughout the FOV. In practice, this means that a reconstructed image of a uniform water-filled cylinder must itself demonstrate low variation in CT number throughout this image. In practice, small circular ROIs are placed at the four corners of the cylinder image, and the mean CT number is compared to that from a region in the center

Table 13. Schedule of CT QC for PET/CT units

Test	Frequency
Water phantom QC	Daily
Tube warm-up	Daily
Air calibration ("fast QC")	Daily
Water phantom checks	Monthly
Slice thickness	
Accuracy	
Positioning	

Table 14. Combined PET/CT QC procedures

Test	Requirement	For information, see paragraph
Registration	Mandatory	1
Attenuation correction accuracy	Mandatory	2

of the phantom; the difference in mean region CT number should not exceed 5 Hounsfield units. Nonuniformities greater than this may produce sufficient quantitative inaccuracies so as to affect PET attenuation correction based on the CT image.

3. **QC schedule for CT used for PET/CT.** Users should consult the manufacturer regarding the specific manner and frequency with which tests should be performed for the CT component of their PET/CT device. A typical schedule is provided in Table 13. For more information regarding ACR recommendation for these tests, please see the ACR Web site.

Combined PET/CT QC procedures. In addition to the (independent) QC tests for the PET and CT portions of the combined system, it is necessary to perform additional tests that assess the combined use of PET and CT (Table 14).

1. **Registration.** The reconstructed PET and CT images must accurately reflect the same 3D locations (ie, the two images must be in registration). Such registration is not as easily achieved, because the PET and CT portions of all commercial combined PET/CT systems are not coincident (ie, the PET and CT "slices" are not in the same plane) and because the PET and CT gantries are contiguous. In practice, this means that the PET and CT acquisitions do not simultaneously image the same slice. In fact, because the bed must travel different distances into the gantry to image the same slice in the patient for PET versus CT, there is ample opportunity for misregistration, via x, y, z misalignment of bed motion or (of perhaps even greater concern) because of differential "bed sag" for the PET and CT portions. In addition, electronic drift can influence the "position" of each image so that calibrations for mechanical registration can become inaccurate over time. Thus it is imperative to check PET-to-CT registration on an ongoing basis. This is usually performed with a specific phantom or jig containing an array of point sources visible in both PET and CT. Errors in co-location in the fused PET-CT images are assessed, such as by means of count profiles generated across transaxial slices. Such errors (after software registration corrections) should be less than 1 mm. It is important to image this registration jig in a number of positions along the bed. It may also be helpful to place a weight on the end of the bed (to produce some bed sag) and repeat the assessment.
2. **Attenuation correction accuracy.** The use of the CT image for PET attenuation correction requires a transformation of the observed CT numbers (in Hounsfield units) to attenuation coefficients at 511 keV. This transformation is usually accomplished with a bilinear calibration curve, "hinged" at a CT value of 0 (ie, hinged at the CT value for water). At a minimum, it is important to image a water-filled cylinder to assess PET field uniformity and PET activity concentrations after CT-based PET attenuation correction. Errors in CT-to-PET attenuation transformations are usually manifest as a corrected PET image without a "flat" profile from edge to center (ie, the activity at the edge is either too high or too low relative to that at the center of the phantom) and with resulting AC absolute PET values that are incorrect (although these values depend on absolute PET scanner calibration as well as accurate CT-based PET attenuation correction). If possible, the CT-based AC PET values should be compared with those from the rotating rod source–based AC PET values in the same phantom. Moreover, if available, more sophisticated phantoms with variable attenuation (and variable activity distributions) can be used to more comprehensively assess any errors in CT-based PET attenuation correction.
3. **Consequences of CT artifacts and misregistration.** As with SPECT/CT, investigators have recently begun documenting the effects of the misregistration between PET and CT transaxial sections on the quantification of myocardial perfusion defects.[28,29] The procedures listed above are intended to provide means of calibrating CT- and PET-acquired data, and to match these properly, and are not capable of correcting for breathing artifacts or the fact that high-quality CT scans are acquired in a fraction of a

second, whereas PET scans are acquired over many minutes.

Clinical QA for each patient procedure. Whereas the recommended QC procedures described in this document will reduce the frequency of SPECT and PET misdiagnosis due to technical problems, ongoing clinical QC for each patient procedure is also needed in order to obtain optimal imaging results. For ongoing clinical PET QC recommendations, please see the section of the guidelines entitled "Positron Emission Tomography Myocardial Perfusion and Glucose Metabolism Imaging." Recommendations for ongoing clinical SPECT QC are as follows:

1. **Patient instructions.** The imaging procedure should be explained to the patient before acquisition.
2. **Patient positioning.** When using 180° orbits for SPECT, every effort should be made to move the patient's left arm from his or her side, either above his or her head (standard) or, if that is not possible, to lower it so it is not attenuating counts from the heart as the camera moves to the left posterior oblique. This is usually accomplished by placing the arm above the head using an arm support device to maximize comfort. With some arm support systems, it is more comfortable to raise both arms into the support system. When using 360° orbits, both arms need to be positioned away from the patient's side. Also, it is important that patients be positioned similarly for additional studies including consistent radius of rotation, such as for both the rest and stress or immediate and delayed portions of a study.
3. **Motion detection/correction.** The patient should be observed throughout the acquisition by a technologist to ensure that patient motion does not occur. Talking, head movement, and irregular breathing should be avoided during the acquisition. Tomographic data should be reviewed for patient motion immediately following completion of an imaging session by the technologist who acquired the data. Acquisitions with motion should be corrected or reacquired before reconstruction. Review of the originally acquired projection data as an endless cine loop is perhaps the single most useful mechanism available to physicians to detect patient motion, to assess the adequacy of motion correction, and to assess the integrity of the collected data, not only for patient motion but also for a wide variety of imaging artifacts.[30] Critical to the accurate reconstruction of the tracer distribution is the fixed alignment of the detector coordinates and the organ being imaged. The most common source of misalignment is the motion of the patient or heart relative to the detector coordinates during acquisition. There is some physiologic cardiac motion over the cardiac cycle, which is unavoidable and accepted as a known source of image degradation. Otherwise, heart motion can result from the patient moving or exaggerated diaphragmatic excursion that can occur with heavy or erratic breathing. With patient or heart motion, count values are erroneously placed back into the tomographic image, resulting in potential artifacts that can corrupt the accuracy of tracer representation. Therefore it is critical that the rotating projection views be played in a cine format and evaluated for motion. If significant motion is detected, a repeat study usually is required. Translational motion along the patient axis ("up" and "down" motion) is the most frequently and most easily detected type of motion since it is perpendicular to the movement of the heart in the rotating cine views. Tomographic image degradation depends on the frame in which motion occurs. For instance, with a single-detector camera, if there is motion in the first frames but no motion for the rest of the study, this will have little effect. However, with multi-detector systems, the single episode of motion will be propagated throughout other frames of the 180° arc. On the other hand, a 1-pixel shift (vertical translation) over as few as 4 frames in the middle of the projection set can produce a clinically significant artifactual defect. Rotational angular motion is less frequently detected since it appears parallel to the motion of the heart in the projection images. Motion toward or away from a detector cannot be detected. A horizontal line of reference drawn on the screen or in one's mind can be used as the reference point for evaluation of the magnitude of motion. If motion is detected, an assessment of its severity must be made. A rule of thumb is that translational motion (eg, the patient moves and remains there throughout the study) on the order of 1 pixel in a 64×64 matrix represents an approximate limit before significant artifacts can result. Motion of one-half pixel can often be detected but generally does not result in clinically significant artifacts and represents the upper limit of motion detectable with automated methods. Translational or "drifting" motion along the patient axis in dual- and multi-detector systems yields unique "jumps" in the position of the myocardium where the detector views are joined. The same criteria for significance of motion for multiple-detector systems should be applied as those described above for single-detector systems. Once motion is detected, manual methods (if available) can be used to shift the frames back to the expected correct position. Manufacturer-specific automated methods can be executed that track the myocardium across the FOV and perform an approximate realignment. As with any automated procedure, automatic motion detection and

Table 15. Expected count ranges in left anterior oblique projection

	Whole heart (×1,000)	Maximum counts
Tl-201 (111 MBq/LEHR/64 stops)	10-28	85-134
Tc-99m (814 MBq/LEHR/64 stops)	21-77	190-298
Tl-201 (111 MBq/LEAP/32 stops)$_{STRESS}$	53-134	91-235
Tl-201 (111 MBq/LEAP/32 stops)$_{REST}$	33-100	66-185

LEHR, Low-energy, high-resolution collimator; *LEAP*, low-energy, all-purpose or general-purpose collimator.

correction are not 100% effective and should therefore not be blindly applied to all patient studies. It is recommended that motion correction only be applied to those studies exhibiting significant motion (as defined above), and that the motion-corrected data sets be carefully examined to ensure they were corrected appropriately.

4. **Detection of inappropriate energy settings.** Occasionally, data may not be acquired with the correct energy setting, such as when data are acquired on a Tc-99m setting for a patient who has been injected with Tl-201. This results in loss of counts, resolution, and contrast. One way to recognize this problem after the fact is to compare information in the header part of the DICOM (Digital Imaging and Communications in Medicine) images, which now have become the standard image storage format, regarding the energy setting of the camera versus the protocol used for patient preparation.[31]
5. **Image count rate.** Manufacturers have various means of making this count rate information available to the user. Some typical count rates for individual projection images are provided in Table 15, representing ranges of counts from acceptable SPECT studies. These values represent average left anterior oblique counts in a planar projection over the left ventricular myocardium, using image acquisition protocols described above.
6. **Attenuation artifact detection/correction.** Ideally, the use of attenuation-correcting hardware/software will eliminate most attenuation artifacts encountered clinically, including left breast and elevated diaphragm or protuberant abdomen. However, users should not expect attenuation correction to totally correct patient attenuation, particularly in patients with unusually large body habitus. There can be more troublesome artifacts that are more difficult to correct, such as those due to metallic objects (eg, metallic electrodes) interposed between the patient and the detectors. Some CT systems are sensitive to such objects; correcting for these may sometimes not be possible. However, review of the original rotating projection data should reveal a distinct shadow traversing the detector's FOV at the location of the foreign metal object.
7. **COR error detection/correction.** COR errors result in a distinct "comet" pattern artifact on myocardial perfusion SPECT data when acquired from the right anterior oblique–45° to left posterior oblique–45° projections. Unlike motion artifacts, these artifacts are highly predictable.[13] Re-acquisition of a point source tomogram should provide a definitive answer as to whether the usual filtered backprojection reconstruction process of data just collected has been compromised due to application of incorrect COR data. If so, and if the manufacturer has provided the means to do so, it is often possible to correct such data after the fact by updating the patient's data file with the newly updated COR information and reconstructing the data again.
8. **Arrhythmia detection.** Equipment manufacturers vary considerably as to R-R information retained for subsequent display. If available, the QA screen that displays the histogram of the patient's R-wave triggers received by the computer during data acquisition for each patient should be reviewed. Some algorithms are available to analyze gated SPECT data after the fact and report patterns of arrhythmias if detected from anomalies in curves of counts plotted versus projection angles from among the different time bins used to acquire data.[32]

SUMMARY

In summary, a thorough QA program involves all aspects of image acquisition, processing, and interpretation and is essential to the high-quality practice of nuclear cardiology.

References

1. Bushberg JT, Seibert JA, Leidholt EM, Boone JM. The essential physics of medical imaging. Baltimore: Williams & Wilkins; 1994.
2. Cherry SR, Sorenson JA, Phelps ME. Physics in nuclear medicine. Philadelphia: Saunders; 2003.
3. DeFilippo FP, Abreu SH, Majmundar H. Collimator integrity. J Nucl Cardiol 2006;13:889-91.

4. O'Connor MK. Instrument- and computer-related problems and artifacts in nuclear medicine. Semin Nucl Med 1996;26:256-77.
5. Shih W-J, Wierzbinski B. Cardiac SPECT: 360° circular acquisition may resolve defects of 180° data. J Nucl Med 2003;44:995-6.
6. Liu Y-H, Lam PT, Sinusas AJ, Wackers FJT. Differential effect of 180° and 360° acquisition orbits on the accuracy of SPECT imaging: quantitative evaluation in phantoms. J Nucl Med 2002;43:1115-24.
7. Cao Z, Maunoury C, Chen CC, Holder LE. Comparison of continuous step-and-shoot versus step-and-shoot acquisition SPECT. J Nucl Med 1996;37:2037-40.
8. American College of Radiology Web site. Available from: URL: http://www.acr.org/accreditation/nuclear.aspx. Accessed July 17, 2007.
9. http://www.icanl.com. Accessed October 6, 2006.
10. American Association of Physicists in Medicine SPECT Task Group. Rotating scintillation camera SPECT acceptance testing and quality control. AAPM Report No. 22. New York: American Association of Physicists in Medicine; 1987.
11. American College of Radiology Web site. Available from: URL: http://www.acr.org/SecondaryMainMenuCategories/quality_safety/guidelines/nuc_med/radiopharmaceuticals.aspx. Accessed November 5, 2007.
12. Intersocietal Commission for the Accreditation of Nuclear Medicine Laboratories Web site. Available from: URL: http://www.icanl.org/icanl/pdfs/2007ICANLStandards.pdf. Accessed November 5, 2007.
13. Nichols KJ, Galt JR. Quality control for SPECT imaging. In: DePuey EG, Berman DS, Garcia EV, editors. Cardiac SPECT imaging. 2nd ed. Philadelphia: Lippincott Williams & Wilkins; 2001. p. 17-40.
14. National Electrical Manufacturers Association. NEMA standards publication NU 1-1994: performance measurements of scintillation cameras. Washington, DC: National Electrical Manufacturers Association; 1994.
15. Esser PD, Graham LS. A quality control program for nuclear medicine cameras. In: Henkin RE, et al. Nuclear medicine. 2nd ed. Philadelphia: Mosby; 2006. p. 246-56.
16. DePuey EG. How to detect and avoid myocardial perfusion SPECT artifacts. J Nucl Med 1994;35:699-702.
17. Galt JR, Faber T. Principles of single photon emission computed tomography (SPECT) imaging. In: Christian PE, Bernier DR, Langan JK, editors. Nuclear medicine and PET: technology and techniques. St Louis: Mosby; 2003. p. 242-84.
18. Cerqueira MD, Matsuoka D, Ritchie JL, Harp GD. The influence of collimators on SPECT center of rotation measurements: artifact generation and acceptance testing. J Nucl Med 1988;29:1393-7.
19. Hines H, Kayayan R, Colsher J, Hashimoto D, Shubert R, Fernando J, et al. National Electrical Manufacturers Association recommendation for implementing SPECT instrumentation quality control. J Nucl Med 2000;41:383-9.
20. Greer KL, Jaszczak RJ, Coleman RE. An overview of a camera-based SPECT system. Med Phys 1982;9:455-63.
21. Goetze S, Wahl RL. Prevalence of misregistration between SPECT and CT for attenuation-corrected myocardial perfusion SPECT. J Nucl Cardiol 2007;14:200-6.
22. Tonge CM, Manoharan M, Lawson RS, Shields RA, Prescott MC. Attenuation correction of myocardial SPECT studies using low resolution computed tomography images. Nucl Med Commun 2005;26:231-7.
23. Fricke H, Fricke E, Weise R, Kammeier A, Lindner O, Burchert W. A method to remove artifacts in attenuation-corrected myocardial perfusion SPECT introduced by misalignment between emission scan and CT-derived attenuation maps. J Nucl Med 2004;45:1619-25.
24. National Electrical Manufacturers Association. NEMA standards publication NU 2-2001: performance measurements of positron emission tomographs. Washington, DC: National Electrical Manufacturers Association; 2001.
25. National Electrical Manufacturers Association. NEMA standards publication NU 2-1994: performance measurements of positron emission tomographs. Washington, DC: National Electrical Manufacturers Association; 1994.
26. Daube-Witherspoon ME, Karp JS, Casey ME, DiFilippo FP, Hines H, Muehllehner G, et al. PET performance measurements using the NEMA NU 2-2001 standard. J Nucl Med 2002;43:1398-409.
27. Radionuclide imaging devices—characteristics and test conditions. Part 1: positron emission tomographs. Geneva: International Electrotechnical Commission; 1998.
28. Le Meunier L, Maass-Moreno R, Carrasquillo JA, Dieckmann W, Bacharach SL. PET/CT imaging: effect of respiratory motion on apparent myocardial uptake. J Nucl Cardiol 2006;13:821-30.
29. Gould KL, Pan T, Loughin C, Johnson NP, Guha A, Sdringola S. Frequent diagnostic errors in cardiac PET/CT due to misregistration of CT attenuation and emission PET images: a definitive analysis of causes, consequences and corrections. J Nucl Med 2007;48:1112-21.
30. DePuey EG. Artifact is SPECT myocardial perfusion imaging. In: DePuey EG, Berman DS, Garcia EV, editors. Cardiac SPECT imaging. 2nd ed. Philadelphia: Lippincott Williams & Wilkins; 2001. p. 231-62.
31. National Electrical Manufacturers Association. The DICOM standard. Available from: URL: http://medical.nema.org/dicom/2004.html. Accessed October 6, 2006.
32. Nichols K, Yao SS, Kamran M, Faber TL, Cooke CD, DePuey EG. Clinical impact of arrhythmias on gated SPECT cardiac myocardial perfusion and function assessment. J Nucl Cardiol 2001;8:19-30.

ASNC IMAGING GUIDELINES FOR NUCLEAR CARDIOLOGY PROCEDURES

First-pass radionuclide angiography

John D. Friedman, MD, Chair,[a] Daniel S. Berman, MD,[a] Salvador Borges-Neto, MD,[b] Sean W. Hayes, MD,[a] Lynne L. Johnson, MD,[c] Kenneth J. Nichols, PhD,[d] Robert A. Pagnanelli, CNMT, RT(R)(T), NCT,[b] and Steven C. Port, MD[e]

ACQUISITION PARAMETERS

Purpose. To assess left ventricular (LV) and right ventricular (RV) function at rest or during stress (evaluation of wall motion, ejection fraction [EF], and other systolic and diastolic parameters). To assess and measure left-to-right shunts (Table 1).

ACQUISITION PROTOCOLS

First-Pass Radionuclide Angiography-LV Function

1. Technetium 99m diethylamine triamine pentaacetic acid (DTPA) is the radionuclide of choice for standard first-pass radionuclide angiography (FPRNA) because of its renal excretion, minimizing patient radiation exposure. Tc-99m pertechnetate may also be used. Other technetium-based compounds, such as the technetium perfusion agents: sestamibi and tetrofosmin, are suitable. The short-lived radionuclides gold 195m and iridium 191m have been used for FPRNA but are not currently approved by the U.S. Food and Drug Administration.
2. The standard dose given is 25 mCi for both rest and exercise studies. A dose as low as 10 mCi may be used as an option in rest studies for multicrystal cameras. Since the study is count dependent and the single crystal cameras have limited count rate capabilities, doses of 20 to 25 mCi are typically recommended. When predicated by dosimetry considerations, lower doses may have to be used. Doses as low as 10 mCi may be used with reasonable clinical success but run the risk of inadequate count rates, especially for wall motion analysis. A rule that should be applied to test if enough counts have been acquired for a diagnostic clinical study is that the end-diastolic frame of the representative cycle should have more than 2500 counts in the LV region of interest (ROI).
3. Because of bolus prolongation and fractionation, no peripheral sites other than the antecubital (preferably medial) and external jugular veins are suitable for FPRNA. The study should not be attempted if those sites are not available.
4. Some users prefer larger-bore cannulae in the 14- to 16-gage range, but they are optional and not highly recommended because of the increased trauma. The cannula should be directly connected to a suitable length of intravenous tubing, preferably 12 to 20 inches. The free end of the tubing should be attached to a three-way stopcock with a sufficiently large bore to accommodate rapid injections. All intravenous connections should be lock-type rather than slip, to avoid contamination. A 10- to 20-mL saline bolus is used to flush the radionuclide bolus into the venous system. The saline bolus should be injected at a continuous, uninterrupted rate so that the entire 10 to 20 mL is injected in 2 to 3 seconds.
5. The injection for LV studies must be rapid. The full width at half maximum (FWHM) of the bolus transit in the superior vena cava should be less than 1 second and, if possible, less than 0.5 second. That will virtually guarantee a technically adequate study, all other variables being equal.
6. The most common position used is the upright, straight anterior view. Its advantages are the ease with which the chest may be stabilized against the detector and the straightforward approach to positioning the patient so that the left ventricle will be in the field of view (FOV). A transmission source or an initial injection of a 1-mCi tracer dose is recommended to ensure proper positioning. The

From the Cedars-Sinai Medical Center,[a] Los Angeles, CA; Duke University Medical Center,[b] Durham, NC; Columbia University,[c] New York, NY; Long Island Jewish Medical Center,[d] Long Island, NY; Cardiovascular Associates, Ltd.,[e] Milwaukee, WI.

Approved by the American Society of Nuclear Cardiology Board of Directors. Last updated on January 15, 2009.

Unless reaffirmed, retired or amended by express action of the Board of Directors of the American Society of Nuclear Cardiology, this guideline shall expire as of March 2014.

Reprint requests: John D. Friedman, MD, Chair, Cedars-Sinai Medical Center, Los Angeles, CA.

1071-3581/$34.00

doi:10.1007/s12350-009-9061-5

Table 1. Acquisition parameters

	Rest	Exercise		For information, see paragraph
A. Radiopharmaceutical dose	Tc-99m	Tc-99m	Standard	1, 2, 13, 19
1. Multicrystal (LV and RV)	10–25 mCi	25 mCi	Standard	
2. Single crystal (LV and RV)	20–25 mCi/0.3–0.5 mL	20–25 mCi/0.3–0.5 mL	Standard	
3. Shunt	10–15 mCi/0.3–0.5 mL		Standard	
B. Injection site				3, 14
1. RV function	Antecubital vein	Antecubital vein	Standard	
	External jugular	External jugular	Optional	
2. LV function	Antecubital vein	Antecubital vein	Standard	
	External jugular	External jugular	Optional	
3. Shunt	Antecubital vein		Preferred	
	External jugular		Optional	
C. Intravenous cannula	18-gauge arm	18-gauge arm	Standard	4
	14-, 16-, or 20-gauge neck	14-, 16-, or 20-gauge neck	Optional	
D. Injection rate				5, 15, 16, 20
1. RV function	Slow (FWHM 2–3 s)	Slow (FWHM 2–3 s)	Preferred	
2. LV function	Rapid (FWHM <1 s)	Rapid (FWHM <1 s)	Standard	
3. Shunt	Rapid (FWHM <1 s)		Standard	
E. Position				6, 17, 21
1. RV function	Upright	Upright	Standard	
	Supine	Supine	Optional	
	20°–30° RAO	20°–30° RAO	Preferred	
	Anterior	Anterior	Optional	
2. LV function	Upright	Upright	Preferred	
	Supine	Supine	Optional	
	Anterior	Anterior	Standard	
	RAO	RAO	Optional	
3. Shunt	Anterior		Standard	
F. ECG signal				7, 22
1. RV and LV function	Multicrystal no	Multicrystal no	Standard	
	Single crystal yes	Single crystal yes	Standard	
2. Shunt	No		Standard	
G. Energy window frame time	120–160 keV	120–160 keV	Standard	8, 9, 23
1. LV and RV function	25 ms	25 ms	Standard	
	50 ms	50 ms	Optional	

Table 1. continued

	Rest	Exercise		For information, see paragraph
2. Shunt	50 ms		Standard	
	100 ms		Optional	
H. Total frames				10, 24
1. LV and RV function	2000	1500–2000	Standard	
2. Shunt	2000		Standard	
I. Matrix: Multicrystal				11, 25
1. RV and LV function	20 × 20	20 × 20	Standard	
	14 × 20	14 × 20	Optional	
2. Shunt	20 × 20 or 14 × 20		Standard	
J. Matrix: Single crystal				11, 25
1. RV function	64 × 64	64 × 64	Preferred	
	32 × 32	32 × 32	Optional	
2. LV function	32 × 32	32 × 32	Preferred	
	64 × 64	64 × 64	Optional	
3. Shunt	32 × 32 or 64 × 64		Standard	
K. Collimator: Single crystal				12, 18, 26
1. LV and RV function and shunt	High sensitivity	High sensitivity	Standard	
2. LV function	Ultrahigh sensitivity	Ultrahigh sensitivity	Preferred	
3. RV function	Ultrahigh sensitivity	Ultrahigh sensitivity	Optional	
4. Shunt	Diverging		Optional	
L. Collimator: Multicrystal				12, 18, 26
1. (SIM 400) (RV, LV, and shunt)	18 mm	18 mm	Standard	
	13 mm to 10 mCi	13 mm to 10 mCi	Optional	
	27 mm to 25 mCi	27 mm to 25 mCi	Optional	
System 77	1 inch	1 inch	Standard	

chief disadvantage of the anterior view is the anatomic overlap that may occur with the descending aorta and the basal portion of the inferoseptal wall and with the left atrium and the basal portion of the left ventricle. The shallow right anterior oblique (RAO) view helps eliminate both of those sources of overlap but is more difficult to standardize. A foam cushion cut at a 30° angle may be used for such positioning. The choice of upright versus supine positioning depends, to some degree, on the clinical situation. The upright position is, in general, preferred. Pulmonary background is reduced in the upright position, which enhances study quality. Positioning of the patient during treadmill exercise is a critical issue since the FOV of the detectors is small. It is suggested that a person should be behind the patient during peak stress for proper positioning of the chest in relation to the detector. This is of crucial importance so that the heart will be within the FOV during acquisition. A point source should also be placed in such a manner (left border of the sternum) that counts from the point source will be acquired during injection of the Tc-99m tracer. It is important to emphasize that for accurate studies of first pass during treadmill exercise, the heart, lung, and point source should all be in the FOV throughout the entire acquisition.

7. In high count rate studies, as are typically acquired with the multicrystal camera, there are enough counts at end diastole and end systole to reliably identify the end-diastolic and end-systolic frames without the aid of an electrocardiographic (ECG) signal. However, for single-crystal gamma cameras, count rates during the LV phase may occasionally be inadequate for reliable identification of the end-diastolic frames. Acquisition of an ECG signal is therefore highly recommended to facilitate data processing. In particular, data acquisition in gated list mode enables bad beat rejection after data has been collected, and enables reformatting images as 32×32 matrices in the event that unusually low counts are obtained. Single-crystal cameras vary widely in their count rate capabilities and thus in how appropriate they are for imaging a first-pass cardiac study. Several state-of-the-art gamma cameras can count at least 150,000 counts per second at a 20% loss of total counts. Use of cameras with lower count rate capabilities could lead to clinically significant inaccuracies in the determination of LVEF and particularly in the assessment of wall motion.
8. The 140-keV photopeak of Tc-99m ± 15% (140 ± 21 keV) is fairly standard and results in adequate count rates. This corresponds very closely to the 120- to 160-keV window used. The window may be widened to ±30% for low-dose injections.
9. Theoretically, the frame time should be varied to suit the heart rate at the time of acquisition. The relationship is fairly linear, with 50 milliseconds being quite adequate at heart rates of less than 80 beats/min and 25 milliseconds for heart rates of 125 to 175 beats/min. At very high heart rates, 10- to 20-millisecond frame times should be considered, especially if diastolic function is of interest. In practice, to avoid the potential errors that might occur if the frame time was constantly being manipulated, a standard of 25 milliseconds per frame is recommended for all acquisitions.
10. Fifteen hundred to 2000 frames should be sufficient, provided that these frames encompass the bolus injection and capture the entire LV phase of bolus transit.
11. The matrix size of the multicrystal camera is fixed due to the inherent design of the systems. However, for single-crystal cameras, the matrix size will largely depend on the computer system being used since most vendors do not offer many, if any, choices for dynamic studies. Most systems that have first-pass software support 64×64 acquisitions. Some systems also support 32×32 matrices. The latter is preferable because count density per pixel is maximized. The 64×64 matrix works reasonably well when count rates are high, but when counts are suboptimal or when the LVEF is high, there is a tendency for the end-systolic frame to have insufficient counts per pixel for assessment of regional wall motion. The actual minimum number of counts per frame needed varies depending on the number of frames per cardiac cycle, the actual LVEF, the amount of background radiation, and whether the study is performed to measure LVEF alone or in conjunction with an assessment of wall motion.
12. The choice of collimators depends on the objectives of the study and the dose to be injected. For standard rest and exercise studies using 20- to 25-mCi doses, the 18-mm-thick collimator provides a good compromise between sensitivity and spatial resolution for multicrystal cameras. A thinner collimator sacrifices spatial resolution but may be necessary for lower dose injections. For single-crystal cameras, most vendors offer high-sensitivity collimators and some offer ultrahigh-sensitivity collimators. It is helpful to categorize the collimators quantitatively in counts per mCi per minute because one vendor's high-sensitivity collimator may be equivalent to another vendor's ultrahigh-sensitivity collimator. For the purposes of first-pass

studies, a high-sensitivity collimator should provide approximately 12,000 to 24,000 counts $\cdot s^{-1} \cdot mCi^{-1}$. This number may vary significantly depending on crystal thickness and dead time of the system. For large (L)FOV systems, it may be desirable to shield part of the peripheral FOV to reduce unwanted pulse pileup, which increases the dead time of the system.

FPRNA-RV Function

13. Since the injection bolus reaches the right ventricle without significant dispersion, lower doses may be adequate; 10- to 25-mCi doses are acceptable. Of note, tricuspid regurgitation will fragment and disperse the radiotracer bolus and prolong RV transit time, often rendering FPRNA evaluation of both the left and right ventricles inadequate and invalid.
14. The use of the antecubital vein is appropriate for RV studies. The external jugular vein may be used but, unlike the LV study, it may result in too rapid an appearance and disappearance of the radionuclide from the chamber.
15. A 10- to 20-mL saline bolus is generally used to flush the radionuclide bolus into the venous system. The saline bolus should be injected at a continuous, uninterrupted rate so that the entire 10 to 20 mL is injected in 3 to 4 seconds.
16. To optimize assessment of RV function, the FWHM of the bolus in the superior vena cava should be 2 to 3 seconds, much slower than that for an LV study. The slower bolus increases the number of beats available for analysis. For assessment of biventricular function, a bolus with an FWHM of 1 to 2 seconds in the superior vena cava may be used as a compromise, realizing that assessment of neither ventricle is optimized.
17. A shallow (20° to 30°) RAO view is recommended to enhance right atrial–RV separation, which is the chief advantage of FPRNA over gated equilibrium radionuclide angiography for the measurement of RVEF.
18. As for LV function studies, the choice of collimators depends on the objectives of the study and the dose to be injected. For standard rest and exercise studies using 10- to 25-mCi doses, the 18-mm collimator from multicrystal cameras provides a good compromise between sensitivity and spatial resolution. A thinner collimator sacrifices spatial resolution but may be necessary for lower dose injections. For single-crystal cameras, the high-sensitivity collimator is the standard.

FPRNA-Shunt Study

19. A 10- to 15-mCi dose of the Tc-99m radiopharmaceutical is typically used.
20. The injection should be rapid for shunt studies. The premise of the shunt study is that the appearance in and clearance of the radionuclide bolus from the pulmonary circulation are monoexponential in character. Absent a shunt, the bolus should be a quite narrow, simple curve. A delayed bolus may result in a pulmonary curve that deviates enough from a monoexponential curve as to make the data uninterpretable. A 10- to 20-mL saline bolus is generally used to flush the radionuclide bolus into the venous system. The saline bolus should be injected at a continuous, uninterrupted rate so that the entire 10 to 20 mL is injected in 2 to 3 seconds.
21. Acquisition in the anterior view is best for imaging the lung fields, which are the areas of interest for the shunt study. If both lung fields cannot be visualized due to the detector size, the lung field of interest should be the right lung for suspected intracardiac shunts and the left lung for a suspected patent ductus arteriosus (PDA).
22. Since only pulmonary data will be quantified, an ECG signal is unnecessary.
23. Frame time is not crucial in a shunt study since the data will ultimately be analyzed using curves whose data points do not require more than 100 milliseconds' temporal resolution. Shorter frame times may be used since they may be added together during the analysis.
24. Total frames acquired should be 2000.
25. For multicrystal systems, the matrix is not an option. For single-crystal systems, a 64×64 matrix is appropriate. A 32×32 matrix may also be used to encompass both lungs in the FOV.
26. Spatial resolution is much less important in the shunt study than in studies performed to evaluate EF and wall motion. Standard high-sensitivity collimators are adequate. If available, a diverging collimator may be used.

PROCESSING PROTOCOLS

Measurement of Ventricular Function

Processing first-pass data has become increasingly automated and considerably faster than in previous years. However, it is unlikely that processing of first-pass data can ever be reliably, totally automated. There are too many variations possible in tracer transit due to

technical and/or pathophysiologic reasons for automated processing to be successful in all cases. The operator must be observant and careful at a few crucial steps in the processing to ensure consistently accurate results.

Preprocessing

Preprocessing of first-pass data is frequently performed, although it is not mandatory. Time smoothing, uniformity correction, and dead-time correction are options that are typically applied when supported by the software.

Processing

First-pass data processing can be divided into four major routines: creation of the initial time–activity curve (TAC), beat selection, and creation of the initial representative cycle, background correction, and creation of the final representative cycle. A fifth optional routine is that of motion correction.

The Initial TAC

Grouping or reformatting. The raw or preprocessed data should be grouped into 0.5- to 1.0-second images to facilitate drawing an ROI around the ventricle. If an ECG signal has been acquired, the raw or preprocessed data may be cyclically added using the R wave to identify end-diastolic frames, thus creating a preliminary representative cycle. The end-diastolic frame of that preliminary representative cycle may then be used to draw an initial ventricular ROI.

Ventricular ROI. The operator or the computer should draw an initial ventricular ROI. This ROI need not be highly accurate since it is only used for generating the initial TAC. A TAC of the raw or preprocessed data using the initial ROI should be displayed using the acquisition frame time.

Beat selection. Most first-pass software allows the operator to identify the first and last beats to be included in the representative cycle. End-diastolic and end-systolic frames may be identified automatically by the computer, but the operator must have the opportunity to override the computer to select only appropriate beats. Because of variable mixing in the chamber, it is advisable to select beats both before and after the beat with the maximum counts. Beats whose end-diastolic counts are below 50% of the maximum end-diastolic count should be excluded as long as this editing does not preclude a statistically adequate representative cycle. Premature ventricular beats and post-premature ventricular contraction (PVC) beats should be excluded. If there are few sinus beats, it may be difficult to generate a statistically adequate representative cycle.

Beat editing is an optional routine in which individual beats of varying duration may be time-corrected so that the final beat lengths are all identical. These algorithms are aided by the display of the actual R-wave trigger information shown superimposed on the transit curves. That approach typically involves an interpolation of the data, but actual end-systolic counts should always be preserved so that the EF is not altered by the time correction.

Background correction. Several approaches to background correction have been proposed. They include the lung frame method, the count threshold method, and the periventricular method. The lung method has been shown to give better results than the other two and is thus the preferred method. The periventricular background region is used as a standard in many single-crystal camera systems.

Lung frame method. In this approach, a frame of data just before the appearance of activity in the LV ROI is chosen as representative of the distribution of the background (nonventricular activity). This is a crucial step since variation in the background frame can substantially alter the calculated EF, volumes, and apparent wall motion. The selected frame should be visualized. That background ''mask,'' after appropriate normalization, is subtracted from the LV representative cycle. A washout factor must be applied to the background since the counts in the background are decreasing throughout the LV phase. This approach has been shown to produce results that compare favorably with contrast angiographic data and is somewhat better than either of the other two approaches.

Count threshold method. A frame of data just before the appearance of the radionuclide in the left ventricle is identified, and the counts in that frame become the new zero level for each subsequent frame of the LV phase.

Periventricular method. This method is quite analogous to the periventricular background method in gated equilibrium imaging. A horseshoe-shaped background ROI is drawn around the ventricle, usually 2 to 3 pixels wide and 1 to 2 pixels away from the LV border.

The final ROI. Once the background correction has been applied to the initial representative cycle, the end-diastolic and end-systolic frames should be displayed again and any necessary modifications of the initial ROI then performed.

Dual-ROI method. For first-pass studies acquired in the anterior view, a separate ROI for the end-diastolic and end-systolic frames is recommended. The operator must manually draw the final ROI on both frames. In drawing the end-systolic ROI, left atrial activity must be

excluded from the end-systolic counts. The LVEF calculated with the dual-ROI approach tends to be higher than that calculated with a single ROI because the valve plane is placed lower during systole compared to diastole.

Single-ROI method. With the single-ROI method, only an end-diastolic ROI is used. This approach works fairly well with studies acquired in the RAO projection, where there is better left atrial–LV separation. In the anterior view, the single-ROI method may result in spuriously low EFs because it can potentially include extra ventricular counts in the end-systolic ROI.

Motion correction. Motion correction of first-pass data is occasionally necessary for studies acquired during bicycle exercise and almost always necessary for studies acquired during treadmill exercise. Motion correction may be performed using either or both of two methods, the ''single-isotope'' method (internal correction method) or ''dual-isotope'' method (external marker correction). The dual-isotope method is preferred for treadmill exercise, while the single-isotope method is usually adequate for bicycle exercise.

Single-isotope motion correction. The position of the ventricle is determined in each frame of the representative cycle by applying a center-of-mass algorithm within an operator-defined ROI. The latter should greatly exceed the actual size of the ventricle. By calculating the average x, y location of the center of mass, the location of the ventricle $x_n y_n$ in any frame may be reregistered to x, y.

Dual-isotope motion correction. An external point source (americium 241, iodine 125) is applied to the chest, usually midsternally or just to the right of the sternum. A dual-energy acquisition is performed at peak exercise such that two first-pass studies are acquired, one using the external marker's photopeak and the other using the standard Tc-99m photopeak. After acquisition, the position of the marker is determined in each frame using a center-of-mass algorithm. The average x, y location of the marker is taken to represent the correct position of the marker had there been no motion. All data frames are then reregistered by the direction and magnitude of the displacement of the marker in that frame.

The final representative cycle. The finalized ROIs are then used to regenerate the TAC and the final representative cycle is created from that curve using the previously determined beat selection. It is this representative cycle that will be used to generate all the quantitative results describing ventricular function.

FPRNA: Quantitation of Results

LVEF. The LVEF is calculated from the final background-corrected representative cycle as follows: (End-diastolic counts End-systolic counts)/End-diastolic counts. On occasion, it is impossible to correct accurately for background activity (very delayed bolus, markedly prolonged RV tracer transit, and so on). In that case, it is appropriate to report an estimated LVEF or LVEF range based on the uncorrected data.

Systolic emptying rates. Systolic emptying rates such as the peak ejection rate may be calculated by applying a Fourier filter (third- to fifth-order harmonic) to the LV representative cycle curve and then taking the first derivative of that filtered curve. The peak ejection rate should be expressed in end-diastolic volumes per second.

Diastolic filling rates. Diastolic filling rates such as the peak filling rate may be calculated by applying a Fourier filter (third- to fifth-order harmonic) to the LV representative cycle curve and then taking the first derivative of that filtered curve. The peak filling rate should be expressed in end-diastolic volumes per second. The time-to-peak filling rate may be calculated and expressed in milliseconds.

Ventricular volumes. LV end-diastolic volume may be measured using either a geometric or count-proportional technique. In the geometric approach, the end-diastolic frame of the representative cycle is displayed using a threshold for edge detection. The area of the left ventricle is measured using the pixel area and the known size of a pixel. The longest length of the left ventricle is identified by the operator and end-diastolic volume calculated using the modified Sandler and Dodge equation. In the countproportional approach, the required data are the total counts in the left ventricle, the counts in the hottest pixel in the left ventricle, and the area of a pixel (m) in centimeters. The end-diastolic volume is then calculated as $1.38\ m^{3/2}\ R^{3/2}$, where R is total LV counts/counts in the hottest pixel.

Left-to-Right Shunt Study

The input function for the first-pass shunt study is a high-count density TAC obtained from a pulmonary ROI. In practice, either the left lung, the right lung, or both may be used. In most cases, the right lung is preferred because it is easier to create a pulmonary ROI that is free of contamination from the cyclic changes in counts in the left heart and great vessels. Regardless of the acquisition frame time, the pulmonary curve should be displayed at a frame time of approximately 100 to 300 milliseconds. That allows the operator to easily visualize the entire curve for qualitative assessment of the presence or absence of a shunt. Not infrequently, the raw curve requires time smoothing to eliminate high-frequency contamination of the curve from cardiac chamber or great vessel counts or from random noise.

The first frame of the curve should unequivocally represent pulmonary activity rather than any superior vena cava, right atrial, or RV activity because the shape of the early part of the curve will determine the shape of the subsequent mathematical fit. It may be helpful to mask out the superior vena cava and right heart from the image before drawing the pulmonary ROI. Careful attention to the statistical content of the pulmonary curve and its freedom from contamination is crucial. The operator may then apply either a gamma variate or an exponential fit to the raw data. Qualitative assessment of the closeness of the fitted curve to the raw curve is important. Varying the initial frame of the fit and the final frame of the fit may be necessary to produce the best fitted curve possible. The fitted curve may then be subtracted from the raw data to leave the shunt component behind, which can, itself, be fitted with another curve that represents the shunt component. The shunt ratio *Qp*:*Qs* is then calculated as $(A1 + A2)/A1$, where $A1$ is the area under the primary fitted curve and $A2$ is the area under the secondary (shunt) fitted curve.

INTERPRETATION AND REPORTING

General Comments

The interpretation of first-pass data should be performed in a consistent, methodical manner, with particular attention to the quality of the data. Unlike equilibrium radionuclide angiography, in which a quick inspection of the cinematic display of the cardiac cycle is sufficient to reassure the interpreting physician of the adequacy of the data, the first-pass study requires considerably more attention to the details of data acquisition and processing to provide consistently accurate interpretations. The final representative cardiac cycle that is used to generate both the quantitative results and the qualitative wall motion assessment can be affected by many factors, including the adequacy of the injection bolus, the count rate, the number and type of beats chosen for inclusion, the manner in which background activity is determined, and occasionally, patient motion. Even in laboratories with extensive experience and well-defined and well-executed acquisition and processing techniques, unavoidable patient-to-patient variability and different cardiac and pulmonary physiology, as well as some degree of interobserver variability in processing, lead to variability in the end product. The physician must therefore exercise due diligence during interpretation of the results (Table 2).

Certain data must be routinely available so that the interpreting physician may quickly assess the technical adequacy of the data and the accuracy of the processing. Most commercial software routines automatically save enough of the intermediate steps of processing to enable the physician to review quickly the processing either directly on the computer display or by reference to hard copy.

Display

27. The final representative cycle should be displayed in a cinematic, endless loop format. Most authorities use a color display in contrast to the recommended display for equilibrium images. The lower pixel count density and the subtle change from cardiac cavities to background make a color display useful. The cine display is typically time-smoothed during data processing and should not need additional smoothing for display. Spatial smoothing may be used after processing if the data are particularly count-poor, but it should not be necessary for the average study. It is preferable to normalize the image to the peak activity in the ventricle because aortic or left atrial activity may be higher, thus making it more difficult to appreciate the count changes in the ventricles. Cinematic displays of the bolus transit through the heart and great vessels are helpful in analyzing aberrations of tracer transit that may occur in patients with congenital anomalies.
28. Hard-copy displays are essential to study interpretation. TACs representing the bolus and the RV and LV phases of the bolus transit, as well as a final representative cycle time–activity (volume) curve, must be available for proper interpretation. Color hard-copy displays of parametric images may be valuable aides in study interpretation. Such displays should not be used to the exclusion of the cinematic display of the representative cycle.

Quality Control

29. *The bolus*. The adequacy of a bolus may be defined quantitatively by generating a TAC from an ROI that includes the superior vena cava. The FWHM of such a curve should ideally be less than 1 second. As a routine quality check, it is helpful to inspect the TAC of the bolus. Alternatively, one may inspect a sequence of images from the early portion of the study to qualitatively assess the bolus. Serial 1-second images are useful for that purpose. The bolus may be assessed as good (FWHM <1 second), adequate (1 to 1.5 seconds), delayed (>1.5 seconds), or split (more than one discrete peak in the TAC). The split bolus is particularly problematic and may preclude accurate data processing. Identification of a delayed or split bolus alerts the physician to the possibility of oversubtraction of

Table 2. First-pass radionuclide angiography: guideline for interpretation

		For information, see paragraph
A. Display		
1. Cinematic display of representative cycle	Standard	27
a. Time smoothing	Standard	27
b. Spatial smoothing	Optional	27
c. Normalization	Standard	27
2. Hard copy 2		
a. Intermediate processing steps	Standard	28
b. Functional images	Optional	28
c. TACs	Standard	28
B. Quality control		
1. Bolus	Standard	29
2. Count statistics	Standard	30
3. Tracer transit	Standard	31
4. Beat selection	Standard	32
5. Background selection	Standard	33
6. Patient motion	Standard	34
C. Results		
1. Cardiac rhythm and conduction	Standard	35
2. Chamber sizes		
a. Qualitative	Standard	36
b. Quantitative	Preferred	36
3. Regional wall motion		
a. Qualitative	Standard	37
b. Quantitative	Optional	37
4. LVEF	Standard	38
5. RVEF	Optional	38
6. LV diastolic filling		
a. Qualitative	Standard	39
b. Quantitative	Optional	39
D. Exercise/intervention studies		
1. Display	Standard	40
2. Regional wall motion: comparison to rest	Standard	41
3. Chamber sizes: comparison to rest	Standard	42
4. EFs: comparison to rest	Standard	43
E. Conclusion		
1. Comparison to previous studies	Standard	44
2. Correlation with clinical findings	Standard	45

background and the resultant spurious increase in LVEF, decrease in LV volume, and overestimation of regional wall motion.

30. *Count statistics*. The adequacy of the count rate may be assessed by use of either the unprocessed data or the representative cycle. When examining the unprocessed data, the count rate in the whole FOV during the RV phase of the study should optimally be greater than 200,000 cps with a multicrystal system and greater than or equal to 150,000 cps on a single-crystal system. When count rates drop below 100,000 cps, it is highly unlikely that adequate studies will be obtained. Alternatively, and more accurately, the count rate of the representative cycle can be checked. This approach is more accurate because it is the representative cycle that is used to generate all quantitative results, and counts in the representative cycle may be inadequate even when the count rate on the raw data is adequate if there are insufficient beats for analysis or background

over-subtraction. In general, LV end-diastolic counts in the representative cycle should not be less than 2000 cps and should preferably exceed 4000 cps. High-resolution wall motion images will require greater than 5000 cps.

31. *Tracer transit*. The transit of the radionuclide should be inspected in every case. Alterations or anomalies of tracer transit may be detected visually by examining serial static images or by a cinematic display of the bolus transiting the central circulation. For example, asymmetric pulmonary transit time or asymmetric maximal tracer concentration may indicate pulmonary vascular pathology or unilaterally decreased pulmonary volume. A cine display may be particularly helpful when the transit seems anomalous. The most common disturbance of tracer transit is prolongation of the transit time through either or both ventricles. Recognition of a prolonged transit time is important because of the potential diagnostic implications and because of the impact on background correction, which in turn affects EF, volumes, and wall motion. Physiologic causes of prolonged tracer transit include valvular insufficiency, severely depressed ventricular function, atrial fibrillation, and a left-to-right shunt. Combining image information such as an enlarged left atrial appendage (see below) and a prolonged tracer transit through the left ventricle suggests mitral valve disease, whereas prolonged LV tracer transit and an enlarged ascending aorta suggest aortic valve disease.
32. *Beat selection*. A hard copy of the TAC should be generated during processing so that one may confirm that the appropriate beats have been selected for inclusion in the representative cycle. Unless the number of beats is very limited, one should preferably select beats whose end-diastolic counts are 70% of the peak end-diastolic counts or greater.
33. *Background selection*. The same curve used to confirm appropriate beat selection may be used to confirm that an appropriate frame was chosen for background correction. A frame as close to the beginning of the LV phase but not including LV activity is desired. Viewing the background frame image is helpful in determining that LV activity is not included and in visualizing any residual activity in the right ventricle that could result in over-subtraction of background. On occasion, the lung frame method of background correction may not be accurate because of poor RV–LV temporal separation. In that case, the physician should demand that a representative cycle be created that has not been subjected to background correction. The uncorrected representative cycle is always generated during the processing but may not be stored. Viewing this image in cine loop format after manually subtracting the background will allow an adequate assessment of regional wall motion.
34. *Patient motion*. Motion of the patient is rarely, if ever, a problem on a resting study. However, motion of the chest during acquisition of an exercise study is seen frequently during treadmill exercise and occasionally during bicycle exercise. Motion should be suspected when typical distortions of the LV TAC are noted and should be confirmed by viewing a cine display of the bolus traveling through the chambers. During treadmill exercise, chest wall motion may be corrected with the use of an external point source. The integrity of the point source, and especially its appearance in each frame of the study, should be confirmed.

Results (Table 3)

35. *Cardiac rhythm and conduction*. Interpretation of the data may be influenced by the rhythm during the acquisition. For example, frequent PVCs, ventricular bigeminy, or very irregular atrial fibrillation may affect the EF or regional wall motion. In the setting of ventricular bigeminy, for example, no true sinus beat EF can be determined. The diagnostic and prognostic significance of post-PVC beats is not completely understood. With atrial fibrillation, the representative cycle may consist of beats with widely varying R–R intervals and, hence, with different volumes and EFs. Pacemaker rhythm confers its own unique contraction sequence, which starts at the apex and proceeds to the base. The latter can be recognized from the cinematic display of the representative cycle. A phase image may be helpful in recognition of this pattern.

    Both regional wall motion and LVEF are typically altered by left bundle branch block. Because most first-pass studies are acquired in the RAO or anterior projections, paradoxical septal motion cannot be detected; however, one may see what appear to be inferoapical or anteroapical wall motion abnormalities. A phase image may aid in recognizing this phenomenon, although it is usually apparent on the cinematic display of the representative cycle. Right bundle branch block does not affect the LV contraction pattern.
36. *Chamber sizes*. Because the overwhelming majority of first-pass studies are performed to evaluate the left ventricle, the final representative cycle will show the left ventricle, the left atrium (in particular its appendage), and the ascending aorta. Most of the

Table 3. First-pass radionuclide angiography: guideline for reporting

		For information, see paragraph
A. Demographics		
1. Name	Standard	
2. Gender	Standard	
3. Age	Standard	
4. Date(s) of acquisition(s)	Standard	
5. Medical record identifier (inpatient)	Standard	
6. Height/weight (taking into account BSA)	Standard	
B. Acquisition parameters		
1. Type(s) of acquisition(s) (rest/exercise/intervention)	Standard	
2. Radionuclide and doses	Standard	45
3. Injection site	Standard	45
4. Indication for study	Standard	48
5. Study quality	Standard	47
C. Results: Hemodynamic and exercise/intervention variables		
1. Rest HR and BP, cardiac rhythm	Standard	46
2. Exercise HR and BP, %MPHR, METS	Standard	46
3. Exercise symptoms, reason for stopping	Standard	46
4. Exercise ECG changes/arrhythmia	Standard	46
D. Results: Resting RNA data		
1. Chamber sizes		
a. Qualitative	Optional	36
b. Quantitative	Standard	36
2. Regional wall motion		
a. Qualitative	Standard	37
b. Quantitative	Optional	37
3. EFs	Standard	38
4. Abnormalities of tracer transit	Standard	31
E. Results: Exercise/intervention RNA data		
1. LV size: Change from rest		
a. Qualitative	Standard	42
b. Quantitative	Preferred	42
2. LV regional wall motion: Change from rest	Standard	41
3. LVEF: Change from rest	Standard	43
4. RVEF: Change from rest	Optional	43
5. Abnormalities of tracer transit	Standard	44
F. Conclusion		
1. Normal/abnormal	Standard	48
(definite, probable, equivocal)	Optional	48
2. Assessment of severity of findings	Standard	48
(diagnostic/prognostic)		48
3. Relationship to perfusion data if acquired	Optional	48
4. Comparison to previous studies	Standard	49

BSA, Body surface area; *HR*, heart rate; *BP*, blood pressure; *%MPHR*, maximum predicted heart rate; *METs*, metabolic equivalents; *RNA*, radionuclide angiography.

left atrium is overlapped with the ascending aorta, and its size is difficult to assess. However, when the left atrium is very dilated, its appendage is quite prominent in the anterior view, and the aortic root will appear to be dilated. Judging the size of the left ventricle qualitatively is more difficult on a first-pass study than on an equilibrium study because one does not have all the surrounding

chambers and great vessels in the same image as references. With enough experience, moderate to severe degrees of LV chamber enlargement can be appreciated. Right atrial, RV, and pulmonary arterial sizes can be evaluated on cinematic display or on serial static 0.5- to 1.0-second images from the raw data but are not particularly reliable.

Actual measurement of LV volume may be performed with either geometric or count-based approaches and offers a more consistent and accurate assessment of chamber size. Normal values for the left ventricle should be established for each laboratory because they will vary depending on the type of processing used, especially the type of background correction and the patient's position during the acquisition (i.e., supine, semisupine, or upright).

37. *Regional wall motion*. The cinematic display of the representative cycle should be viewed and regional wall motion assessed qualitatively by use of the conventional terms of hypokinesis, akinesis, and dyskinesis. For hypokinesis, the qualifiers of mild, moderate, and severe are useful for communicating the severity of the abnormality. In addition, the extent and location of the abnormality should also be reported, such as the basal (proximal) half or the apical (distal) quarter of the anterior wall. An aneurysm should be identified when an akinetic or dyskinetic segment can be clearly and discretely distinguished from the adjacent contractile myocardium. When available, previous studies should be compared by use of side-by-side cine analysis. Standardized nomenclature for the myocardial segments visualized in the typical FPRNA study (i.e., acquired in the anterior view) is shown in Figure 1. If biplane FPRNA is performed, segmental analysis may also be applied to the left anterior oblique projection. It is recommended that the visualized segments be designated as the basal anterolateral, mid anterolateral, apical, mid inferoseptal, and basal inferoseptal segments. For a left anterior oblique acquisition, the visualized segments include the septal, inferoseptal, inferoapical, inferolateral, and lateral segments.

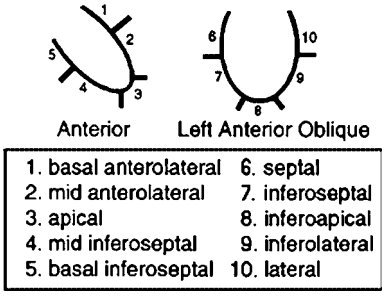

Figure 1. FPRNA segmentation.

Even though the final representative cycle is corrected for background, it may be necessary to display the cine with the lower level raised to 10% to 20% depending on the signal-to-noise ratio in the study. Any one of the number of color schemes may be used to view the cine. Whether one is more representative of actual wall motion than another is speculative. The operator should choose the scheme that works best clinically, but one should avoid color tables that condense all the three-dimensional information into a few colors that make the image appear two-dimensional, as if all the information were in the moving edges.

Many parametric images are available to the interpreting physician that may be used to reinforce one's subjective opinion. Occasionally, an abnormality will be evident on a parametric image that is not obvious on the cinematic display, especially when the regional dysfunction is occurring in a plane that is perpendicular to the detector. The parametric images may be thought of as an independent, unbiased observer similar to the way in which quantitative displays of perfusion images are used. They are also useful as quantitative measures of regional dysfunction. For example, one physician's impression of moderate hypokinesis may be different than another physician's, but a regional EF of 28% is clear to anyone receiving the information. The most commonly used images are the regional EF image, the stroke volume image, and the amplitude and phase images. The latter three may be used in processing, as well as in interpretation. One must keep in mind that the accuracy of the parametric image is highly dependent on the statistics in the image and may be influenced by translational movement of the heart; therefore, the parametric image should not be used to the exclusion of the representative cycle cine because the latter gives the operator the best visual feedback on the statistical quality of the data. Very little literature is available to document the accuracy of parametric images for diagnosis.

38. *LVEF and RVEF*. The LVEF is calculated from the background-corrected end-diastolic and end-systolic counts in either ventricle. Published ranges for a normal EF vary, but most laboratories accept a range of 50% to 80% for the left ventricle. The variability of the LVEF has been reported to be ±4% at rest for the same individual studied on different days. It is very important when interpreting the LVEF, and most especially when interpreting changes in LVEF

from one study to another, to keep in mind that the LVEF is not a fixed number for any patient. It will vary with the heart rate, the blood pressure, the level of circulating catecholamines, position (upright vs supine), and medications. When there are an adequate number of beats to choose for the EF calculation, it is preferable to select those beats whose end-diastolic counts are 70% of the peak end-diastolic counts or greater. The normal values for the RVEF vary with the type of processing used. With the use of separate end-diastolic and end-systolic ROIs, the lower limit of normal can be expected to be 40%, ranging up to 65%.

39. Diastolic filling of the left ventricle may be assessed by qualitative inspection of the TAC (volume curve) of the LV representative cycle. Obviously, decreased early rapid filling, a prolonged time to peak filling, and an increase in the atrial contribution to filling may be recognized by visual inspection of the LV volume curve. The quantitative values for peak early filling and the time to peak filling should be expressed in end-diastolic volumes per second and in milliseconds, respectively. The atrial contribution to filling may be expressed as a ratio of the atrial to early peak filling or vice versa. The atrium typically contributes 15% to 25% of total LV filling. The interpreting physician should not accept any diastolic values without confirmation by visual inspection of the LV volume curve.

    It is difficult to evaluate diastolic filling during exercise because the increase in heart rate usually results in a loss of the transition between early peak filling and atrial filling. At best, one can measure peak diastolic filling, but without the requisite temporal sampling necessary for high heart rates (i.e., 10 to 20 ms/frame), any measured values may not be reliable. Some investigators have used filling fractions (i.e., the fraction of filling achieved during the first third or first half of diastole). It is not clear that such values offer any advantage over the conventional values, and they are certainly a departure from the values typically measured in gated equilibrium studies.

Exercise/Intervention Studies

40. The representative cycles of both resting and exercise or pharmacologic intervention studies should be viewed in a split-screen cinematic display. Each study should be normalized to itself.
41. Regional wall motion of an exercise or intervention study should be compared visually with regional wall motion of the resting study by use of standard qualitative or semiquantitative terms (see paragraph 11). During exercise or during administration of inotropic or afterload-reducing agents, regional wall motion is expected to increase. Regional wall motion may decrease during ischemia, during protocols that result in abrupt increase in afterload such as isometric or sudden strenuous aerobic exercise, or during administration of drugs that acutely increase afterload. A semiquantitative scoring system or quantitative regional EFs may be useful for comparison of rest to exercise or interventional studies.
42. The size of the left ventricle may be qualitatively evaluated on the cine displays. During exercise in the upright position, LV volume usually increases. The magnitude of the increase is typically in the 10% to 20% range, although larger increases do occur in control subjects. When the volume increases by 50% or greater above baseline, coronary artery disease should be suspected even in the absence of a regional wall motion abnormality, especially if there is a concomitant, significant drop in LVEF. LV volume may fail to increase or may actually decrease even in the upright position in patients with pericardial or valvular heart disease.
43. During exercise in the upright position, one can anticipate that the EFs of both ventricles will increase. At one point in time, failure to increase the LVEF during exercise was invariably considered pathologic. However, it is quite clear that some individuals may show a flat response to exercise and, occasionally, even a decrease in EF (especially elderly subjects) in the absence of coronary or valvular heart disease. The higher the resting EF, the less of an increase one tends to see during exercise. For diagnostic purposes, an absolute value of exercise EF may be more useful than the change from rest to exercise. Most normal individuals will have a peak exercise LVEF of 56% or greater. A decrease in LVEF to less than 56% should be considered abnormal in individuals aged younger than 70 years, but in the absence of regional dysfunction, the finding is not specific for coronary artery disease. The change in EF during exercise may also be influenced by the type of exercise protocol used. A standard graded exercise protocol should always be used.

    RVEF typically increases during exercise but may decrease in patients with pulmonary hypertension, including those in whom pulmonary hypertension develops during exercise, such as those with mitral stenosis or severe exercise-induced LV dysfunction. In particular, patients with proximal right coronary artery lesions may show decreases in RVEF during exercise.

44. LV tracer transit may be prolonged during exercise because of the appearance of mitral insufficiency resulting from LV ischemia. This finding may be recognized most readily on a TAC of the bolus transit through the left ventricle. Occasionally, this finding is accompanied by exercise-induced enlargement of the left atrium.

Conclusion

45. The radionuclide and doses used for the study, as well as the injection site, should be permanently archived in the report. These are more important for future reference in case a patient returns to the laboratory for serial studies. Having the data is particularly useful in avoiding pitfalls if the previous study was technically suboptimal.
46. The report should include the most important variables from a stress or intervention that will help the referring physician assess the clinical significance of the findings. These variables are also important because they have independent diagnostic and prognostic information.
47. Overall study quality should be mentioned in the report. This serves to appropriately increase or decrease the confidence of the physicians using the report for clinical decision making. It is also useful for subsequent screening of studies for inclusion in research databases.
48. The initial interpretation of the study should be made without reference to clinical data to avoid bias. The physician should then correlate the findings and interpretation with the clinical information to avoid an obvious misinterpretation and to guarantee that the clinical question has been addressed. Including the indication for the study in the report serves to focus the interpreting physician's attention to the clinical question and is also useful for subsequent coding issues related to reimbursement. Studies should be classified as normal or abnormal. Categories of probably normal, equivocal, and probably abnormal may be added. Both the diagnostic and prognostic contents of the data should be addressed. If perfusion scan data are available, a statement about the significance of the two datasets is appropriate.
49. Whenever previous studies are available, the cine displays of the representative cycles should be displayed side by side. When rest and exercise/intervention data are available, a quad-screen display is optimal. Interpretation of serial changes in EFs should always take into account differences in the heart rates, blood pressures, and medications.

Acknowledgments *The authors indicated that they have no financial conflicts of interest.*

Suggested Reading

1. Aroney CN, Ruddy TD, Dighero H, et al. Differentiation of restrictive cardiomyopathy from pericardial constriction: Assessment of diastolic function by radionuclide angiography. J Am Coll Cardiol 1989;13:1007-14.
2. Berger HJ, Matthay RA, Loke J, et al. Assessment of cardiac performance with quantitative radionuclide angiocardiography: RV ejection fraction with reference to findings in chronic obstructive pulmonary disease. Am J Cardiol 1978;41:897-905.
3. Berger H, Reduto L, Johnstone D, et al. Global and regional left ventricular response to bicycle exercise in coronary artery disease assessment by quantitative radionuclide angiocardiography. Am J Med 1979;66:13-21.
4. Borges-Neto S, Coleman RE, Jones RH. Perfusion and function at rest and treadmill exercise using technetium-99m sestamibi: Comparison of one and two day protocols in normal volunteers. J Nucl Med 1990;31:1128-32.
5. Borges-Neto S, Coleman RE, Potts JM, Jones RH. Combined exercise radionuclide angiocardiography and single photon emission computed tomography perfusion studies for assessment of coronary disease. Semin Nucl Med 1991;21:223-9.
6. Borges-Neto S, Shaw L. The added value of simultaneous myocardial perfusion and left ventricular function. Curr Opin Cardiol 1999;14:460-3.
7. Borges-Neto S. Perfusion and function assessment by nuclear cardiology techniques. Curr Opin Cardiol 1997;12:581-6.
8. Campos CT, Chu HW, D'Agostino HJ Jr, Jones RH. Comparison of rest and exercise radionuclide angiocardiography and exercise treadmill testing for diagnosis of anatomically extensive coronary artery disease. Circulation 1983;67:1204-10.
9. DePace NL, Iskandrian AS, Hakki A, et al. Value of left ventricular ejection fraction during exercise in predicting the extent of coronary artery disease. J Am Coll Cardiol 1983;1:1002-10.
10. Foster C, Dymond DS, Anholm JD, et al. Effect of exercise protocol on the left ventricular response to exercise. Am J Cardiol 1983;51:859-64.
11. Friedman JD, Berman DS, Kiat H, et al. Rest and treadmill exercise first-pass radionuclide Ventriculography: Validation of left ventricular ejection fraction measurements. J Nucl Cardiol 1994;4:382-8.
12. Gal R, Grenier RP, Carpenter J, et al. High count first-pass radionuclide angiography using a digital gamma camera. J Nucl Med 1986;27:198-206.
13. Gal R, Grenier RP, Schmidt DH, Port SC. Background correction in first-pass radionuclide angiography: Comparison of several approaches. J Nucl Med 1986;27:1480-6.
14. Gal R, Grenier RP, Port SC, Dymond DS. Left ventricular volume calculation using a count-based ratio method applied to first-pass radionuclide angiography. J Nucl Med 1992;33:2124-32.
15. Johnson LL, Rodney RA, Vaccarino RA, et al. Left ventricular perfusion and performance from a single radiopharmaceutical and one camera. J Nucl Med 1992;33:1411-6.
16. Jones RH, McEwen P, Newman GE, et al. Accuracy of diagnosis of coronary artery disease by radionuclide measurement of left ventricular function during rest and exercise. Circulation 1981;64:586-601.

17. Lee KL, Pryor DB, Pieper KS, Hasell FE Jr. Prognostic value of radionuclide angiography in medically treated patients with coronary artery disease. Circulation 1990;82:1705-17.
18. Maltz DL, Treves S. Quantitative radionuclide angiocardiography: determination of Qp:Qs in children. Circulation 1973;47:1048-56.
19. Morrison DA, Turgeon J, Quitt T. Right ventricular ejection fraction measurements: contrast ventriculography versus gated blood pool and gated first-pass method. Am J Cardiol 1984;54: 651-3.
20. Nichols K, DePuey EG, Gooneratne N, et al. First-pass ventricular ejection fraction using a single crystal nuclear camera. J Nucl Med 1994;35:1292-300.
21. Nichols K, DePuey EG, Rozanski A. First-pass radionuclide angiocardiography using single crystal gamma cameras. J Nucl Cardiol 1997;4:61-73.
22. Nickel O, Schad N, Andrews EJ, et al. Scintigraphic measurement of left ventricular volumes from the count-density distribution. J Nucl Med 1982;23:404-10.
23. Philippe L, Mena I, Darcourt J, French WJ. Evaluation of valvular regurgitation by factor analysis of first-pass angiography. J Nucl Med 1988;29:159-67.
24. Potts JM, Borges-Neto S, Smith LR, Jones RH. Comparison of bicycle and treadmill radionuclide angiocardiography. J Nucl Med 1991;32:1918-22.
25. Reduto LA, Wickemeyer WJ, Young JB, et al. Left ventricular diastolic performance at rest and during exercise in patients with coronary artery disease. Circulation 1981;63:1228-37.
26. Updated imaging guidelines for nuclear cardiology procedures, part 1. J Nucl Cardiol 2001;8:G1-58.
27. Upton MT, Rerych SK, Newman GE, et al. The reproducibility of radionuclide angiographic measurements of LV function in normal subjects at rest and during exercise. Circulation 1980;62:126-32.
28. Verani MS, Lacy JL, Guidry GW, et al. Quantification of left ventricular performance during transient coronary occlusion at various anatomic sites in humans: a study using tantalum-178 and a multiwire gamma camera. J Am Coll Cardiol 1992;19:297-306.
29. Williams KA, Bryant TA, Taillon LA. First-pass radionuclide angiographic analysis with two regions of interest to improve left ventricular ejection fraction accuracy. J Nucl Med 1998;39:1857-61.

ASNC IMAGING GUIDELINES FOR NUCLEAR CARDIOLOGY PROCEDURES

Equilibrium radionuclide angiocardiography

James R. Corbett, MD, Chair,[a] Olakunle O. Akinboboye, MD, BS, MPH, MBA,[b] Stephen L. Bacharach, PhD,[c] Jeffrey S. Borer, MD,[d] Elias H. Botvinick, MD,[e] E. Gordon DePuey, MD,[f] Edward P. Ficaro, PhD,[g] Christopher L. Hansen, MD,[h] Milena J. Henzlova, MD,[i] and Serge Van Kriekinge, PhD[j]

I. PLANAR IMAGING

A. Purpose

Planar equilibrium radionuclide angiocardiography (ERNA) is used to determine global and regional measures of ventricular function (primarily left ventricular [LV] function) at rest and/or during exercise stress or pharmacologic intervention. These measures of ventricular function may include evaluations of ventricular wall motion, ejection fraction (EF), and other parameters of systolic and diastolic function. The following sections provide a technical description of the techniques to acquire and process the data necessary to assess parameters of ventricular performance.

B. Radiopharmaceuticals

1. Inject the patient with technetium 99m-labeled red blood cells, with activity of approximately 20 to 25 mCi/70 kg body weight (11 to 13 MBq/kg) to provide the radioisotope tag for resting studies (Table 1). For exercise studies, the activity can be increased to 25 to 35 mCi/70 kg patient. The radiation dosimetry to the patient from 20 mCi of Tc-99m-labeled red blood cells labeled in vitro is 0.3 to 0.52 rem effective dose equivalent. With in vivo labeling of red blood cells, doses will run at the higher end of this range.[1]
2. Labeling methods.
   a. In vivo or modified in vivo/in vitro methods (e.g., using 2 to 3 mg stannous pyrophosphate 15 minutes before injection of the radiopharmaceutical).[2]
   b. Commercial in vitro kit.[3]

Quality control-labeling efficiency. Poor labeling of red blood cells can be easily recognized on ERNA images. Free Tc-99m-pertechnetate accumulates in the mucosa of the stomach and in the thyroid gland. A number of frequently used drugs and solutions are known to interfere with red blood cell labeling (Table 2).[4] Heparin unfavorably affects labeling efficiency. Thus, if at all possible, Tc-99m-pertechnetate should not be injected in heparinized intravenous lines, or they should be flushed thoroughly. Similarly, intravenous lines containing dextrose solution may alter labeling efficiency. In addition, antibodies against red blood cells may inhibit labeling. Antibodies may develop as a result of drugs such as methyldopa and penicillin. Antibodies may also be present in patients with chronic lymphocytic leukemia, non-Hodgkin's lymphoma, and systemic lupus erythematosus.

Labeling efficiency is also diminished when ''old'' Tc-99m-pertechnetate of low specific activity is used. Tc-99m decays to Tc-99, which is no longer useful for imaging but nevertheless competes with the radioactive form of stannous ions. To prevent the presence of carrier Tc-99, the Tc-99m dose should be taken from relatively fresh (<24 hours after elution) eluate from the generator.[5]

C. Acquisition Parameters—Rest/Exercise Imaging

1. *Collimator.* For resting studies, use of a parallel-hole, high-resolution collimator with spatial resolution of approximately 8 to 10 mm full width at half

Unless reaffirmed, retired, or amended by express action of the Board of Directors of the American Society of Nuclear Cardiology, this Imaging Guideline shall expire as of January 2014.

From the University of Michigan Health System,[a] Ann Arbor, MI; New York Hospital,[b] Flushing, NY; UCSF,[c] San Francisco, CA; New York Hospital-Cornell,[d] New York, NY; UCSF Department of Medicine,[e] San Francisco, CA; St. Lukeós-Roosevelt Hospital,[f] New York, NY; University of Michigan,[g] Ann Arbor, MI; Jefferson Heart Institute,[h] Philadelphia, PA; Mount Sinai Medical Center,[i] New York, NY and Cedars-Sinai Medical Center,[j] Los Angeles, CA.

Reprint requests: James R. Corbett, MD, Chair, University of Michigan Health System, Ann Arbor, MI.

1071-3581/$34.00

doi:10.1007/s12350-008-9027-z

Table 1. Radiopharmaceuticals used for planar ERNA

	Rest	Exercise		For information, see paragraph
Radiopharmaceutical	Tc-99m-labeled RBCs	Tc-99m-labeled RBCs	Standard	1
Dose	20–25 mCi/70 kg	25–35 mCi/70 kg	Preferred	1
Labeling method	In vivo	In vivo	Not recommended	2
	Modified in vivo/ in vitro	Modified in vivo/ in vitro	Standard	2
	In vitro	In vitro	Preferred	2

Table 2. Causes of poor red blood cell labeling

Cause	Mechanism
Hydralazine	Oxidation of stannous ion
Prazosin	Decreases labeling rate
Propranolol	Increases dissociation
Digoxin	Decreases labeling rate
Doxorubicin	?
Iodinated contrast	?
Heparin	Complexes with Tc-99m Oxidation of stannous ion
Dextrose	Complexes with Tc-99m
Methyldopa	Induces RBC antibodies Oxidation of stannous ion
Penicillin	Induces RBC antibodies
Quinidine	Induces RBC antibodies
Immune disorders	Induces RBC antibodies
Prolonged generator ingrowth	Increased carrier
Decreased hematocrit	Relative increase in plasma which oxidizes stannous ion (?)
Excess stannous ion	Tc-99m reduced outside the RBC
Insufficient stannous ion	Incomplete reduction with free Tc-99m pertechnetate

RBC, Red blood cell
From Gerson MC. Cardiac nuclear medicine. 3rd ed. New York: McGraw-Hill; 1997. Reproduced with permission of the McGraw-Hill Companies

maximum (FWHM) (of a line spread function) or better at 10 cm distance from the collimator, as well as a sensitivity (for Tc) of approximately 4,000 to 5,000 counts $\cdot$ s^{-1} $\cdot$ mCi^{-1} (108 to 135 counts $\cdot$ s^{-1} $\cdot$ MBq^{-1}), is preferred (Table 3). If a time-limited stress study (e.g., bicycle exercise) is to be performed, a higher sensitivity (and therefore poorer spatial resolution) collimator may be considered, such as a low-energy all-purpose (LEAP) collimator (typically 12 mm FWHM at 10 cm and sensitivity of approximately 10,000 counts $\cdot$ s^{-1} $\cdot$ mCi^{-1}, or approximately 280 counts $\cdot$ s^{-1} $\cdot$ MBq^{-1}), or optionally a high-sensitivity collimator. In this case, it is especially important to keep the collimator–chest wall distance minimized. It is recommended that the same collimator be used for both the rest and stress study, with parallel-hole LEAP collimator being preferred. If caudal tilt is used (see paragraph 10), a slant-hole collimator may be considered instead of a parallel-hole collimator to provide 10° to 15° of caudal tilt while maintaining minimal collimator–chest wall distance.

2. *Pixel size*. Any matrix size that results in a pixel size less than approximately 4 mm/pixel (with approximately 2 to 3 mm/pixel being preferred) can be used. These acquisitions are usually performed using a zoomed 64 $\times$ 64 matrix of 16-bit (word) pixels. The zoom required to meet the less than 4 mm/pixel criteria will depend on the field of view (FOV) of the camera used. Minimal to no zoom is recommended for small-FOV cameras (circular, 10 inch diameter, or square, 8 inch) to zoom factors of 1.5 to 2.2 for large-FOV (rectangular, 21 inch) cameras. Smaller-FOV cameras, if available, are preferred. In any case, pixel size should not exceed 5 mm. See paragraph 5.
3. *FOV*. The effective FOV is dependent on the camera size and acquisition zoom utilized. Typically, an 18 $\times$ 18-cm^2 FOV will be sufficient, but any FOV size sufficient to encompass all four cardiac chambers and at least 2 cm beyond the cardiac blood pool (for positioning of a background region of interest [ROI]) is acceptable. Larger FOVs are acceptable, provided that they (1) do not inhibit minimizing collimator–chest distance and (2) are not so large as to cause increased gamma camera dead time. If large FOVs are used, care must be taken to prevent

Table 3. Camera/computer setup[6-11]

	Rest	Exercise		For information, see paragraph
Collimator	Parallel—LEAP	Parallel—LEAP	Preferred	1
(rest/exercise)	Parallel—high sensitivity	Parallel—high sensitivity	Optional	1
Collimator	Parallel—high resolution		Preferred	1
(rest only)	Parallel—LEAP		Optional	1
	Slant hole	Slant hole	Optional	1
Pixel size	<4 mm/pixel	<4 mm/pixel	Standard	2, 3
	2-3 mm/pixel	2-3 mm/pixel	Preferred	2, 3
Energy window	140 keV, ±10%	140 keV, ±10%	Standard	4
Bad beat	Buffered beat	Buffered beat	Preferred	5
	On-the-fly:	On-the-fly:	Standard	5
	Reject beat and next beat	Reject beat and next beat	Preferred	5
Beat length window	±10-15%	±10-15%	Standard	5
	Check trigger	Check trigger	Preferred	5
Acquisition method	Frame mode	Frame mode	Standard	7
	List mode	List mode	Optional	7
Frame rate (EF)	>16 frames/cycle	16-32 frames/cycle	Standard	8
	24-32 frames/cycle	24-32 frames/cycle	Preferred	8
Count density	>1800/pixel (3 mm) or 20,000/cm^2 (high-resolution collimator)	Not applicable	Standard	9
	>3600/pixel (3 mm) or 40,000/cm^2 (high-sensitivity collimator)	2-3 minutes acquisition	Standard	9
Positioning	LAO (best right/left separation)	LAO (best right/left separation)	Standard	10a
	LAO (caudal tilt)	LAO (caudal tilt)	Optional	10a
	Plus anterior, lateral		Standard	10b and 10c
Quality control	View cine loop	View cine loop	Preferred	6
	R-R histogram	R-R histogram	Preferred	6

acquisitions terminated on liver or spleen overflow and to ensure that data are displayed with cardiac structures at maximum intensity. Use of a lead apron as a shield for the liver/spleen may be appropriate, positioned with the aid of a persistence scope.

4. *Energy window.* 140 keV, ±10% window.
5. *Bad beat/beat length window (arrhythmia rejection).*[8,12,13] If systolic function only (EF) is to be assessed, accepting less than 10% to 15% arrhythmic beats are acceptable. If the examination is performed to determine diastolic function, beat length windowing (arrhythmia rejection) is necessary. The preferred arrhythmia rejection mode is buffered beat, where each beat is temporarily stored in memory to assess whether its beat length is within the (typical) ±10% to 15% R-R beat length window. If the beat is outside the window, it is rejected without contaminating the gated data acquired. Standard arrhythmia rejection methods typically terminate data acquisition if a premature beat is seen outside of the (±10% to 15%) beat length window (a portion of the bad beat will be acquired). Rejection of the short or long beat along with rejection of the subsequent (compensatory) beat is preferred. The typical beat length window is ±10% to 15% but will vary depending on heart rate and rhythm. If the study is acquired with significant arrhythmias, poor statistics may result, and accurate computation of EF may be compromised. The beat length window may require lengthening to improve statistics but will compromise measurement of diastolic function and may adversely affect cine-loop displays if end frames are not corrected or deleted. See paragraph 8. With regard to triggers, assessment of the adequacy of the R-wave trigger prior to instigation of the gated acquisition should be performed. It is recommended that the electrocardiographic (ECG) trigger point be checked to ensure that the ECG gating circuitry is synchronized to the peak of the ECG R-wave. Checks can be either performed visually, with a dual-trace oscilloscope, or checked with a commercially available dynamic phantom. Poor-quality or delayed triggers can adversely affect the ventricular volume curve.
6. *Post-acquisition quality control of the ERNA study is also recommended.* Visualization of the beating cine loop after acquisition allows evaluation of data drop-off due to inadequate triggers, significant arrhythmias, rhythm disorders, poor tag, or poor count statistics. Review of the beat-length R–R interval histogram can be used to assess cardiac rhythm abnormalities or determine if significant arrhythmias were present. Quality control can anticipate errors associated with inadequate ERNA studies prior to the reporting of ventricular performance.
7. *Acquisition method.* Frame mode gating is standard (forward framing), although forward/backward, as well as forward/backward by thirds, methods are optional. If arrhythmias are present, the frames at the end of the cardiac cycle (containing data acquired over shorter total acquisition time) should be either corrected or deleted (preferred). List-mode data acquisition is optional and offers increased beat length windowing flexibility, particularly for analysis of diastolic function.[6]
8. *Frame rate.*[12] A frame rate of less than 50 milliseconds/frame is preferred for resting EF. A frame rate of less than 30 milliseconds/frame is preferred if ejection and filling rates are to be computed. For rest studies, a minimum of 16 to 19 frames per cardiac cycle is recommended, with 24 or 32 being preferred for EF calculation and for calculation of ejection and filling parameters. For stress studies (R–R <600 milliseconds), 32 frames/cycle is preferred for EF calculation and calculation of peak ejection and filling rates.
9. *Count density.* Studies containing approximately 20,000 counts/cm^2 (1,800 counts/pixel for a 3-mm pixel) over the center of the left ventricle at rest using high-resolution collimation, or about 40,000 counts/cm^2 at rest with the higher-sensitivity collimators (LEAP or high sensitivity), as used in rest/exercise studies, are preferred (which corresponds to about 3 to 4 million counts in a 15 × 15-cm^2 FOV with high-resolution collimator). This count density is measured by summing all images in the gated series together and determining the count density from a small ROI at the center of the left ventricle in the left anterior oblique (LAO) projection. Total counts are not a reliable indicator, as they depend too strongly on the FOV. Nevertheless, a practical rule has been to acquire at least 200,000 counts per image frame for a 16-frame resting study using a high-resolution collimator. Similarly, acquisition time will give variable results depending on collimator sensitivity. To calculate a typical acquisition time, for a particular collimator and dose, sum all frames in the study together, and using a small ROI at the center of the left ventricle, determine the time necessary to achieve the above-mentioned counts per square centimeter. During stress, acquisition time is often the limiting factor. When this is the case, at least 2 minutes (preferably 3 minutes) of acquisition time at peak stress is recommended using the LEAP or high-sensitivity collimator, as previously specified.

10. *Camera positioning—imaging angles.* To acquire the ERNA study, position the patient supine (for greatest patient comfort) or in the right lateral decubitus position (to minimize interference from diaphragm and spleen). Three views should be recorded for assessment of wall motion of the left ventricle.

    a. *LAO view.* The LAO view is optimized to visualize the septum (best septal view—usually the 45° LAO, but the angle will depend on body habitus and cardiac orientation) (Figure 1). In the LAO view, the orientation should be such that the long axis of the ventricle is approximately vertical, with the apex pointing down and left ventricle on the right side of the image. Caudal tilt of the LAO view, typically 10° to 15°, is helpful to separate the atria from the ventricle and may be particularly useful in patients with vertical hearts. The degree of caudal tilt is limited by the detector yoke suspension and the necessity to keep the camera face as close as possible to the chest. As an alternative to achieve a 10° to 15° caudal tilt, a slant-hole collimator may be used, if available. When using a caudal tilt, depending on the imaging conditions, the LV and left atrial separation still may not be apparent. This may result in inclusion of more left atrium than desired, if the atrial-ventricular border is difficult to discern, as the superior aspect of the ROI may encroach into the left atrium. If the atrial-ventricular border is not evident, use the standard LAO view. On a correctly angulated LAO projection, the photopenic area of the septum is more or less vertical. To the left is the foreshortened right ventricle. The right atrium is partially hidden behind and superior to the right ventricle. At the viewer's right, the LV blood pool is well isolated from the surrounding structures by the myocardium as a photopenic halo. The appendage of the left atrium can occasionally be seen superior to the left ventricle, usually separated from the LV blood pool by the photopenic area of myocardium. As a rule, LV blood pool is projected as nearly a ''short-axis'' view. In other

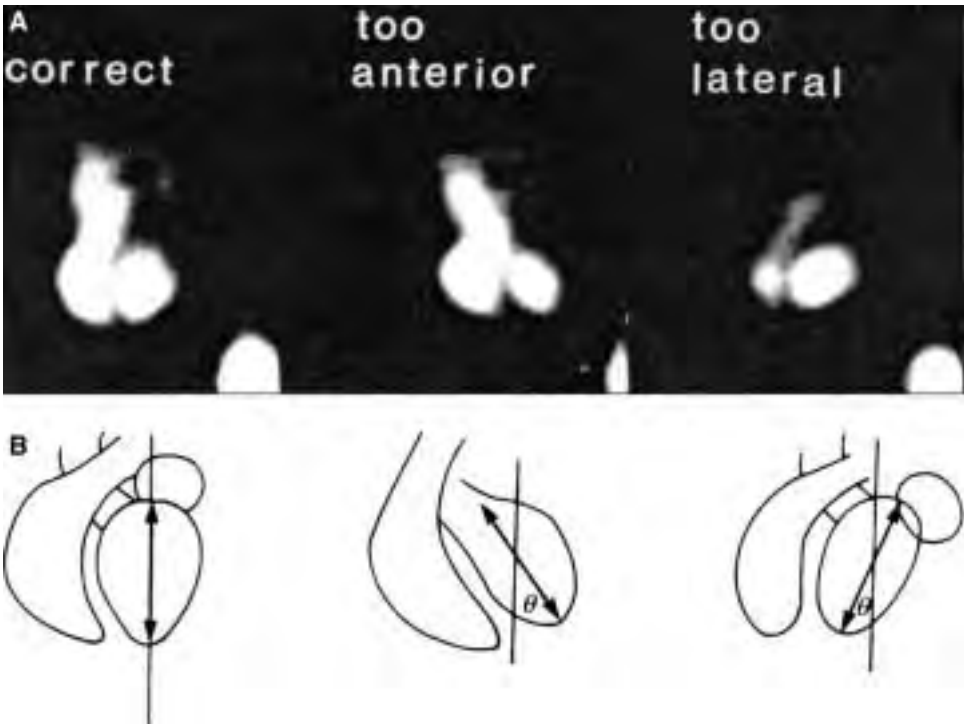

Figure 1. Correct positioning to image left ventricle.[8] **A**, LAO images that are optimal, too anterior, and too lateral in obliquity. **B,** In an optimized LAO view the axis of the left ventricle should be vertical. In images that are too anterior, there is a rightward tilting of the axis from base to apex. In images that are too laterally positioned, there is a leftward tilting of the axis from base to apex. (Reproduced with permission from DePuey.[8]).

words, one looks ''down the barrel'' of the left ventricle. In some patients, the heart is vertically oriented. This anatomic variant can be recognized because of the elongated shape of both ventricles and visualization of both the right atrium and left atrium superior to the ventricles. The pulmonary artery and ascending aorta can also be evaluated in the LAO view. The myocardial segments typically visualized in the LAO view are the septal, inferoseptal, inferoapical, inferolateral, and lateral. The two other preferred views are as follows:

b. *Anterior view*. The anterior view ideally should be −45° more anterior than the LAO selected. On the anterior view, the border-forming contour on the right side of the heart (left side of image) is the right atrium. To the viewer's right, the border-forming contour of the heart on this view is the left ventricle. Because of the overlying activity of the right ventricle, only the anterolateral wall and apex can be evaluated. The inferior wall is frequently completely obscured by the right ventricular (RV) blood pool. Further structures that can be evaluated on the anterior view are the pulmonary artery and the ascending aorta. The myocardial segments typically visualized in the anterior view are the basal anterolateral, mid anterolateral, apical, mid inferoseptal, and basal inferoseptal.
c. *Lateral view*. The left lateral or left posterior oblique (LPO) view; the LPO view angle selected is +45° more lateral than the LAO view angle selected. These views are best acquired with the patient lying on his or her right side. An optimal left lateral view shows the long axis of the left ventricle. ''Long axis'' is defined as the longest dimension from valve plane to apex. Because there is individual variation among patients, either the straight left lateral or the LPO view may show the long axis of the left ventricle best. In the left lateral projection, the left ventricle is superimposed on activity of the right ventricle. Anterior and superior to the left ventricle, the RV outflow tract and the pulmonary artery can be noted. The mitral valve plane is often well demarcated by a linear photopenic area caused by attenuation by fatty tissue in the atrioventricular groove. Posterior to the left ventricle are the left atrium and the descending aorta. The spleen is usually visualized in the right lower corner of the image. The myocardial segments typically visualized in the lateral or LPO view are the basal anterior, mid anterior, apical, mid inferior, and basal inferior.

D. Assessments of Ventricular Function—ERNA at Rest: Image Display and Quantification (Table 4)

1. *Display.*[6,8,10,11] Multiple-view ERNA (LAO, anterior, and left lateral or posterior oblique projections) are usually displayed simultaneously as endless-loop movies in quadrants of the computer screen. The display should visualize the entire heart and its surroundings. ERNA images are best viewed by use of a linear gray scale. Color display is strongly discouraged. Occasionally, intense extracardiac activity may cause a problem with image display. Computer images are usually normalized to the hottest pixel within the image over all time points. In the presence of intense extracardiac activity, radioactivity in the heart is at the darker (lower) end of the gray scale and may be almost invisible. Rather than using lead shielding, normalization of the cardiac image to the hottest pixel within the heart usually deals adequately with this display problem. Alternatively, the extracardiac activity may be subtracted or ''masked out''.
2. *Smoothing*.[15,16] The smoothing process is designed to remove statistical fluctuations from image data by modifying individual data points within the image. Multiframe digitized ERNA data are often temporally and spatially smoothed. For temporal smoothing, pixels are modified by weighted averaging of data from preceding and following frames in time, usually 3 to 5, with the center pixel replaced with this average value. For spatial smoothing, pixels are modified by weighted averaging of counts from a group of neighboring pixels within the same image, usually 9, with the center pixel in the group replaced with this weighted average value. This is referred to as Gaussian 9-point weighted smoothing. The exact number of temporal or spatial points used for the smoothing will depend on the number of time points acquired and the acquisition resolution. Images of adequate count density rarely require spatial smoothing.
3. *LV volume curve generation.*[17-20] Most parameters describing ventricular function are extracted from a complete LV volume curve or time-activity curve (TAC). This curve can be obtained either from a single ROI drawn at end diastole (and modified at end systole, if necessary, to include any dyskinetic regions) or preferably using multiple ROIs drawn at each time point. ROIs should be edited on an amplitude or difference image to exclude overlapping atrial counts. Manually drawn ROIs are the most consistently accurate, though time consuming. Many

Table 4. Quantitative parameters of ventricular function–planar ERNA[6,8,10,11,14]

Parameter	Method		For information, see paragraph
LV volume curve generation	Manual ROI at ED and ES	Preferred	3
	Manual or automatic ROIs at each time point	Optional	3
	Manual or automatic ROIs at ED only	Optional	3
Background	Manual at ED	Preferred	4
	Automatic at ED	Standard	4
	Automatic or manual at ES	Optional	4
LVEF	From end-diastolic and end-systolic ROIs	Preferred	5
	From Fourier-filtered curve	Optional	5
	From single end-diastolic ROI (not recommended)	Optional	5
LV wall motion	Visual assessment of cine loop	Preferred	6a
	Phase and amplitude analysis	Optional	6b
	Principal component or factor analysis	Optional	6c
	Regional EF	Optional	6d
LV emptying	Peak rate of emptying	Preferred	7a
	Average rate of emptying	Optional	7b
	Time to peak emptying rate	Optional	7a
LV filling	Peak rate of filling	Preferred	8
	Average rate of filling	Optional	8
	Time to peak filling rate	Optional	8
LV volumes	Counts based	Optional	9
	Geometric based	Optional	9
RVEF	Not widely accepted at equilibrium	Optional	10
Heart/lung ratio	Counts based LV/lung	Optional	13

automatic techniques exist for drawing ROIs. It is important that the resulting ROIs be checked visually and altered manually if necessary. Irregularities in LV contours occasionally occur using automatic algorithms, especially for exercise studies, and for ROIs drawn near end systole. These irregularities can have significant effects on parameters extracted from the LV curve. If EF only is to be determined, the preferred method (and the simplest) for LV volume curve generation is from manually drawn ROIs over end diastole and end systole, with the volume curve being processed by weighted interpolation of curves from end-diastolic and end-systolic ROIs (weighted to end diastole near the beginning and end of the curve and weighted to end systole at curve minimum). If ejection and filling rates are to be computed, ROIs drawn on all frames are preferred. **NOTE:** Single ROI definition at end diastole may underestimate EF. Optionally, automatic edge detection may be used, if each frame is reviewed, and the ROI corrected, if necessary.

4. *Background*. Background is critical for the measurement of many LV parameters. Usually an ROI 5 to 10 mm away from the end-diastolic border, drawn from approximately 2 o'clock to 5 o'clock, is used, although the exact location used is less important than consistent placement, ensuring that atrial counts, counts from the spleen or descending thoracic aorta, LV counts, or a gastric air bubble is excluded. With automatic routines, visual verification of the background ROI is essential. A visual examination of the TAC produced from the background ROI (it should be flat) is useful to determine if LV activity or atrial activity is spilling into the background ROI. If the background curve is flat, this indicates that the background ROI has not been positioned over any periodically beating structures and that all time points may be averaged for good statistics. An ROI adjacent to the end-systolic border can be used to estimate background, but care must be taken to use only those time points that do not include LV activity. A rule of thumb is that the background count rate/pixel is

typically 30% to 70% of the end-diastolic LV counts, and exceptions to this rule occur infrequently.

5. *LVEF*.[6-8,13,14] Many methods are commercially available for computation of LVEF. In general, LVEF is calculated based on the assumption that LV volumes throughout the cardiac cycle are proportional to LV counts. LV counts at end diastole and at end systole or throughout the cardiac cycle are measured by constructing LV ROIs. The measured LV counts within these LV ROIs are corrected for background scatter. Background is measured using ROIs constructed adjacent to the lateral or inferoapical walls of the ventricle. LV ROI counts are corrected for background by subtracting background counts from LV ROI counts. This is referred to as background correction (BkCorr). LVEF then is calculated using the usual equation: ([End-diastolic volume (EDV) − End-systolic volume (ESV)]/EDV) × 100 or, as applied to ERNA, LVEF = ([BkCorr end-diastolic counts − BkCorr end-systolic counts]/BkCorr end-diastolic counts) × 100.

   Three basic approaches are commonly employed.

   a. LVEF can be computed by selecting only the end-diastolic and end-systolic frames and constructing the appropriate LV and background ROIs. This is just as effective as using all frames from the entire cardiac cycle, and if regions are being constructed manually, this greatly decreases processing time. No matter what the approach, care must be taken to ensure that LV ROIs are appropriately fitted to include all LV counts, but only LV counts (i.e., LV ROIs) should not extend to include the activity from any adjacent structures such as the left atrium above, right ventricle to the left, an adjacent intensely active spleen below and to the right, or a grossly ectatic descending aorta immediately to the right. Automatically generated LV ROIs may need to be edited or redrawn by the operator if they do not tightly fit the apparent LV boundaries. This is especially the case at end systole, where automatically generated ROIs often do not fit well, extending irregularly beyond the ventricle frequently including the aortic root to the left and beyond the apex above. If the end-systolic LV ROI is not correctly drawn, the calculated LVEF will generally be underestimated.
   b. If all frames throughout the cardiac cycle are employed to generate an LV TAC, one optional method that can be used fits two or four Fourier harmonics to the LV TAC, extracting the first and the minimum points, as the end-diastolic and end-systolic count values. Because this method uses the entire curve, it reduces statistical fluctuations, even for very short (stress) acquisitions. If the first point of the filtered curve is used, one must ensure that the ECG gate is correctly set up, with gating occurring no later than the peak of the R wave, preferably during the upslope of the R wave to ensure that the first point truly corresponds to end diastole. If the R-wave trigger is not precisely at end diastole (see section I.C.5, ''Bad beat/beat length window [arrhythmia rejection]''), then the maximum value of the filtered curve can be used to identify the end-diastolic counts. Fourier fitting may fail to provide reliable results if there is ''drop off'' in TAC counts at the end of the curve due to heart rate variability from sinus arrhythmia or other arrhythmias varying the R–R′ interval. This effectively reduces the time of acquisition of frames at the end of the diastolic phase of the cardiac cycle and the corresponding TAC. Fourier filtering should be applied only to curves that have no drop off or that have been corrected for drop off.
   c. EF can also be computed from the LV counts produced from a single end-diastolic ROI, applied to both the end-diastolic and the end-systolic images. In this case, the EF will be consistently underestimated compared to the above methods. The single end-diastolic LV ROI approach is discouraged.

6. *LV wall motion*.[15,16,21-27]

   a. Visual assessment of all three standard views is preferred. It is critical that the cine loop consist of approximately 12 to 16 frames (fewer frames may lose temporal information, greater may compromise statistics). If the acquisition is performed with more than 16 frames for improved temporal resolution, it is imperative that the frames be appropriately added/recombined or filtered before visual assessment. Spatial filtering and temporal filtering are often employed in cine-loop presentations. Spatial filtering is typically a 9-point spatial smooth and reduces the apparent quantum mottle or image noise. Temporal filtering typically weights the current frame two parts and the previous and postframes one part to recreate the cine-loop image with 16 frames or more. Both types of filtering tend to make the cine loop appear more visually pleasing. If rest and stress are to be compared, it is preferred to show both cine loops simultaneously. Optionally, modern application of principal components analysis (PCA) or factor analysis can create a mathematically derived cine loop which separates various types of wall motion

(atrial, ventricular), producing a more visually pleasing motion image, reducing the appearance of noise in the cine. However, the effects of PCA analysis on the assessment of regional wall motion have not been completely evaluated.

b. Phase and amplitude images have been reported to be of use for the detection and quantification of wall motion defects. It is preferred that this method supplement, not replace, visual assessment of the cine loop. Analyses of the phase image and phase histogram, as well as visual assessment of a dynamic phase image, have both been reported to be useful in reducing the subjectivity associated with visual assessment of wall motion defects using cine loops. Also, in patients with conduction abnormalities, phase analysis has proven useful in identifying the pattern, location, and/or point of origin of arrhythmic foci.

c. PCA or factor analysis creates a mathematically derived set of functional images expressing significant motion components in the image. Displayed as amplitude images and associated time signatures, they may add to the assessment of regional wall motion and can be viewed in similar fashion to phase and amplitude images or applied to process the cine-loop display (see above). This method is clearly a supplement at this point and should be used in conjunction with standard cine-loop assessment of wall motion. (d) Regional EF (i.e., dividing the left ventricle into 6 to 8 subregions and applying the conventional formulation for EF) has been reported to aid in the assessment of regional or segmental wall motion. It is preferred that this method supplement, not replace, visual assessment of the cine loop.

Cardiac rhythm and conduction.[8,13,28,29] Because the ERNA is formatted and displayed as an endless-loop cine of a single representative beat, the ''rhythm'' always looks regular. Abnormalities of rhythm can only be discerned by the relationship of atrial to ventricular contraction. The most common sustained disturbance of rhythm is atrial fibrillation. Atrial fibrillation or flutter can be assumed to be present when no atrial contraction is detected. Occasionally, one may diagnose flutter or atrial tachycardia by a difference between the atrial and ventricular contraction rates—that is, 2 or 3 atrial contractions to each ventricular contraction. A pacemaker rhythm is usually apparent because the LV activation starts at the apex, and the wave front of contractions proceeds to the base. Left bundle branch block can be diagnosed by the typical paradoxical pattern of septal motion.

7. *LV emptying*.[12,30]

   a. The maximal LV emptying rate is determined by measuring the peak slope of the LV curve, expressed in units of EDV/second. The counts in the end-diastolic ROI are used to represent the EDV, and the counts in subsequent frames are referenced to this value to compute EDV/second. The time to peak emptying (from the end-diastolic frame) may also be computed and expressed in milliseconds. Measurement error in the down slope of the LV volume curve is greatly amplified by statistical noise in the unprocessed (unfiltered) curve. For this reason, either the LV curve is generally first filtered or a small region of the curve is fitted to a polynomial, or other similar techniques are employed to minimize noise without distorting the value of slope. Measurements of peak emptying at exercise are often considered too heart rate dependent or statistically inadequate to be of clinical use. When computing peak or maximal emptying rate, 32 frames per cardiac cycle is preferred to ensure accurate assessment of maximal rate.

   b. The slope of a line connecting the end-diastolic and end-systolic points can be used as a measure of the average LV emptying rate. Alternatively, methods that depend on the time it takes for the left ventricle to empty one-third (or any other arbitrary fraction) of the way from end diastole to end systole have been reported.

8. *LV filling/diastolic function*.[8,12,31-35] The same techniques described in paragraph 7 above can be used to measure diastolic filling rates. All of the same considerations mentioned above for emptying also hold for filling. Note that the gating requirements for adequate representation of diastolic parameters are more stringent than for systolic ejection parameters, due to data drop off at the end of the cardiac cycle.

   Qualitative. Visual analysis of the shape of the LV TAC is frequently sufficient to detect gross abnormalities of diastolic filling. Prolongation of isovolumic relaxation, a delay in the onset of rapid filling, a decrease in the slope of the rapid filling phase, or an exaggerated contribution of atrial contraction to LV filling may be readily apparent and should be noted. Such findings are typical of hypertrophic ventricles. Aging, pericardial disease, and restrictive myocardial disease are also

associated with changes in the pattern of filling and a decrease in the rate of filling.

Quantitative. Peak diastolic filling rate can be quantified from the first derivative of the diastolic portion of the LV TAC. To obtain reliable values for diastolic filling, the LV volume curve should have sufficient temporal resolution. Values for normal studies vary from laboratory to laboratory, but a generally accepted lower limit of normal for the peak diastolic filling rate (PFR) is 2.50 EDV/second. PFR tends to decrease with age in otherwise healthy older subjects. In addition to the PFR, the time to PFR (tPFR) can also be measured from the LV TAC and is expressed in milliseconds. As with the PFR, the tPFR also varies from laboratory to laboratory but on average should be expected to be less than 180 milliseconds. The relative contribution of atrial filling to LV filling may be quantified as the ratio of the atrial peak to the peak of the rapid filling phase on the first derivative curve. Ratios of less than 1:4 are normal but may increase with aging.

9. *LV volumes*.[36-40] Acceptable results have been reported in the literature using both counts-based and (to a lesser extent) geometrically based methods, although counts-based methods are preferred. Geometric methods are based on the standard ''area-length'' methods and are hampered by the limited spatial resolution of ERNA. Both the counts-based and geometrically based methods may produce highly inaccurate results unless extraordinary attention is paid to methodological detail. These methods are not widely used. Assessments of LV volume are affected by photon attenuation and Compton scatter. Counts-based methods include the ''aortic arch'' method or methods involving blood draws and calibration of the counts-to-volume ratio. The latter method is highly influenced by photon attenuation. Calculation of absolute volumes is not recommended, except for laboratories that have the ability to independently validate their methodology.
10. *RVEF*.[41-44] Because of overlap with other cardiac chambers, ERNA is not the procedure of choice for measurement of RVEF. Frequently, there is overlap of right atrial activity during RV systole, which will lead to an erroneously low calculation of RVEF. Overlap of the right atrial activity with the right ventricle may be partially circumvented by acquiring a separate shallower LAO, about 20° LAO, chosen to optimize the separation of the right ventricle from both the right atrium and left ventricle. Although optimal separation is generally impossible, improved separation usually is relatively easily accomplished. Rotating slant-hole collimators, if available, may be quite useful in optimizing atrioventricular separation. Either true first-pass or ''gated first-pass'' radionuclide angiocardiography is the preferred approach. Both of those techniques yield RVEF values that are higher than those measured on a standard ERNA study. The lower limit of normal with these methods is 0.40.
11. *RV size*. This is best evaluated in the anterior view. Assuming that ERNA images are routinely acquired with the same gamma camera and same zoom factor, abnormal enlargement of the right ventricle can be identified by visual inspection and mental comparison to normal studies. There is no reliable quantitative measurement method for the RV volume with ERNA.
12. *RV regional wall motion*. This is best assessed by use of the information from both the anterior and LAO views. Any single view may be inadequate. Regional wall motion is usually qualitatively graded as normal, mildly hypokinetic, severely hypokinetic, akinetic, or dyskinetic.
13. *Heart/lung ratio.* Optionally, heart/lung ratio can be computed. The ratio of the counts in the cardiac blood pool to the counts in the lung can be useful to assess ventricular compensation. Pooling of blood in the lungs has been reported to be indicative of LV failure.

E. Assessment of Ventricular Function During Exercise and Interventions: Image Display and Quantification[7,8,11,45,46]

1. *Display*. ERNA images acquired at baseline and during exercise or pharmacologic interventions should be displayed side by side on quadrants of the computer screen for evaluation of changes between the two sets of images.
2. *Regional wall motion changes from rest*.[45,47-49] One should expect an increase in regional excursion during exercise, during inotropic stimulation, and during administration of afterload-reducing agents such as nitroglycerin. The standard approach to detection of changes in regional wall motion between two studies is to visually assess the change on the side-by-side display. A somewhat more rigorous approach is the semiquantitative method in which ventricular segments are assigned scores where 4 is normal, 3 is mildly hypokinetic, 2 is moderately

hypokinetic, 1 is severely hypokinetic, 0 is akinetic, and −1 is dyskinetic. A significant change in regional wall motion between two studies is defined as a change in score of 2 or greater.

3. *Chamber size changes from rest*.[50-52] During interventions, changes in chamber size may occur. A mild increase in end-diastolic volume is normal during physical exercise, especially with patients in the upright position.[50] During dobutamine stress, a decrease in LV chamber size may be observed. These changes may be too small to be appreciated by visual analysis but can be quantified either as a relative change (from decay-corrected count changes) or absolute volume change. Visually, only moderate to severe dilation of the ventricles should be reported. Such marked volume changes are almost always abnormal. If volume is measured quantitatively, one should expect increases in LV EDV of only 10% to 20% during exercise and concomitant decreases in ESV.
4. *LVEF and RVEF changes from rest*.[12,43,47,48,53-57] Both LVEF and RVEF typically increase during exercise. Many authors have suggested that the normal response is an increase of at least 5%, or 5 EF units. That criterion is based on the reproducibility of the ERNA measurements of LVEF. Nevertheless, this criterion does not hold true under all circumstances. For instance, with increasing age, the ability to augment LVEF during exercise decreases. The type of exercise protocol, the subject's gender, acquisition during submaximal exercise, isometric exercise, markedly hypertensive responses to exercise, and coexisting noncoronary heart disease may all alter the response of the EF to exercise. Consequently, a failure to increase LVEF of at least 5% is a sensitive but very nonspecific criterion for diagnosis of coronary heart disease. In the absence of an exercise-induced regional wall motion abnormality, changes in LVEF alone are nonspecific. Coupled with a large (>20%) increase in EDV during exercise, a drop in LVEF with normal regional wall motion during exercise should be viewed as highly suspicious for coronary artery disease.

   A more important parameter is the absolute level of LVEF at peak exercise. Even if angiographic coronary artery disease is documented, a peak exercise LVEF greater than 50% indicates a favorable prognosis. It is important to ensure that acquisition of radionuclide data is performed during peak exercise. In most patients, with and without significant disease, a significant increase in LVEF can be noted immediately after discontinuation of exercise. Abnormalities in RVEF during exercise are most often seen in patients with chronic pulmonary diseases and in particular in those with pulmonary hypertension. Patients with cardiomyopathy and bi-ventricular dysfunction or proximal right coronary artery stenoses may also demonstrate abnormal RV responses.
5. *Comparison to previous studies and correlation with clinical data*.[45,55,58] When a patient has undergone previous radionuclide studies, the results of this study should be compared with the previous ones. Ideally, one should display the old and new studies side by side. Serial LVEF data are particularly important in patients undergoing chemotherapy for cancer and also in patients with heart failure, myocarditis, or cardiomyopathy or after undergoing transplantation. For this reason, it is helpful to record and reproduce the camera angles at which the three planar cardiac views are acquired for each study. Interpretation of ERNA data may be performed without knowledge of the clinical data; however, once an initial interpretation is made, the interpreting physician should always review the available clinical information to avoid obvious misinterpretation and to guarantee that the interpretation appropriately addresses the clinical question that prompted the study.
6. *Study quality*. Poor-quality studies cannot be interpreted with confidence and a high degree of reproducibility. Studies can be subjectively graded as (a) excellent, (b) average, (c) suboptimal but interpretable, and (d) uninterpretable. Placing such a designation in the report communicates a level of confidence in the data that is helpful to recipients of the report. It may also be used to screen studies from inclusion in research data. If possible poor-quality (suboptimal and uninterpretable) studies should be repeated but, if for some reason, they cannot be, the subjective grade of study quality will at least alert the referring clinician to the limited reliability of the reported results.
7. *Type of exercise or intervention protocol*.[50,59] The type of exercise should be specified in the report: physical exercise on treadmill or supine or upright bicycle. The exercise protocol should be stated. Exercise ERNA studies are performed with bicycle ergometers, and the levels of stress during each image acquisition are reported in watts or kilogrammeters of work and duration. Treadmill protocols such as the Bruce, modified Bruce, and Naughton protocol are not used with exercise ERNA. For pharmacologic intervention, the generic name of the

drug (e.g., dobutamine) and maximal dose (e.g., 40 mg · kg^{-1} · min^{-1}) infused should be stated. Furthermore, whether drugs were administered to either enhance or counteract the effect of the pharmacologic stressor should be reported.

8. *Symptoms, heart rate and blood pressure response, ECG changes, and endpoint of stress.* Within the report of the radionuclide study, a succinct description should be given of important clinical parameters: duration of exercise or stress protocol, baseline and peak stress heart rate, maximal workload (in metabolic equivalents when applicable), baseline and peak stress blood pressure, symptoms during test, (re)production of symptoms and chest pain, and ECG changes compared with baseline.

F. Image Analysis/Interpretation[7,8,10,11,39]

1. *Overall cardiac assessment.* The initial assessment of ERNA studies should include an overall general assessment of the size, position, and rotation of the cardiac blood pool (heart) and proximal great arteries. In most patients there is not a great deal of variability in regard to position and rotation if the standard best septal LAO, anterior, and lateral projections have been acquired. In patients with severe obstructive airways disease and patients with congenital heart disease, often previously undiagnosed, to mention only a few causes of significant variability, size, position, and rotation can differ greatly from the expected. The best septal projection can on rare occasion be as shallow as straight anterior or as steep as 10° to 30° LPO. If the technologist has not carefully identified and noted the angulation of the best septal LAO projection and the standard ''anterior'' (−45°) and ''lateral'' (+45°) projections, the quantification of ventricular function will be significantly impaired and the interpretation of segmental function of the left and right ventricles hampered by either chamber overlap or misidentification of segments or both. For example, if the interpreting physician does not note that the rotation of the heart in the sagittal oblique plane is quite steep in a patient with severe chronic obstructive pulmonary disease and depressed diaphragm, that individual may interpret motion at the base of the left ventricle in the LAO projection as anterior wall motion, as is more commonly the case in patients without overinflated lungs, rather than motion of the mitral valve plane. In patients with pulmonary hypertension, the right ventricle is often greatly dilated and, with this, the septum is often rotated to a steep LAO, lateral, or LPO projection. If the technologist does not recognize and note this during image acquisition, chamber overlap may be so severe that the left ventricle cannot be assessed at all.
2. *Attenuation artifacts*. As is the case for myocardial perfusion imaging, breast attenuation may also affect ERNA imaging. On the LAO view, the entire heart may be in the ''shadow'' of the left breast. At times, this may give the illusion of a halo around the heart and suggest pericardial fluid. Lack of ''swinging'' of the heart and the typical configuration of the shadow may provide clues for the artifact.
3. *Activity outside the heart and great vessels*. Any vascular structure (tumor, etc.) with a sufficient volume of red blood cells can be visualized by ERNA imaging. Therefore, it is important to be attentive for any unusual radioactivity outside the heart and great vessels and seek clinical correlation. Free Tc-99m-pertechnetate accumulates in the thyroid gland and gastric mucosa.
4. *Chamber sizes.*
   a. *LV size*. One can qualitatively assess the relative size of various cardiac chambers. This assumes that the same camera and magnification are used routinely. Because in many patients the right ventricle is normal in size and function, RV end-diastolic size may serve as a benchmark for qualitative assessment of the relative size of other cardiac structures. On a normal study, the right ventricle is usually somewhat larger than the left ventricle and the RV inferior wall and apex extends below the left ventricle. A normally sized left ventricle ''fits'' within the crescent of the right ventricle on the LAO view. The presence or absence of marked LV hypertrophy (LVH) can be estimated by qualitative assessment of the thickness of the septum. The septum is well delineated by RV and LV blood pool, and thus the thickness of the myocardium can be assessed. In severe LVH, a thick photopenic halo typically surrounds the LV blood pool.
   b. *RV size*. This is best evaluated in the anterior view. Assuming that ERNA images are routinely acquired with the same gamma camera and same zoom factor, abnormal enlargement of the right ventricle can be identified by visual inspection and mental comparison to normal studies. There is no reliable quantitative measurement method for the RV volume with ERNA.
   c. *Atrial sizes*. The right atrium forms the left lower border on the anterior view of the cardiac image. Size and contraction of the right atrium can be evaluated in this view during ventricular systole.

The left atrium is best evaluated on the left lateral view during ventricular systole. Because of overlying and surrounding radioactivity, frequently no clear outline of the left atrium is present. However, the general size and contractility of the left atrium usually can be appreciated. The size of the left atrium should be judged in comparison to the long axis of the left ventricle. The contraction of the left atrium is appreciated as a change in count density during ventricular diastole and is sometimes discernible on radionuclide studies.

Atrial contraction does, however, occur at the very end of the acquisition cycle. Atrial contraction is shorter than the ventricular cycle. In the presence of ventricular ectopy or irregular rhythm, the last frames have lower count density, resulting in ''flicker'' of the endless-loop cine. During processing, one or two frames at the end of the cycle may be ''cut off''' for aesthetic reasons. As a result, atrial contraction may no longer be evaluable.

5. *LVH*. The presence of LVH is best assessed in the LAO view as more than normal thickening of the septum. This is a subjective evaluation that requires familiarity with the normal appearance of the septum on ERNA images acquired with a particular gamma camera. In severe LVH, the LV blood pool is surrounded by a thick photopenic area—that is, the hypertrophied myocardium. During systole, there can be almost complete LV cavity obliteration.
6. *Pericardial space*. Pericardial fluid accumulation can be identified on ERNA studies. When a large amount of fluid is present, a photopenic area surrounds the heart, extending up to the roots of the large vessels. On the cine display, a swinging motion of the heart can be appreciated. When estimating the extent of the photopenic area around the ventricular blood pool, one should account for both the thickness of the myocardium and the presence of epicardial fat before deciding that pericardial fluid is present. Consequently, small amounts of fluid are impossible to distinguish from normal variants. The shadow of a large overlying breast may, particularly in the LAO view, mimic pericardial fluid. Only swinging motion of the heart is a certain sign of a large amount of pericardial fluid. The preferred technique to assess pericardial fluid continues to be echocardiography.
7. *Size of pulmonary artery and aorta*. The pulmonary artery and the ascending and descending aorta can also be evaluated visually on good-quality ERNA studies. Only qualitative assessments, such as dilation of the pulmonary artery and dilation and tortuosity of the ascending aorta, aortic arch, or descending aorta, can be made. The three conventional views allow for visual assessment from different angles.
8. *Conclusion*. It is important to summarize the results of the test as either ''normal'' or ''abnormal.'' Equivocal statements should be avoided if at all possible. In addition, the report should reflect the degree to which the test is abnormal: ''markedly,'' ''moderately,'' or ''mildly'' abnormal. Finally, a comparison should be made to previous results, if applicable. A serious attempt should be made to provide an answer to the clinical questions and indication for study.

II. SINGLE-PHOTON EMISSION COMPUTED TOMOGRAPHY IMAGING

A. Purpose

Single-photon emission computed tomography (SPECT) ERNA is used to determine global and regional measures of ventricular function (primarily LV function) at rest and/or during pharmacologic intervention. These measures of ventricular function may include evaluations of ventricular wall motion, EF, and other parameters of systolic and diastolic function. The following sections provide a technical description of the techniques to acquire and process the data necessary to assess parameters of ventricular performance.

B. Radiopharmaceuticals (Table 5)

1. Inject the patient with Tc-99m-labeled red blood cells, with activity of approximately 25 to 30 mCi/70 kg body weight (14–17 MBq/kg) to provide the radioisotope tag. With in vivo labeling or red blood cells, doses will run at the higher end of this range.[1]
2. Labeling methods.
   a. In vivo or modified in vivo/in vitro methods (e.g., using 2 to 3 mg stannous pyrophosphate 15 minutes before injection of the radiopharmaceutical).[2]
   b. Commercial in vitro kit.[3]

C. Acquisition Parameters and Reconstructions—Gated SPECT ERNA (Table 6)

1. *Camera*. Use of dual-detector (two-head) SPECT cameras in the 90° configuration are the most common preferred camera setup (90° gantry rotation required), but three-head cameras in 120° configurations are another preferred approach (120° rotation). For 360° image acquisitions, three-head SPECT systems (120° configuration) are the most efficient systems for image acquisition (120°

Table 5. Radiopharmaceuticals used for SPECT ERNA

			For information, see paragraph
Radiopharmaceutical	Tc-99m-labeled RBCs	Standard	1
Dose	25-35 mCi/70 kg	Preferred	1
Labeling method	In vivo	Not recommended	2
	Modified in vivo/in vitro	Standard	2
	In vitro	Preferred	2

RBC, Red blood cells

Table 6. Camera and computer setup and reconstruction[7,60-64]

	Data/method		For information, see paragraph
Camera and computer setup			
Camera	Dual-head—90° configuration	Preferred	1
	Three-head—120° configuration	Optional	1
	Single head	Optional	1
Collimator	Parallel—high resolution (dual head)	Preferred	2
	Parallel—LEAP (single head)	Preferred	2
Pixel size	4.8-6.6 mm/pixel	Standard	3
Energy window	140 keV, ±15%	Standard	4
Beat length window	±15-35%	Standard	5
Bad beat rejection	Reject beat	Standard	5
	Reject beat and next beat	Preferred	5
Acquisition method	Frame mode	Standard	6
Frame rate	16 frames/cycle over full cycle	Standard	7
	16 frames/cycle over partial cycle	Optional	7
Number of views	60-64	Standard	8
	30-32	Optional	8
	30-32 (single head)	Standard	8
Time per view (seconds)	20-30	Standard	8
	40-60	Optional	8
	40-60 (single head)	Standard	8
Acquisition stop mode	Time per view	Standard	8
	Cardiac cycles per view	Preferred	8
	Acquisition time per view	Preferred	8
Rotation	180°	Standard	9
	360°	Optional	9
Gated SPECT reconstruction parameters			
SPECT reconstruction	Filtered backprojection or iterative	Standard	10
Reconstruction filter	Butterworth 0.55 Nyquist cutoff		
	Order = 7	Standard	10
	Butterworth 0.45 Nyquist cutoff	Optional	10
Oblique reorientation	Short-axis oblique	Standard	11
	Long-axis coronal	Optional	11
	Long-axis sagittal	Optional	11

rotation acquisitions) followed by dual-head SPECT systems in a 180° configuration (180° rotation acquisitions). Single-head SPECT cameras are the least efficient systems for both 180° and 360° acquisitions, requiring 180° and 360° rotations, respectively, to acquire a full study. With multidetector SPECT systems, ERNA SPECT can be performed in half the time, about 15 minutes, of a 3-view planar ERNA series and are highly recommended. Dual-headed cameras in the 180° configuration are optional but are not recommended unless 360° image acquisitions are desired (180° rotations are required). Single-head SPECT cameras with 180° rotations are optional, but not recommended. Acquisition time with a single-head camera (180° rotation) is approximately 30 minutes.

2. *Collimator.* High-resolution parallel-hole collimators (resolution of approximately 8 to 10 mm FWHM or better at 10 cm and sensitivity [Tc] of approximately 4,000 to 5,000 counts $\cdot$ s^{-1} $\cdot$ mCi^{-1} [108 to 135 counts $\cdot$ s^{-1} $\cdot$ MBq^{-1}]) are preferred when using multidetector SPECT systems. LEAP collimators (typically 12 mm FWHM at 10 cm and sensitivity of approximately 10,000 counts $\cdot$ s^{-1} $\cdot$ mCi^{-1}, or approximately 280 counts $\cdot$ s^{-1} $\cdot$ MBq^{-1}) may be preferred when using a single-head SPECT camera.
3. *Pixel size*. A 64 $\times$ 64 matrix size of 16-bit word pixels or a 128 $\times$ 128 matrix size of 8-bit byte pixels is preferred. Acquisition zooms that result in pixels 4.8 to 6.6 mm^2 in the acquired planar projection images and comparably sized cubic voxels in the reconstructed SPECT image sets are standard of practice. Acquisitions may be performed using acquisition zooms as high as 1.75 with large-FOV cameras (1.75 for patients with small body habitus) providing pixels as small as 4 mm^2. However, it is critical that the entire cardiac blood pool be in the FOV in all projections or severe truncation artifacts may result. If pixel sizes smaller than 4.8 mm are desired, a test rotation with observation of the blood pool using a persistence scope in all views is recommended. With large-FOV rectangular detectors, common on most modern and currently available SPECT systems, a test orbit is only required in patients with very severely dilated hearts. Most quantification programs are validated at only one or two pixel/voxel sizes, and it is generally recommended that an acquisition zoom (voxel size) be used on all patients in keeping with the image input requirements of the quantification software used.
4. *Energy window*. 140 keV, ±15% window.
5. *Bad beat/beat length window (arrhythmia rejection)*. The preferred arrhythmia rejection mode is on-the-fly bad beat rejection. Typically, the standard arrhythmia rejection methods interrupt data acquisition if a premature beat is detected outside of the beat length acceptance window. Rejection of the short or long beat is typical, with rejection of subsequent beat preferred. The typical beat length acceptance window for SPECT is the mean R–R′ interval ±15% to 35% but will vary depending on heart rate and rhythm. This window is generally somewhat larger than that used for planar ERNA, as significant arrhythmias may result in poor statistics, which, depending on the acquisition stop mode employed, can adversely affect the quality of the gated SPECT reconstruction. The beat length window may require widening in some patients if there is significant variation in cycle length due to either sinus arrhythmia or premature beats. Regarding acquisition stop mode, SPECT image reconstructions assume equal sampling (acquisition time) at each camera view. If several cardiac cycles are excluded due to cycle lengths falling outside the acceptance window, severe reconstruction artifacts can occur including severe streaking of the reconstructed images. For this reason, although not commonly employed, ‘‘acquisition stop for accepted beats’’ with normalization of the actual acquisition time at each projection to a common time (e.g., 30 seconds) and ‘‘acquisition stop for accepted time’’ at each projection (e.g., 30 seconds) are the preferred stop modes. Both stop for accepted beats and stop for accepted time ensure virtually identical sampling at each projection, whereas simple acquisition for camera dwell time at each projection with bad beat rejection turned on can result in some projections having no accepted beats (in the worst case) if there is a run of frequent premature beats or a drift of heart rate outside the acceptance window. As with planar studies, it is recommended that the ECG trigger point be checked to ensure that the ECG gating circuitry is gating on the upslope or peak of the ECG R-wave. The ECG gate setup should be checked with either a dual-trace oscilloscope or strip chart recorder output from the ECG gate on each patient. Since most gating devices are designed to recognize a rapid increase in QRS voltage, the optimal input to these devices is an ECG lead that is predominately a large monophasic R-wave accompanied by relatively small P-waves and T-waves and an artifact-free baseline. In most cases if the negative electrode (typically the right arm lead) is placed just below

the right clavicle in the mid-clavicular line, the positive electrode (typically the left arm lead) is placed above the costal margin 2 to 4 cm below the V4, V5, or V6 position so as to avoid overlapping the cardiac FOV, and the ground lead is placed in a similar position on the right lower chest, a good signal will be obtained. Care should be taken to carefully prepare the electrode sites with alcohol or other skin preparation materials to ensure a stable artifact-free signal. In difficult cases, a quick review of a standard 12-lead electrocardiogram may be helpful in planning electrode placement, and usually only repositioning the positive electrode will be the only required change. The ECG lead wires should be positioned so that they have no tension on them and so that neither the patient nor camera can either displace, snag, or bump them during acquisition setup and imaging, resulting in interruption of gating and/or artifacts. Bad ECG gating devices including gating devices with excessive delays between QRS onset and output of signal to the camera can adversely affect the ventricular volume curve and severely lengthen image acquisition time or result in poor statistics. ECG gating devices can be checked with commercially available dynamic phantoms.

6. *Acquisition method*. Frame mode (forward framing) is standard. However, when available, forward–backward gating should be considered, especially in patients with significant arrhythmia where the diastolic phase of the volume curve and cine displays of wall motion may be severely distorted when only forward framing is used.
7. *Frame rate*. Sixteen frames per cardiac cycle are preferred because of the poor temporal resolution of 8-frame studies. LVEF values may be decreased significantly if 8 gated frames per cycle are acquired. The statistics of SPECT acquisitions typically preclude the use of higher frame rates. An alternative to higher frame rates per cycle is to acquire 16 frames, over one half or two-thirds of the cardiac cycle, if systolic ejection parameters and EF only are required. However, with this optional acquisition mode, diastolic function analyses will be compromised if not precluded entirely.
8. *Number of projections (views) and time per view*. When using dual-head SPECT cameras, 60 or 64 projections (30 or 32 projections per head) over a 180° rotation (right anterior oblique to LPO) at approximately 30 seconds per view are preferred when (total acquisition time of about 15 or 16 minutes). Optionally, 30 or 32 views may be used (15 or 16 views per head) at 60 seconds per view for enhanced statistics in very large or severely arrhythmic patients (total acquisition time of about 15 or 16 minutes). With 3-headed systems, the total number of projections acquired over a 180° orbit and the acquisition time per projection are the same as for dual-head systems. This will require approximately 30% more total acquisition time for a 180° study. However, this 180° approach throws away half of the acquired data (i.e., in the same time required for a 180° study, a 360° study has actually been acquired). Some laboratories take advantage of all the acquired projections and reconstruct with the full 360° projection data set. This permits reduced time per projection and reduced total acquisition time with the same or greater total acquired counts for 360° reconstructions. When using a single-head gamma camera, 30 or 32 projections at 60 seconds per view are recommended (total acquisition time of about 30 to 32 minutes).
9. *Rotation*. With single- and dual-head SPECT cameras, 180° rotation is preferred; 360° rotation is optional with either a single- or dual-head camera but is not recommended unless a three-head SPECT camera is used.
10. *SPECT reconstruction/filter*. Filtered backprojection is the suggested reconstruction method. Iterative methods can also be used when available and are required if attenuation correction is performed. Different SPECT reconstruction filters are preferred by different clinical sites. The suggested filter for each of the 16 gated frames is a Butterworth filter with 0.55 Nyquist frequency cutoff, and order of 7. If the study is count-poor (due to significant arrhythmias, poor tag, or other technical reasons), a Butterworth filter with 0.45 Nyquist frequency cutoff, and order of 7 may decrease statistical noise and improve the quality of the reconstruction. As algorithms become commercially available, iterative reconstruction methods will probably become the preferred approach. Temporal filling analogous to that employed in planar imaging (I.D.2) should be applied to raw data or to transverse reconstructed images of count-poor studies.
11. *Oblique reorientation*. Preferably, each of the 16 gated frames' transverse reconstructions are reoriented in short-axis oblique slices and, optionally, long-axis coronal slices, most commonly referred to as horizontal long-axis slices, and long-axis sagittal slices, most commonly referred to as vertical long-axis slices. Typical three-dimensional (3D) reconstructions of the SPECT ERNA data are accomplished using the short-axis oblique data only. However, long-axis views are often important when observing regional wall motion by cine-loop display of the oblique reformatted slice data. See paragraph 5 in the next section.

D. Assessment of Ventricular Function—Gated SPECT ERNA Imaging: Image Display and Quantification (Table 7)

1. *LV volume curve generation*.[66-71] Most parameters describing ventricular function are extracted from a complete LV volume curve in a manner similar to that employed for planar ERNA studies. Techniques that obtain this curve from either a single two-dimensional ROI drawn at end diastole (and modified at end systole as necessary) or using multiple ROIs drawn at each time point over the summed short-axis slices, which include the entire left ventricle but exclude the left atrium, have been used on occasion in the past but are outmoded and should be avoided. Most methods described for the quantification of LV volumes from SPECT ERNA employ 3D regions encompassing the entire left ventricle, but only the left ventricle, at each frame throughout the cardiac cycle. Like methods used to quantify LV volumes from gated SPECT perfusion studies, these methods sum the calibrated voxels and partial voxels within the defined 3D LV volume throughout the cardiac cycle. Unlike planar ERNA methods that employ TACs where background subtraction is required, SPECT methods are inherently volumetric and do not typically employ background subtraction. Several automatic or semiautomatic methods have been described, which in most patients are quick and accurate, although it is important that the automatic results be checked visually and modified as necessary. Irregularities in the LV contour occasionally occur using automatic algorithms and can have significant effects on the parameters extracted from the LV curve if not manually or semiautomatically corrected during user quality assurance. Definition of the mitral and aortic valve planes is the most difficult step in this quantification—this is the result of the activities within the LV, left atrium, and aortic blood pools all being generally of similar intensity and separated only by the relatively thin and sometimes poorly defined mitral and aortic valve planes.
2. *Background*. Background subtraction is not required and generally not performed for SPECT imaging. The inherently 3D nature of reconstructed SPECT images and the 3D surface rendering of the LV blood pool employed in most quantitative methods obviate the need for background correction (see paragraph 1 above).
3. *LVEF*. As discussed in paragraph 3 above, LVEF can be computed by applying an end-diastolic ROI to end-diastolic images and an end-systolic ROI to end-systolic images reconstructed from slices summed to include the entire left ventricle (but excluding other cardiac chambers). These are essentially adaptations of gated SPECT ERNA data sets to planar ERNA quantification programs. These are outdated and to be discouraged. Automatic or semiautomatic programs which are inherently volumetric and consider the left ventricle as a 3D object are the current standard. LV

Table 7. Quantitative parameters of ventricular function-gated SPECT ERNA imaging[7,63-65]

Parameter	Method		For information, see paragraph
LV volume curve generation	Automatic ROIs at end diastole or at each time point	Preferred	1
	Manual ROI at end diastole	Standard	1
Background LVEF	None	Standard	2
	Counts-based 2D/3D method	Preferred	3
	Geometrically based method	Optional	3
	Automated method	Optional	3
	From single end diastolic ROI	Optional	3
RVEF	Not well validated at this point	Optional	4
Wall motion	3D visual assessment of movie loop	Preferred	5
	Slice-based visual assessment of movie loop	Optional	5
	Regional EF	Optional	5
LV emptying	Peak/average rate of emptying	Optional	6
LV filling	Peak/average rate of filling	Optional	7
LV volumes	Counts based	Standard	8
	Pixel based	Optional	8

volume curves can be generated and LVEFs can be computed in a manner similar to what is done with planar ERNA. Although count-based methods can be used, with SPECT, volume-based methods are preferred. Optionally, a geometric-based method may be used to compute LVEF from EDVs and ESVs. LVEFs obtained from SPECT ERNA are likely to be higher than LVEF values determined from the planar ERNA method due to the complete removal of all activity from the left atrium. Preliminary results indicate that SPECT ERNA LVEFs are approximately 7 to 10 EF units higher than those determined from planar studies.[72] Fitting the LV curve with two or three harmonics and extracting the maximum and minimum points as the EDV and ESV values are sometimes employed. Volumetric methods are generally less affected by variations in sampling at the end of the cardiac cycle due to cycle length variation. Therefore, the end-diastolic frame may occur at either the beginning or the end of the cardiac frame cycle (frame 14, 15, or 16). If a nonvolumetric activity-based method is employed and the original TAC is produced from a single end-diastolic ROI, the EFs will be consistently lower than if the TAC is produced from multiple ROIs. In this case, SPECT ERNA LVEF values may be comparable to or less than multi-ROI planar ERNA calculations. Care must be taken when applying SPECT ERNA LVEF values to the evaluation of chemotherapy patients where standards have been established using planar methods. A thorough understanding of the differences between LVEF normal values between SPECT and planar studies is required.

4. *RVEF*. Unlike planar ERNA studies, accurate computation of RVEF may be possible with SPECT ERNA due to the removal of chamber overlap and the 3D nature of SPECT. Automatic volume-based methods to date have not been as well validated as those used for the left ventricle. Some studies validating RVEF values from SPECT ERNA have yielded positive results, although others have not.[73-75] The same activity-based techniques described in paragraphs 1 and 3 above can be applied for the measurement of RVEF, but as was the case for the left ventricle, they are also discouraged for RV analysis. All of the same considerations mentioned above for the left ventricle also hold for the right ventricle, but since the RV chamber is geometrically more complex than the left ventricle, final results may vary.
5. *Wall motion*.[60,66,67,76,77] Regional wall motion in SPECT ERNA may be determined from cine displays of multiple long- and short-axis slices and from 3D displays of the cardiac chambers in cine-loop fashion (preferred). The 3D displays may be shaded-surface and/or wire-frame displays or, optionally, volume-rendered displays. These 3D images are best displayed in multiple cardinal views or rotated under user control. Cine-loop displays of long- and short-axis slices are standard on most commercial computer systems as part of gated SPECT software packages. Wall motion analyses by SPECT ERNA may be the most useful application of this technique and can be performed on most commercial systems. Optionally, regional EFs can be computed from the segmented left ventricle and have been shown to be helpful in identifying wall motion defects in patients with coronary artery disease. Alternatively, two-dimensional planar projections can be easily generated from the 3D data sets to permit viewing of cine images from a variety of projection angles.

   SPECT ERNA has been used for the assessment of left and right ventricular activation sequences and the identification of the sites of AV nodal bypass tracks, as well as LV and RV arrhythmias.[78-81] A newer application of SPECT ERNA has been the study of activation sequences to calculate parameters of ventricular synchrony such as the site of last activation useful in guiding resynchronization therapy for congestive heat failure.[82] These uses have been recently reviewed, but unfortunately, these applications currently remain available only to research laboratories since there is no commercially available software that performs these functions.[64,82]
6. *LV emptying*. LV emptying, average and maximum, may be computed in similar fashion to planar ERNA methods, as can the systolic ejection period.
7. *LV filling*. LV filling, average and maximum, may be computed in similar fashion to planar ERNA methods, as can the diastolic filling period(s).
8. *LV volumes*.[66-71] LV volumes can be accurately computed using SPECT ERNA techniques. LV surface rendering methods are inherently volumetric and are less hampered by chamber overlap. Moreover, the spatial distribution of the left ventricle is more clearly delineated. The most straightforward approach for LV volume determination that involves no geometric assumptions is to sum the 3D pixels (voxels) contained within the LV volume of interest, excluding all other structures, and multiply the number of voxels by the calibrated voxel volume. With the calibrated voxel volume (a standard system measurement on all modern SPECT systems), LV volumes at end diastole and end systole and throughout the cardiac cycle can be easily computed. Although many individual studies have compared LV volumes to those derived from cardiac contrast ventriculography going back as far as the early 1980s and, more recently, against cardiac

III. EQUILIBRIUM RADIONUCLIDE ANGIOCARDIOGRAPHY: GUIDELINE FOR INTERPRETATION (TABLE 8)

Table 8. Guideline for interpretation

		For information, see paragraph	
		Planar	**SPECT**
Display			
Quad screen cinematic display	Standard	I.D.1	II.D.1 and .5
Time smoothing	Standard	I.D.2	II.C.10
Spatial smoothing	Optional	I.D.2	II.C.10
Quality control			
Image quality			
Statistics-qualitative	Standard	I.B.2	II.C.10
Statistics-quantitative	Optional	I.C.9	II.C.8 and .10
Labeling efficiency-qualitative	Standard	I.B.2	I.B.2
Appropriate imaging angles	Standard	I.C.10	II.C.8 and .9
Appropriate zoom	Standard	I.C.2	II.C.3
Attenuation	Standard	I.F.2	-
Processing accuracy			
Ventricular ROIs	Standard	I.D.3 and .5	II.D.1 and .3
Background ROIs	Standard	I.D.4	II.D.2
Volume curve(s)	Standard	I.D.3	II.D.1
Image analysis			
Cardiac rhythm and conduction	Standard	I.D.6	II.C.5 and II.D.5
LV size			
Qualitative	Standard	I.F.4.a	II.D.8
Quantitative volume	Preferred	I.D.9	II.D.8
LV regional wall motion			
Qualitative	Standard	I.D.6	II.D.5
Semiquantitative	Optional	I.D.6	II.D.5
Quantitative	Optional	I.D.6	II.D.5
LVEF	Standard	I.D.5	II.D.3
LV diastolic filling			
Qualitative	Standard	I.D.8	II.D.7
Quantitative	Preferred	I.D.8	II.D.7
RV size			
Qualitative	Standard	I.D.11 and I.F.4.b	II.D.4
Quantitative	Optional	I.D.11 and I.F.4.b	II.D.4
RV regional wall motion	Standard	I.D.12	II.D.5
RVEF	Optional	I.D.10	II.D.4
Atrial sizes	Standard	I.F.4.c	-
Aortic and pulmonary artery sizes	Standard	I.F.7	-
LV hypertrophy	Optional	I.F.5	-
Pericardial space	Standard	I.F.6	-
Activity outside heart and great vessels	Standard	I.F.3	-
Exercise/intervention study			
Display	Standard	I.E.1	-
Regional wall motion: Changes from rest	Standard	I.E.2	-
Chamber size: Changes from rest	Standard	I.E.3	-
LVEF, RVEF: Changes from rest	Standard	I.E.4	-
Conclusion			
Correlation with clinical data	Standard	I.E.5	I.E.5
Comparison to previous studies	Standard	I.E.5	I.E.5

IV. EQUILIBRIUM RADIONUCLIDE ANGIOCARDIOGRAPHY: GUIDELINE FOR REPORTING (TABLE 9)

Table 9. Guideline for reporting

		For information, see paragraph	
		Planar	**SPECT**
Demographic data			
Name	Standard		
Gender	Standard		
Age	Standard		
Ethnic background	Optional		
Date acquisition	Standard		
Medical record number for inpatient	Standard		
Height/weight body surface area	Standard		
Acquisition parameters			
Type of study	Standard		
Radionuclide/dose	Standard		
Indication for study	Standard	I.A. and V.	I.A. and V.
Study quality	Optional	I.B.2 and I.C.6 and I.E.6	II.C.5 and .10
Results: Rest			
LV size			
Qualitative	Standard	I.F.4.a	II.D.8
Quantitative	Optional	I.D.9	II.D.8
LV regional wall motion	Standard	I.D.6	II.D.5
LV hypertrophy	Optional	I.F.5	-
LVEF	Standard	I.D.5	II.D.3
LV diastolic function			
Qualitative	Standard	I.D.8	II.D.7
Quantitative	Preferred	I.D.8	II.D.7
RV size			
Qualitative	Standard	I.D.11 and I.F.4.b	-
Quantitative	Standard	I.D.11	II.D.4
RV regional wall motion	Standard	I.D.12	II.D.5
RVEF	Optional	I.D.10	II.D.4
Atrial sizes	Optional	I.F.4.c	-
Aortic and pulmonary artery size	Optional	I.F.7	-
Results: Exercise/intervention parameters			
Type of exercise/intervention protocol	Standard	I.E.7	-
Symptom(s)	Standard	I.E.8	-
Peak heart rate and blood pressure	Standard	I.E.8	-
METS achieved or percent maximum heart rate	Optional	I.E.8	-
Results: Exercise/intervention ERNA data			
LV size: Change from rest			
Qualitative	Standard	I.E.3	II.D.5
Quantitative	Preferred	I.E.4	II.D.3
LV regional wall motion Change from rest	Standard	I.E.2	II.D.5
LVEF exercise	Standard	I.E.4	NA
RV size: Change from rest	Standard	I.E.3	-
RV regional wall motion: Change from rest	Standard	I.E.2	-
RVEF exercise	Optional	I.E.4	-

Table 9 continued

		For information, see paragraph	
		Planar	**SPECT**
Conclusion			
Normal or abnormal	Standard	I.F.8	I.F.8
Diagnostic significance of rest/exercise response	Standard	I.F.8	NA
Prognostic significance of rest/exercise response	Optional	I.F.8	NA
Comparison to previous results	Standard	I.E.5	I.E.5

NA, Not applicable; *METs*, metabolic equivalents

contrast ventriculography and gated magnetic resonance imaging (see cautions discussed in paragraph 3 above), as a caution, LV volumes have not been validated extensively with any one of the commercially available quantitative programs.[83]

V. GUIDELINES FOR CLINICAL USE OF RADIONUCLIDE ANGIOCARDIOGRAPHY

The American College of Cardiology, American Heart Association, and American Society of Nuclear Cardiology have developed guidelines for the use of radionuclide imaging of the heart. Table 10 has been adapted from these guidelines. Note that items may be categorized as class III if not enough data are presently available to substantiate routine clinical implementation.[84,85]

Table 10. Indications for equilibrium radionuclide angiocardiography (rest and/or exercise)

	Planar	**SPECT**
Diagnosis of acute coronary end diastole syndromes		
Suspected ACS in the ED with nondiagnostic electrocardiogram and biomarkers	III	III
Detection of AMI when conventional measures are nondiagnostic	III	III
Diagnosis of STE AMI	III	III
Risk assessment and assessment of prognosis and therapy after STE AMI		
Rest LV function	I	I
Rest RV function after suspected RV infarction	IIa	IIa
Presence of stress-induced ischemia and myocardium at risk	IIb	III
Detection of infarct size and residual viable myocardium	III	III
Predicting improvement in regional and global LV function after revascularization	IIb	IIb
Diagnosis, prognosis and assessment of therapy in patients with unstable angina/NSTEMI		
Measurement of LV function	I	I
Identification of ischemia in the distribution of the culprit lesion or in remote areas	IIb	III
Identification of severity and extent of disease in stabilized patients on medical therapy	IIb	III
Identification of severity/extent of disease with ongoing ischemia and nondiagnostic electrocardiogram	IIb	III
Diagnosis of myocardial ischemia when history and ECG changes are unreliable	IIb	III
Diagnosis of chronic CAD		
Assessment of ventricular performance (rest/exercise)	I/I	I/III
Diagnosis of symptomatic and selected asymptomatic patients with myocardial ischemia	IIb	III
Planning PTCA—identifying lesions causing ischemia, if not otherwise known	III	III
Risk stratification before noncardiac surgery in selected patients	IIb	III
Screening of asymptomatic patients with low likelihood of disease	III	III

Table 10 continued

	Planar	SPECT
Assessment of severity, prognosis, and risk stratification of chronic CAD		
Assessment of LV performance	I	I
Identification of extent, severity, and localization of ischemia	IIb	IIb
Risk stratification of patients with intermediate risk Duke treadmill score	III	IIb
Assessment of functional significance of intermediate coronary stenosis	IIb	IIb
Assessment of interventions in chronic CAD		
Assessment for restenosis after PCI (symptomatic)	IIb	III
Assessment of ischemia in symptomatic patients after CABG	IIb	III
Assessment 3–5 years after CABG or PCI in select patients, high-risk asymptomatic	IIb	III
Routine assessment of asymptomatic patients after PTCA or CABG	III	III
CHF		
Determination of initial LV and RV performance	I	I
RV dysplasia	IIa	IIb
Initial or serial assessment of ventricular function with exercise	IIb	III
Routine serial assessment of LV and RV function at rest	IIb	IIb
Initial and followup evaluation of LV function in patients receiving cardiotoxic drugs	I	IIb
Assessment of myocardial viability in patients with CAD and LV dysfunction	III	III
Assessment of the co-presence of coronary heart disease in patients without angina	IIb	III
Detection of myocarditis	III	III
Diagnosis and serial monitoring of hypertensive hypertrophic heart disease	IIb	IIb
Diagnosis of CAD in patients with hypertrophic cardiomyopathy	III	III
Diagnosis and serial monitoring of hypertrophic cardiomyopathy	III	III
After cardiac transplantation		
Assessment of ventricular performance	I	I
Detection and assessment of coronary vasculopathy	IIb	IIb
Valvular heart disease		
Initial and serial assessment of LV and RV function at rest	I	I
Initial and serial assessment of LV and RV function with exercise	IIb	III
Assessment of concomitant CAD	IIb	III
Congenital heart disease		
Initial and serial assessment of LV and RV function	I	I

Acknowledgement

Dr. Van Kriekinge receives partial royalties from the licensing of the Quantitative Blood Pool SPECT (QBS) algorithm owned by Cedars-Sinai Medical Center.

References

1. Recalculated dose data for 19 frequently used radiopharmaceuticals from ICRP Publication 53. Technetium-labelled erythrocytes (RBC) Tc-99m. Ann ICRP 1998;28:61.
2. Callahan RJ, Froelich JW, McKusick KA, Leppo J, Strauss HW. A modified method for the in vivo labeling of red blood cells with Tc-99m: Concise communication. J Nucl Med 1982;23:315–8.
3. UltraTag RBC. St. Louis: Mallinckrodt Medical; 1992 [package insert].
4. Gerson MC, editor. Cardiac nuclear medicine. 3rd ed. New York: McGraw-Hill, Health Professions Division; 1997.
5. Kelly MJ, Cowie AR, Antonino A, Barton H, Kalff V. An assessment of factors which influence the effectiveness of the modified in vivo technetium-99m-erythrocyte labeling technique in clinical use. J Nucl Med 1992;33:2222–5.
6. Bacharach SL, Green MV, Borer JS. Instrumentation and data processing in cardiovascular nuclear medicine: evaluation of ventricular function. Semin Nucl Med 1979;9:257–74.
7. Groch MW. Cardiac function: gated cardiac blood pool and first pass imaging. St. Louis: Mosby; 1996.
8. DePuey EG. Evaluation of cardiac function with radionuclides. In: Gottschalk A, Hoffer PB, Potchen EJ, editors. Diagnostic nuclear medicine. Baltimore: Williams and Wilkins; 1998.
9. Garcia EV. Physics and instrumentation of radionuclide imaging. Philadelphia: Saunders; 1991.
10. Garcia EV, Bateman TM, Berman DS, Maddahi J. Computer techniques for optimal radionuclide assessment of the heart. Baltimore: Williams and Wilkins; 1988.
11. Wackers FJT. Equilibrium radionuclide angiocardiography. 3rd ed. New York: McGraw Hill; 1997.
12. Bacharach SL, Green MV, Borer JS, Hyde JE, Farkas SP, Johnson GS. Left ventricular peak ejection rate, filling rate and ejection fraction: frame rate requirements at rest and exercise. J Nucl Med 1979;20:189–93.

13. Bacharach SL, Green MV, Bonow RO, Findley SL, Ostrow HG, Johnston GS. Measurement of ventricular function by ECG gating during atrial fibrillation. J Nucl Med 1981;22:226–31.
14. Strauss HW, Zaret BL, Hurley PJ, Natarajan TK, Pitt B. A scintiphotographic method for measuring left ventricular ejection fraction in man without cardiac catheterization. Am J Cardiol 1971;28:575–80.
15. Miller TR, Goldman KJ, Epstein DM, Biello DR, Sampathkumaran KS, Kumar B, et al. Improved interpretation of gated cardiac images by use of digital filters. Radiology 1984;152:795–800.
16. Steckley RA, Kronenberg MW, Born ML, Rhea TC, Bateman JE, Rollo FD, et al. Radionuclide ventriculography: Evaluation of automated and visual methods for regional wall motion analysis. Radiology 1982;142:179–85.
17. Cahill PT, Ornstein E, Ho SL. Edge detection algorithms in nuclear medicine. IEEE Trans Nucl Sci 1976;23:555–9.
18. Chang W, Henkin RE, Hale DJ, Hall D. Methods for detection of left ventricular edges. Semin Nucl Med 1980;10:39–53.
19. Jackson PC, Allen-Narker R, Davies ER, Rees JR, Wilde P, Watt I. The assessment of an edge detection algorithm in determining left ventricular ejection fraction using radio-nuclide multiple gated acquisition and contrast ventriculography. Eur J Nucl Med 1982;7:62–5.
20. Groch MW, Erwin WD, Murphy PH, Ali A, Moore W, Ford P, et al. Validation of a knowledge-based boundary detection algorithm: a multicenter study. Eur J Nucl Med 1996;23:662–8.
21. Zaret BL, Strauss HW, Hurley PJ, Natarajan TK, Pitt B. A noninvasive scintiphotographic method for detecting regional ventricular dysfunction in man. N Engl J Med 1971;284: 1165–70.
22. Pavel DG, Byron E, Bianco JA, Zimmer AM. A method for increasing the accuracy of the radionuclide measurement of ejection fraction and left ventricular volume curve [abstract]. J Nucl Med 1977;18:641.
23. Maddox DE, Holman BL, Wynne J, Idoine J, Parker JA, Uren R, et al. Ejection fraction image: A noninvasive index of regional left ventricular wall motion. Am J Cardiol 1978;41:1230–8.
24. Murphy PH. ECG gating: does it adequately monitor ventricular contraction? J Nucl Med 1980;21:399–401.
25. Cavailloles F, Bazin JP, Di Paola R. Factor analysis in gated cardiac studies. J Nucl Med 1984;25:1067–79.
26. Wendt RE, Murphy PH, Treffert JD, Groch MW, Erwin WD, Schneider PM, et al. Application and interpretation of principal component analysis of gated cardiac images [abstract]. J Nucl Med 1993;34:175P.
27. Wendt RE, Murphy PA, Schneider PM, Treffert JD, Groch MW, Ford PV, et al. Lossy compression of dynamic studies using eigenimage methods [abstract]. J Nucl Med 1994;35:P178.
28. Rosenbush SW, Ruggie N, Turner DA, Von Behren PL, Denes P, Fordham EW, et al. Sequence and timing of ventricular wall motion in patients with bundle branch block. Assessment by radionuclide cineangiography. Circulation 1982;66:1113–9.
29. Watson DD, Liedholdt EM, Carabello ME, et al. Gated blood pool imaging in patients with atrial fibrillation [abstract]. J Nucl Med 1981;22:P153.
30. Wagner RH, Halama JR, Henkin RE, Dillehay GL, Sobotka PA. Errors in the determination of left ventricular functional parameters. J Nucl Med 1989;30:1870–4.
31. Bonow RO, Bacharach SL, Green MV, Kent KM, Rosing DR, Lipson LC, et al. Impaired left ventricular diastolic filling in patients with coronary artery disease: assessment with radionuclide angiography. Circulation 1981;64:315–23.
32. Mancini GB, Slutsky RA, Norris SL, Bhargava V, Ashburn WL, Higgins CB. Radionuclide analysis of peak filling rate, filling fraction, and time to peak filling rate. Response to supine bicycle exercise in normal subjects and patients with coronary disease. Am J Cardiol 1983;51:43–51.
33. Lee FA, Fetterman R, Zaret BL, Wackers FJT. Rapid radionuclide derived systolic and diastolic cardiac function using cycle-dependent background correction and Fourier analysis. Proc Comput Cardiol 1985;443–6
34. Seals AA, Verani MS, Tadros S, Mahmarian JJ, Roberts R. Comparison of left ventricular diastolic function as determined by nuclear cardiac probe, radionuclide angiography, and contrast cineangiography. J Nucl Med 1986;27:1908–15.
35. Bauch TD, Rubal BJ, Lecce MD, Smith TE, Groch MW. S2 triggered gated blood pool imaging for assessment of diastole. Biomed Sci Instrum 1995;31:201–6.
36. Slutsky R, Karliner J, Ricci D, Kaiser R, Pfisterer M, Gordon D, et al. Left ventricular volumes by gated equilibrium radionuclide angiography: A new method. Circulation 1979;60:556–64.
37. Dehmer GJ, Firth BG, Lewis SE, Willerson JT, Hillis LD. Direct measurement of cardiac output by gated equilibrium blood pool scintigraphy: Validation of scintigraphic volume measurements by a nongeometric technique. Am J Cardiol 1981;47:1061–7.
38. Bourguignon MH, Schindledecker JG, Carey GA, Douglass KH, Burow RD, Camargo EE, et al. Quantification of left ventricular volume in gated equilibrium radioventriculography. Eur J Nucl Med 1981;6:349–53.
39. Links JM, Becker LC, Shindledecker JG, Guzman P, Burow RD, Nickoloff EL, et al. Measurement of absolute left ventricular volume from gated blood pool studies. Circulation 1982;65:82–91.
40. Massardo T, Gal RA, Grenier RP, Schmidt DH, Port SC. Left ventricular volume calculation using a count-based ratio method applied to multigated radionuclide angiography. J Nucl Med 1990;31:450–6.
41. Berger HJ, Matthay RA, Loke J, Marshall RC, Gottschalk A, Zaret BL. Assessment of cardiac performance with quantitative radionuclide angiocardiography: Right ventricular ejection fraction with reference to findings in chronic obstructive pulmonary disease. Am J Cardiol 1978;41:897–905.
42. Brent BN, Mahler D, Matthay RA, Berger HJ, Zaret BL. Noninvasive diagnosis of pulmonary arterial hypertension in chronic obstructive pulmonary disease: Right ventricular ejection fraction at rest. Am J Cardiol 1984;53:1349–53.
43. Winzelberg GG, Boucher CA, Pohost GM, McKusick KA, Bingham JB, Okada RD, et al. Right ventricular function in aortic and mitral valve disease: Relation of gated first-pass radionuclide angiography to clinical and hemodynamic findings. Chest 1981;79:520–8.
44. Maddahi J, Berman DS, Matsuoka DT, Waxman AD, Stankus KE, Forrester JS, et al. A new technique for assessing right ventricular ejection fraction using rapid multiple-gated equilibrium cardiac blood pool scintigraphy. Description, validation and findings in chronic coronary artery disease. Circulation 1979;60:581–9.
45. Pryor DB, Harrell FE, Lee KL, Rosati RA, Coleman RE, Cobb FR, et al. Prognostic indicators from radionuclide angiography in medically treated patients with coronary artery disease. Am J Cardiol 1984;53:18–22.
46. Lee KL, Pryor DB, Pieper KS, Harrell FE, Califf RM, Mark DB, et al. Prognostic value of radionuclide angiography in medically treated patients with coronary artery disease. A comparison with clinical and catheterization variables. Circulation 1990;82:1705–17.
47. Borer JS, Bacharach SL, Green MV, Kent KM, Epstein SE, Johnston GS. Real-time radionuclide cineangiography in the noninvasive evaluation of global and regional left ventricular function at rest and during exercise in patients with coronary-artery disease. N Engl J Med 1977;296:839–44.

48. Borer JS, Kent KM, Bacharach SL, Green MV, Rosing DR, Seides SF, et al. Sensitivity, specificity and predictive accuracy of radionuclide cineangiography during exercise in patients with coronary artery disease. Comparison with exercise electrocardiography. Circulation 1979;60:572–80.
49. Turner DA, Shima MA, Ruggie N, Von Behren PL, Jarosky MJ, Ali A, et al. Coronary artery disease: Detection by phase analysis of rest/exercise radionuclide angiocardiograms. Radiology 1983;148:539–45.
50. Poliner LR, Dehmer GJ, Lewis SE, Parkey RW, Blomqvist CG, Willerson JT. Left ventricular performance in normal subjects: A comparison of the responses to exercise in the upright and supine positions. Circulation 1980;62:528–34.
51. Dehmer GJ, Lewis SE, Hillis LD, Corbett J, Parkey RW, Willerson JT. Exercise-induced alterations in left ventricular volumes and the pressure-volume relationship: A sensitive indicator of left ventricular dysfunction in patients with coronary artery disease. Circulation 1981;63:1008–18.
52. Dehmer GJ, Firth BG, Nicod P, Lewis SE, Hillis LD. Alterations in left ventricular volumes and ejection fraction during atrial pacing in patients with coronary artery disease: Assessment with radionuclide ventriculography. Am Heart J 1983;106:114–24.
53. Port S, Cobb FR, Coleman RE, Jones RH. Effect of age on the response of the left ventricular ejection fraction to exercise. N Engl J Med 1980;303:1133–7.
54. Port S, McEwan P, Cobb FR, Jones RH. Influence of resting left ventricular function on the left ventricular response to exercise in patients with coronary artery disease. Circulation 1981;63:856–63.
55. Gibbons RJ, Lee KL, Cobb F, Jones RH. Ejection fraction response to exercise in patients with chest pain and normal coronary arteriograms. Circulation 1981;64:952–7.
56. Port SC, Oshima M, Ray G, McNamee P, Schmidt DH. Assessment of single vessel coronary artery disease: Results of exercise electrocardiography, thallium-201 myocardial perfusion imaging and radionuclide angiography. J Am Coll Cardiol 1985;6:75–83.
57. Wackers FJ, Berger HJ, Johnstone DE, Goldman L, Reduto LA, Langou RA, et al. Multiple gated cardiac blood pool imaging for left ventricular ejection fraction: Validation of the technique and assessment of variability. Am J Cardiol 1979;43:1159–66.
58. DePace NL, Iskandrian AS, Hakki AH, Kane SA, Segal BL. Value of left ventricular ejection fraction during exercise in predicting the extent of coronary artery disease. J Am Coll Cardiol 1983;1:1002–10.
59. Foster C, Dymond DS, Anholm JD, Pollock ML, Schmidt DH. Effect of exercise protocol on the left ventricular response to exercise. Am J Cardiol 1983;51:859–64.
60. Moore ML, Murphy PH, Burdine JA. ECG-gated emission computed tomography of the cardiac blood pool. Radiology 1980;134:233–5.
61. Corbett JR, Jansen DE, Willerson JT. Radionuclide ventriculography: I. Technical aspects. Am J Physiol Imaging 1987;2:33–43.
62. Corbett JR, Jansen DE, Willerson JT. Radionuclide ventriculography: II. Anatomic and physiologic aspects. Am J Physiol Imaging 1987;2:85–104.
63. Corbett JR. Gated blood-pool SPECT. In: DePuey EG, Berman DS, Garcia EV, editors. Cardiac SPECT imaging. New York: Raven Press; 1995. p. 257–73.
64. Ficaro EP, Corbett JR. Gated blood-pool SPECT. In: DePuey EG, Berman DS, Garcia EV, editors. Cardiac SPECT imaging. 2nd ed. Philadelphia: Lippincott Williams & Wilkins; 2001. p. 321–37.
65. Quaife RA, Corbett JR. Radionuclide ventriculography. In: McGhie AI, editor. Handbook of non-invasive cardiac testing. New York: Oxford University Press; 2001. p. 55–98.
66. Gill JB, Moore RH, Tamaki N, Miller DD, Barlai-Kovach M, Yasuda T, et al. Multigated blood-pool tomography: New method for the assessment of left ventricular function. J Nucl Med 1986;27:1916–24.
67. Corbett JR, Jansen DE, Lewis SE, Gabliani GI, Nicod P, Filipchuk NG, et al. Tomographic gated blood pool radionuclide ventriculography: Analysis of wall motion and left ventricular volumes in patients with coronary artery disease. J Am Coll Cardiol 1985;6:349–58.
68. Faber TL, Stokely EM, Templeton GH, Akers MS, Parkey RW, Corbett JR. Quantification of three-dimensional left ventricular segmental wall motion and volumes from gated tomographic radionuclide ventriculograms. J Nucl Med 1989;30:638–49.
69. Groch MW, Leidholdt EM, Marshall RA, et al. Gated blood pool SPECT imaging: Sources of artifacts [abstract]. Clin Nucl Med 1991;16:717
70. Chin BB, Bloomgarden DC, Xia W, Kim HJ, Fayad ZA, Ferrari VA, et al. Right and left ventricular volume and ejection fraction by tomographic gated blood-pool scintigraphy. J Nucl Med 1997;38:942–8.
71. Groch MW, Schippers DJ, Marshall RC, Barnett C. A quantitative program for gated blood pool SPECT imaging [abstract]. Clin Nucl Med 1991;16:713.
72. Bartlett ML, Srinivasan G, Barker WC, Kitsiou AN, Dilsizian V, Bacharach SL. Left ventricular ejection fraction: Comparison of results from planar and SPECT gated blood-pool studies. J Nucl Med 1996;37:1795–9.
73. Nichols K, Humayun N, De Bondt P, Vandenberghe S, Akinboboye OO, Bergmann SR. Model dependence of gated blood pool SPECT ventricular function measurements [see comment]. J Nucl Cardiol 2004;11:282–92.
74. Nichols K, Saouaf R, Ababneh AA, Barst RJ, Rosenbaum MS, Groch MW, et al. Validation of SPECT equilibrium radionuclide angiographic right ventricular parameters by cardiac magnetic resonance imaging [see comment]. J Nucl Cardiol 2002;9:153–60.
75. Slart RH, Poot L, Piers DA, van Veldhuisen DJ, Jager PL. Evaluation of right ventricular function by NuSMUGA software: Gated blood-pool SPECT vs. first-pass radionuclide angiography. Int J Cardiovasc Imaging 2003;19:401–7.
76. Underwood SR, Walton S, Ell PJ, Jarritt PH, Emanuel RW, Swanton RH. Gated blood-pool emission tomography: A new technique for the investigation of cardiac structure and function. Eur J Nucl Med 1985;10:332–7.
77. McGhie AL, Faber TL, Willerson JT, Corbett JR. Evaluation of left ventricular aneurysm after acute myocardial infarction using tomographic radionuclide ventriculography. Am J Cardiol 1995;75:720–4.
78. Daou D, Lebtahi R, Faraggi M, Petegnief Y, Le Guludec D. Cardiac gated equilibrium radionuclide angiography and multiharmonic Fourier phase analysis: Optimal acquisition parameters in arrhythmogenic right ventricular cardiomyopathy. J Nucl Cardiol 1999;6:429–37.
79. Botvinick EH, O'Connell JW, Kadkade PP, Glickman SL, Dae MW, Cohen TJ, et al. Potential added value of three-dimensional reconstruction and display of single photon emission computed tomographic gated blood pool images. J Nucl Cardiol 1998;5:245–55.
80. Le Guludec D, Gauthier H, Porcher R, Frank R, Daou D, Benelhadj S, et al. Prognostic value of radionuclide angiography in patients with right ventricular arrhythmias. Circulation 2001;103:1972–6.
81. Le Guludec D, Slama MS, Frank R, Faraggi M, Grimon G, Bourguignon MH, et al. Evaluation of radionuclide angiography in

diagnosis of arrhythmogenic right ventricular cardiomyopathy. J Am Coll Cardiol 1995;26:1476–83.
82. Botvinick EH. Scintigraphic blood pool and phase image analysis: the optimal tool for the evaluation of resynchronization therapy. J Nucl Cardiol 2003;10:424–8.
83. Cahill JM, Chen MY, Ficaro EP, Corbett JR, Quaife RA. Validation of 4D-MSPECT analysis method for Tc-99m gated blood pool tomography: comparison of LV ejection fractions and volumes to magnetic resonance imaging [abstract]. J Nucl Cardiol 2003;10:S20.
84. Lee TH, Udelson JE. Nuclear cardiology. In: Zipes DP, Libby P, Bonow RO, Braunwald E, editors. Braunwald's heart disease: A textbook of cardiovascular medicine. 7th ed. Philadelphia: Saunders; 2005.
85. Klocke FJ, Baird MG, Bateman TM, Berman DS, Carabello BA, Cerquerira MD, et al. ACC/AHA/ASNC guidelines for the Clinical Use of Cardiac Radionuclide Imaging. A report of the American College of Cardiology/American Heart Association Task Force on Practice Guidelines (ACC/AHA/ASNC Committee to Revise the 1995 Guidelines for the Clinical Use of Radionuclide Imaging) 2003. American College of Cardiology web site. Available from: URL: http://www.acc.org/qualityandscience/clinical/guidelines/radio/index.pdf. Accessed February 11, 2008.

ASNC IMAGING GUIDELINES FOR NUCLEAR CARDIOLOGY PROCEDURES

Stress protocols and tracers

Milena J. Henzlova, MD,[a] Manuel D. Cerqueira, MD,[b] Christopher L. Hansen, MD,[c] Raymond Taillefer, MD,[d] and Siu-Sun Yao, MD[e]

EXERCISE STRESS TEST

Exercise is the preferred stress modality in patients who are able to exercise to an adequate workload (at least 85% of age-adjusted maximal predicted heart rate and five metabolic equivalents).

Exercise Modalities

1. Treadmill exercise is the most widely used stress modality. Several treadmill exercise protocols are described which differ in the speed and grade of treadmill inclination and may be more appropriate for specific patient populations. The Bruce and modified Bruce protocosls are the most widely used exercise protocols.
2. Upright bicycle exercise is commonly used in Europe. This is preferable if dynamic first-pass imaging is planned during exercise. Supine or semi-supine exercise is relatively suboptimal and should only be used while performing exercise radionuclide angiocardiography.

Indications

Indications for an exercise stress test are:

1. Detection of obstructive coronary artery disease (CAD) in the following:
   (a) Patients with an intermediate pretest probability of CAD based on age, gender, and symptoms.
   (b) Patients with high-risk factors for CAD (e.g., diabetes mellitus, peripheral, or cerebral vascular disease).
2. Risk stratification of post-myocardial infarction patients before discharge (submaximal test at 4-6 days), and early (symptom-limited at 14-21 days) or late (symptom-limited at 3-6 weeks) after discharge.
3. Risk stratification of patients with chronic stable CAD into a low-risk category that can be managed medically or into a high-risk category that should be considered for coronary revascularization.
4. Risk stratification of low-risk acute coronary syndrome patients (without active ischemia and/or heart failure 6-12 hours after presentation) and of intermediate-risk acute coronary syndrome patients 1-3 days after presentation (without active ischemia and/or heart failure symptoms).
5. Risk stratification before noncardiac surgery in patients with known CAD or those with high-risk factors for CAD.
6. To evaluate the efficacy of therapeutic interventions (anti-ischemic drug therapy or coronary revascularization) and in tracking subsequent risk based on serial changes in myocardial perfusion in patients with known CAD.

Absolute Contraindications

Absolute contraindications for exercise stress testing include:

1. High-risk unstable angina. However, patients with chest pain syndromes at presentation, who are otherwise stable and pain-free, can undergo exercise stress testing.
2. Decompensated or inadequately controlled congestive heart failure.
3. Uncontrolled hypertension (blood pressure >200/110 mm Hg).
4. Uncontrolled cardiac arrhythmias (causing symptoms or hemodynamic compromise).

From the Mount Sinai Medical Center,[a] New York, NY; Cleveland Clinic Foundation,[b] Cleveland, OH; Jefferson Heart Institute,[c] Philadelphia, PA; Centre Hospitalier de lóUniversite de Montreal,[d] St. Jean-sur-Richelieu, QC, Canada and St. Lukeós-Roosevelt Hospital,[e] Jericho, NY.

Approved by the American Society of Nuclear Cardiology Board of Directors on June 24, 2008. Last updated on January 16, 2009.

Unless reaffirmed, retired or amended by express action of the Board of Directors of the American Society of Nuclear Cardiology, this guideline shall expire as of March 2014.

Reprint requests: Milena J. Henzlova, MD, Mount Sinai Medical Center, New York, NY.

J Nucl Cardiol
1071-3581/$34.00

doi:10.1007/s12350-009-9062-4

5. Severe symptomatic aortic stenosis.
6. Acute pulmonary embolism.
7. Acute myocarditis or pericarditis.
8. Acute aortic dissection.
9. Severe pulmonary hypertension.
10. Acute myocardial infarction (<4 days).
11. Acutely ill for any reason.

Relative Contraindications

Relative contraindications for exercise stress testing include:

1. Known left main coronary artery stenosis.
2. Moderate aortic stenosis.
3. Hypertrophic obstructive cardiomyopathy or other forms of outflow tract obstruction.
4. Significant tachyarrhythmias or bradyarrhythmias.
5. High-degree atrioventricular (AV) block.
6. Electrolyte abnormalities.
7. Mental or physical impairment leading to inability to exercise adequately.
8. If combined with imaging, patients with complete left bundle branch block (LBBB), permanent pacemakers, and ventricular pre-excitation (Wolff-Parkinson-White syndrome) should preferentially undergo pharmacologic vasodilator stress test (not dobutamine stress test).

Limitations

Exercise stress testing has a lower diagnostic value in patients who cannot achieve an adequate heart rate and blood pressure response due to a noncardiac physical limitation such as pulmonary, peripheral vascular, or musculoskeletal abnormalities or due to lack of motivation. These patients should be considered for pharmacologic stress with myocardial perfusion imaging.

Procedure

1. Patient preparation: Nothing to eat 2 hours before the test. Patients scheduled for later in the morning may have a very light (cereal, fruit) breakfast.
2. A large-bore (18- to 20-gauge) intravenous (IV) cannula should be inserted for radiopharmaceutical injection during exercise.
3. The electrocardiogram should be monitored continuously during the exercise test and for at least 5 minutes into the recovery phase or until the resting heart rate is <100 beats/minute and/or dynamic exercise-induced ST-segment changes have resolved. A 12-lead electrocardiogram should be obtained at every stage of exercise, at peak exercise, and at the termination or recovery phase.
4. The heart rate and blood pressure should be recorded at least every 3 minutes during exercise, at peak exercise, and for at least 5 minutes into the recovery phase.
5. **All exercise tests should be symptom-limited. Achievement of 85% of maximum, age-adjusted, predicted heart rate is not an indication for termination of the test.**
6. The radiopharmaceutical should be injected as close to peak exercise as possible. Patients should be encouraged to exercise for at least 1 minute after the radiotracer injection.
7. In patients who cannot exercise adequately and are being referred for a diagnostic stress test the patients may be considered for conversion to a pharmacologic stress test.
8. Blood pressure medication(s) with antianginal properties (β-blocker, calcium channel blocker, and nitrates) will lower the diagnostic accuracy of a stress test. Generally, discontinuation of these medicines may be left to the discretion of the referring physician.

Indications for Early Termination of Exercise

Indications for early termination of exercise include:

1. Moderate-to-severe angina pectoris.
2. Marked dyspnea or fatigue.
3. Ataxia, dizziness, or near-syncope.
4. Signs of poor perfusion (cyanosis and pallor).
5. Patient's request to terminate the test.
6. Excessive ST-segment depression (>2 mm).
7. ST elevation (>1 mm) in leads without diagnostic Q waves (except for leads V_1 or aVR).
8. Sustained supraventricular or ventricular tachycardia.
9. Development of LBBB or intraventricular conduction delay that cannot be distinguished from ventricular tachycardia.
10. Drop in systolic blood pressure of >10 mm Hg from baseline, despite an increase in workload, when accompanied by other evidence of ischemia.
11. Hypertensive response (systolic blood pressure >250 mm Hg and/or diastolic pressure >115 mm Hg).
12. Technical difficulties in monitoring the electrocardiogram or systolic blood pressure.

PHARMACOLOGIC VASODILATOR STRESS

There are currently three vasodilator agents available: dipyridamole, adenosine and, most recently approved, regadenoson. They all work by producing stimulation of A2A receptors. Methylxanthines (caffeine, theophylline, and theobromine) are competitive inhibitors of this effect which requires withholding methylxanthines prior to testing and permits the reversal of the effect with theophylline when clinically indicated.

Note: Some of the pharmacologic stress protocols described in this section fall outside of manufacturer package insert guidelines but have been documented in the literature and are now used commonly in the clinical practice of nuclear cardiology. The practitioner should be familiar with the package insert for each medication.

Adenosine

Mechanism of Action. Adenosine induces direct coronary arteriolar vasodilation through specific activation of the A2A receptor. This results in a 3.5- to 4-fold increase in myocardial blood flow. Myocardial regions supplied by stenotic coronary arteries have an attenuated hyperemic response. Depending upon the severity of coronary stenosis and coronary flow reserve limitation, a relative flow heterogeneity is induced. Adenosine generally does not cause myocardial ischemia since myocardial blood flow increases to a variable degree in all coronary artery vascular beds with minimal or no increase in rate-pressure product (i.e., myocardial oxygen demand). However, in a small percentage of patients with severe CAD, true ischemia may also be induced because of a coronary steal phenomenon. Since the myocardial tracer uptake is proportional to the regional myocardial blood flow, a heterogeneous distribution of radiotracer occurs in the myocardium. Activation of A1, A2b, and A3 receptors may cause undesirable side effects of adenosine infusion: AV block (A1 receptor), peripheral vasodilation (A2b receptor), and bronchospasm (A2b and A3 receptors).

Adenosine Dose. Adenosine should be given as a continuous infusion at a rate of 140 mcg/kg/min over a 6-minute period. A shorter-duration adenosine infusion, lasting 4 minutes, has been found to be equally effective for the detection of CAD compared to the standard 6-minute infusion. For shorter duration protocols, the minimum time to tracer injection should be 2 minutes and the infusion should continue for at least 2 minutes after tracer injection.

Side Effects of Adenosine.

1. Minor side effects are common and occur in approximately 80% of patients. The common side effects are flushing (35-40%), chest pain (25-30%), dyspnea (20%), dizziness (7%), nausea (5%), and symptomatic hypotension (5%). Chest pain is nonspecific and is not necessarily indicative of the presence of CAD.
2. AV block occurs in approximately 7.6% of cases. However, the incidence of second-degree AV block is only 4%, and that of complete heart block is less than 1%. Most cases (>95%) of AV block do not require termination of the infusion.
3. ST-segment depression of 1 mm or greater occurs in 5-7% of cases. However, unlike chest pain, this is usually indicative of significant CAD.
4. Fatal or nonfatal myocardial infarction is extremely rare.
5. Due to an exceedingly short half-life of adenosine (<10 seconds), most side effects resolve in a few seconds after discontinuation of the adenosine infusion, and aminophylline infusion is only very rarely required.

Hemodynamic Effects. Adenosine results in a modest increase in heart rate and a modest decrease in both systolic and diastolic blood pressures.

Indications. The indications for adenosine stress perfusion imaging are the same as for exercise myocardial perfusion imaging and in the presence of the following conditions:

1. Inability to perform adequate exercise due to noncardiac physical limitations (pulmonary, peripheral vascular, musculoskeletal, or mental conditions) or due to lack of motivation. Of note, as with exercise testing, anti-ischemic cardiac medications (including β-blockers, nitrates, and calcium antagonists) have been reported to decrease the diagnostic accuracy of vasodilator stress testing.
2. Baseline electrocardiographic (ECG) abnormalities: LBBB, ventricular pre-excitation (Wolff-Parkinson-White syndrome), and permanent ventricular pacing. Falsely positive imaging results are much less frequent with adenosine (approximately 10%) as compared to stress imaging with exercise (approximately 50%).
3. Risk stratification of clinically stable patients into low- and high-risk groups very early after acute myocardial infarction (≥1 day) or following presentation to the emergency department with a presumptive acute coronary syndrome.

Contraindications. Contraindications for adenosine stress testing include:

1. Asthmatic patients with ongoing wheezing should not undergo adenosine stress testing. However, it has

been reported that patients with adequately controlled asthma can undergo an adenosine stress test and can have pre-treatment with two puffs of albuterol or a comparable inhaler. Bronchospasm is listed as an absolute contraindication in the package insert.
2. Second- or third-degree AV block without a pacemaker or sick sinus syndrome.
3. Systolic blood pressure <90mm Hg.
4. Recent use of dipyridamole, dipyridamole-containing medications (e.g., Aggrenox).
5. Methyl xanthines such as aminophylline caffeine or theobromine block the effect of adenosine and should be held for at least 12 hours prior to the test. Pentoxifylline (Trental) does not appear to block the effects of adenosine.
6. Known hypersensitivity to adenosine.
7. Unstable acute myocardial infarction or acute coronary syndrome.

Relative Contraindications. Relative contraindications for adenosine stress testing include:

1. Profound sinus bradycardia (heart rates <40/min).

Procedure.

1. Patient preparation: Nothing to eat for at least 2 hours; no caffeine-containing beverages or medications for at least 12 hours prior to testing.
2. An infusion pump is required for adenosine to be administered at a constant infusion rate.
3. An IV line with a dual-port Y-connector is required for the injection of the radiotracer during adenosine infusion.
4. ECG monitoring should be carried out as with exercise stress testing. A 12-lead electrocardiogram will be recorded every minute during the infusion.
5. Blood pressure should be monitored every minute during infusion and 3-5 minutes into recovery or until stable. Adenosine infusion should be given at a rate of 140 mcg/kg/min for 3 minutes followed by the injection of the radiotracer. The infusion should be continued for another 3 minutes. For patients deemed to be at a higher risk for complications (borderline hypotension, controlled asthma), adenosine infusion may be started at a lower dose (70-100 mcg/kg/min). If this dose is tolerated well for 1 minute, the infusion rate should be increased to 140 mcg/kg/min and should be continued for 4 minutes. The radiotracer should be injected 1 minute after starting the 140 mcg/kg/min dose.

Combination of Low-Level Exercise with Adenosine Infusion. The combination of low-level upright treadmill exercise (1.7 mph, 0% grade) during the adenosine infusion has been found to be safe. This results in a significant reduction in the side effects of adenosine (flushing, dizziness, nausea, and headache) and attenuates the adenosine-induced drop in blood pressure. Image quality is improved by decreasing high hepatic and gut radiotracer uptake, which is common with pharmacologic stress perfusion imaging. Therefore low-level exercise may be performed in combination with pharmacologic stress. However, since it is desirable not to increase the heart rate of patients with LBBB undergoing pharmacologic stress, low-level exercise supplementation is not recommended in patients with LBBB.

Indications for Early Termination of Adenosine Infusion. The adenosine infusion should be stopped early under any of the following circumstances:

1. Severe hypotension (systolic blood pressure <80 mm Hg).
2. Development of symptomatic, persistent second-degree or complete heart block.
3. Wheezing.
4. Severe chest pain associated with ST depression of 2 mm or greater.
5. Signs of poor perfusion (pallor, cyanosis, and cold skin).
6. Technical problems with the monitoring equipment.
7. Patient's request to stop.

Regadenoson

Mechanism of Action. Regadenoson is an A2A adenosine receptor agonist that is a coronary vasodilator. Regadenoson is a low affinity agonist (Ki $\approx$ 1.3 μM) for the A2A adenosine receptor, with at least 10-fold lower affinity for the A1 adenosine receptor (Ki $>$ 16.5 μM), and weak, if any, affinity for the A2B and A3 adenosine receptors. Activation of the A2A adenosine receptor by regadenoson produces coronary vasodilation and increases coronary blood flow (CBF), the same way adenosine and dypyridamole produce coronary vasodilation. The maximal plasma concentration of regadenoson is achieved within 1-4 minutes after injection and parallels the onset of the pharmacodynamic response. The half-life of this initial phase is approximately 2-4 minutes. An intermediate phase follows, with a half-life on average of 30 minutes coinciding with loss of the pharmacodynamic effect. The last phase consists of a decline in plasma concentration with a half-life of approximately 2 hours.

Regadenoson Dose. The recommended intravenous dose of regadenoson is 5 mL (0.4 mg regadenoson) and should be given as a rapid (approximately 10 seconds) injection into a peripheral vein using

a 22 gauge or larger catheter or needle. Administer a 5-mL saline flush immediately after the injection of regadenoson. Administer the radionuclide myocardial perfusion imaging agent 10-20 seconds after the saline flush. The radionuclide may be injected directly into the same catheter as regadenoson.

Side Effects of Regadenoson.

1. The most common reactions to administration of regadenoson during MPI are shortness of breath, headache, and flushing.
2. Less common reactions are chest discomfort, angina pectoris or ST, dizziness, chest pain, nausea, abdominal discomfort, dysgeusia, and feeling hot.
3. In patients with a prior adenosine stress study, rhythm or conduction abnormalities were seen in 26% with regadenoson (30% for Adenosine). First degree AV block was detected in 3% with regadenoson (7% with adenosine), second degree AV block in 0.1% (1% with adenosine).
4. Most adverse reactions begin soon after dosing and generally resolve within approximately 15 minutes, except for headache which resolves in most patients within 30 minutes.
5. Aminophylline may be administered in doses ranging from 50 to 250 mg by slow intravenous injection (50-100 mg over 30-60 seconds) to attenuate severe and/or persistent adverse reactions to regadenoson.

Hemodynamic Effects. In clinical studies, the majority of patients had an increase in heart rate and a decrease in blood pressure within 45 minutes after administration of regadenoson. Maximum hemodynamic changes after regadenoson or adesosine were as follows: increase in heart rate of more than 40 bpm in 5% (3% for adenosine), decrease in systolic blood pressure of more than 35 mm Hg in 7% (8% for adenosine), and decrease in diastolic blood pressure of more than 25 mm Hg in 4% (5% with adenosine).

Indications. Regadenoson injection is a pharmacologic stress agent indicated for radionuclide myocardial perfusion imaging in patients unable to undergo adequate exercise stress, more specifically in the presence of the following conditions:

1. Inability to perform adequate exercise due to noncardiac physical limitations (pulmonary, peripheral vascular, musculoskeletal, or mental conditions) or due to lack of motivation. Of note, as with exercise testing, anti-ischemic cardiac medications (including β-blockers, nitrates, and calcium antagonists) should be discontinued for at least 48 hours prior to performing a diagnostic imaging test.

Contraindications. Contraindications for regadenoson stress testing include:

1. Patients with second or third degree AV block or sinus node dysfunction unless these patients have a functioning artificial pacemaker.
2. Patients with bronchospasm. The safety profile of Regadenoson has not yet been definitively established in patients with bronchospasm. Two pilot studies reported on the use of regadenoson in patients with bronchoconstrictive disease. The incidence of bronchoconstriction (FEV1 reduction >15% from baseline) was assessed in a randomized, controlled study of 49 outpatients with stable, moderate to severe COPD. A bronchoconstriction rate of 12% and 6%, for Regadenoson and placebo groups, respectively, was observed. In a randomized, controlled study of 48 patients with stable mild-to-moderate asthma who had previously been shown to have bronchoconstrictive reactions to adenosine monophosphate, the rate of bronchoconstriction was the same (4%) for both the Regadenoson and placebo groups. In both studies, dyspnea was reported as an adverse reaction in the Regadenoson group (61% for patients with COPD; 34% for patients with asthma) while no subjects in the placebo group experienced dyspnea. As these small sample size studies were pilot in nature, inadequate data exists to confidently use regadenoson in patients with these conditions.
3. Systolic blood pressure <90 mm Hg. Adenosine receptor agonists including regadenoson induce arterial vasodilation and hypotension. Decreased systolic blood pressure (>35 mm Hg) was observed in 7% of patients and decreased diastolic blood pressure (>25 mm Hg) was observed in 4% of patients within 45 minutes of regadenoson administration. The risk of serious hypotension may be higher in patients with autonomic dysfunction, hypovolemia, left main coronary artery stenosis, stenotic valvular heart disease, pericarditis or pericardial effusions, or stenotic carotid artery disease with cerebrovascular insufficiency.
4. Use of dipyridamole, dipyridamole-containing medications in last 48 hours, aminophylline in last 24 hours or ingestion of caffeinated foods (e.g., chocolate) or beverages (e.g., coffee, tea, and sodas) within the last 12 hours should be avoided.
5. Known hypersensitivity to regadenoson.

Relative Contraindications. Relative Contraindications for regadenoson stress testing include:

1. Profound sinus bradycardia (heart rate <40/minute).

Procedure.

1. Patient preparation: avoid consumption of any products containing methylxanthines, including caffeinated coffee, tea or other caffeinated beverages, caffeine-containing drug products, and theophylline for at least 12 hours prior to the testing. Dipyridamole should be withheld for at least 2 days prior to regadenoson administration.
2. ECG monitoring should be carried out as with exercise stress testing. A 12-lead electrocardiogram will be recorded every minute during the infusion.
3. Blood pressure should be monitored every minute during infusion and 3-5 minutes into recovery.
4. Regadenoson (5 mL, containing 0.4 mg of regadenoson) should be given as a rapid (approximately 10 seconds) injection into a peripheral vein using a 22 gauge or larger catheter or needle. Administer a 5-mL saline flush immediately after the injection of regadenoson. Administer the radionuclide myocardial perfusion imaging agent 10-20 seconds after the saline flush. The radionuclide may be injected directly into the same catheter as regadenoson.

Indications for Reversal of Regadenoson Infusion. Indications for reversal of regadenoson include:

1. Severe hypotension (systolic blood pressure <80 mm Hg).
2. Development of symptomatic, persistent second-degree or complete heart block.
3. Wheezing.
4. Severe chest pain associated with ST depression of 2 mm or greater.
5. Signs of poor perfusion (pallor, cyanosis, and cold skin).
6. Technical problems with the monitoring equipment.
7. Patient's request to stop.

Dipyridamole

Mechanism of Action. Dipyridamole is an indirect coronary artery vasodilator that increases the tissue levels of adenosine by preventing the intracellular reuptake and deamination of adenosine. Dipyridamole-induced hyperemia lasts for more than 15 minutes.

Dipyridamole Dose. Dipyridamole is administered at 0.56 mg/kg intravenously over a 4-minute period (142 mcg/kg/min).

Side Effects. Over 50% of patients develop side effects (flushing, chest pain, headache, dizziness, or hypotension). The frequency of these side effects is less than that seen with adenosine, but they may last for a longer period of time (15-25 minutes) and may vary significantly in individual patients. Aminophylline (125-250 mg intravenously) is often required to reverse these side effects. The incidence of AV block with dipyridamole is less than that observed with adenosine (2%). Aminophylline should also be used in the presence of ischemic ECG changes after dipyridamole.

Hemodynamic Effects. Dipyridamole results in similar hemodynamic changes as seen with adenosine with a modest increase in heart rate and a modest decrease in both systolic and diastolic blood pressures.

Indications. The indications for dipyridamole stress perfusion imaging are the same as for adenosine myocardial perfusion imaging.

Contraindications. The contraindications for dipyridamole stress testing are the same as with adenosine. In patients taking oral dipyridamole, IV dipyridamole may be administered safely and efficaciously.

Procedure.

1. Patient preparation: Nothing to eat for at least 2 hours and no caffeine-containing beverages or medication at least 12 hours prior to testing.
2. The drug is infused intravenously over 4 minutes. Although an infusion pump is preferable, dipyridamole can also be administered by hand injection or drip. The radiotracer is injected 3-5 minutes after the completion of dipyridamole infusion. The half-life of dipyridamole is approximately 30-45 minutes.

Combination of Low-Level Exercise with Dipyridamole Infusion. Patients who are ambulatory may undergo low-level treadmill exercise (1.7 mph, 0% grade) for 4-6 minutes soon after the completion of dipyridamole infusion. Radiotracer is injected during this low-level exercise, and the exercise continues for two additional minutes to allow for tracer uptake in the myocardium. This significantly reduces the side effects and improves image quality. Low-level exercise supplementation is not recommended for patients with LBBB.

Dobutamine

Mechanism of Action. Dobutamine infusion results in direct β_1 and β_2 stimulation with a dose-related increase in heart rate, blood pressure, and myocardial contractility. Dobutamine increases regional myocardial blood flow based on physiologic principles of coronary flow reserve. A similar dose-related increase in subepicardial and subendocardial blood flow occurs within vascular beds supplied by normal coronary arteries. However, blood flow increases minimally within

vascular beds supplied by significantly stenosed arteries, with most of the increase occurring within the subepicardium rather than the subendocardium. However, at a dose of 20 mcg/kg/min, dobutamine-induced coronary flow heterogeneity is similar to exercise but less than that induced by adenosine or dipyridamole.

Dobutamine Dose. Dobutamine is infused incrementally starting at a dose of 5-10 mcg/kg/min, which is increased at 3-minute intervals to 20, 30, and 40 mcg/kg/min. The half-life of dobutamine is approximately 2 minutes. As with exercise stress, achieving >85% of the predicted heart rate is desirable.

Side Effects. Side effects occur in about 75% of patients. The common side effects are palpitation (29%), chest pain (31%), headache (14%), flushing (14%), dyspnea (14%), and significant supraventricular or ventricular arrhythmias (8-10%). Ischemic ST-segment depression occurs in approximately one-third of patients undergoing dobutamine infusion. Severe side effects may require IV administration of a short-acting β-blocker (esmolol, 0.5 mg/kg over 1 minute).

Indications. Indications for dobutamine stress testing include:

1. Dobutamine is a secondary pharmacologic stressor that is recommended only in patients who cannot undergo exercise stress and who also have contraindications to pharmacologic vasodilator stressors (mainly bronchospastic airway disease).
2. Dobutamine perfusion imaging has not been studied as extensively as adenosine or dipyridamole perfusion imaging in the evaluation and prognostication of patients with CAD.

Contraindications. Contraindications for dobutamine stress testing include:

1. Recent (<1 week) myocardial infarction.
2. Unstable angina.
3. Hemodynamically significant left ventricular outflow tract obstruction.
4. Severe aortic stenosis.
5. Atrial tachyarrhythmias with uncontrolled ventricular response.
6. Prior history of ventricular tachycardia.
7. Uncontrolled hypertension (blood pressure >200/110 mm Hg).
8. Patients with aortic dissection or large aortic aneurysm.
9. Patients who are on β-blockers where the heart rate and inotropic responses to dobutamine will be attenuated.

Procedure.

1. Patient preparation: Nothing to eat for at least 2 hours.
2. An infusion pump is necessary for dobutamine administration.
3. An IV line with a dual-port Y-connector is required for injecting radioisotope during dobutamine infusion.
4. ECG monitoring and blood pressure monitoring should be performed as with other pharmacologic stressors.
5. Dobutamine infusion should start at a dose of 5-10 mcg/kg/min. The dobutamine dose should then be increased at 3-minute intervals up to a maximum of 40 mcg/kg/min. The radiotracer should be injected at 1 minute into the highest dobutamine dose, and dobutamine infusion should be continued for 2 minutes after the radiotracer injection.
6. Some investigators recommend the addition of atropine (divided doses of 0.25-0.5 mg up to 1-2 mg) in patients who do not achieve target heart rate with dobutamine alone.

Indications for Early Termination of Dobutamine. The indications for early termination of dobutamine are similar to those for exercise stress. Termination for ventricular tachycardia or ST-segment depression is more likely with dobutamine than with other stressors.

RADIOTRACERS AND PROTOCOLS

Currently utilized myocardial perfusion tracers for myocardial perfusion imaging include thallium 201 and two technetium 99m agents (Tc-99m sestamibi and Tc-99m tetrofosmin). Information related to PET perfusion radiotracers are described in the PET Imaging Guidelines. Characteristics for each tracer, injected doses (Table 1), typical protocol, and dosimetry are presented.

Note: The suggested radiopharmaceutical doses in this section are for current camera and processing protocols as defined in the SPECT Imaging Guidelines. Some of the radiopharmaceutical doses described in this section fall outside of the manufacturer package insert guidelines but are now commonly used in the clinical practice of nuclear cardiology.

Note: The radiation dosimetry values are point estimates of doses to a typical patient. Doses were determined using average administered activities, most recent International Commission on Radiological Protection (ICRP) dose coefficients, and ICRP Publication 103 tissue weighing factors. TC-99m doses represent an average for sestamibi and tetrofosmin.

Gated imaging is recommended where feasible. Results of gating are most reliable with higher doses of technetium-based perfusion tracers but satisfactory results have been reported with lower dose technetium as well as thallium-201.

Table 1. Suggested radiopharmaceutical doses for myocardial perfusion imaging protocols

Tl-201 Protocol	Stress (mCi)	Rest (mCi)	Reinjection (mCi)
Stress/Rest	2.5-4.0	-	-
Stress/Rest/Reinjection	2.5-4.0	-	1.0-2.0
Viability Only	-	3.0-4.0	-
Tc-99m Protocol	**Stress (mCi)**		**Rest (mCi)**
Two day	24-36		24-36
One day, Stress/Rest	8-12		24-36
One day, Rest/Stress	24-36		8-12
Dual isotope	24-36		2.5-4.0

Tl-201

Mechanism of Action. Tl-201 is an analog of potassium (monovalent cation), with a physical half-life of 73.1 hours, decay by electron capture to Hg-201 with principal emission of 68-80 keV x-rays, high first-pass extraction (85%), active membrane transport into the myocyte, rapid clearance from the intravascular space, and monoexponential washout (redistribution) which starts 10-15 minutes after injection. Washout depends on initial tracer concentration in the myocyte and on myocardial blood flow. Clearance occurs via the kidneys. The whole body effective dose for Tl-201 is approximately 6.3 mSv per mCi of Tl-201 injected.

Imaging Protocols. A single dose of 2.5-4.0 mCi of Tl-201 is injected prior to peak exercise stress or at peak pharmacologic vasodilatation, and SPECT imaging starts 10-15 minutes later. Redistribution (rest) imaging is done 2.5-4.0 hours later. In cases where standard stress-redistribution imaging shows a fixed or minimally reversible perfusion abnormality, myocardial viability can be assessed with a rest image at 18-24 hours or following reinjection of an additional 1-2 mCi dose of Tl-201. An alternative method for viability assessment is injection of 3-4 mCi of Tl-201 at rest followed by 3- to 4-hour redistribution imaging. Protocol options and timing for assessment of perfusion and viability are shown in Figure 1.

Tc-99m-Labeled Tracers

Mechanism of Action. Tc-99m sestamibi and Tc-99m tetrofosmin have very similar characteristics: lipid-soluble, cationic, physical half-life of 6 hours, produces 140-keV photons, first-pass extraction less than Tl-201, uptake and mitochondrial retention dependent on blood flow and transmembrane energy potentials. Their myocardial washout (redistribution) is clinically negligible. These agents are excreted via the hepatobiliary system and excreted into the gastrointestinal tract. Lacking significant redistribution, Tc-99m-labeled tracers require two separate injections at stress and rest. The two agents have sufficiently similar characteristics that the recommended protocols use similar camera setup and acquisition times and vary only in the optimal time for image acquisition following rest, exercise, and pharmacologic stress. Optimal validation

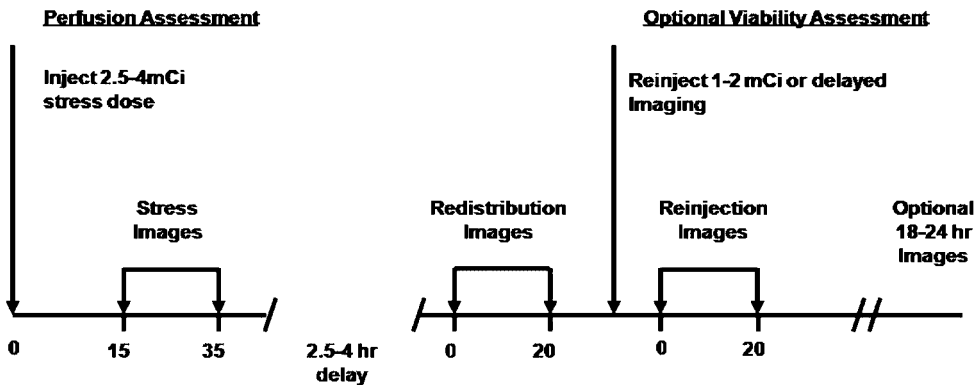

Figure 1. Stress/redistribution/reinjection/18- to 24-hour Tl-201 imaging protocol.

of imaging times has not been extensively studied, and factors such as camera availability and the presence of liver and gastrointestinal activity influence the optimal imaging times. In the figures, a range of imaging times is suggested. The whole body effective dose for Tc-99m is approximately 0.3 mSv per mCi of Tc-99m injected.

Imaging Protocols. *Tracer-Specific Imaging Times* For Tc-99m sestamibi, minimum delays of 15-20 minutes for exercise, 45-60 minutes for rest, and 60 minutes for pharmacologic stress are recommended. For Tc-99m tetrofosmin, minimum delays of 10-15 minutes for exercise, 30-45 minutes for rest, and 45 minutes for pharmacologic stress are optimal. Since there is minimal redistribution with these agents, longer delays, up to 2 hours, between the radiotracer injection and imaging can be used when needed.

Two-Day Protocol Ideally, stress and rest imaging with Tc-99m agents should be performed on two separate days, as shown in Figure 2, to avoid having residual activity from the first study contaminate the second study. In overweight patients (i.e., >250 lb or body mass index >30) or in female patients where significant breast attenuation is anticipated, a low dose of Tc-99m radiotracer may result in suboptimal images and a 2-day imaging protocol is preferable.

One-Day Protocols For most patients, 2-day imaging is impractical; stress and rest studies are usually performed using a 1-day protocol as shown in Figures 3-7 for exercise and pharmacologic stress. This requires administration of a low dose (one-fourth of the total dose, or 8-12 mCi) for the first study and a larger dose (three-fourths of the total dose, or 24-36 mCi) for the second study. One-day rest/stress Tc-99m protocols are now performed almost universally with no delay between the rest and subsequent stress images. The initially proposed 1990 protocol specified a 2-hour delay between rest and stress to allow the rest dose to decay in order to maximize the stress/rest count density ratio and minimize rest-to-stress ''shine-through'' or ''crosstalk.'' However, simply increasing the stress dose provides the same stress/rest count density ratio achieved by letting the rest dose decay (20% in 2 hours). Thus a 3:1 stress/rest dose ratio with a 2-hour delay and a 3.5-4:1 ratio with no delay provide the same result. Note that the 2-hour delay is the total time between rest injection and starting the post-stress imaging. Thus the waiting time to stress is not fixed but depends on the sum of intervals from rest injection to the post-stress imaging. In contrast, for the 1-day stress/rest protocol, wherein the stress scan is performed first and relative tracer uptake in the myocardium is increased consequent to the stress-induced coronary hyperemia, a delay between the stress injection and the subsequent resting injection is essential and should be as close to 4 hours as possible between the stress injection and starting the post-rest imaging. Stated administered activities are commonly used in the United States, but these vary in other countries. Issues regarding the imaging sequence (stress vs. rest first) and the minimum time interval between the two radiotracer injections are not fully settled.

In patients without a prior history of CAD with an intermediate pre-test likelihood based on risk factors, a low-dose stress/high-dose rest Tc-99m protocol may have theoretical advantages since a significant percentage of these patients will have normal stress studies, thereby avoiding additional radiation exposure from a rest study. Due to higher tracer uptake during low-dose stress, the waiting time to high-dose rest imaging needs to be longer (3-4 hours) or the rest dose needs to be higher to achieve a rest/stress ratio of at least 1:4.

Dual-Isotope Imaging Use of Tl-201 for initial rest imaging and a Tc-99 labeled tracer for stress perfusion imaging, as shown in Figure 8 allows a shorter duration of the entire imaging protocol, but there is a significantly higher radiation dose to the patient. Use of rest/3- to 4-hour redistribution Tl-201 imaging prior to the stress, Tc-99m study provides valuable information on myocardial viability and should be considered in patients with prior infarction or heart failure.

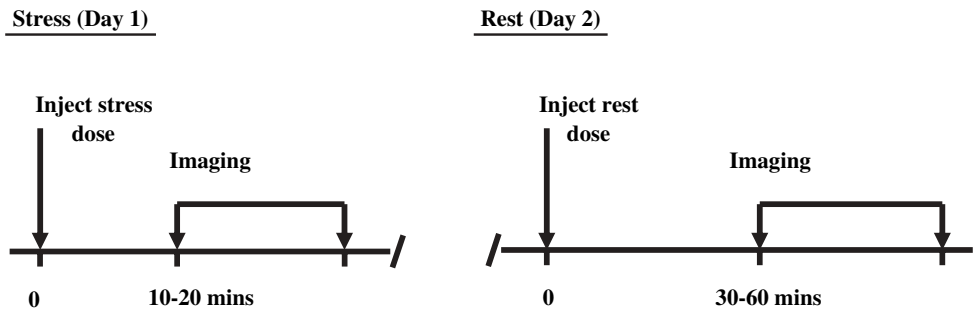

Figure 2. Tc-99m imaging protocols: Two-day exercise stress/rest.

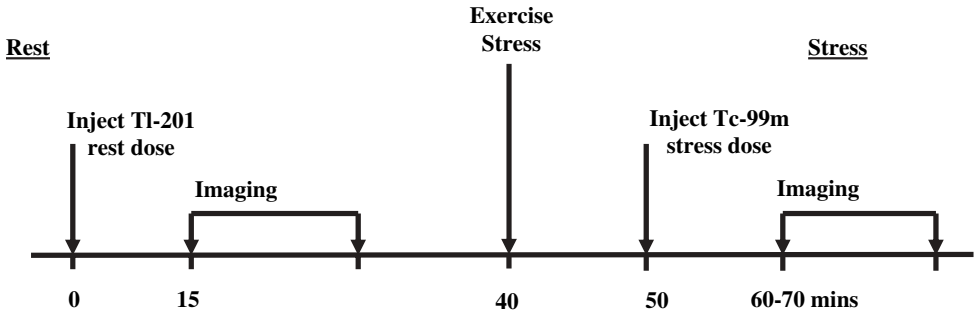

Figure 3. Rest Tl-201/stress Tc-99m separate-acquisition dual-isotope protocol.

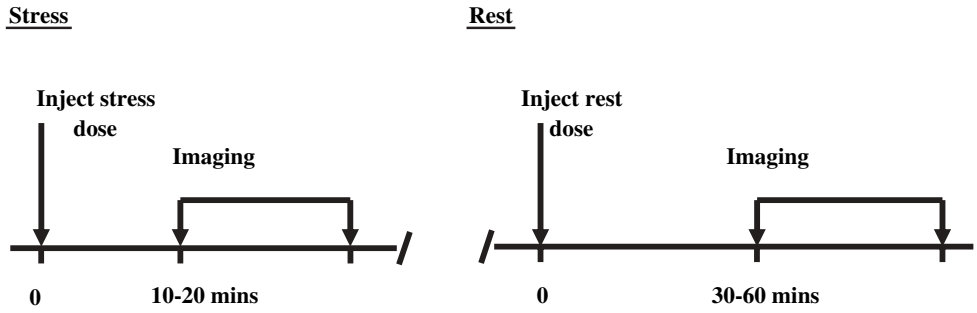

Figure 4. Tc-99m imaging protocols: One-day exercise stress/rest.

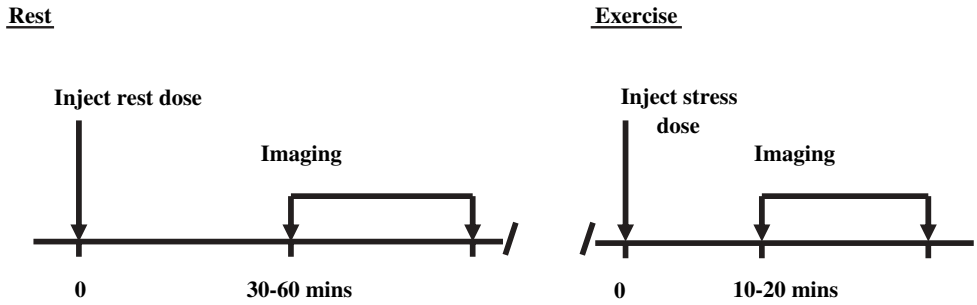

Figure 5. Tc-99m imaging protocols: One-day rest/exercise stress.

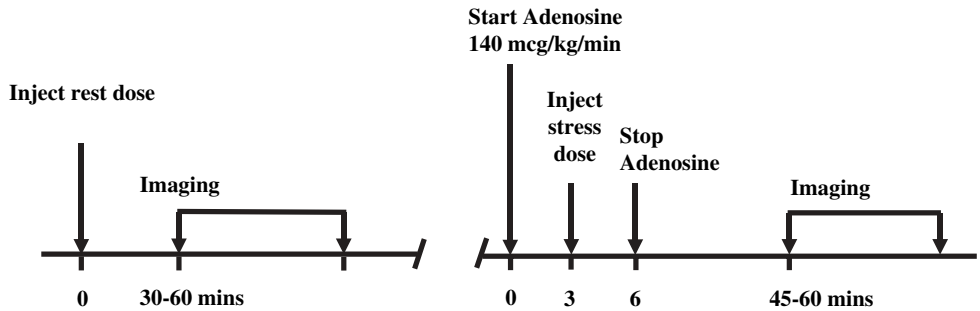

Figure 6. Tc-99m imaging protocols: One-day rest/adenosine pharmacologic stress.

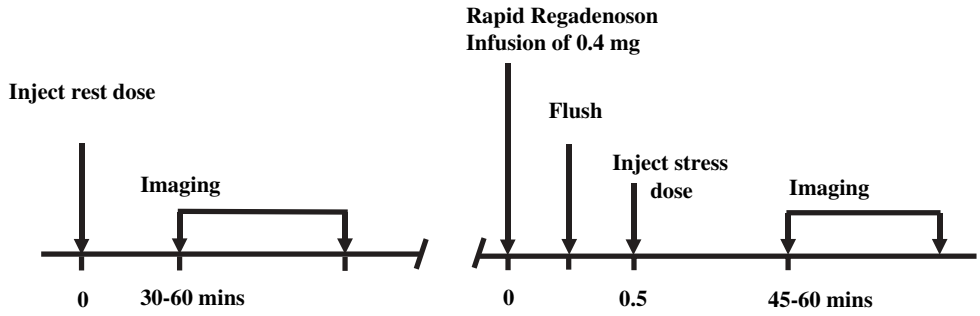

Figure 7. Tc-99m imaging protocols: One-day rest/regadenoson pharmacologic stress.

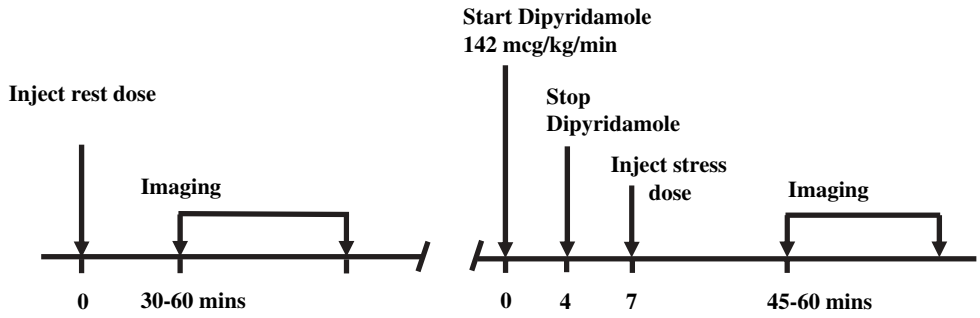

Figure 8. Tc-99m imaging protocols: One-day rest/dipyridamole pharmacologic stress.

Acknowledgment

The authors have indicated that they have no financial conflicts of interest.

Suggested Reading

1. Abbott BG, Afshar M, Berger AK, Wackers FJT. Prognostic significance of ischemic electrocardiographic changes during adenosine infusion in patients with normal myocardial perfusion imaging. J Nucl Cardiol 2003;10:9-16.
2. Amanullah AM, Berman DS, Erel J, et al. Incremental prognostic value of adenosine myocardial perfusion single-photon emission computed tomography in women with suspected coronary artery disease. Am J Cardiol 1998;82:725-30.
3. Amanullah AM, Berman DS, Hachamovitch R, et al. Identification of severe or extensive coronary artery disease in women by adenosine technetium-99m sestamibi SPECT. Am J Cardiol 1997;80:132-7.
4. Aqel RA, Zoghbi GJ, Trimm JR, Baldwin SA, Iskandrian AE. Effect of caffeine administered intravenously on intracoronary-administered adenosine-induced coronary hemodynamics in patients with coronary artery disease. Am J Cardiol 2004;93:343-6.
5. Berman DS, Kiat H, Friedman JD, et al. Separate acquisition rest thallium-201/stress technetium-99m sestamibi dual-isotope myocardial perfusion single-photon emission computed tomography: A clinical validation study. J Am Coll Cardiol 1993;22:1455-64.
6. Bokhari S, Ficaro EP, McCallister BD. Adenosine stress protocols for myocardial perfusion imaging. J Nucl Med 2007;14:415-6.
7. Braat SH, Leclercq B, Itti R, Lahiri A, Sridhara B, Rigo P. Myocardial imaging with technetium-99m-tetrofosmin: Comparison of one-day and two-day protocols. J Nucl Med 1994;35:1581-5.
8. Candell-Riera J, Santana-Boado C, Castell-Conesa J, et al. Simultaneous dipyridamole/maximal subjective exercise with Tc-99m-MIBI SPECT: improved diagnostic yield in coronary artery disease. J Am Coll Cardiol 1997;29:531-6.
9. Cerqueira MD, Nguyen P, Staehr P, et al. ADVANCE-MPI Trial Investigators. Effects of age, gender, obesity, and diabetes on the efficacy and safety of the selective A2A agonist regadenoson versus adenosine in myocardial perfusion imaging: Integrated ADVANCE-MPI Trial Results. J Am Coll Cardiol Img 2008;1:307-16.
10. Cerqueira MD, Verani MS, Schwaiger M, Heo J, Iskandrian AS. Safety profile of adenosine stress perfusion imaging: Results from Adenoscan Multicenter Trial Registry. J Am Coll Cardiol 1994;23:384-90.
11. Dakik HA, Wendt JA, Kimball K, Pratt CM, Mahmarian JJ. Prognostic value of adenosine Tl-201 myocardial perfusion imaging after acute myocardial infarction: Results of a prospective clinical trial. J Nucl Cardiol 2005;12:276-83.
12. Eagle KA, Berger PB, Calkins H, et al. ACC/AHA guideline update on perioperative cardiovascular evaluation for noncardiac surgery. American College of Cardiology/American Heart Association Task Force on Practice Guidelines (Committee to Update the 1996 Guidelines on Perioperative Cardiovascular Evaluation for Noncardiac Surgery). Circulation 2002;105:1257-67.
13. Eggbrecht H, Gössl M. Regadenoson (CV therapeutics/astellas). Curr Opin Investig Drugs 2006;7:264-71.
14. Einstein AJ, Moser KW, Thompson RC, Cerqueira MD, Henzlova MJ. Radiation dose to patients from cardiac diagnostic imaging. Circulation 2007;116:1290-305.
15. Elliott MD, Holly TA, Leonard SM, Hendel RC. Impact of an abbreviated adenosine protocol incorporating adjunctive treadmill exercise on adverse effects and image quality in patients undergoing stress myocardial perfusion imaging. J Nucl Cardiol 2000;7:584-9.

16. Gaemperli O, Schepis T, Koepfli P, Siegrist PT, Fleischman S, Nguyen P, et al. Interaction of caffeine with regadenoson-induced hyperemic myocardial blood flow as measured by positron emission tomography: A randomized, double-blind, placebo-controlled crossover trial. J Am Coll Cardiol 2008;51:328-9.
17. Gibbons RJ, Balady GJ, Bricker JE, et al. ACC/AHA 2002 guideline update for exercise testing: Summary article: A report of the American College of Cardiology/American Heart Association Task Force on Practice Guidelines (Committee to Update the 1997 Exercise Testing Guidelines). Circulation 2002;106:1883-92.
18. Gordi T, Frohna P, Sun HL, et al. A population pharmacokinetic/pharmacodynamic analysis of regadenoson, an adenosine A(2A)-receptor agonist, in healthy male volunteers. Clin Pharmacokinet 2006;45:1201-12.
19. Hansen CL, Goldstein RA, Akinboboye OO, et al. ASNC Imaging guidelines for nuclear cardiology procedures: Myocardial perfusion and function: Single photon emission computed tomography. J Nucl Cardiol 2007;14:e39-60.
20. Hays JT, Mahmarian JJ, Cochran AJ, Verani MS. Dobutamine thallium-201 tomography for evaluating patients with suspected coronary artery disease unable to undergo exercise or vasodilator pharmacologic stress testing. J Am Coll Cardiol 1993;21:1583-90.
21. Hendel RC, Bateman TM, Cerqueira MD, Iskandrian AE, Leppo JA, Blackburn B, et al. Initial clinical experience with regadenoson, a novel selective A2A agonist for pharmacologic stress single-photon emission computed tomography myocardial perfusion imaging. J Am Coll Cardiol 2005;46:2069-75.
22. Hesse B, Tagil K, Cuocolo A, Anagnostopoulos C, Bardies M, Bax J, et al. EANM/ESC procedural guidelines for myocardial perfusion imaging in nuclear cardiology. Eur J Nucl Med Mol Imaging 2005;32:855-97.
23. Higley B, Smith FW, Smith T, et al. Technetium-99m-1,2 bis[-bis(2-ethoxyethyl)phosphino]ethane: Human biodistribution, dosimetry and safety of a new myocardial perfusion imaging agent. J Nucl Med 1993;34:30-8.
24. Holly TA, Satran A, Bromet DS, Mieres JH, Frey MJ, Elliott MD, et al. The impact of adjunctive adenosine infusion during exercise myocardial perfusion imaging: Results of the Both Exercise and Adenosine Stress Test (BEAST) trial. J Nucl Cardiol 2003;10:291-6.
25. Iskandrian AE, Bateman TM, Belardinelli L, Blackburn B, Cerqueira MD, Hendel RC, et al. Adenosine versus regadenoson comparative evaluation in myocardial perfusion imaging: Results of the ADVANCE phase 3 multicenter international trial. J Nucl Cardiol 2007;14:645-58.
26. Iskandrian AS, Verani MS, Heo J. Pharmacologic stress testing: Mechanism of action, hemodynamic responses, and results in detection of coronary artery disease. J Nucl Cardiol 1994;1:94-111.
27. Jain D. Technetium labeled myocardial perfusion imaging agents. Semin Nucl Med 1999;29:221-36.
28. Jain D, FJTh Wackers, Mattera J, McMahon M, Sinusas AJ, Zaret BL. Biokinetics of technetium-99m-tetrofosmin: Myocardial perfusion imaging agent: Implications for a one day imaging protocol. J Nucl Med 1993;34:1254-9.
29. Jamil G, Ahlberg AW, Elliott MD, Hendel RC, Holly T, McGill CC, et al. Impact of limited treadmill exercise on adenosine Tc-99m sestamibi single-photon emission computed tomographic myocardial perfusion imaging in coronary artery disease. Am J Cardiol 1999;84:400-3.
30. Kelly JD, Forster AM, Higley B, et al. Technetium-99m-tetrofosmin as a new radiopharmaceutical for myocardial perfusion imaging. J Nucl Med 1993;34:222-7.
31. Klodas E, Miller TD, Christian TF, Hodge DO, Gibbons RJ. Prognostic significance of ischemic electrocardiographic changes during vasodilator stress testing in patients with normal SPECT images. J Nucl Cardiol 2003;10:4-8.
32. Leaker BR, O'Connor B, Hansel TT, Barnes PJ, Meng L, Mathur VS, et al. Safety of regadenoson, an adenosine A2A receptor agonist for myocardial perfusion imaging, in mild asthma and moderate asthma patients: A randomized, double-blind, placebo-controlled trial. J Nucl Cardiol 2008;15:329-36.
33. Lette J, Tatum JL, Fraser S, Miller DD, et al. Safety of dipyridamole testing in 73,806 patients: The Multicenter Dipyridamole Safety Study. J Nucl Cardiol 1995;2:3-17.
34. Lieu HD, Shryock JC, von Mering GO, et al. Regadenoson, a selective A(2A) adenosine receptor agonist, causes dose-dependent increases in coronary blood flow velocity in humans. J Nucl Cardiol 2007;14:514-20.
35. Machac J, Bacharach SL, Bateman TM, et al. ASNC Imaging guidelines for nuclear cardiology procedures: Positron emission tomography myocardial perfusion and glucose metabolism imaging. J Nucl Cardiol 2006;13:e121-51.
36. Mahmarian JJ, Shaw LJ, Olszewski GH, Pounds BK, Frias ME, Pratt CM, et al. Adenosine sestamibi SPECT post-infarction evaluation (INSPIRE) trial: A randomized, prospective multicenter trial evaluating the role of adenosine Tc-99m sestamibi SPECT for assessing risk and therapeutic outcomes in survivors of acute myocardial infarction. J Nucl Cardiol 2004;11:458-69.
37. Mahmood S, Gunning M, Bomanji JB, et al. Combined rest thallium-201/stress technetium-99m-tetrofosmin SPECT: Feasibility and diagnostic accuracy of a 90-minute protocol. J Nucl Med 1995;36:932-5.
38. Mieres JH, Shaw LJ, Arai A, Budoff MJ, Flamm SD, Hundley WG, et al. Role of noninvasive testing in the clinical evaluation of women with suspected coronary artery disease. Circulation 2005;111:682-96.
39. O'Keefe JH, Bateman TM, Handlin LR, Barnhart CS. Four- versus 6-minute infusion protocol for adenosine thallium-201 single photon emission computed tomography imaging. Am Heart J 1995;129:482-7.
40. Pennell DJ, Mavrogeni S, Forbat SM, Karwatowski SP, Underwood SR. Adenosine combined with dynamic exercise for myocardial perfusion imaging. J Am Coll Cardiol 1995;25:1300-9.
41. Pennell DJ, Underwood SR, Ell PJ. Safety of dobutamine stress for thallium myocardial perfusion tomography in patients with asthma. Am J Cardiol 1993;71:1346-50.
42. Pennell DJ, Underwood SR, Swanton RH, Walker JM, Ell PJ. Dobutamine thallium myocardial perfusion tomography. J Am Coll Cardiol 1991;18:1471-9.
43. Samady H, Wackers FJTh, Joska TM, Zaret BL, Jain D, et al. Pharmacologic stress perfusion imaging with adenosine: Role of simultaneous low-level treadmill exercise. J Nucl Cardiol 2002;9:188-96.
44. Stein RA, Chaitman BR, Balady GJ, et al. Safety and utility of exercise testing in emergency room chest pain centers: An advisory from the Committee on Exercise, Rehabilitation, and Prevention, Council on Clinical Cardiology, American Heart Association. Circulation 2000;102:1463-7.
45. Taillefer R. Radionuclide myocardial perfusion imaging protocols. In: Heller GV, Hendel RC, editors. Nuclear cardiology: Practical applications. New York: McGraw-Hill Medical Publishing Division; 2004.
46. Taillefer R, Laflamme L, Dupras G, Picard M, Phaneuf DC, Leveille J. Myocardial perfusion imaging with $^{99\,m}$Tc-methoxy-isobutyl-isonitrile (MIBI): Comparison of short and long time

intervals between rest and stress injections. Preliminary results. Eur J Nucl Med 1988;13:515-22.
47. Thomas GS, Prill NV, Majmundar H, Fabrizi RR, Thomas JJ, Hayashida C, et al. Treadmill exercise during adenosine infusion is safe, results in fewer adverse reactions, and improves myocardial perfusion image quality. J Nucl Cardiol 2000;7:439-46.
48. Thomas GS, Tammelin BR, Schiffman GL, Marquez R, Rice DL, Milikien D, et al. Safety of regadenoson, a selective adenosine A2A agonist, in patients with chronic obstructive pulmonary disease: A randomized, double-blind, placebo-controlled trial (RegCOPD trial). J Nucl Cardiol 2008;15:319-28.
49. Trueth MG, Reyes GA, He ZX, Cwaig E, Mahmarian JJ, Verani MS. Tolerance and diagnostic accuracy of an abbreviated adenosine infusion for myocardial scintigraphy: A randomized, prospective study. J Nucl Cardiol 2001;8:548-54.
50. Vaduganathan P, He ZX, Raghavan C, Mahmarian JJ, Verani MS. Detection of left anterior descending coronary artery stenosis in patients with left bundle branch block: Exercise, adenosine or dobutamine imaging. J Am Coll Cardiol 1996;28:543-53.
51. Vitola JV, Brambatti JC, Caligaris F, Lesse CR, Nogueira PR, Joaquim AI, et al. Exercise supplementation to dipyridamole prevents hypotension, improves electrocardiogram sensitivity, and increases heart-to-liver activity ratio on Tc-99m sestamibi imaging. J Nucl Cardiol 2001;8:652-9.
52. Wackers FJTh, Berman DS, Maddahi J, et al. Technetium-99m hexakis 2-methoxyisobutyl isonitrile: Human biodistribution, dosimetry, safety and preliminary comparison to thallium-201 for myocardial perfusion imaging. J Nucl Med 1989;30:301-11.
53. Zhao G, Messina E, Xu X, et al. Caffeine attenuates the duration of coronary vasodilation and changes in hemodynamics induced by regadenoson (CVT-3146), a novel adenosine A2A receptor agonist. J Cardiovasc Pharmacol 2007;49:369-75.

Myocardial perfusion planar imaging

Peter L. Tilkemeier, MD, Chair,[a] and Frans J. Th. Wackers, MD, PhD[b]

Although single photon emission computed tomography (SPECT) is preferable for myocardial perfusion scintigraphy, in a minimal number of circumstances, planar imaging may be useful or may be the only modality available.

Purpose. To evaluate regional myocardial perfusion and function. Planar imaging is an acceptable method for myocardial perfusion imaging. The anatomy of the heart is sufficiently simple that the imaging specialist can comprehend the location and extent of defects from multiple projections without need of computer reconstruction. Although SPECT imaging is presently considered state-of-the-art for myocardial perfusion imaging and preferable, planar imaging still has a role in the daily routine of a laboratory. Imaging at the bedside of acutely ill patients, or instrumented patients, can only be performed using planar imaging technique and portable gamma cameras. Planar views can be quickly repeated if the patient moves during acquisition. Planar imaging may be the only way to acquire images in very obese patients, who are too heavy for the imaging table of a SPECT camera. It may also be the only way to acquire images in severely claustrophobic patients.

Electrocardiography (ECG)-gated planar images can be obtained using standard software for equilibrium radionuclide angiography studies. Finally, planar imaging is the basis for good SPECT imaging. The ability to obtain high-quality planar images is an essential skill, even for those who routinely use SPECT imaging.[1]

PROCEDURE

Exercise

Adequate exercise is most important if the aim of the study is to detect coronary artery disease (CAD). In patients with mild and moderate CAD, myocardial blood flow may become abnormal only at high heart rates or at high double products. At lower heart rates, myocardial blood flow may be normal and perfusion images will be correspondingly normal. In patients with known CAD who are being evaluated for extent and severity of inducible myocardial ischemia, submaximal exercise can provide clinically relevant information.[2]

Positioning

The most important part of positioning is the ability to reproduce the same position on initial and delayed (or rest) images. Even slight differences in angulation of the camera, positioning of breasts or other soft tissue, or the pressure of the camera on the chest wall can produce artifacts and inaccuracies in comparing rest and stress images. It is vital to bring the camera head as close to or touching the patient's chest in order to get the highest possible count rates, as opposed to SPECT imaging, where some distance is necessary to avoid collisions with the patient during rotational acquisition.

The standard imaging positions are supine anterior, supine 45° left anterior oblique (LAO), and a right side-decubitus 90° left lateral (LL). The 90° LL decubitus view provides optimal visualization of the inferior wall and reduces subdiaphragmatic and breast attenuation artifacts. Admittedly, the right-side decubitus position is less stable than the supine position, making it somewhat more difficult to obtain identical repositioning. An alternate LL view is the shallow 70° LAO position. The latter position is suboptimal at times due to frequent occurrence of artifacts: subdiaphragmatic attenuation of the inferior wall and breast attenuation of the anterior wall.[3]

The LAO view should be chosen in such a way that the right ventricle and left ventricle are well separated by a vertically visualized septum (i.e., ''best septal'' view). One should be aware that in individual patients the heart may not always be in the same position. Hearts may be rotated clockwise or counterclockwise so that a ''straight'' 45° LAO will not always display the desired image. It is preferred to search for the ''best septal'' view instead of a straight 45° LAO. The angulation of the detector head for acquisition of anterior and LL views should then be correspondingly modified. The advantage of this option is that it provides greater

From Miriam Hospital,[a] Providence, RI; Yale University School of Medicine,[b] New Haven, CT.

Approved by the American Society of Nuclear Cardiology Board of Directors, December 11, 2008.

Unless reaffirmed, retired or amended by the American Society of Nuclear Cardiology, this Imaging Guideline shall expire as of March 2014.

Reprint requests: Peter L. Tilkemeier, MD, Chair, Miriam Hospital, Providence, RI.

1071-3581/$34.00

doi:10.1007/s12350-009-9057-1

standardization of the imaged left ventricle, which will simplify quantitative analysis. The disadvantage of this option is the increased complexity, and it carries the potential for non-reproducible positioning.

Female patients should be imaged consistently with the bra off and without camera pressure, which might produce variable tissue displacement.

Planar imaging may be particularly useful in patients who are unable to maintain the supine position for a prolonged period of time. New camera designs allow for imaging in upright or seated position. As for supine acquisition, images are to be obtained in multiple views as listed in the table below. Position of cameras and patients must be exactly reproduced for rest and stress imaging, whether supine or upright.

Positioning

View	Patient position	Detector position	Alternative
Shallow LAO	Supine/upright	45°	"Best septal"
Anterior	Supine/upright	0°	"Best septal" minus 45°
Steep LAO	Supine/upright	70°	"Best septal" plus 25°
Left lateral	Right decubitus or upright	0° or 90° if upright	Not applicable

Positions of cameras and patients must be exactly reproduced for rest and stress imaging.

IMAGE ACQUISITION

Gamma camera positions are as shown in the previous table. Using either thallium 201 (Tl-201) or technetium 99m (Tc-99m)-labeled agents, one may optionally use ECG-synchronized gating and acquire in 16-frame, multiple-gated acquisition (equilibrium radionuclide angiography) mode. No beat rejection should be used. In patients with atrial fibrillation, ECG gating should not be performed. ECG-gated acquisition allows for cine review of wall thickening and motion. The multiple frames of the ECG-gated myocardial perfusion images can be summed to produce a single static planar image for conventional visual and quantitative analysis.[4]

The total imaging time for static planar Tl-201 imaging should be 8 to 10 minutes per view, whereas the total imaging time for static planar Tc-99m-labeled agents can be reduced to 5 minutes per view. When ECG gating is used, imaging time per view using Tc-99m agents should be extended to 8 to 10 minutes. For ECG-gated image acquisition with Tl-201, image acquisition time per view should be at least 10 minutes per view. Planar images acquired with a 10-inch-diameter gamma camera should have at least 600,000 counts (1 million counts preferred) in the field of view. Alternatively, optimal count density can be defined as at least 100 counts in the pixel with maximal counts in the left ventricle.[5,6]

In female patients an optional 1-minute image of a line source marker that delineates the contour of the breast can be acquired to aid in identifying breast attenuation artifacts.

Cardiac shields or other masking devices should not be used. The extracardiac background cannot be determined correctly unless both the cardiac activity and extracardiac activity have been recorded in the raw data.

Acquisition

	Tc-99m	Tl-201
Collimator	High resolution	Low energy, medium resolution
Field of view	Full 10-inch field of small camera or 1.2-1.5 zoom with large-field-of-view camera	Same
Matrix	128 × 128	128 × 128
Window	140 keV 20% centered	78 keV, 30% centered
Gating	Optional 16 frames/cardiac cycle	Same
Imaging time (per view)	5 minutes (10 minutes ECG-gated)	8-10 minutes (10 minutes ECG-gated)
Imaging counts	At least 1 million	At least 1 million

QUANTITATIVE PROCESSING OF PLANAR IMAGES

Quantitative processing includes using the computer to produce standardized raw images for visual evaluation. The gray scale should be fully utilized to display the heart normalized to maximal left ventricular (LV) count density, and not scaled to visceral activity.

Background subtraction is performed. The background-subtracted images are useful for visual evaluation and are used for measurements of myocardial activity. These measurements provide quantitative determination of a suspected defect so that consistent standards can be set for defect detection. The measurements are especially useful in comparing defects in stress and rest images and to detect subtle defect reversibility. Registration of the stress and rest images also can be performed to ensure that the same myocardial region is being sampled. A normal database also may be incorporated in the quantitative program so that segmental tracer activity can be compared with the average obtained from the normal database.[7-11]

There is no single ''generic'' description for what all good computer programs should offer. There are common features among several successful programs. In the following section we review these features and comment on acceptable variations.

Regions of Interest

The first step in quantification is to locate the heart by placing reference regions of interest around the heart. Regions can be rectangular or elliptical. Elliptical regions fit the heart better. Rectangular regions are best used by having the operator set the boundaries by touching the apparent ''edge'' of the heart and then moving the region outward approximately 4 pixels. This operation is highly reproducible. The reference boundaries are used to separate the region containing myocardial activity from background activity.

Background Subtraction

Background subtraction is the removal of the background or, more precisely, the ''tissue cross-talk'' from the raw image. For each image, a background image is generated from the smoothed image using the above-mentioned reference background region. The background is then subtracted from the unsmoothed raw image, leaving behind the myocardial activity.

Background subtraction is essential to planar imaging both for valid quantitation and to restore defect contrast adequate for visual assessment. Background correction is in fact more critical for planar imaging with Tc-99m-labeled agents than for imaging with Tl-201. The relative tissue distribution of Tc-99m-labeled agents at rest and after exercise may be markedly different compared to that of Tl-201.[12]

A modified version of the conventional interpolative background algorithm has worked well for both Tl-201 and Tc-99m sestamibi planar images. The modification allows the background-defining regions to cross regions of intense extracardiac activity without causing significant background error in the background-subtracted cardiac image.[13]

Rescaling the Image Gray Scale

When Tl-201 is used as the imaging agent, the heart is usually the organ with the most intense activity. When using myocardial tracers labeled with Tc-99m, activity in the abdominal viscera often exceeds that of the heart. This normally causes the computer to scale image intensities to the extracardiac activity, which will cause erratic and suboptimal visualization of the heart. Any computer program for quantitative image processing should have a convenient mechanism to suppress activity outside the heart if it becomes greater than the activity in the heart. When comparing initial and delayed images or images obtained after reinjection, each image should be individually scaled to the area of most intense cardiac activity. If the images were scaled to different maxima, the appearance of defect reversibility would be distorted.

Image Registration

Comparison of rest and exercise images to detect redistribution or reversibility can be accurate only if the same myocardial segments are being compared. Image registration so that stress and rest images are precisely aligned facilitates accurate comparisons. There are several ways of doing this. Maximizing the cross-correlation coefficient between the two images is a robust method that can be performed by the computer without operator intervention.

Profile Generation

After subtraction of the reference (background) plane to compensate for tissue crosstalk and registration of the images to allow precise comparisons, quantification becomes the relatively simple matter of finding a convenient way of indicating image count density. Again, there are several ways of doing this. One basic way is to display count profiles across the heart. Four profiles will sample the myocardial count distribution adequately within the limitations of image resolution (each profile represents an average of about a 1-cm-wide slice across the heart) and produce an intelligible display. A more commonly used alternative for graphic display of myocardial activity is the circumferential count distribution profile. The circumferential profile method provides a more compact and dense single-curve display of counts sampled around the myocardial ''rim''

and allows the simple plot of a second profile indicating normal limits. Either method, transverse count profiles or circumferential count profiles, will provide an adequate and ultimately equivalent quantitative representation of myocardial activity. Either method facilitates standardization and reproducibility of image interpretation.[14]

A more fundamental choice is what parameter to use to quantify myocardial activity. Many programs, including most methods used to generate bull's-eye maps for SPECT imaging, perform a search across the myocardium for the maximum pixel count in a transmural myocardial sample. The other choice is to take an average of counts in the transmural sample. The advantage of the latter method is that it reduces statistical noise because it is an average, and it is intuitively more representative in regions of subendocardial scar or ischemia. The disadvantage is that the transmural average is quite sensitive to the accurate definition of endocardium and epicardium. Variability in locating the epicardial and endocardial limits probably nullifies the gain in precision from the averaging of more pixels. The use of maximum counts provides a quantitative parameter that is less sensitive to edge location. This parameter has been used extensively and has been reasonably robust in practice. Either method is usable. Normal standards and normal limits will be quite different for those using the transmural average. They are not comparable with values based on transmural maximum.[15]

Normal Database

Data from ''normal'' subjects may be incorporated into the computer program and indicated in the output as normal limits. Because of variations in equipment and positioning, the normal database should not be used until it has been validated in-house using standardized imaging protocols.

Along with the average values obtained from the normal database, the standard deviations (SDs) also need to be obtained. Different myocardial segments will have different degrees of normal variability, which should be accounted for in deciding if a segment is outside normal limits. Individual segments may be flagged using limits of 2.0 to 2.5 SDs. The computer may also flag reversible segments, but this is a more complex operation. The database must have SDs comparing stress and rest segments. If a segment has a significant stress defect, reversibility may be indicated if that defect changes toward normal by more than 1 SD. Additional ''expert logic'' may also be incorporated to scan for secondary segments with nonsignificantly reduced initial uptake and significant reversibility.[1,16]

Limitations

Well-trained readers consistently outperform readings even from relatively sophisticated computer programs. The programs are valuable in standardizing the images and image processing and in maintaining consistent interpretive standards. However, the judgment of a well-trained reader should override the computer logic. Computer programs that dogmatically indicate normal and abnormal scans or scan segments can be intimidating and misleading. Readers must be prepared to disagree and overrule the computer. Otherwise, the readers will be no better than the computer.

INTERPRETATION AND REPORTING

Images should be assessed initially for technical adequacy, including target-to-background activity, splanchnic tracer uptake, count adequacy in the cardiac region of interest, adequacy of count normalization and masking, appropriate orientation of the planar projections, and registration of the stress and delay (Tl-201) or stress and rest (Tc-99m agents) planar projections and appropriate location and alignment of the ventricular region of interest utilized for quantitative analysis, if performed.

Display

Planar perfusion images may be displayed by use of the computer screen, x-ray film, or paper copy. The use of the computer screen is strongly recommended and is the preferred medium. Counts should preferably be represented by a linear gray scale. If a color table is used, the scale should be simultaneously displayed on screen. Otherwise, the adequacy of the display medium (film or paper) should be established by inspection of a standard test pattern, which provides testing of both resolution and gray scale.

The initial set of images is typically displayed together with the subsequent set of images aligned adjacent to or underneath it. The interpreting physician should confirm that the imaging angles have not changed between image sets. Images are typically normalized to themselves. Planar images should be interpreted without any processing. Background-subtracted images may be generated for quantitative analysis but should not be interpreted without viewing the unsubtracted images as well.

Evaluation for Technical Sources of Artifacts

The images should then be carefully inspected for potential image artifacts, the most common of which is

attenuation.[17] Suspected soft-tissue attenuation should be thoroughly evaluated and its effect on the interpretation carefully considered. The use of breast marker images may be helpful in distinguishing true perfusion defects from breast attenuation.[18] Attenuation of the inferior wall by the diaphragm or an enlarged right ventricle should also be considered. Other sources of attenuation (e.g., pleural effusions or infiltrates, foreign objects, other soft tissues) should be noted.

Adjacent subdiaphragmatic activity, as is frequently seen in liver and bowel, may create overlap artifacts that spuriously increase the activity in the inferior wall, creating the appearance of a relative paucity of counts in other myocardial segments. Intense noncardiac activity may cause scaling artifacts in the myocardial images. Techniques for masking such noncardiac activity are available.

Count-poor studies are subject to misinterpretation. Apparent perfusion abnormalities may resolve when a statistically adequate study is available. The factors leading to suboptimal count statistics include body habitus, radionuclide dose, collimation, window, acquisition time, and the level of myocardial blood flow.

Patient motion is rarely a problem because of the short duration of imaging.

Initial Perfusion Image Analysis and Interpretation

The initial interpretation of the perfusion scan should be performed without any clinical information other than the patient's gender, height and weight, and presence of left bundle-branch block. This approach minimizes the bias in study interpretation. All relevant clinical information should be reviewed after a preliminary impression is formed.

Before segmental analysis of myocardial perfusion, the reader should note whether there is LV cavity dilation at rest or during exercise or pharmacologic challenge. Dilation on both the stress and resting studies suggests LV dysfunction but may occur in volume-overload states with normal ventricular function. Transient ischemic dilation is a marker for multivessel CAD. It is typically described qualitatively but may be quantified.[19]

The presence of increased lung uptake should be noted by comparison of the pulmonary to myocardial counts. This is especially important when imaging with Tl-201. Although qualitative assessment is standard, calculation of lung-to-heart ratios is preferred. Lung uptake may be increased on stress images if the exercise was submaximal. Lung uptake during dipyridamole and adenosine imaging tends to be higher than that seen during adequate exercise. Both the likelihood of CAD and the risk of an adverse outcome are increased when lung uptake is increased.

Right ventricular (RV) intensity is normally about 50% of the peak LV intensity. Increased RV uptake is indicative of RV pressure overload, most typically because of pulmonary hypertension. RV intensity may also appear increased when LV uptake is globally reduced.

The images should be examined for the presence of activity in organs other than the heart and pulmonary vasculature. Thyroid uptake, breast uptake, pulmonary parenchymal (tumor) uptake, or uptake in other thoracic or upper abdominal structures should be noted. Hepatic or splenic enlargement and the apparent absence of a gallbladder on technetium studies may be of clinical significance.

A statement regarding the overall quality of the study is helpful for two reasons. First, it alerts physicians using the report to any shortcomings that might reduce the accuracy of the data and their interpretation. Second, it is useful as an inclusion/exclusion criterion for subsequent acceptance of the study for research or other statistical analyses.[20]

Segmental Perfusion Assessment

The detection and localization of perfusion defects is typically performed by use of visual analysis of the unprocessed images. Perfusion defects are assigned to a particular myocardial segment or segments. Standardized nomenclature is recommended (Figure 1). In the anterior planar image, the anterolateral and inferior walls are divided into basal (1 and 5), and mid (2 and 4) segments, and the apex (3) separates the inferior and anterolateral walls. In the LAO view, the septum is divided into anteroseptal (6) and inferoseptal (7) segments, whereas the lateral wall is divided into inferolateral (9) and anterolateral (10) segments, and the inferior segment (8) separates the septum from the lateral wall. In the lateral view, the anterior and

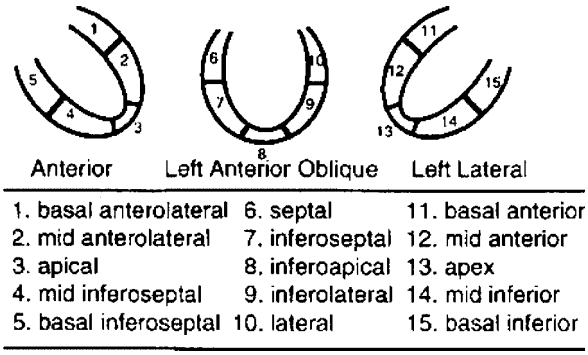

Figure 1. Planar MPI segmentation.

inferior walls are divided into basal (11 and 15) and mid (12 and 14) segments, whereas the apex (13) separates the anterior and inferior walls. Perfusion defect severity is typically expressed qualitatively with terms such as mild, moderate, or severe. Defect extent may be characterized qualitatively as small, medium, or large.

Rather than the qualitative evaluation of perfusion defects, it is preferred that the physician apply a semiquantitative method on the basis of a validated segmental scoring system. This approach standardizes the visual interpretation of scans, reduces the likelihood of overlooking significant defects, and provides an important semiquantitative index that is applicable to diagnostic and prognostic assessments. Furthermore, semiquantitative scoring can be used to more reproducibly and objectively designate segments as normal or abnormal. A 5-point model has been recommended for semiquantitative scoring of segments.

Category	Score
Normal perfusion	0
Mild reduction in counts—not definitely abnormal	1
Moderate reduction in counts—definitely abnormal	2
Severe reduction in counts	3
Absent uptake	4

The summed scores may also be calculated by adding all segment scores together to provide an integrated index of severity and extent. This may be done on the initial and resting or delayed images, and a summed difference score could then be used to represent the amount of defect reversibility.[21]

Perfusion Defect Severity and Extent: Quantitative

Quantitative analysis can be useful to supplement visual interpretation of the images. In planar perfusion imaging, quantitative analysis requires that a background subtraction be applied. The physician should review the background-subtracted images for technical adequacy. Quantitative data may be displayed as graphs of counts versus angular sampling location or as profiles that compare counts in contralateral walls of each image. Supporting data exist for both approaches. When counts are graphed versus radial sampling location, the resultant curve is typically compared with a gender-matched, reference database. The 2.0- to 2.5-SD curve is usually graphed with the patient's curve, and segments where the patient's curve drops below the reference curve are considered abnormal. The area between the patient's curve and the reference curve is a quantitative index of the combined extent and severity of the perfusion abnormality.[7-9]

Separate gender-based reference databases are recommended for thallium and technetium-based perfusion agents because the myocardial distribution and, in particular, the extracardiac activity are significantly different. Separate databases are also preferred, when available, for pharmacologic and exercise studies. Quantitative analysis of the data should not be used as a surrogate for visual analysis but rather as an expert opinion that may be used to modify the physician's impression.

Reversibility of perfusion defects may be categorized qualitatively as minimal, partial, or complete. Reversibility can be defined quantitatively as defects in which pixels improve to fewer than 2.5 SDs from the normal reference distribution at that location. The number of pixels that must show improvement for reversibility to be deemed present is arbitrary.

The so-called reverse redistribution may be seen in stress-delayed thallium imaging sequences. Reverse redistribution refers to segments with decreased or normal intensity on the initial set of images that show even less relative intensity on the delayed images. The interpretation of the finding remains controversial.

Acknowledgment

The authors have indicated that they have no financial conflicts of interest.

References

1. Maddahi J, Rodrigues E, Berman DS, Kiat H. State-of-the-art myocardial perfusion imaging. Cardiol Clin 1994;12:199-222.
2. Mahmarian JJ, Verani MS. Exercise thallium-201 perfusion scintigraphy in the assessment of coronary artery disease. Am J Cardiol 1991;67:2D-11D.
3. Port SC, Oshima M, Ray G, McNamee P, Schmidt DH. Assessment of single vessel coronary artery disease: Results of exercise electrocardiography, thallium-201 myocardial perfusion imaging and radionuclide angiography. J Am Coll Cardiol 1985;6:75-83.
4. Verzijlbergen JF, Suttorp MJ, Ascoop CA, Zwinderman AH, Niemeyer MG, van der Wall EE, et al. Combined assessment of technetium-99m SESTAMIBI planar myocardial perfusion images at rest and during exercise with rest/exercise left ventricular wall motion studies evaluated from gated myocardial perfusion studies. Am Heart J 1992;123:59-68.
5. Watson DD, Smith WH. Sestamibi and the issue of tissue cross-talk. J Nucl Med 1990;31:1409-11.

6. Smith WH, Watson DD. Technical aspects of myocardial planar imaging with technetium-99m sestamibi. Am J Cardiol 1990;66: 16E-22E.
7. Berger BC, Watson DD, Taylor GJ, Craddock GB, Martin RP, Teates CD, et al. Quantitative thallium-201 exercise scintigraphy for detection of coronary artery disease. J Nucl Med 1981;22:585-93.
8. Garcia E, Maddahi J, Berman D, Waxman A. Space/time quantitation of thallium-201 myocardial scintigraphy. J Nucl Med 1981;22:309-17.
9. Kaul S, Chesler DA, Boucher CA, Okada RD. Quantitative aspects of myocardial perfusion imaging. Semin Nucl Med 1987;17:131-44.
10. Van Train KF, Berman DS, Garcia EV, Berger HJ, Sands MJ, Friedman JD, et al. Quantitative analysis of stress thallium-201 myocardial scintigrams: A multicenter trial. J Nucl Med 1986;27: 17-25.
11. Wackers FJ, Fetterman RC, Mattera JA, Clements JP. Quantitative planar thallium-201 stress scintigraphy: A critical evaluation of the method. Semin Nucl Med 1985;15:46-66.
12. Sinusas AJ, Beller GA, Smith WH, Vinson EL, Brookeman V, Watson DD. Quantitative planar imaging with technetium-99m methoxyisobutyl isonitrile: Comparison of uptake patterns with thallium-201. J Nucl Med 1989;30:1456-63.
13. Koster K, Wackers FJ, Mattera JA, Fetterman RC. Quantitative analysis of planar technetium-99m-sestamibi myocardial perfusion images using modified background subtraction. J Nucl Med 1990; 31:1400-8.
14. Kaul S, Chesler DA, Okada RD, Boucher CA. Computer versus visual analysis of exercise thallium-201 images: A critical appraisal in 325 patients with chest pain. Am Heart J 1987;114: 1129-37.
15. Sigal SL, Soufer R, Fetterman RC, Mattera JA, Wackers FJ. Reproducibility of quantitative planar thallium-201 scintigraphy: Quantitative criteria for reversibility of myocardial perfusion defects. J Nucl Med 1991;32:759-65.
16. Reisman S, Maddahi J, Van Train K, Garcia E, Berman D. Quantitation of extent, depth, and severity of planar thallium defects in patients undergoing exercise thallium-201 scintigraphy. J Nucl Med 1986;27:1273-81.
17. Wackers FJ. Artifacts in planar and SPECT myocardial perfusion imaging. Am J Card Imaging 1992;6:42-57.
18. Schechter D, Bocher M, Karger H, Gotsman MS, Chisin R. Breast artifact in planar cardiac imaging: A comparison of 201T1 to sestamibi-99mTc. Cardiology 1994;84:339-44.
19. Weiss AT, Berman DS, Lew AS, Nielsen J, Potkin B, Swan HJ, et al. Transient ischemic dilation of the left ventricle on stress thallium-201 scintigraphy: A marker of severe and extensive coronary artery disease. J Am Coll Cardiol 1987;9:752-9.
20. Wackers FJ, Bodenheimer M, Fleiss JL, Brown M. Factors affecting uniformity in interpretation of planar thallium-201 imaging in a multicenter trial. The Multicenter Study on Silent Myocardial Ischemia (MSSMI) Thallium-201 Investigators. J Am Coll Cardiol 1993;21:1064-74.
21. Porenta G, Dorffner G, Kundrat S, Petta P, Duit-Schedlmayer J, Sochor H. Automated interpretation of planar thallium-201-dipyridamole stress-redistribution scintigrams using artificial neural networks. J Nucl Med 1994;35:2041-7.

ASNC IMAGING GUIDELINES FOR NUCLEAR CARDIOLOGY PROCEDURES

Myocardial perfusion and function: Single photon emission computed tomography

Christopher L. Hansen, MD,[a] Richard A. Goldstein, MD,[a]
Olakunle O. Akinboboye, MBBS, MPH, MBA,[b] Daniel S. Berman, MD,[b]
Elias H. Botvinick, MD,[b] Keith B. Churchwell, MD,[b] C. David Cooke, MSEE,[b]
James R. Corbett, MD,[b] S. James Cullom, PhD,[b] Seth T. Dahlberg, MD,[b]
Regina S. Druz, MD,[b] Edward P. Ficaro, PhD,[b] James R. Galt, PhD,[b] Ravi K. Garg, MD,[b]
Guido Germano, PhD,[b] Gary V. Heller, MD, PhD,[b] Milena J. Henzlova, MD,[b]
Mark C. Hyun, CNMT, NCT, RT(N)(R),[b] Lynne L. Johnson, MD,[b]
April Mann, CNMT, NCT, RT(N),[b] Benjamin D. McCallister, Jr, MD,[b]
Robert A. Quaife, MD,[b] Terrence D. Ruddy, MD,[b] Senthil N. Sundaram, MD, MPH,[b]
Raymond Taillefer, MD,[b] R. Parker Ward, MD,[b] John J. Mahmarian, MD[c]

Purpose. To evaluate regional myocardial perfusion and function.

ACQUISITION PROTOCOLS

Protocols for the various nuclear cardiology single photon emission computed tomography (SPECT) acquisition studies are presented in the following pages (Tables 1-6). For each of the protocols, the acquisition parameters are listed along with their corresponding value for exercise and rest. Implementation of these protocol acquisition parameters has been shown to provide acceptable images of good quality for routine clinical interpretation and quantitation. However, protocol parameters other than those listed may be preferred at some institutions, and ongoing research into corrections for attenuation, scatter, and camera response depth dependence may result in better parameters in the future. Therefore these protocols should be viewed as a consensus of opinion on the parameters that will provide acceptable images. A description for each of the acquisition parameters is listed below.

1. **Dose.** The doses for each of the protocols represent standard doses commonly used clinically. The standard doses described are given for an average 70-kg patient. Doses may be adjusted upward for heavier patients by 0.04 mCi/kg for thallium 201 and by 0.31 mCi/kg for technetium 99m. Other options are increased imaging times, the use of multidetector systems, or 2-day imaging. Tl-201 imaging times can be adjusted based on the counts acquired for a preliminary 4-minute planar study in order to ensure acquiring at least 500,000 background-subtracted myocardial counts.
2. **Position.** Factors influencing patient position include camera/gantry design, minimization of artifacts, and patient comfort. The supine position is routinely used for SPECT imaging with most currently available systems and protocols. Prone imaging has been reported to produce less patient motion and less inferior wall attenuation than supine imaging.[1,2] The combination of supine and prone images may be helpful in identifying attenuation artifacts due to breast and/or excessive lateral chest-wall fat, due to the shift in position of the attenuating structures that occurs in the prone position. In some laboratories the advantages of prone imaging in clarifying artifactual defects has led to a routine use of the combination of supine followed by prone acquisitions.[3] It appears that prone imaging does not eliminate attenuation artifact but rather simply changes the location. By comparing supine and prone images, artifactual defects will change their location whereas true perfusion defects will remain fixed.[4,5] Therefore it is suggested that prone imaging be done in combination with supine imaging and not simply replace it. When being used in this fashion, the acquisition time for the secondary (prone) image set is reduced by 20% to 40%. Using a dual-detector camera with 25 to 30 mCi of a Tc-99m perfusion agent, supine acquisitions are performed for 25 seconds per stop and prone acquisitions for 15

Co-Chair[a] Member[a] Board Reviewer[a]
J Nucl Cardiol 2007;14:e39-60.
1071-3581/$32.00

doi:10.1016/j.nuclcard.2007.09.023

Table 1. Patient protocol: Same-day rest-stress Tc-99m acquisition

	Rest study	Stress study		For information, see paragraph
Dose	8-12 mCi	24-36 mCi	Standard	1
Position	Supine	Supine	Standard	2
	Prone	Prone	Optional	2
	Upright/semi-upright	Upright/semi-upright	Optional	
Delay time (intervals)				
Injection → imaging	30-60 min	15-60 min	Standard	3
Rest → stress		30 min to 4 h	Standard	3
Acquisition protocol				
Energy window	15%-20% symmetric	Same	Standard	4
Collimator	LEHR	Same	Preferred	5
Orbit	180° (45° RAO to 45° LPO)	Same	Preferred	6
Orbit type	Circular	Same	Standard	7
	Non-circular	Same	Standard	7
Pixel size	6.4 ± 0.4 mm	Same	Standard	8
Acquisition type	Step and shoot	Same	Standard	9
	Continuous	Same	Optional	9
No. of projections	60-64	Same	Standard	10
Matrix	64 × 64	Same	Standard	11
Time/projection	25 s	20 s	Standard	12
ECG gated	Optional	Standard	Preferred	14
Frames/cycle	8	8	Standard	14
	8	16	Optional	
	16	16	Optional	14
R-to-R window	100%	100%	Preferred	14

RAO, Right anterior oblique; *LPO*, left posterior oblique.

seconds per stop, with 30 to 32 stops per detector being obtained per acquisition along a 180° orbit (right anterior oblique 45° to left posterior oblique 45°). With Tl-201, imaging should be begun approximately 10 to 15 minutes after stress testing, and if soft-tissue attenuation or patient motion compromises a study, the benefit of repeating the acquisition is questionable. In contrast, Tc-99m sestamibi or Tc-99m tetrofosmin permits stress testing and tracer injection to take place at a location remote from the imaging laboratory and image acquisition can simply be repeated when patient motion, soft-tissue attenuation, or other artifact is considered to be responsible for the production of a perfusion defect. Some camera/gantry designs require the patient to be positioned in a more upright position. Changes in patient positioning from those described above will likely cause changes in the distribution of adjacent soft-tissue attenuation and need to be considered in image interpretation. New normal databases will most likely need to be generated for different patient positions.

3. **Delay time.** These times are listed as ranges; specific values are optional. The objectives are to allow the patient to recover fully from exercise, thus allowing heart rate to return to baseline (reducing gating artifact), avoiding "upward creep" from changes in respiratory patterns while dyspnea resolves, and to minimize interference from hepatic uptake.[6] Provided that imaging times fall within the specified ranges, clinically useful SPECT images should result.
4. **Energy windows.** Energy window position is determined by the radioisotope employed, 140 keV for technetium-based perfusion agents and 70 keV for thallium. It is reasonable to simultaneously acquire the higher energy peaks of thallium (135 and 167 keV) on cameras that are capable of doing this. The window sizes are determined largely by convention and reflect the tradeoff between image counts and resolution. The values shown are the most commonly used and have been found to be acceptable for most cameras. On systems offering improved energy resolution, the window size may be reduced, result-

Table 2. Patient protocol: Same-day stress-rest Tc-99m acquisition

	Stress study	Rest study		For information, see paragraph
Dose	8-12 mCi	24-36 mCi	Standard	1
Position	Supine	Supine	Standard	2
	Prone	Prone	Optional	2
	Upright/semi-upright	Upright/semi-upright	Optional	
Delay time (intervals)				
Injection → imaging	15 min to 1 h	30-60 min	Standard	3
Stress → rest		30 min to 4 h	Standard	3
Acquisition protocol				
Energy window	15%-20% symmetric	Same	Standard	4
Collimator	LEHR	Same	Preferred	5
Orbit	180° (45° RAO to 45° LPO)	Same	Preferred	6
Orbit type	Circular	Same	Standard	7
	Non-circular	Same	Standard	7
Pixel size	6.4 ± 0.4 mm	Same	Standard	8
Acquisition type	Step and shoot	Same	Standard	9
	Continuous	Same	Optional	9
No. of projections	60-64	Same	Standard	10
Matrix	64 × 64	Same	Standard	11
Time/projection	25 s	20 s	Standard	12
ECG gated	Optional	Standard	Preferred	14
Frames/cycle	8	8	Standard	14
	16	16	Optional	14
R-to-R window	100%	100%	Preferred	14

RAO, Right anterior oblique; *LPO*, left posterior oblique.

ing in decreased scatter and improved image resolution, so long as imaging times are extended to acquire the same clinically useful number of counts. The same energy windows used in performing patient studies should be used for routine daily quality control (QC).

5. **Collimator.** Parallel-hole collimators are most commonly employed for cardiac SPECT acquisitions. They fall into two categories: low-energy all-purpose (LEAP), used mostly for Tl-201 studies, and low-energy high-resolution (LEHR), used for Tc-99m studies. Compared with LEAP collimators, LEHR collimators have longer bores, thinner septa, and smaller holes, which provide better resolution at the expense of reduced sensitivity. Therefore, to use LEHR collimators, imaging agents providing high count rates are required (ie, Tc-99m agents). Generally, LEAP collimators are used for 3-mCi Tl-201 studies, including gated SPECT acquisitions. For dual-isotope studies, LEHR collimators are suggested.
6. **Orbit.** Due to the anterior position of the heart in the left hemithorax, much higher count rates are obtained per given period of imaging time for a 180° orbit (45° right anterior oblique to 45° left posterior oblique) compared to a 360° orbit.[7] The recommendation of which orbit will depend on the camera configuration; it does not seem to be worthwhile to increase imaging time to complete a 360° orbit since much better count statistics will be obtained if that time is used to increase acquisition on a 180° orbit.[8] A 360° orbit is appropriate for 3-headed cameras with a 360° configuration where a 360° orbit is acquired in the same time as a 180° orbit. The utility of the posterior 180° of a 360° orbit is much greater for higher-energy radioisotopes (such as technetium) compared to low-energy radioisotopes (such as thallium).
7. **Orbit type.** The main orbit options in SPECT myocardial perfusion imaging are circular versus noncircular (elliptical or body-contoured) orbits. Noncircular orbits follow the contour of the patient, bringing the camera closer to the patient, thereby improving spatial resolution. Circular orbits maintain a fixed radius of rotation and on average result in the detector being further from the patient. In

Table 3. Patient protocol: Two-day stress Tc-99m acquisition

	Stress study	Rest study		For information, see paragraph
Dose	30 mCi	30 mCi	Standard	1
Position	Supine	Supine	Standard	2
	Prone	Prone	Optional	2
Delay time (intervals)				
Injection → imaging	15-60 min	30-60 min	Standard	3
Acquisition protocol				
Energy window	15%-20% symmetric	Same	Standard	4
Collimator	LEHR	Same	Preferred	5
Orbit	180° (45° RAO to 45° LPO)	Same	Preferred	6
Orbit type	Circular	Same	Standard	7
	Non-circular	Same	Standard	7
Pixel size	6.4 ± 0.4 mm	Same	Standard	8
Acquisition type	Step and shoot	Same	Standard	9
	Continuous	Same	Optional	9
No. of projections	60-64	Same	Standard	10
Matrix	64 × 64	Same	Standard	11
Time/projection	20 s	20 s	Standard	12
ECG gated	Standard	Standard	Preferred	14
Frames/cycle	8	8	Standard	14
	16	16	Optional	14
R-to-R window	100%	100%	Preferred	14

RAO, Right anterior oblique; *LPO*, left posterior oblique.

general, there is reduced (but more uniform) spatial resolution with circular orbits since the detector-to-source distance is greater with this technique. Circular acquisitions continue to be the most frequently used option, but some manufacturers do provide noncircular orbit capability. Imaging artifacts have been observed when noncircular orbits are used, due to increased variation of source-to-detector distance, resulting in variation of spatial resolution.[9]

8. **Pixel size.** The SPECT protocols listed here specify a 6.4 ± 0.4–mm pixel size for a 64 × 64 image matrix. This size offers satisfactory image resolution for interpretation and quantitation of both Tl-201 and Tc-99m tomograms.
9. **Acquisition type.** The most widespread mode of tomographic acquisition is the "step-and-shoot" method. In this approach, the camera acquires a projection and then stops recording data when moving to the next angle; this results in a small amount of dead time since the camera is not acquiring data while it is moving. An alternative is "continuous" mode, where the camera moves continuously and acquires each projection over an angular increment. This eliminates dead time and thus increases image counts at the expense of a small amount of blurring due to the motion of the camera head while acquiring. It seems likely that the increase in count statistics more than offsets the small amount of blurring due to camera motion.
10. **Number of projections.** The optimal number of projections for emission studies depends on matching the number of projections to the resolution of the system. A thallium SPECT acquisition with a LEAP collimator is a relatively low-resolution study, for which 32 projections over 180° are sufficient. A higher-resolution study using Tc-99m agents should be collected with a high-resolution collimator; this requires at least 60 to 64 projections over 180° to prevent loss of resolution. Larger numbers of projections are not necessary at this time but could become beneficial if technical innovations result in improved overall system resolution.
11. **Matrix.** The standard matrix size for emission SPECT is 64 × 64 pixels.
12. **Time/projection.** The emission acquisition times listed have been found to produce images of acceptable and comparable quality for rest and stress studies.
13. **Total time.** For single-detector systems, the total time for an emission acquisition ultimately is based

Table 4. Patient protocol: Separate dual-isotope acquisition

	Rest study	Stress study		For information, see paragraph
Dose	2.5-3.5 mCi Tl-201	30 mCi Tc-99m	Standard	1
Position	Supine	Supine	Standard	2
	Prone	Prone	Optional	
	Upright/semi-upright	Upright/semi-upright	Optional	
Delay time (intervals)				
Injection → imaging	10-15 min	15-60 min	Standard	3
Rest → stress		No delay	Standard	3
Acquisition protocol				
Energy window	25%-30% symmetric, 70 keV 20% symmetric, 167 keV	15%-20% symmetric, 140 keV	Standard	4
Collimator	LEHR	Same	Preferred	5
Orbit	180° (45° RAO to 45° LPO)	Same	Preferred	6
Orbit type	Circular	Same	Standard	7
	Non-circular	Same	Standard	7
Pixel size	6.4 ± 0.4 mm	Same	Standard	8
Acquisition type	Step and shoot	Same	Standard	9
	Continuous	Same	Optional	9
No. of projections	32-64	60-64	Standard	10
Matrix	64 × 64	Same	Standard	11
Time/projection	40 s (32 fr), 25 s (64 fr)	20 s	Standard	12
ECG gated	Optional	Standard	Preferred	14
Frames/cycle	8	8	Standard	14
	16	16	Optional	
R-to-R window	100%	100%	Preferred	14

RAO, Right anterior oblique; *LPO*, left posterior oblique.

on how long a patient can tolerate the procedure without moving, balanced by the need to acquire sufficient counts. The maximum practical time is on the order of 30 minutes. For 90° dual-detector systems, this time can be halved, and many laboratories obtain gated perfusion SPECT studies in only 12 to 15 minutes using biplane cameras. Consideration may be made for increasing imaging time in patients likely to have lower count statistics (eg, obese patients) if it is felt that they can tolerate it.

14. **Gated SPECT.** Incorporation of wall motion and wall thickening information from gated SPECT has been shown to increase specificity and confidence by helping to differentiate breast and diaphragmatic attenuation artifacts from true perfusion defects. Likewise, assessment of regional wall motion and/or thickening can be a valuable tool for detecting viability within a stress-induced perfusion defect. Left ventricular (LV) ejection fractions (EFs) and volumes, as well as regional wall motion and thickening, now are computed routinely from gated SPECT data using commercially available software.[10] The majority of stress myocardial perfusion radionuclide studies currently are acquired as gated SPECT data. However, there is mounting evidence that the information content of the post-stress acquisition may be different from that of the resting data in patients who have post-ischemic stunning of myocardium.[11] Discrepancies may also be present if the count density is suboptimal due to the lower tracer dose in the resting scan (same-day rest/stress protocol) and/or hypoperfusion of a segment at stress. Providing that there is adequate count density, particularly with regard to the lower-dose acquisitions, both stress and rest SPECT perfusion studies may be acquired as gated data sets. Optimizing protocols for which both stress and rest gated data are acquired remains an area of investigation.
15. **Multidetector systems.** It is recommended for multidetector systems that total imaging time be adjusted to obtain greater than the minimum counts listed in the "Instrumentation Quality Assurance and Performance" section of these guidelines (in the subsection entitled "Clinical QA for Each Patient

Table 5. Patient protocol: Stress/redistribution Tl-201 acquisition

	Stress study	Redistribution rest study		For information, see paragraph
Dose	2.5-3.5 mCi Tl-201	Not applicable	Standard	1
Position	Supine	Supine	Standard	2
	Prone	Prone	Optional	
	Upright/semi-upright	Upright/semi-upright	Optional	
Delay time (intervals)				
Injection → imaging	10-15 min*	Not applicable	Standard	3
Stress → rest		3-4 h	Standard	3
Acquisition protocol				
Energy window	30% symmetric, 70 keV 20% symmetric, 167 keV	Same	Standard	4
Collimator	LEAP	Same	Preferred	5
Orbit	180° (45° RAO to 45° LPO)	Same	Preferred	6
Orbit type	Circular	Same	Standard	7
	Non-circular	Same	Standard	7
Pixel size	6.4 ± 0.4 mm	Same	Standard	8
Acquisition type	Step and shoot	Same	Standard	9
	Continuous	Same	Optional	9
No. of projections	32-64	Same	Standard	10
Matrix	64 × 64	Same	Standard	11
Time/projection	40 s (32 fr), 25 s (64 fr)	40 s (32 fr), 25 s (64 fr)	Standard	12

RAO, Right anterior oblique; *LPO*, left posterior oblique.
*An anterior planar image may be acquired during this interval to evaluate Tl-201 lung uptake.

Procedure") but less than a maximum total imaging time of 30 minutes.

16. The following acquisition parameters are recommended for the imaging protocols described in the "Stress Protocols and Tracers" section of these guidelines.

PROCESSING PROTOCOLS

1. **Filtering.** Image filtering is a very complex topic that encompasses techniques for image enhancement, reconstruction, and feature extraction.[12,13] The main area of concern for an interpreter of SPECT studies is image enhancement by reducing noise prior to image reconstruction. All forms of imaging are plagued by statistical variation in the acquired image counts commonly referred to as noise. The quality of an image can be described as the signal-to-noise ratio, which describes the relative strength of the signal component (what is actually being imaged) compared to noise. The signal-to-noise ratio is much higher at lower spatial frequencies (broad features that are constant over many pixels) and decreases at higher spatial frequencies (features that change over few pixels such as edges). In general, the greater the count statistics, the better the signal-to-noise ratio. A low-pass filter is generally used to reduce noise because it allows low spatial frequencies to pass through and attenuates the high frequencies where image noise predominates. Low-pass filters such as the Hanning and Butterworth can be characterized by a cutoff frequency where they begin to affect the image. The cutoff frequency can be adjusted, depending on the signal-to-noise ratio, to preserve as much of the signal and suppress[14] as much noise as possible. If the cutoff is too high, there is significant noise in the image; if the cutoff is too low, significant information in the signal is suppressed. Nuclear cardiology images, because of their relatively low count statistics, tend to have greater amounts of image noise, and filtered backprojection, because of its dependence on ramp filtering, tends to amplify this noise. The optimal filter for a given image depends on the signal-to-noise ratio for that image; under-filtering an image leaves significant noise in the image, and over-filtering unnecessarily blurs image detail; both over-filtering and under-filtering can reduce image accuracy. Software reconstruction packages are set with default filter selection and cutoff values that are optimized for the average patient. Adjustment of the filter cutoff can be

Table 6. Patient protocol: Stress/reinjection/redistribution Tl-201 acquisition

	Stress study	Reinjection	(Redistribution) rest study		For information, see paragraph
Dose	2.5-3.5 mCi	1.0-1.5mCi	Not applicable	Standard	1
Position	Supine		Supine	Standard	2
	Prone		Prone	Optional	2
	Upright/semi-upright		Upright/semi-upright	Optional	
Delay time (intervals)					
Injection → imaging	10-15 min		Not applicable	Standard	3
Stress → redistribution			3-4 h	Standard	3
Reinjection → imaging (MI)			20-30 min	Standard	3
24-h imaging				Optional	3
Acquisition protocol					
Energy window	30% symmetric, 70 keV 20% symmetric, 167 keV		Same	Standard	4
Collimator	LEAP		Same	Preferred	5
Orbit	180° (45° RAO to 45° LPO)		Same	Preferred	6
Orbit type	Circular		Same	Standard	7
	Non-circular		Same	Standard	7
Pixel size	6.4 ± 0.4 mm		Same	Standard	8
Acquisition type	Step and shoot		Same	Standard	9
	Continuous		Same	Optional	9
No. of projections	32-64		Same	Standard	10
Matrix	64 × 64		Same	Standard	11
Time/projection	40 s (32 fr), 25 s (64 fr)		40 s (32 fr), 25 s (64 fr)	Standard	12

RAO, Right anterior oblique; *LPO*, left posterior oblique.

done in patients with poor count statistics (eg, obese patients) to optimally filter their images. However, this is discouraged unless the physician is thoroughly familiar with filter adjustment and the potential effects. Changing the filter cutoff may have unexpected effects on the output of commercially available analysis programs, especially those that employ edge detection such as defect quantitation and LV volumes and EF. Deconvolving filters, such as the Metz and Wiener filters, can correct for blurring that occurs from scatter as photons travel through the body. Although images may look sharper with these filters, these filters have not yet been shown to improve image accuracy.[12]

2. **Reconstruction.** The traditional method of image reconstruction has been filtered backprojection, a technique based on a mathematical proof, which assumes no attenuation, no scatter, and an infinite number of projections. It is relatively straightforward and comparatively fast.[15] The vast majority of clinical experience is based upon it, and it has withstood the test of time despite its inability to model attenuation and scatter. There is a different class of reconstruction algorithms that are based on iterative techniques. These algorithms start with a rudimentary guess of the distribution, generate projections from the guess, and compare these projections to the acquired projections. The guess is refined based on the differences between the generated and actual projections, and the process is repeated (hence the term "iterative") usually for a fixed number of iterations but can also be repeated until the error between the generated and actual projections is acceptably small. A main advantage of these algorithms is that the process of generating projections from the guess can be made as sophisticated as desired and can incorporate such variables as attenuation, scatter, and depth-dependent blur. The main disadvantage is the computational intensity of the algorithm; it takes many times longer to complete than filtered backprojection. However, due to contin-

ual increases in computer processor speed, these algorithms can now be completed in an acceptable time for routine clinical use. Nonetheless, iterative techniques have not yet been proven to be unequivocally superior to filtered backprojection.

3. **Reorientation.** A critical phase of myocardial processing is reorientation of tomographic data into the natural approximate symmetry axes of an individual patient's heart. This is performed either by an observer or automatically and results in sectioning the data into vertical long-axis, horizontal long-axis, and short-axis planes. Long-axis orientation lines should be parallel to long-axis walls of the myocardium and should be consistent between rest and stress studies. Inappropriate plane selections can result in misaligned myocardial walls between rest and stress data sets, potentially resulting in incorrect interpretation. It is crucial that all axis choices be available as QC screens, and that these are reviewed by the technologist and the physician who reads each study to verify that axes were selected properly.
4. **Display–cine review.** The most important post-acquisition QC procedure is to view the raw tomographic data in cine mode. This presentation offers a sensitive method for detecting patient and/or heart motion, "upward creep," breast shadow due to attenuation, diaphragmatic attenuation, and superimposed abdominal visceral activity, all of which can create artifacts in the reconstructed images. Review of the raw tomograms in cine mode is performed twice: once by the technologist immediately after the acquisition and again by the physician during image interpretation. For gated studies, usually it is only the sum of all gated tomograms that is reviewed in this manner; this will alert the observer to most types of gating errors due to arrhythmias manifested by an intermittent flashing of the images. However, for the detection of gating errors due to some types of transient arrhythmias, a full display of all count-versus-projection curve data is helpful. Cine reviews occasionally show abnormalities in the abdomen or thorax such as renal cysts or abnormal uptake that may be suspicious for neoplasm. The accuracy and clinical utility of these findings have not yet been established.
5. **Display–study review.** It is strongly recommended that physicians use the active computer screen for reviewing images and use film and paper hard copies only for record-keeping purposes. Images produced by formatters onto transparency film or photographic paper can have variable contrast, also termed gamma, and result in inconsistent image interpretation. Computer screen outputs are relatively more stable and always have readily available monochromatic contrast bars or color code bars to the side of the images, enabling more consistent viewing conditions. In addition, computer screens offer rapid sequential and/or cinematic displays of image data. For all of these reasons, screen interpretation is strongly recommended over relying on interpretations from hard copies.[16]

PERFUSION QUANTITATION

The display medium and translation table employed can have a significant impact on image interpretation, going as far as to make a normal perfusion scan appear abnormal or vice versa. Quantitative analysis is a direct way of measuring relative uptake of a perfusion tracer that is independent of the display medium and translation table and can thus greatly reduce variations in interpretation due to subjective analysis and inconsistent image display. Quantitative analysis also allows for the comparison of a study with a gender-specific normal database. For this reason, quantitative analysis is recommended as part of image interpretation. Traditional, circumferential profile-based quantitative analysis consists of the following steps:

1. **Image quantitation.** This measures the relative activity, most often in a short-axis slice, by generating a circumferential profile also known as a radial plot. This is done by first identifying the center of the lumen and the inner and outer boundaries of the ventricle. The activity in each part of the slice is determined by measuring the activity in each pixel lying on a radius between the inner and outer boundaries, analogous to moving along a spoke of a wagon wheel from the hub to the rim. The radius is then rotated slightly (analogous to going to the next spoke of the wagon wheel), and the activity is again measured. This is repeated until the entire circumference has been traversed. Determination of activity along each radius can be as simple as identifying the maximal pixel or as complicated as fitting the profile to a Gaussian curve.
2. **Normalization and scaling.** Myocardial perfusion imaging can only measure relative uptake. In order to compare different studies or compare with normal databases, the images must be normalized to a certain value. Each slice can be normalized to its own maximum, but it is much more common to normalize to the maximal pixel in the ventricle. All values are multiplied by 100/value of the maximum pixel, which sets the maximum pixel to 100 and all others to a fraction of that. Finally, the ventricle is "scaled" to a constant number of curves; smaller ventricles with fewer short-axis slices are interpolated up, and larger

ventricles with more short-axis slices are decimated down to achieve a constant number of curves. Thus relative activity can be compared for any location in two ventricles regardless of their absolute tracer uptake or chamber size.

3. **Polar plot generation (optional).** Each radial plot generated in step 1 generates a series of numbers that can be displayed as a graph. The entire LV volume would be represented by a series of graphs, which is difficult to assimilate. Alternatively, these plots can be used to make a "bulls-eye" or polar plot.[17] Instead of generating a graph, the radial profiles are used to make a series of rings of activity, where the intensity of the ring corresponds to the relative activity of the corresponding polar plot and the diameter of the rings grows moving toward the base of the heart. These can then be fused into a single image where each successive ring is formed around the one preceding it, analogous to the rings of a tree. This creates a 2-dimensional image that reflects the relative activity in the 3-dimensional left ventricle with the apex at the center of the polar plot and the base as the outer ring.[17,18] The width of the rings can be adjusted to reflect the relative size of the corresponding short-axis images so that a given area of the polar plot corresponds to a constant fraction of the volume of the left ventricle in a process known as "volume weighting."
4. **Database construction and analysis.** It is frequently difficult to differentiate true perfusion defects from soft-tissue attenuation; women tend to have anterior defects from breast attenuation, and men tend to have inferior wall defects from diaphragmatic attenuation.[19] A range for "normal" soft-tissue attenuation can be defined by creating a normal database; gender-specific normal databases are usually employed due to the different attenuation patterns for men and women. These can be generated by performing radial plot analysis on "normals"—that is, patients proven not to have coronary disease or, more often, patients with an acceptably low probability of having coronary disease (usually $<5\%$ or $<1\%$). The mean and standard deviation of activity for each point of the ventricle are calculated for the male and female normals; the result is the normal database for each gender. The normalized and scaled activity for each point of the ventricle of a patient is compared to the mean of the corresponding gender-based normal database; if the activity is more than a predetermined number of standard deviations below the mean of the normals (2.5 standard deviations is most frequently used), it is considered abnormal. It should be realized that this definition of normal is statistical, not absolute. There will still be overlap between normal and abnormal uptake.
5. **Parameters.** Different parametric images can be generated to show the results of quantitative analysis, such as "blackout," "severity," and "reversibility" maps. A blackout map generates a polar plot for the patient marking those points that fall a predetermined number of standard deviations below the gender-based normal limits and thus demonstrates the size or extent of the perfusion defect. Another type of parametric image can be generated which shows the number of standard deviations that activity falls below the mean of normals and thus demonstrates severity. A third can be generated which quantitates the activity on the stress and rest images and demonstrates which areas show improved perfusion at rest, which is known as a reversibility map.

GATED SPECT

Acquisition. The introduction of technetium-based perfusion tracers has resulted in images with sufficient count density to allow for cardiac gating adding parameters of wall motion, wall thickening, and EF to myocardial perfusion imaging.[20-23] Gating requires a stable and consistent heart rhythm as well as sufficient temporal resolution to correctly characterize the cardiac cycle. A stable heart rate and rhythm can be achieved by rejecting heartbeats that fall out of range at the expense of an increase in image time. This "beat length acceptance window" can vary from 20% to 100% of the expected R-to-R duration, the recommended value being 20% if an "extra frame" is provided that allows the accumulation of rejected counts. Most laboratories gate the heart for 8 frames per cycle, although an increasing number of laboratories have reported good results with 16 frames per cycle and have used the increased temporal sampling to derive more accurate estimates of LVEF as well as parameters of diastolic function. For either 8- or 16-frame gating, the recommendations are to avoid beat rejection. The lower count statistics achieved with Tl-201 imaging make gating more challenging with this isotope, but many laboratories have reported satisfactory results using 8-frame gating in selected patients.[24] Processing is done using commercially available software.

INTERPRETATION AND REPORTING

General Comments

The interpretation of myocardial perfusion SPECT images should be performed in a systematic fashion to include (1) repeat evaluation of the raw tomographic images to determine the presence of technical sources of abnormalities and extracardiac activity; (2) interpretation of images with respect to the location, size, severity, and

reversibility of defects as well as chamber sizes and, for Tl-201, presence or absence of pulmonary uptake; (3) incorporation of the results of quantitative analysis; (4) consideration of functional data obtained from the study; and (5) consideration of clinical factors that may have influenced the presence of any findings. All of those factors contribute to the production of a final clinical report. Guidelines for interpreting and reporting myocardial perfusion SPECT are listed in Tables 8 and 9.

Display

1. **Recommended medium for display.** It is strongly suggested that the reading physician use the computer monitor screen rather than hard copy to interpret the study since a monitor screen is capable of displaying more variations in gray scale or color (making it easier to discern smaller variations in uptake) and is more consistent than film. Moreover, it is not possible to properly view moving images (eg, raw tomographic data or gated images) on hard copy. A linear gray-scale translation table is generally preferred to color tables since it demonstrates consistent grades of uptake compared to pseudocontouring seen with color scales, but this is also dependent on how familiar the reader is with a given translation table.[16,25] The reader should be aware that the appearance of an image can change significantly when changing from one translation table to another. A linear scale is preferred to nonlinear (eg, sigmoidal) scales since it most faithfully characterizes uptake over the range of activity. A logarithmic scale may be used for evaluating regions of lower-count density such as soft-tissue uptake and the right ventricle but should never be used for interpreting LV uptake.[16,25]
2. **Conventional slice display of SPECT images.** Three sets of images should be displayed: (a) a view generated by slicing perpendicular to the long axis of the left ventricle (short axis); (b) a view of long-axis tomograms generated by slicing in the vertical plane (vertical long axis); and (c) a view of long-axis tomograms generated by slicing in the horizontal plane (horizontal long axis). The short-axis tomograms should be displayed with the apical slices to the far left with progression of slices toward the base in a left-to-right fashion. The vertical long axis should be displayed with septal slices on the left and progression through the midventricular slices to the lateral slices in a left-to-right fashion. Similarly, the horizontal long-axis tomographic display should proceed left to right from the inferior to the superior (anterior) surface. It is also recommended that, for purposes of interpretation and comparison of sequential images (eg, stress and rest, rest and redistribution), these images be displayed aligned and adjacent to each other serially. There are two widely used approaches to image normalization. Each series (vertical, horizontal, short axis) may be normalized to the brightest pixel in the entire image set, which is known as "series normalization." This is considered to provide the most intuitively easy way to evaluate the extent and severity of perfusion defects. The drawbacks of this approach are its sensitivity to focal hot spots, the frequently poor visualization of normal structures at the base and apex of the left ventricle, and the lack of an ideal display of each individual slice.

   The other approach is "frame normalization" in which each image is normalized to the brightest pixel within the frame. That method provides optimal image quality of each slice. The drawback of this approach is that the brightness of each slice is unrelated to the peak myocardial activity in the entire series such that gradations in activity between slices of a series may be lost. That drawback is mitigated by the display of three orthogonal planes.
3. **Three-dimensional display.** Most commercial software programs allow creation of 3-dimensional displays. These help less experienced readers identify coronary distributions associated with perfusion defects. These should be used only as an adjunct to, not a replacement for, the conventional image formatting described above.

Evaluation of Images for Technical Sources of Error

4. **Patient motion.** The interpreting physician should also review the raw tomographic images for possible sources of artifact. Images should again be inspected for the presence of patient motion. A cine display of the planar projection data is highly recommended because motion in both the craniocaudal and horizontal axes is readily detectable. Additionally, a static "sinogram" and sometimes "linogram" may be used to detect motion. Software routines are available for quantitation and correction of motion. The experienced reader should be familiar with the normal appearance of raw tomograms and be able to identify motion artifact. In patients who have had a technetium-based perfusion agent, consideration should be made for repeating the image acquisition where feasible when significant motion is detected. Alternatives such as planar imaging or prone positioning may be considered as well. The effect of patient motion on the final reconstructions is complex.[6,26-28] Generally, up-and-down motion (espe-

cially when the heart returns to the same baseline) has less of an effect on the accuracy of the study than sideways motion. Also, up-and-down motion is much easier to correct either manually or with semiautomated software. Rotation currently cannot be corrected either manually or with available motion correction software. Since motion correction software may sometimes introduce motion artifact, corrected raw tomographic images should be evaluated in the same way for adequacy of the correction.

5. **Attenuation and attenuation correction.** The cine display of the planar projection images is also recommended for the identification of sources of attenuation, the most common being diaphragmatic in men and the breast in women.[29] Breast attenuation artifact is most problematic when it is different between the rest and stress images. When breast attenuation artifact is more prominent on the stress images than on the rest, it can be very challenging to exclude ischemia. Breast attenuation can sometimes be improved by repeating the acquisition with the breast repositioned. Diaphragmatic attenuation and breast attenuation may be reduced by imaging the patient prone. Hardware and software for attenuation and scatter correction are commercially available and may obviate or at least mitigate these common attenuation artifacts. The evaluation of attenuation-corrected (AC) images is performed with the same approach as that used for non-AC images. As with the interpretation of non-AC studies, it is essential that the interpreting physician be familiar with the segment-by-segment normal variation of uptake of radioactivity at stress and rest associated with the specific attenuation correction system that is being used.[30-32] AC images are displayed in the same manner as uncorrected images. Because the currently available correction algorithms are imperfect, it is recommended that the uncorrected data be interpreted along with the AC data.
6. **Reconstruction artifacts.** Superimposed bowel loops or liver activity may create artifactually intense uptake in adjacent myocardium that could mask a real perfusion defect or be misinterpreted as reduced uptake in adjacent or contralateral segments. Non-superimposed but adjacent extracardiac activity may also affect the reconstructed myocardial images. Intense activity in bowel loops or adjacent liver may cause a negative reconstruction artifact, resulting in an apparent reduction in activity in the adjacent myocardial segments. There is currently no reliable correction for such artifacts, although they may be less prominent with iterative as opposed to filtered backprojection techniques. They can often be eliminated by repeating the acquisition after the activity level in the adjacent structure has decreased.
7. **Myocardial statistics.** Many factors are involved in the final count density of perfusion images including body habitus, exercise level, radiopharmaceutical dose, acquisition time, energy window, and collimation. The interpreting physician should make note of the count density in the planar projection images because the quality of the reconstructed data is a direct reflection of the raw data. Perfusion defects can be artifactually created simply because of poor statistics. As a general rule, peak pixel activity in the LV myocardium in an anterior planar projection should exceed 100 counts for a Tl-201 study and 200 counts in a Tc-99m study.

Initial Image Analysis and Interpretation

The initial interpretation of the perfusion study should be performed without any clinical information other than the patient's gender, height and weight, and peak exercise heart rate. Such an approach minimizes the bias in study interpretation. All relevant clinical data should be reviewed after a preliminary impression is formed.

8. **Ventricular dilation.** Before segmental analysis of myocardial perfusion, the reader should note whether there is LV enlargement at rest or during stress. Dilation on both the stress and resting studies usually indicates LV dysfunction, although it may be seen in volume overload states with normal ventricular function. Transient ischemic dilation (TID) has been described as a marker for high-risk coronary disease.[33] It is most likely due to diffuse subendocardial ischemia[34,35] and can be seen in other conditions, such as microvascular disease, that cause diffuse subendocardial ischemia even in the absence of epicardial disease. TID is typically described quantitatively but may be quantified.[36] Normal limits by quantitation will depend on both the software and perfusion agents being used.
9. **Lung uptake.** The presence of increased lung uptake after thallium perfusion imaging has been described as an indicator of poor prognosis and should therefore be evaluated in all patients when using this perfusion agent.[34,35,37] No clear consensus has emerged as to the significance of lung uptake with technetium-based perfusion agents.
10. **Right ventricular uptake.** Right ventricular (RV) uptake may be qualitatively assessed on the raw projection data and on the reconstructed data. There are no established quantitative criteria for RV uptake, but in general, the intensity of the right ventricle is approximately 50% of peak LV intensity. RV uptake increases in the presence of RV hypertrophy,

most typically because of pulmonary hypertension.[38] The intensity of the right ventricle may also appear relatively increased when LV uptake is globally reduced.[39-41] Regional abnormalities of RV uptake may be a sign of ischemia or infarct in the distribution of the right coronary artery. The size of the right ventricle should be noted.

11. **Noncardiac findings.** Both thallium- and technetium-based agents can be concentrated in tumors, and uptake outside the myocardium may reflect unexpected pathology. However, the accuracy and, in particular, the specificity of myocardial perfusion imaging for diagnosing noncardiac conditions have not been established. Splanchnic Tl-201 activity following adequate exercise stress (>85% maximum predicted heart rate) is generally reduced compared to resting images. This difference is not present following pharmacologic Tl-201 stress testing with dipyridamole, adenosine, or dobutamine.
12. **Perfusion defect location.** Myocardial perfusion defects should be identified by use of visual analysis of the reconstructed slices. The perfusion defects should be characterized by their location as they relate to specific myocardial walls—that is, apical, anterior, inferior, and lateral. The term posterior should probably be avoided because it has been variably assigned either to the lateral wall (circumflex distribution) or to the basal inferior wall (right coronary distribution) and is thus ambiguous. Standardization of segment nomenclature is highly recommended. (See the segmentation models described below.)
13. **Perfusion defect severity and extent: Qualitative.** Defect severity is typically expressed qualitatively as mild, moderate, or severe. Mild defects may be identified by a decrease in counts compared to adjacent activity without the appearance of wall thinning, moderate defects demonstrate wall thinning, and severe defects are those that approach background activity.[42,43] Defect extent may be qualitatively described as small, medium, or large. In semiquantitative terms, small represents 5% to 10%, medium represents 15% to 20%, and large represents 20% of the left ventricle or greater.[43] Alternatively, defect extent may also be estimated as a fraction such as the "basal one half" or "apical one third" of a particular wall or as extending from base to apex. Defects whose severity and extent do not change between image sets (eg, stress and rest) are typically categorized as "fixed" or nonreversible. When changes do occur, a qualitative description of the degree of reversibility is required.
14. **Perfusion defect severity and extent: Semiquantitative.** In addition to the qualitative evaluation of perfusion defects, it is preferred that the physician may also apply a semiquantitative method on the basis of a validated segmental scoring system. This approach standardizes the visual interpretation of scans, reduces the likelihood of overlooking significant defects, and provides an important semiquantitative index that is applicable to diagnostic and prognostic assessments. It is generally considered preferable to use a system with at least 16 segments.

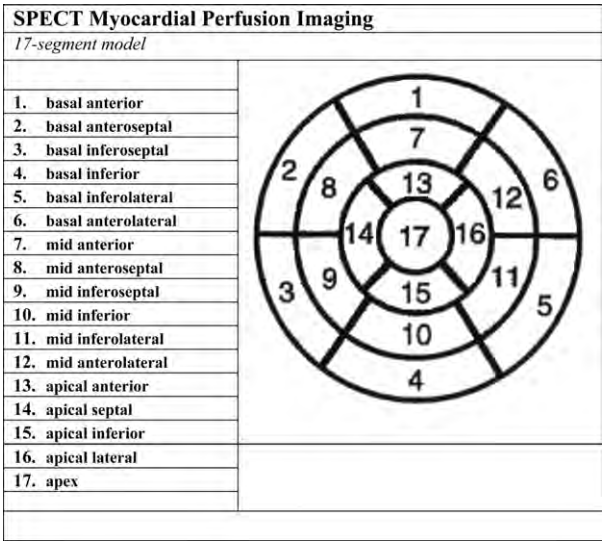

Figure 1. SPECT myocardial perfusion imaging: 17-segment model.

The quality assurance (QA) committee of the American Society of Nuclear Cardiology has considered several models for segmentation of the perfusion images and has previously recommended either a 17- or 20-segment model for semiquantitative visual analysis. The models use three short-axis slices (apical, mid, and basal) to represent most of the ventricle and one vertical long-axis slice to better represent the LV apex. In both the 17- and 20-segment models, the basal and mid short-axis slices are divided into 6 segments. In the 17-segment model, the apical short-axis slice is divided into 4 segments, whereas in the 20-segment model, the apical short-axis slice is divided into 6 segments. In the 17-segment model, a single apical segment is taken from the vertical long-axis slice, whereas in the 20-segment model, the apex is represented by 2 segments. Each segment has a specific name. In order to facilitate consistency of nomenclature with other imaging modalities, the 17-segment model has become the preferred nomenclature.

Seventeen-segment nomenclature (Figure 1). Segments 1, 7, and 13 represent the basal (1), mid (7), and apical (13) anterior segments. Segments 4, 10, and 15 represent the basal (4), mid (10), and apical (15)

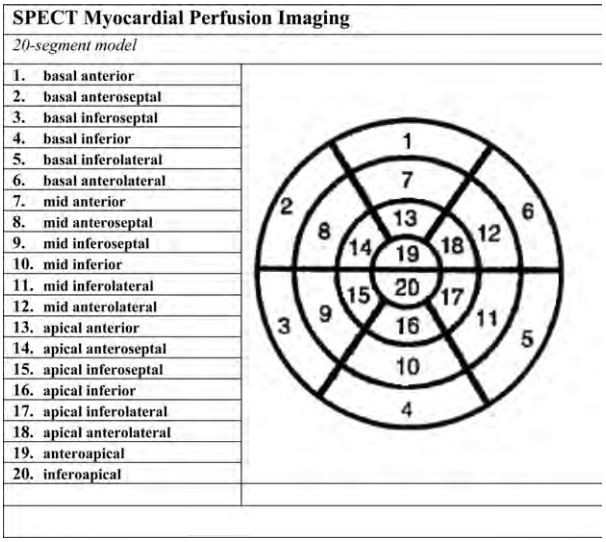

Figure 2. SPECT myocardial perfusion imaging: 20-segment model.

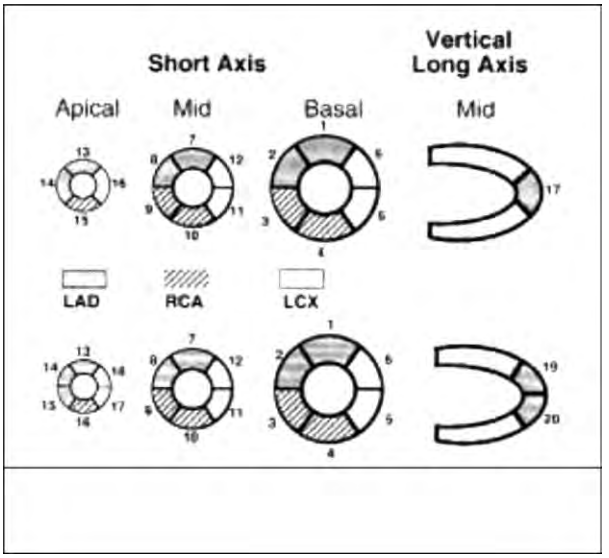

Figure 3. SPECT myocardial perfusion imaging: coronary artery territories. *LAD*, Left anterior descending artery; *RCA*, right coronary artery; *LCX*, left circumflex artery.

inferior segments. The septum contains 5 segments, the basal anteroseptal (2), the basal inferoseptal (3), the mid anteroseptal (8), the mid inferoseptal (9), and the apical septal (14). Similarly, the lateral wall is divided into the basal anterolateral (6), the basal inferolateral (5), the mid anterolateral (12), the mid inferolateral (11), and the apical lateral (16). The long-axis apical segment is called the apex.

Twenty-segment nomenclature (Figure 2). Segments 1, 7, and 13 represent the basal (1), mid (7), and apical (13) anterior segments. Segments 4, 10, and 16 represent the basal (4), mid (10), and apical (16) inferior segments. The septum contains 6 segments, the basal (2), mid (8), and apical (14) anteroseptal and the basal (3), mid (9), and apical (15) inferoseptal. Similarly, the lateral wall contains 6 segments, the basal (6), mid (12), and apical (18) anterolateral and the basal (5), mid (11), and apical (17) inferolateral segments. The apex from the vertical long-axis slice is divided into anteroapical (19) and inferoapical (20) segments.

The myocardial segments may be roughly assigned to coronary arterial territories as indicated in Figure 3 as long as the reader realizes that there can be considerable variation among patients especially in the inferior and inferolateral segments of the left ventricle due to the variable extent of the circumflex and right coronary artery territories.

Semiquantitative Scoring System: The Five-Point Model

The use of a scoring system provides a reproducible semiquantitative assessment of defect severity and extent. A consistent approach to defect severity and extent is clinically important because both of those variables contain independent prognostic power. Furthermore, semiquantitative scoring can be used to more reproducibly and objectively designate segments as normal or abnormal. Points are assigned to each segment in direct proportion to the perceived count density of the segment (Table 7).

Table 7. Semiquantitative scoring system: 5-point model

Category	Score
Normal perfusion	0
Mild reduction in counts—not definitely abnormal	1
Moderate reduction in counts—definitely abnormal	2
Severe reduction in counts	3
Absent uptake	4

In addition to individual scores, it has been recommended that summed scores be calculated. The summed stress score equals the sum of the stress scores of all the segments, and the summed rest score equals the sum of the resting scores or redistribution scores of all the segments. The summed difference score equals the difference between the summed stress and the summed resting (redistribution) scores and is a measure of reversibility. In particular, the summed stress score has been shown to have significant prognostic power.[43] Before

scoring, it is necessary for the interpreting physician to be familiar with the normal regional variation in count distribution of myocardial perfusion SPECT.

15. **Perfusion defect severity and extent: Quantitative.** Quantitative analysis is useful to supplement visual interpretation.[42-44] Most techniques of quantitative analysis are based on radial plots of short-axis slices. Different techniques analyze the apex separately. These plots are then normalized to allow creation of or comparison to normal databases. Defects can be defined as where activity falls a given amount below the mean of a normal database to evaluate size and severity of defects. Quantitation of the stress images is compared to the rest images to assess the degree of ischemia versus infarction. It is customary to generate separate normal databases based on gender as well as the perfusion agent used. This quantitative analysis is usually displayed as a "bulls-eye" or polar plot.[45] The quantitative programs are effective in providing an objective interpretation that is inherently more reproducible than visual analysis, eliminates the variability of the appearance of a defect when viewed in different media (with different gammas) and different translation tables, and is particularly helpful in describing changes between two studies in the same patient. Quantitative analysis also serves as a guide for the less experienced observer who may be uncertain about normal variations in uptake. Quantitative programs are by no means sophisticated enough to unequivocally differentiate perfusion defects from artifact but help in understanding the range of uptake that can be encountered in patients without disease. Because of artifacts during imaging and also the nature of coronary blood flow, there will always be an overlap between normals and patients with mild perfusion defects; this overlap can be reduced but not completely eliminated by careful attention to image acquisition and reconstruction. Therefore quantitative analysis should only be used as an adjunct to and not a substitute for visual analysis.

    Defect extent may be quantitatively expressed as a percentage of the entire left ventricle or as a percentage of individual vascular territories, the latter being less reliable because of the normal variations in coronary anatomy. Defect severity may be quantitatively expressed as the number of standard deviations by which the segment varies from the normal range for that particular segment or segments. Defect reversibility may also be expressed as a percentage of the entire left ventricle or of a vascular territory.

16. **Reversibility.** Reversibility of perfusion defects may be categorized qualitatively as partial or complete, the latter being present when the activity in the defect returns to a level comparable to surrounding normal myocardium. The semiquantitative scoring system may be used to define reversibility as a $\geq$2-grade improvement or improvement to a score of 1. Reversibility on a quantitative polar plot or on 3-dimensional displays will depend on the particular software routine in use and the normal reference databases used in the program. Areas of reversibility are typically described by pixels that improve to less than 2.5 SDs from the normal reference redistribution or resting database. How many pixels have to improve for reversibility to be deemed present is arbitrary.

    So-called reverse redistribution may be seen in stress delayed thallium imaging sequences and has been described in rest delayed technetium sestamibi sequences. Reverse redistribution refers to segments with decreased or normal intensity on the initial set of images that show even less relative intensity on the delayed images. The interpretation of the finding remains controversial, but in certain clinical situations, it seems to represent segments with a mixture of viable and nonviable myocardium that are frequently supplied by patent infarct-related arteries.[46]

GATED MYOCARDIAL PERFUSION SPECT

Because of the comparatively low additional cost and substantial benefit of the information obtained, gated studies of ventricular function should be a routine part of myocardial perfusion SPECT.[20] A systematic approach to display and interpretation of the ventricular function derived from gated SPECT is important.

17. **Gated SPECT display.** Multiple ventricular slices should be evaluated. At a minimum, a quad-screen display of apical and mid-basal short-axis, a mid-ventricular horizontal long-axis, and a mid-ventricular vertical long-axis slice should be viewed. Other slices may be viewed for completeness or to resolve a discrepancy between the clinical impression and what is seen on the four standard cine views. Ideally, the software should allow the user to scroll through any of the slices in any axis in cine mode. Each view should be normalized to the series of end-diastolic to end-systolic slices to maintain the count density changes that reflect wall thickening. When available, software routines that automatically define epicardial and endocardial borders and that subsequently calculate ventricular volumes and EF should be applied.

Table 8. Myocardial perfusion SPECT: Guidelines for interpretation

		For information, see paragraph
A. Display		
1. Medium		
a. Computer screen	Preferred	1
b. Film hard copy	Discouraged	1
2. Format		
a. Conventional slice display	Preferred	2
i. Frame normalization	Optional	2
ii. Series normalization	Preferred	2
b. Three-dimensional display	Optional	3
B. Technical sources of error		
1. Motion	Standard	4
2. Attenuation	Standard	5
a. Attenuation correction	Optional	5
3. Reconstruction artifacts	Standard	6
4. Myocardial statistics	Standard	7
C. Initial image interpretation		
1. Ventricular dilation		
a. Qualitative	Standard	8
b. Quantitative	Optional	8
2. Lung uptake		
a. Qualitative	Standard	9
b. Quantitative	Preferred	9
3. Non-cardiac	Standard	11
4. Perfusion defect assessment		
a. Location	Standard	12
b. Extent/severity		
i. Qualitative	Standard	13
ii. Semiquantitative	Optional	14
iii. Quantitative	Optional	15
5. Reversibility	Standard	16
D. Gated SPECT		
1. Display	Standard	17
2. QC	Standard	18
3. Regional wall motion	Standard	19
4. Regional wall thickening	Standard	19
5. LVEF		
a. Qualitative	Standard	20
b. Quantitative	Preferred	20
6. LV volume		
a. Qualitative	Standard	20
b. Quantitative	Recommended	20
E. Integration of perfusion and function results	Standard	21
F. Myocardial viability		
1. Qualitative	Standard	22
2. Semiquantitative	Optional	23
3. Quantitative	Preferred	24
G. Modification of interpretation	Preferred	25

Table 9. Myocardial perfusion SPECT: Guideline for reporting

		For information, see paragraph
A. Demographic data		
1. Name	Standard	26
2. Gender	Standard	26
3. Age	Standard	26
4. Date(s) of acquisition(s)	Standard	26
5. Medical record identification	Standard	26
6. Height/weight (body surface area)	Standard	26
7. Relevant medications	Optional	26
8. Indication for study	Standard	28
B. Acquisition parameters		
1. Type(s) of studies	Standard	27
2. Radionuclide(s) and doses	Standard	27
C. Results: Exercise/intervention data		
1. Resting ECG findings	Standard	29
2. Exercise/intervention parameters		
a. Heart rate, blood pressure, % maximal predicted heart rate, metabolic equivalents	Standard	30
b. Symptoms	Standard	30
c. Reason for terminating	Standard	30
d. ECG changes with exercise	Standard	30
D. Results: perfusion scan data		
1. Potential sources of error		
a. Motion	Standard	4
b. Attenuation	Standard	5
c. Adjacent/overlapping uptake	Standard	6
2. Chamber sizes	Standard	8
3. Lung uptake (thallium)		
a. Qualitative	Standard	9
b. Quantitative	Preferred	9
4. Initial defect location	Standard	12
5. Initial defect severity and extent		
a. Qualitative	Standard	13
b. Semiquantitative	Preferred	14
c. Quantitative	Optional	15
6. Reversibility		
a. Qualitative	Standard	16
b. Semiquantitative	Preferred	16
c. Quantitative	Optional	16
7. RV uptake	Standard	10
8. Abnormal noncardiac uptake	Standard	11
E. Results: gated SPECT		
1. Regional wall motion	Standard	19
2. Regional wall thickening	Standard	19
3. EF		
a. Qualitative	Recommended	20
b. Quantitative	Recommended	20
4. LV volume	Optional	20
F. Overall study quality	Optional	31

Table 9. (Continued)

		For information, see paragraph
G. Conclusion		
1. Normal/abnormal		
a. Three categories	Recommended	16
b. Five categories	Optional	16
2. Probability of CAD	Optional	32
3. Estimated risk of adverse events	Optional	32

Regional wall motion should be interpreted with a gray-scale display. When computer edge analysis software is available, the physician may choose to analyze wall motion by use of the assigned endocardial and epicardial contours, but reference should also be made to the wall motion without computer-derived edges. Regional wall thickening may be analyzed in gray scale or in a suitable color scheme, although color displays may make it easier to see changes in count intensity.

18. **Gated SPECT QC.** All the QA procedures for routine SPECT are applicable to gated SPECT with the addition of the evaluation of the adequacy of the electrocardiographic (ECG) gate.[21] The most common manifestation of poor gating is the appearance of a flashing pattern on the rotating planar projection images that results from count loss in the later frames. Ideally, a heart rate histogram should also be viewed to verify beat length uniformity. Inspecting the time-volume curve is particularly useful since gating errors may distort the curve. As yet, there is no clear consensus on the beat length window for gated SPECT acquisitions. As in blood pool imaging, the narrower the window, the more physiologic the data, but this runs the risk of compromising the quality of the SPECT perfusion images unless the acquisition software allows for an "extra frame" to accumulate rejected counts during the gated acquisition. Another important aspect of QC is a visual or quantitative determination that the number of counts acquired in each frame of the gated study was adequate for assessment of function. Software that collects all counts into a separate bin for the summed image can minimize the effect that gating errors have on the summed image.
19. **Gated SPECT: Regional wall motion and thickening.** Regional wall motion should be analyzed by use of standard nomenclature: normal, hypokinesis, akinesis, and dyskinesis. Hypokinesis may be further qualified as mild, moderate, or severe. A semiquantitative scoring system is recommended, where 0 is normal, 1 is mild hypokinesis, 2 is moderate hypokinesis, 3 is severe hypokinesis, 4 is akinesis, and 5 is dyskinesis.

This is comparable to the 5-point scoring system used in both contrast and radionuclide ventriculography. As in any assessment of regional ventricular function, one must be cognizant of expected normal and abnormal variations such as the reduced wall excursion at the base compared with the apex, the greater excursion of the basal lateral wall compared with the basal septum, and paradoxical septal motion, which may result from left bundle branch block, post pericardiotomy, or pacing from the right ventricle.

Normal myocardial wall thickness is below the resolution of image reconstruction from currently available SPECT systems. However, regional wall thickening can be estimated by use of the count increase from end diastole to end systole. Visually, it is not as easy to assign degrees of abnormality of thickening as it is to wall motion. However, the evaluation of thickening with gated perfusion SPECT lends itself to quantitation because it is characterized by count changes.

Wall motion and wall thickening are generally concordant. The principal exception to this occurs in patients who have undergone cardiac surgery where septal wall motion is frequently abnormal (paradoxical) but there is normal wall thickening. Rather than separately scoring wall motion and wall thickening, it is commonly accepted to incorporate the two findings into a single score while noting the presence of discordance in wall motion and wall thickening when it occurs. In addition to noting LV wall motion, wall thickening, and EF, the size of the left and right ventricles should be observed, and the function of the right ventricle should be noted.

Quantitative normal databases are now available for assessment of regional wall thickening.

20. **LVEF and volume.** LVEF and LV and RV chamber sizes should routinely be evaluated qualitatively.[47]

EF may be categorized as normal or mildly, moderately, or severely reduced.[22] Volume may be categorized as normal or mildly, moderately, or severely increased. Alternatively, LVEF and end-diastolic and end-systolic volumes may be calculated with geometric models applied to the reconstructed data set. Several software routines that correlate well with contrast and other radionuclide measurements are commercially available.[22]

21. **Integration of perfusion and function results.** The results of the perfusion and gated SPECT data sets should be integrated into a final interpretation. The wall motion is particularly helpful in distinguishing real nonreversible perfusion defects from attenuation or motion artifacts. Fixed perfusion defects that do not show a corresponding abnormality of motion or thickening are more likely to be due to artifacts, especially if the clinical data do not support prior infarction.[29]

Myocardial Viability

22. **Viability: Qualitative assessment.** The assessment of myocardial viability is a complex issue made even more difficult by the lack of consensus in the literature of the precise meaning of the term viability—whether it refers merely to the absence of scar or requires improvement in wall motion after revascularization. It is, however, clear that the quantitative uptake of radionuclides such as Tl-201 and the available technetium agents does correlate with myocardial viability as defined by post-revascularization improvement in both tracer uptake and regional function. Myocardial segments with normal or mildly reduced tracer uptake at rest or on delayed imaging almost invariably prove to be viable. The majority of myocardial segments in which there is unequivocal improvement of uptake on either redistribution or resting images also prove to be viable. The more difficult challenge for the single photon assessment of viability is in segments with severely reduced tracer uptake.
23. **Myocardial viability: Semiquantitative assessment.** The semiquantitative scoring system described above may be used to assess viability as follows. Segments with rest, reinjection, or redistribution scores of 0 (normal perfusion) and 1 (slight reduction in counts) are considered viable. Segments with rest, redistribution, or reinjection scores of 2 (moderately decreased perfusion) are consistent with a combination of viable and nonviable myocardium, and segments with scores of 3 and 4 are generally nonviable. Segments with final scores of 4 are considered nonviable.
24. **Myocardial viability: Quantitative assessment.** An alternate and perhaps more rigorous approach to the assessment of the viability of any segment is the quantitative determination of ischemic-to-normal ratios. Regions of interest may be placed over the segment in question and over the most normal segment of the myocardium in that particular series of images. The analysis should be applied to the resting images for technetium images or to the resting, redistribution, or reinjection images for thallium. When this approach is used, one must take into account the normal count variations such as the relatively reduced counts in the normal inferior wall. Segments with ratios of less than 0.30 are considered nonviable. Areas with ratios greater than 0.50 are considered viable, whereas areas with ratios of 0.30 to 0.50 are equivocal for viability. As indicated above for the semiquantitative approach, such regions require additional data such as wall motion of the region, exercise perfusion in the region, the change in perfusion or wall motion after nitroglycerin, the response of regional function to low-dose dobutamine, or myocardial metabolic imaging with fluorine 18 fluorodeoxyglucose.[22]

    It is also important to recognize that viability of a given segment does not necessarily equate to improvement in clinical outcome after revascularization unless enough segments that are viable are available. The critical number of segments necessary to justify revascularization strategies has not been adequately studied.

Modification of Interpretation by Relevant Clinical Information

25. Due to imperfections in the technology as well as the gradual impairment of coronary blood flow as stenoses become hemodynamically significant, there will always be overlap between normal and mildly abnormal perfusion scans. In these patients it is often particularly helpful to incorporate other clinical information (eg, symptoms, risk factors, ST-segment changes, exercise tolerance) as well as prognostic information in order to help the referring physician make the most appropriate management decisions for patients. Homogeneous perfusion images of patients who have other markers of severe ischemia, such as marked ST-segment changes, should be carefully evaluated for adjunctive markers of ischemia such as TID or increased lung uptake (with thallium) in order to identify those patients with balanced ischemia. The majority of artifacts encountered will produce mild defects; therefore moderate or severe defects, in the absence of dramatic artifact,

should be considered as reflecting pathology. Finally, it needs to be understood that not all pathology detected by perfusion imaging reflects epicardial coronary artery disease (CAD).

Reporting of SPECT Myocardial Perfusion Scan Results

26. **Subject information.** The age, gender, height, weight, and body surface area should be included in the report because they may directly affect the image results and interpretation. For medical records purposes, any identification number should be included. Pertinent medications that may influence the results may be included.
27. **Type of study.** The imaging protocol should be specified, including the radiopharmaceutical and dose, imaging technique (gated vs ungated, supine or prone), imaging sequence (stress/4-hour redistribution, 1-day or 2-day rest/stress or stress/rest, and so on), and a specific statement about whether images were or were not corrected for attenuation. The date(s) of study acquisitions should also be included.
28. **Indication for study.** Placing the indication for the study in the report helps focus the interpreting physician on the clinical question raised by the ordering physician and may be subsequently important for reimbursement issues.
29. **Resting ECG findings.** Inclusion of ECG findings that may have a direct bearing on the study interpretation should be included such as the presence of left bundle branch block or LV hypertrophy.
30. **Summary of stress data.** The type of stress (bicycle or treadmill) and the protocol should be identified (Bruce, modified Bruce, Naughton, manual). For pharmacologic stress, the agent, route of administration, and dose should be indicated. The reason for stopping the test should be noted. All symptoms experienced by the patient during stress (eg, chest pain, dyspnea, claudication, dizziness) should be mentioned.

    If a separate stress test report is generated, then the stress variables that could impact on the perfusion study quality or findings should be included in the perfusion scan report. At a minimum, the report should include the total exercise duration, maximal heart rate and percent of predicted maximum heart rate, resting and maximal blood pressure achieved and workload achieved (estimated metabolic equivalents), and magnitude (in millimeters) and location of any ST-segment deviation.

    If only one report is used for both the exercise or pharmacologic study and the perfusion results, then more detail about the stress test should be included such as time of onset, duration and exact ECG leads with ST-segment changes, the type of chest pain (typical, atypical, non-anginal) and its severity (mild, moderate, severe), and the presence of arrhythmia.
31. **Overall study quality.** Including a statement about the quality of the study is helpful, as it alerts the physicians using the report to any shortcomings that might reduce the accuracy of the data and their interpretation.
32. **Conclusions.** The final interpretation of the scan should obviously reflect the reader's impression as to whether the scan is normal or abnormal. This may be refined to address uncertainty by adding 3 or 5 categories reflecting certainty. That is, the scan may be on a 2-category scale as normal or abnormal; a 3-category scale as normal, equivocal, or abnormal; or a 5-category scale as normal, probably normal, equivocal, probably abnormal, or abnormal.
33. **Diagnosis and prognosis of CAD.** The probability of CAD may be determined with available algorithms that use the pre-scan likelihood of CAD as determined by age, gender, character of chest pain, the number of coronary risk factors, and the results of the stress electrocardiogram. The perfusion data are then added to the model to produce a probability of CAD. A qualitative probability may be reported on the basis of the definite presence or absence of a perfusion defect, the severity and extent of any perfusion defects, and the presence of other markers of CAD such as transient LV dilation, post-stress stunning, or increased lung uptake. When CAD is known to be present, the likelihood of stress-induced ischemia is reported instead of the likelihood of significant CAD.

    Though not widely available, some large laboratories have enough internal follow-up data to be able to statistically predict outcomes (death and nonfatal myocardial infarction) on the basis of perfusion image scores. If such data are available, incorporation of the likelihood of an adverse event in the report is desirable. Otherwise, a qualitative statement about risk may be appropriate because the likelihood of an adverse event increases with the presence of any of the following: perfusion defects in multiple vascular territories, transient LV dilation, increased lung uptake, and decreased LV systolic function.
34. **Clinical interpretation of AC SPECT studies.** The interpretation of AC SPECT myocardial perfusion images follows a similar approach to that used for uncorrected myocardial perfusion images, but there are differences, and these should be taken into account in order to obtain good results. The normal

distributions of perfusion tracer uptake are significantly different with AC compared to uncorrected studies, and because of this, it is important that the interpreting physician have available and learn databases of normal tracer distribution(s). Although from system to system these normal distributions are generally relatively similar, there can be differences that are dependent on the geometry of the imaging system, acquisition protocol, and processing algorithms.[31] There can also be differences in normal distribution(s) related to patient gender and ventricular volume. The interpreting physician must be aware of these differences if they exist for their imaging system(s) and take them into account on a patient-by-patient basis when assessing clinical studies.

AC SPECT studies generally have more uniform regional activity in the anterior, septal, inferior, and lateral walls, but mild reductions in apical and distal anterior activity are typical of the normal AC image distribution. This apical and distal anterior activity reduction is similar to that seen with positron emission tomography myocardial perfusion imaging. This finding becomes more prominent when resolution recovery and scatter correction are included in the AC processing workflow and is often more prominent in patients with larger hearts. In low-likelihood normal patients, this reduction in distal activity is generally more prominent in men than in women, as men generally have larger hearts. If men and women with similar heart sizes are compared, the difference disappears. The unsuspecting observer may mistake this expected normal activity reduction for a distal or mid and distal left anterior descending coronary perfusion defect. In general, the success of AC SPECT appears related to the diligence of the clinical laboratory in following recommended procedures for image acquisition, reconstruction, QA, display, and quantification. Although it may seem reasonable that AC SPECT should simply provide better images, like those without correction, but with the bothersome artifacts that often result in false-positive tests removed, the normal distributions are significantly different and must be accounted for to achieve optimal clinical benefit. The distribution of normal activity is different with AC SPECT. If these differences are not understood by interpreting physicians, AC SPECT will be unreliable. Likewise, quantification and display programs without appropriate normal AC databases should not be used for quantification, as spurious results will occur.

QA requirements are more demanding with AC than non-AC images and should be carefully assessed for each patient study. Artifacts due to movement, either respiration or patient movement, misregistration, and extracardiac radiotracer uptake can be amplified by the iterative algorithms that are employed in AC reconstructions and processing. The quality and registration of the attenuation maps (or mu maps) with the emission image data are additional key factors that must be ensured, and if they cannot be ensured, the associated AC images should be read with greater caution. QA tools to aid these assessments of registration and mu map quality are still not uniformly available, but this should improve in the near future.

For the clinical interpretation of AC SPECT myocardial perfusion images, it is recommended that AC and non-AC images be displayed side by side with displays of the normal activity distribution(s) and their variance distribution available as required for comparison. This requires the availability of normal databases specific for the imaging device, imaging protocol, and processing approach employed clinically. Extracardiac activity especially when combined with respiratory and/or patient movement can introduce artifacts and/or normalization errors that may require renormalization or abandonment of the AC images altogether. Artifactual reductions in activity most often affecting the apparent anterior and/or lateral wall perfusion tracer uptake can occur when there is misregistration of SPECT and mu map images such that the myocardial activity from the SPECT images is matched with the relatively low attenuation coefficients for adjacent lung tissue in the mu maps. Some attenuation correction–capable SPECT systems acquire the SPECT and the transmission image data sequentially rather than simultaneously. If there is a change in position of arm(s) or breasts between emission and transmission imaging, even though there may be perfect registration of the heart in the emission and transmission images, there can be artifactual defects introduced into the SPECT perfusion images by the misregistration of tissues outside the thorax.

The SPECT/CT systems that have become available recently require sequential emission and transmission imaging with a change in bed position between acquisitions. Although the quality of the mu maps with these systems will consistently far exceed the quality of sealed-source transmission system mu maps, the greatly improved resolution of the mu maps they provide make it even more important that registration of emission and transmission reconstructions be exact to a tolerance of less than 1 pixel.

Acknowledgment

We acknowledge the excellent editorial assistance of Patricia Upchurch, Director of Quality Assurance, American Society of Nuclear Cardiology.

References

1. Segall GM, Davis MJ. Prone versus supine thallium myocardial SPECT: a method to decrease artifactual inferior wall defects. J Nucl Med 1989;30:548-55.
2. Kiat H, Van Train KF, Friedman JD, Germano G, Silagan G, Wang FP, et al. Quantitative stress-redistribution thallium-201 SPECT using prone imaging: methodologic development and validation. J Nucl Med 1992;33:1509-15.
3. Esquerre JP, Coca FJ, Martinez SJ, Guiraud RF. Prone decubitus: a solution to inferior wall attenuation in thallium-201 myocardial tomography. J Nucl Med 1989;30:398-401.
4. Nishina H, Slomka PJ, Abidov A, et al. Combined supine and prone quantitative myocardial perfusion SPECT: method development and clinical validation in patients with no known coronary artery disease. J Nucl Med 2006;47:51-8.
5. Slomka PJ, Nishina H, Abidov A, et al. Combined quantitative supine-prone myocardial perfusion SPECT improves detection of coronary artery disease and normalcy rates in women. J Nucl Cardiol 207;14:44-52.
6. Friedman J, Van Train K, Maddahi J, Rozanski A, Prigent F, Bietendorf J, et al. "Upward creep" of the heart: a frequent source of false-positive reversible defects during thallium-201 stress-redistribution SPECT. J Nucl Med 1989;30:1718-22.
7. Eisner RL, Nowak DJ, Pettigrew R, Fajman W. Fundamentals of 180 degree acquisition and reconstruction in SPECT imaging. J Nucl Med 1986;27:1717-28.
8. Liu YH, Lam PT, Sinusas AJ, Wackers FJ. Differential effect of 180 degree acquisition and reconstruction in SPECT imaging. J Nucl Med 2002;43:1115-24.
9. Maniawski PJ, Morgan HT, Wackers FTH. Orbit-related variation in spatial resolution as a source of artifactual defects in thallium-201 SPECT. J Nucl Med 1991;32:871-5.
10. Germano G, Kiat H, Kavanagh PB, Moriel M, Mazzanti M, Su HT, et al. Automatic quantification of ejection fraction from gated myocardial perfusion SPECT. J Nucl Med 1995;36:2138-47.
11. Johnson LL, Verdesca SA, Aude WY, Xavier RC, Nott LT, Campanella MW, et al. Postischemic stunning can affect left ventricular ejection fraction and regional wall motion on post-stress gated sestamibi tomograms. J Am Coll Cardiol 1997;30: 1641-8.
12. Hansen C. Digital image processing for clinicians, part II: filtering. J Nucl Cardiol 2002;9:429-37.
13. Hansen CL, Kramer M, Rastogi A. Lower accuracy of Tl-201 SPECT in women is not improved by size-based normal databases or Wiener filtering. J Nucl Cardiol 1999;6:177-82.
14. King MA, Glick SJ, Penney BC, Schwinger RB, Doherty PW. Interactive visual optimization of SPECT prereconstruction filtering. J Nucl Med 1987;28:1192-8.
15. Hansen C. Digital image processing for clinicians, part III: SPECT reconstruction. J Nucl Cardiol 2002;9:542-9.
16. Hansen CL. The role of the translation table in cardiac image display. J Nucl Cardiol 2006;13:571-5.
17. Eisner R, Churchwell A, Noever T, Nowak D, Cloninger K, Dunn D, et al. Quantitative analysis of the tomographic thallium-201 myocardial bullseye display: critical role of correcting for patient motion. J Nucl Med 1988;29:91-7.
18. Klein JL, Garcia EV, DePuey EG, Campbell J, Taylor AT, Pettigrew RI, et al. Reversibility bull's-eye: a new polar bull's-eye map to quantify reversibility of stress-induced SPECT thallium-201 myocardial perfusion defects. J Nucl Med 1990;31:1240-6.
19. Wackers FJ. Artifacts in planar and SPECT myocardial perfusion imaging. Am J Card Imaging 1992;6:42-58.
20. Bateman TM, Berman DS, Heller GV, Brown KA, Cerqueira MD, Verani MS, et al. American Society of Nuclear Cardiology position statement on electrocardiographic gating of myocardial perfusion SPECT scintigrams. J Nucl Cardiol 1999;6:470-1.
21. Cullom SJ, Case JA, Bateman TM. Electrocardiographically gated myocardial perfusion SPECT: technical principles and quality control considerations. J Nucl Cardiol 1998;5:418-25.
22. DePuey EG, Nichols K, Dobrinsky C. Left ventricular ejection fraction assessed from gated technetium-99m-sestamibi SPECT. J Nucl Med 1993;34:1871-6.
23. Smanio PE, Watson DD, Segalla DL, Vinson EL, Smith WH, Beller GA. Value of gating of technetium-99m sestamibi single-photon emission computed tomographic imaging. J Am Coll Cardiol 1997;30:1687-92.
24. He ZX, Cwajg E, Preslar JS, Mahmarian JJ, Verani MS. Ejection fraction determined by gated myocardial perfusion SPECT with Tl-201 and Tc-99m sestamibi: comparison with first-pass radionuclide angiography. J Nucl Cardiol 1999;4:412-7.
25. Hansen C. Digital image processing for clinicians, part I: basics of image formation. J Nucl Cardiol 2002;9:343-9.
26. Cooper JA, Neumann PH, McCandless BK. Effect of patient motion on tomographic myocardial perfusion imaging. J Nucl Med 1992;33:1566-71.
27. Friedman J, Berman DS, Van Train K, Garcia EV, Bietendorf J, Prigent F, et al. Patient motion in thallium-201 myocardial SPECT imaging. An easily identified frequent source of artifactual defect. Clin Nucl Med 1988;13:321-4.
28. Goerres GW, Burger C, Kamel E, Seifert B, Kaim AH, Buck A, et al. Respiration-induced attenuation artifact at PET/CT: technical considerations. Radiology 2003;226:906-10.
29. Choi JY, Lee KH, Kim SJ, Kim SE, Kim BT, Lee SH, et al. Gating provides improved accuracy for differentiating artifacts from true lesions in equivocal fixed defects on technetium 99m tetrofosmin perfusion SPECT. J Nucl Cardiol 1998;5:395-401.
30. Ficaro EP, Fessler JA, Shreve PD, Kritzman JN, Rose PA, Corbett JR. Simultaneous transmission/emission myocardial perfusion tomography. Diagnostic accuracy of attenuation-corrected 99mTc-sestamibi single-photon emission computed tomography. Circulation 1996;93:463-73.
31. Fricke H, Fricke E, Weise R, Kammeier A, Lindner O, Burchert W. A method to remove artifacts in attenuation-corrected myocardial perfusion SPECT. Introduced by misalignment between emission scan and CT-derived attenuation maps. J Nucl Med 2004;45: 1619-25.
32. Grossman GB, Garcia EV, Bateman TM, Heller GV, Johnson LL, Folks RD, et al. Quantitative Tc-99m sestamibi attenuation-corrected SPECT: development and multicenter trial validation of myocardial perfusion stress gender-independent normal database in obese population. J Nucl Cardiol 2004;11:263-772.
33. Weiss AT, Berman DS, Lew AS, Nielsen J, Potkin B, Swan HJ, et al. Transient ischemic dilation of the left ventricle on stress thallium-201 scintigraphy: a marker of severe and extensive coronary artery disease. J Am Coll Cardiol 1987;9:752-9.
34. Hansen CL, Cen P, Sanchez B, Robinson R. Comparison of pulmonary uptake with transient cavity dilation after dipyridamole Tl-201 perfusion imaging. J Nucl Cardiol 2002;9:47-51.
35. Hansen CL, Sangrigoli R, Nkadi E, Kramer M. Comparison of pulmonary uptake with transient cavity dilation after exercise

thallium-201 perfusion imaging. J Am Coll Cardiol 1999;33: 1323-7.
36. Chouraqui P, Rodrigues EA, Berman DS, Maddahi J. Significance of dipyridamole-induced transient dilation of the left ventricle during thallium-201 scintigraphy in suspected coronary artery disease. Am J Cardiol 1990;66:689-94.
37. Gill JB, Ruddy TD, Newell JB, Finkelstein DM, Strauss HW, Boucher CA. Prognostic importance of thallium uptake by the lungs during exercise in coronary artery disease. N Engl J Med 1987;317:1486-9.
38. Wackers FJT. On the bright side. J Nucl Cardiol 2005;12:378-80.
39. Berger HJ, Matthay RA, Loke J, Marshall RC, Gottschalk A, Zaret BL. Assessment of cardiac performance with quantitative radionuclide angiocardiography: right ventricular ejection fraction with reference to findings in chronic obstructive pulmonary disease. Am J Cardiol 1978;41:897-905.
40. Brent BN, Mahler D, Matthay RA, Berger HJ, Zaret BL. Noninvasive diagnosis of pulmonary arterial hypertension in chronic obstructive pulmonary disease: right ventricular ejection fraction at rest. Am J Cardiol 1984;53:1349-53.
41. Williams KA, Schneider CM. Increased stress right ventricular activity on dual isotope perfusion SPECT: a sign of multivessel and/or left main coronary artery disease. J Am Coll Cardiol 1999;34:420-7.
42. Reisman S, Maddahi J, Van Train K, Garcia E, Berman D. Quantitation of extent, depth, and severity of planar thallium defects in patients undergoing exercise thallium-201 scintigraphy. J Nucl Med 1986;27:1273-81.
43. Caldwell JH, Williams DL, Harp GD, Stratton JR, Ritchie JL. Quantitation of size of relative myocardial perfusion defect by single-photon emission computed tomography. Circulation 1984; 70:1048-56.
44. Kaul S, Chesler DA, Okada RD, Boucher CA. Computer versus visual analysis of exercise thallium-201 images: a critical appraisal in 325 patients with chest pain. Am Heart J 1987;114:1129-37.
45. Burow RD, Pond M, Schafer AW, Becker L. "Circumferential profiles:" a new method for computer analysis of thallium-201 myocardial perfusion images. J Nucl Med 1979;20:771-7.
46. Weiss AT, Maddahi J, Lew AS, et al. Reverse redistribution of thallium-201: a sign of nontransmural myocardial infarction with patency of the infarct-related coronary artery. J Am Coll Cardiol 1986;7:61-7.
47. DePace NL, Iskandrian AS, Hakki AH, Kane SA, Segal BL. Value of left ventricular ejection fraction during exercise in predicting the extent of coronary artery disease. J Am Coll Cardiol 1983;1:1002-10.

ASNC IMAGING GUIDELINES FOR NUCLEAR CARDIOLOGY PROCEDURES

PET myocardial perfusion and metabolism clinical imaging

Vasken Dilsizian, MD,[a] Stephen L. Bacharach, PhD,[b] Robert S. Beanlands, MD,[c] Steven R. Bergmann, MD, PhD,[d] Dominique Delbeke, MD,[e] Robert J. Gropler, MD,[f] Juhani Knuuti, MD, PhD,[g] Heinrich R. Schelbert, MD, PhD,[h] and Mark I. Travin, MD[i]

INTRODUCTION

Positron emission tomography (PET) utilizes radionuclide tracer techniques that produce images of in vivo radionuclide distribution using measurements made with an external detector system. Similar to computed tomography (CT), the images acquired with PET represent cross-sectional slices through the heart. However, with PET, the image intensity reflects organ function as opposed to anatomy. The functional information that is illustrated in PET images depends upon the radiopharmaceutical employed for that particular study. PET allows noninvasive evaluation of myocardial blood flow, function, and metabolism, using physiological substrates prepared with positron-emitting radionuclies, such as carbon, oxygen, nitrogen, and fluorine. These radionuclides have half-lives that are considerably shorter than those used in single photon emission CT (SPECT). Positron emitting radionuclides are produced using a cyclotron, such as fluoro-2-deoxyglucose (F-18 FDG) with a 110 minute half-life or a generator such as rubidium-82 (Rb-82) with a 75 second half-life.

PET radionuclides reach a more stable configuration by the emission of a positron. Positrons are positively charged particles with the same rest mass as electrons. When a positron collides with an electron, two 511 keV gamma rays are emitted. These emitted photons are nearly collinear, travelling in opposite directions, almost exactly 180° apart.[1]

The PET detectors are configured to register only photon pairs that strike opposing detectors at approximately the same time, termed coincidence detection. Over the course of a typical scan, millions of coincidence events are recorded and projections of the activity distribution are measured at all angles around the patient. These projections are subsequently used to reconstruct an image of the in vivo radionuclide distribution using the same algorithms as those used in x-ray CT. The resulting PET images have improved spatial and temporal resolution when compared to SPECT.

Recent advances in the instrumentation of multichannel spiral CT allow detailed visualization of the coronary arteries, noninvasively, as an adjunct to PET imaging. Whereas multichannel CT angiography provides information on the presence and extent of anatomical luminal narrowing of epicardial coronary arteries, stress myocardial perfusion PET provides information on the downstream functional consequences of such anatomic lesions. Thus, with hybrid PET/CT systems, such complementary information of anatomy and physiology can be obtained during the same imaging session. The ability to determine coronary artery disease, myocardial perfusion, viability, and ventricular function from a hybrid PET/CT system has the potential to be an important tool in the clinical practice of cardiology.

The current document is an update of an earlier version of PET guidelines that was developed by the American Society of Nuclear Cardiology.[2] The publication is designed to provide imaging guidelines for physicians and technologists who are qualified to practice nuclear cardiology. While the information supplied in this document has been carefully reviewed by experts in the field, the document should not be considered

From the University of Maryland Medical Center,[a] Baltimore, MD; UCSF,[b] San Francisco, CA; University of Ottawa Heart Institute,[c] Ottawa, Ontario, Canada; Beth Israel Medical Center,[d] New York, NY; Vanderbilt University Medical Center,[e] Nashville, TN; Washington University,[f] St. Louis, MO; Turku University Hospital,[g] Turku, Finland; UCLA School of Medicine,[h] Los Angeles, CA; Montefiore Medical Center,[i] Pleasantville, NY.

Unless reaffirmed, retired or amended by express action of the Board of Directors of the American Society of Nuclear Cardiology, this Imaging Guideline shall expire as of May 2014.

Reprint requests: Vasken Dilsizian, MD, University of Maryland Medical Center, Baltimore, MD.

1071-3581/$34.00

doi:10.1007/s12350-009-9094-9

medical advice or a professional service. We are cognizant that PET and PET/CT technology is evolving rapidly and that these recommendations may need further revision in the near future. Hence, the imaging guidelines described in this publication should not be used in clinical studies until they have been reviewed and approved by qualified physicians and technologists from their own particular institutions.

PET AND PET/CT INSTRUMENTATION

PET Imaging Systems (2D and 3D)

The majority of dedicated PET cameras consist of rings of small detectors that are typically a few millimeters on a side, and tens of millimeters deep. Coincidences between detectors in a single ring produce one tomographic slice of data. Usually one or more adjacent rings may also contribute to counts in that slice. In a 2-dimensional (2D) or ''septa-in'' PET scanner, there is a septum (e.g., lead or tungsten) between adjacent rings. This septum partially shields coincidences from occurring between detectors in one ring and detectors in a non-adjacent or more distant ring. By minimizing coincidences between a ring and its more distant neighboring rings, the septa greatly reduce scattered events.

A scanner with no septa in place is referred to as a three-dimensional (3D) or ''septa-out'' scanner. This permits coincidences between all possible pairs of detectors, greatly increasing sensitivity but also greatly increasing scatter. The increased sensitivity is the greatest for the central slice and falls rapidly, and usually linearly, for slices more distant from the central slice. The slices near the edge have the sensitivity of about the same as in a 2D scanner but with greater scatter. Scatter is measured with standards given by the National Electrical Manufacturers Association (NEMA)[3-5] and is typically in the order of 10-15% for 2D scanners and 30-40% or more for 3D scanners. In chest slices encompassing the heart, as opposed to the relatively small NEMA phantom, there is an even larger increase in scattered counts for 3D imaging. For cardiac applications, scatter tends to increase the counts in cold areas surrounded by higher-activity regions (e.g., a defect surrounded by normal uptake).

Some manufacturers have scanners that have retractable septa, permitting the user to choose between 2D and 3D operation. Many PET/CT manufacturers have opted for scanners that operate only in 3D mode, since these are preferred for oncology studies. Situations in which 3D mode may be advantageous include those in which:

1. Whole-body patient throughput is important (e.g., a busy oncology practice).
2. Radiation exposure is critical, so that reductions in injected activity are desired.
3. Special (i.e., usually research) radiopharmaceuticals are being used, which can only be produced in low radioactivity quantities.

As noted above, although 3D acquisition is in principle many times more sensitive than 2D, random events (termed randoms), dead time, and scatter can greatly reduce the effective sensitivity of images acquired in 3D, especially at high doses. Thus, in order to prevent poor quality images, lower doses are administered. When using 3D imaging with a bismuth germanate (BGO) crystal camera, for example, 3D imaging had often been used when the dose had to be minimized (e.g., in normal volunteers, in children, or when multiple studies are planned) or when scatter was minimal (e.g., brain imaging). The advent of lutetium oxyothosilicate (LSO)- and gadolinium oxyorthosilicate (GSO)-based PET scanners, and even BGO scanners with new-generation optimized photo multiplier/crystal coupling schemes and high-speed electronics, has made 3D imaging more practical. Improvements in software, coupled with improvements in electronics and crystal technology can, in part, compensate for the increase in randoms, dead time, and scattered events.[6] The use of 3D cardiac imaging with new-generation machines continues to be evaluated. The degree to which any of these improvements is achieved in practice for cardiac imaging may vary between manufacturers.

PET Imaging-Crystal Types

Four different crystal types are commonly employed—BGO, GSO, LSO, and lutetium yttrium orthosilicate (LYSO)—although other crystal types have also been used. Each of them can be used successfully for cardiac imaging. BGO has the highest stopping power, but relatively poor energy resolution (i.e., limiting energy-based scatter reduction) and timing resolution (i.e., limiting its ability to reduce randoms). GSO, LSO, and LYSO have better timing resolution and, in theory, better energy resolution. For 2D imaging, GSO, LSO, and LYSO may not offer significant advantage over BGO, given the inherently high sensitivity of BGO. The main advantage of the newer crystals is their much reduced dead time, which enables them to acquire data at the much higher count rates associated with operating in 3D mode, and to better minimize the effects of randoms. One minor disadvantage of LSO and LYSO is their intrinsic radioactivity, which contributes to a small increase to the random event rate.

The better energy resolution of GSO, LSO, or LYSO, and consequent reduction of scatter in 3D mode, would make these detector types advantageous. At present, the theoretical energy resolution for these detectors does not seem to have been fully realized in practice, leaving all three crystal types with similar energy-based scatter rejection (i.e., GSO, LSO, and LYSO giving only slight potential improvement over BGO) and making 2D imaging still the method of choice if scatter rejection is critical. Modern image reconstruction algorithms incorporate improved models for scatter correction, and as a result, the impact of scatter for state-of-the-art scanners operating in 3D mode is usually acceptable for clinical imaging. The suitability of 3D mode for cardiac PET imaging should be evaluated by the user.

PET TOF Imaging

Machines that incorporate time-of-flight (TOF) information in the acquisition process have recently been commercially introduced. TOF refers to the time difference between the two 511 keV annihilation photons reaching their respective detectors, 180° apart. For example, if the positron annihilation occurred at the center of the machine, the two photons would reach their respective detectors at exactly the same time, while if the annihilation occurred closer to one detector than the other, the photon would reach the closer detector first. Adding TOF capability improves the statistical quality of the data (i.e., the noise).[7-9] If one could measure the time accurately enough, it would be possible to determine exactly where the photon originated. Unfortunately, current detector and instrumentation technology is not nearly good enough to achieve this level of accuracy. As machines with TOF ability have only recently been introduced, no quality control (QC) or other aspects of such machines are described here.

PET/CT Imaging

The latest trend in PET instrumentation is the addition of a CT system to the PET scanner. In all cases, the manufacturer starts with a state-of-the-art PET scanner, whose characteristics have been described in the section above. The manufacturer then adds a CT system, consisting of a 2-, 4-, 6-, 8-, 16-, 32-, 64-, or greater slice scanner. These combined systems, in practice, demonstrate a range of integration. At one end of the spectrum, the hardware and software of the CT systems are completely integrated within the PET scanner. In this approach, a common, unified gantry is used and a single, unified software system with an integrated PET/CT interface is provided. At the other end of the spectrum, the hardware and software of the CT system are less integrated. In some machines, a separate CT gantry is carefully placed in front of or behind the PET gantry, and a separate workstation is used to control the CT system.

PET Imaging-Attenuation Correction

For dedicated PET scanners, rotating rod sources of germanium-68 (Ge-68)/gallium-68 (Ga-68) or Cesium-137 (Cs-137) are used to acquire a transmission scan for attenuation correction. Typical transmission scans with a rotating rod add about 3-6 minutes to the overall imaging time. This is acceptable for cardiac imaging, but a significant drawback for multi-bed position oncology scans. Since oncology applications have been the driving force behind recent sales of PET scanners, manufacturers looked for a way to reduce this transmission scan time. For this reason, and because of other advantages of CT, nearly all current commercially available PET scanners are hybrid PET/CT systems. These scanners, in general, have eliminated the rotating rod source and instead rely on CT scans for attenuation correction.

CT-based attenuation correction typically adds less than 20 seconds to the scan time of a cardiac scan. The use of either CT or the rotating rod for attenuation correction requires precise alignment between the transmission image and the emission image. An advantage of CT over transmission sources is a much reduced scan time, which helps reduce overall patient motion. The high speed of CT scans, however, freezes the heart at one phase of the respiratory cycle, causing potential misalignment between the CT-based transmission image and the emission data. The latter, of course, are averaged over many respiratory cycles. The respiratory misalignment between the CT image and emission data can produce significant artifacts and errors in apparent uptake at the myocardial segments adjacent to lung tissue.[10] Errors in attenuation correction from misregistration are typically worse if the CT is acquired at full inspiration. At present, software realignment, usually manual, must be performed to minimize this misalignment. Other techniques (e.g., slow CT, respiratory gating, and 4D-CT) are under development for compensating for respiratory motion, but are still in the research phase and are not further described here.

PET AND PET/CT IMAGING QC

PET QC Procedures

The procedures below should be suitable for ensuring overall proper basic operation of a PET scanner. Table 1 lists recommended PET imaging QC

Table 1. Suggested QC procedures: dedicated PET imaging devices

Procedure	Frequency
Acceptance testing (NU 2-2007)	Once upon delivery and upon major hardware upgrades
Daily QC, as recommended by vendor (attenuation blank scan, phantom scan, etc.)	Daily
Sensitivity and overall system performance	Weekly (or at least monthly)
Accuracy (corrections for count losses and randoms)	At least annually
Scatter Fraction	At least annually
Accuracy of attenuation correction	At least annually
Image quality	At least annually
Measurements specified by the manufacturer	As per the manufacturer

schedules. Note that, unlike planar and SPECT imaging, there are no widely accepted, published QC procedures for PET. Some additional procedures may be required by particular manufacturers.

Acceptance testing. It is recommended that the NEMA performance measurements, as defined by NU 2-2007,[5] be made before accepting the PET scanner. Many of these tests can be performed by the company supplying the PET scanner. If so, it is recommended that the purchaser's representative work with the manufacturer's representatives during these tests. The NU 2-2007 recommendations have superseded the NU 2-2001 recommendations.[4] In scope, the tests are nearly equivalent between NU 2-2007 and NU 2-2001, the primary difference being NU 2-2007 addresses the intrinsic radioactivity in LSO and LYSO crystals. For cardiac imaging, these standards should be used rather than NU 2-1994 recommendations,[3] as they better reflect the imaging of objects of the size of a typical adult thorax region by incorporating measurements of the International Electrotechnical Commission (IEC) body phantoms.[11]

There are two reasons for making these performance measurements:

1. To ensure that the new PET scanner meets specifications published by the manufacturer.
2. To provide a standard set of measurements that allows the user to document the limitations of the scanner, and to provide a standard against which to track changes that may occur over time.

Daily QC scan. Each day the PET detectors should be evaluated to ensure proper operation before commencing with patient injections or scans. The daily quality procedure varies according to the design of the scanner and recommendations of the vendor. For example, some scanners utilize an attenuation blank scan to evaluate detector constancy, and others may use a scan of a standard phantom. In addition to numerical output of the scanners software (chi-square, uniformity, etc.), the raw sinogram data also should be inspected to evaluate detector constancy.

Sensitivity. NEMA NU 2-2007 provides recommended procedures for measuring system sensitivity. Subtle changes in PET system sensitivity may occur slowly over time. More dramatic changes in sensitivity may reflect hardware or software malfunction. There are simple tests designed to monitor such changes in sensitivity. Ideally, these tests should be performed weekly, but no less than monthly. For many systems, the daily QC scan also provides a measure useful for tracking changes in sensitivity.

Spatial resolution. Spatial resolution is measured using a point source as specified in the NEMA NU 2-2007 or NEMA NU 2-2001.

Scatter fraction. Intrinsic scatter fraction is measured according to either NEMA NU 2-2007 or NEMA NU 2-2001 specifications.

Accuracy of attenuation correction and overall clinical image quality. Attenuation correction should be assessed using the IEC phantom, as specified in the NU 2-2007 recommendations.[11] If this phantom is not readily available, it is suggested that similar measurements be performed with a phantom approximating a typical human body shape and size (e.g., a 20 by 30-cm elliptical phantom or anthropomorphic phantom). It should have at least one cold sphere or cylinder and one hot sphere or cylinder, as well as at least some material simulating lung tissue to ensure proper performance in the presence of non-uniform attenuating substances.

Variations among manufacturers. The above recommendations regarding PET scanner quality assurance are general guidelines. In addition, each manufacturer has its own periodic QC recommendations for parameters such as ''singles'' sensitivity, coincidence timing, energy calibration, and overall system

performance. These, by necessity, require different measurement protocols that may vary even between models for the same manufacturer. These measurements must be performed as detailed by the manufacturer. However, the measurements specified above are not intended to replace these basic system-specific QC measurements.

CT QC Procedures

The procedures below should be suitable for ensuring overall proper basic operation of a CT scanner. Table 2 lists recommended CT imaging QC schedules. Some additional procedures may be required by particular manufacturers.

Calibration. The reconstructed CT image must exhibit accurate, absolute CT numbers in Hounsfield Units (HU). This is critical for the use of CT images for PET attenuation correction, because the quantitative CT values are transformed, usually via a bilinear or trilinear function with one hinge at or near the CT value for water, to attenuation coefficients at 511 keV. Any errors in CT numbers will be propagated as errors in estimated 511 keV attenuation coefficients, which in turn will adversely affect the attenuation-corrected PET values. CT system calibration is performed with a special calibration phantom that includes inserts of known CT numbers. This calibration is done by the manufacturer's field service engineers. The CT calibration is then checked daily with a water-filled cylinder, usually 24 cm in diameter provided by the manufacturer. In practice, if the error is greater than 5 HU (i.e., different than the anticipated value of 0 HU), the CT system is considered to be out of calibration. The technologist will usually then do an air calibration, to determine if this corrects the overall calibration (i.e., brings the CT number for water back to within 5 HU of 0). If it does not, the manufacturer's field service engineer must be called. On an annual basis, or after any major repair or calibration, calibration is checked by the manufacturer's service engineer.

Field uniformity. The reconstructed CT image must exhibit uniform response throughout the field of view (FOV). In practice, this means that a reconstructed image of a uniform water-filled cylinder must itself demonstrate low variation in CT number throughout this image. In practice, small circular regions of interest (ROIs) are placed at the four corners of the cylinder image, and the mean CT number is compared to that from a region in the center of the phantom; the difference in mean region CT number should not exceed 5 HU. Non-uniformities greater than this may produce sufficient quantitative inaccuracies so as to affect PET attenuation correction based on the CT image.

Table 3 lists recommended CT QC schedules for combined PET/CT Units. Users should consult the manufacturer regarding the specific manner and frequency with which tests should be performed for the CT component of their PET/CT device. Both the American College of Radiology (ACR) and American Association of Physicists in Medicine (AAPM) have published CT testing procedural guidelines.[12,13]

Table 2. CT QC procedures

Test	Requirement	Frequency
Calibration	Mandatory	Monthly*
Field Uniformity	Mandatory	Monthly*

*Or as recommended by the manufacturer.

Combined PET/CT QC Procedures

The PET and CT portion of the combined system should be assessed as described for the dedicated PET and CT imaging devices. In addition to the independent QC tests for the PET and CT portions of the combined system, it is necessary to perform additional tests that assess the combined use of PET and CT. Table 4 lists recommended QC procedures for combined PET/CT units.

Registration. The reconstructed PET and CT images must accurately reflect the same 3D locations (i.e., the two images must be in registration). Such registration is often difficult because the PET and CT portions of all commercial combined PET/CT systems are not coincident (i.e., the PET and CT ''slices'' are not in the same plane) and because the PET and CT gantries are contiguous. In practice, this means that the PET and CT acquisitions do not simultaneously image the same

Table 3. Schedule of CT QC for PET/CT units

Test	Frequency
Water phantom QA	Daily
Tube warm-up	Daily
Air calibration ("fast QA")	Daily
Water phantom checks: slice thickness, accuracy, positioning	Monthly

Table 4. Combined PET/CT QC procedures

Test	Requirement
Registration	Mandatory
Attenuation correction accuracy	Mandatory

slice. In fact, because the bed must travel different distances into the gantry to image the same slice in the patient for PET versus CT, there is ample opportunity for misregistration via x, y, z misalignment of bed motion—or, of perhaps even greater concern, because of differential ''bed sag'' for the PET and CT portions, depending on the table design.

In addition, electronic drift can influence the ''position'' of each image, so that calibrations for mechanical registration can become inaccurate over time. Thus, it is imperative to check PET-to-CT registration on an ongoing basis. This is usually performed with a specific phantom or jig containing an array of point sources visible in both PET and CT.

Errors in co-location in the fused PET-CT images are assessed, such as by means of count profiles generated across transaxial slices. Such errors, after software registration corrections, should be less than 1 mm. It is important to image this registration jig in a number of positions along the bed. It may also be helpful to place a weight on the end of the bed to produce some bed sag and repeat the assessment.

Note: The above considerations are in addition to the patient-specific alignment QC clinically necessary to assess possible patient or respiratory motion (not described here).

Attenuation correction accuracy. The use of the CT image for PET attenuation correction requires a transformation of the observed CT numbers in HU to attenuation coefficients at 511 keV. This transformation is usually accomplished with a bilinear or trilinear calibration curve, with one ''hinge'' at a CT value of 0 (i.e., hinged at the CT value for water).

At a minimum, it is important to image a water-filled cylinder to assess PET field uniformity and PET activity concentrations after CT-based PET attenuation correction. Errors in CT-to-PET attenuation transformations are usually manifest as a corrected PET image without a ''flat'' profile from edge to center (i.e., the activity at the edge is either too high or too low relative to that at the center of the phantom) and with resulting attenuation-corrected absolute PET values that are incorrect (although these values depend on absolute PET scanner calibration as well as accurate CT-based PET attenuation correction).

If possible, the CT-based attenuation-corrected PET values should be compared with those from the rotating rod source-based attenuation-corrected PET values in the same phantom. Moreover, if available, more sophisticated phantoms with variable attenuation and variable activity distributions can be used to more comprehensively assess any errors in CT-based PET attenuation correction.

The accuracy of CT attenuation-corrected PET images is still under investigation.[14] Recent work has reported that even after correcting for potential PET/CT misalignment, tracer uptake maps derived from CT-based attenuation correction differ from those derived using transmission source correction.[10,15,16]

PET ACQUISITION AND PROCESSING PARAMETERS

The acquisition and processing parameters defined in this section apply to both the perfusion and metabolic PET tracers in the sections that follow.

Patient Positioning

Ideally, the patient should be placed in the supine position, with the arms out of the camera FOV. This can be tolerated by nearly all patients, provided that some care is given to a method to support the arms. Alternatively, an overhead bar has often been used as a handhold for arm support. In patients with severe arthritis, whose arms cannot be positioned outside the camera's FOV, cardiac images should be obtained with the patient's arms resting on his/her side. In the latter case, the transmission scan time may have to be increased, and it is of critical importance that the arms do not move between transmission and emission, or artifacts will result. Note that when performing perfusion/metabolism PET studies, it is best to keep the patient positioned similarly for both studies. In patients undergoing PET/CT imaging, arms resting inside the FOV will result in beam-hardening artifacts on the CT-based transmission scan, which usually lead to streak artifact of the corrected emission scans.

Dose Considerations

In determining appropriate patient doses, the following issues should be considered:

1. Staff exposure could be high because of the limited effectiveness of shielding and the potential for large doses (e.g., Rb-82 PET). Thus, standing in close proximity to an Rb-82 generator or the patient during injection should be avoided.
2. Large patients may benefit from higher doses.
3. 3D imaging requires less dosage than 2D imaging due to the improved sensitivity of the system.

Total Counts

The counts per slice necessary to yield adequate quality images will vary from camera to camera depending, in part, on scatter and randoms corrections, as well as the amount of smoothing that is performed. If

one tries to achieve on the order of 7 mm full width at half maximum (FWHM) in-plane resolution and has 10-15% scatter (NEMA), then a typical good-quality study in 2D mode might have on the order of 50,000 true counts per millimeter of transaxial distance over the region of the heart (e.g., for a 4.25-mm slice separation, the counts would be $50{,}000 \times 4.25 = 250{,}000$ counts per slice). These numbers are very approximate and may differ from one scanner to the next. If one is willing to accept a lower resolution (e.g., more smoothing) or more noise, imaging time can be reduced. Since 3D scanners have greater scatter, they usually require more counts than a 2D scanner to achieve the same noise level.

Pixel Size

It is recommended that 2-3 mm per pixel be used. A ''rule of thumb'' in nuclear medicine physics is that one needs at least 3 pixels for every FWHM of resolution in the image. For example, if the data are reconstructed to 8 mm FWHM, then one needs roughly $8 \text{ mm}/3 = 2.7$ mm/pixel. Many institutions achieve a 3 mm sampling rate or better with a 256×256 array over the entire FOV of the camera. Other institutions choose to use a 128×128 array over a limited FOV (e.g., 25-35 cm diameter) centered over the heart, in which case, 2-3 mm/pixel is easy to achieve, cutting out extraneous structures in the FOV, even with a 128×128 array. Either method is acceptable to achieve the desired 2-3 mm/pixel. Greater than 3 mm/pixel may be acceptable for older PET cameras with resolution worse than 1 cm.

Imaging Mode (Static, Gated or Dynamic)

Static PET acquisition produces images that allow relative assessment of tracer uptake on a regional basis. Comparison of regional tracer uptake in relation to the normal tracer distribution is the current standard for the identification regional abnormalities.

Usually, PET tracer counts are sufficiently high to yield good quality ventricular function study. Electrocardiographic (ECG)-gated images are acquired in 8-16 time frames per R to R interval, in a manner similar to SPECT gated perfusion studies but at higher spatial resolution. Given that ventricular contraction and thickening are often clinically useful for assessing viability, gating should be performed when possible. It is important that the gating software does not adversely affect the ungated images (e.g., by loss of counts as a result of beat length rejection). Monitoring the length and number of the accepted beats is critical to assure the accuracy of the gated data. Arrhythmias such as atrial fibrillation, frequent premature ventricular contractions (PVCs), or other abnormal rythms can lead to highly erroneous gated information.

For a dynamic acquisition, PET data are acquired in multiple time sequenced frames. A potential advantage of the dynamic over static acquisition is in the case of patient motion artifact. For example, if a patient should move at the end of the study, one can select and utilize only those dynamic frames with no motion (i.e., summing them together to make one static image). This is easily implemented and takes almost no additional operator time. A more elaborate dynamic acquisition beginning with tracer injection may optionally be used when kinetic analysis over the entire uptake period is to be performed (e.g., compartmental analysis or Patlak analysis). Kinetic analysis permits absolute quantification of the tracer's kinetic properties (e.g., blood flow for Rb-82 and N-13 ammonia, rate of FDG utilization). Performing and interpreting such kinetic analyses can be complex and require expertise.

List mode acquisitions are now available with many new cameras, which enable simultaneous dynamic and ECG-gated acquisitions. This is considered an optional acquisition mode, although it is routinely used by some vendors' processing software.

Image Reconstruction

Several corrections are required for creating data sets that can be used for reconstruction. PET data must be corrected for randoms, scatter, dead time, attenuation, and decay before reconstruction can begin. Once these corrections are applied, the data can be reconstructed with either filtered backprojection (FBP) or iterative algorithms. FBP is the standard method used for reconstruction on older PET systems. FBP images are subject to streak artifacts, especially when the subject is obese or large. This can affect visual analysis but usually does not adversely affect quantitative analysis with regions of interest (i.e., the streaks tend to average out properly over typical volumes of interest). Newer PET/CT systems employ iterative reconstruction methods (e.g., the method of ordered-subsets expectation maximization [OSEM]) yielding images with better noise properties. Although high uptake structures, such as the heart, may not improve their noise characteristics with OSEM, the surrounding lower uptake structures do improve, and streak artifacts are nearly eliminated, thus greatly improving the visual appearance of the image. However, low uptake areas, such as myocardial defects and the left ventricular (LV) cavity at late times, may have slightly or artificially elevated activity levels unless sufficient iterations are performed. It is recommended that one thoroughly characterizes the PET machine and its reconstruction algorithm's behavior with a realistic cardiac phantom.

For rest/stress comparisons, the rest/stress images must have matched resolution. Filtering is usually necessary to achieve adequate noise properties. Care must be taken to match reconstructed resolution when making pixel-by-pixel comparisons of paired myocardial perfusion and metabolism data.

For GSO systems, the images are reconstructed using a row action maximum likelihood algorithm (RAMLA) reconstruction technique, which includes a texture/filter factor. Thus, an additional reconstruction filter should not be performed.

Attenuation Correction

PET cardiac imaging should only be performed with attenuation correction. Attenuation correction can be accomplished with a rotating line source in a dedicated PET system or with CT in a PET/CT system.

For dedicated PET systems, two techniques are typically used for creating the patient-specific transmission maps: direct measurement of patient attenuation with a rotating line source of either Ge-68 or Cs-137 or segmentation of patient-specific attenuation maps. The former are very sensitive to the choice of reconstruction algorithm and, depending on reconstruction algorithm used, could require 60-600 seconds' acquisition time to produce a reasonable attenuation map. Segmentation algorithms are relatively insensitive to noise but are very dependent on the quality of the program used for performing the transmission scan segmentation and are influenced by lung attenuation inhomogeneities (e.g., partial-volume effects from the liver).

Transmission data are typically acquired sequentially, so it is essential that the patient remain still between transmission and emission images. Either pre- or post-scan transmission imaging is satisfactory, providing that the system's software can adequately correct for residual emission activity. Transmission imaging simultaneous with emission imaging is not recommended unless the high count rate and rapidly changing distribution of the emission tracer can be assured to not adversely affect the transmission scan. If the transmission scan is performed at the beginning of the study, attention should be made for potential misregistration with the emission images, possibly due to gradual upward creep of the diaphragm, due to pressure from visceral fat.[17]

For PET/CT systems, x-ray CT can be used for acquiring a transmission map for attenuation correction. An advantage of this approach is the rather rapid (15-30 seconds) acquisition of the transmission map, which can be repeated for each imaging session, rest and stress perfusion studies as well as for subsequent metabolic imaging, if necessary. The CT scan can be reviewed for additional, independent diagnostic information, such as coronary calcium visualization and other extra-cardiac anatomic information. To acquire a CT-based transmission scan, it is necessary to first acquire a planar scout CT acquisition. This scan is used to measure the axial limits of the CT acquisition. Following this acquisition, the CT transmission scan is acquired. The best approach for CT transmission imaging is still evolving, and therefore this guideline can only suggest some considerations. Some of the considerations for CT scanning are as follows (Table 5):

1. If CT is used for either attenuation correction or anatomical evaluation, this will have an effect on the kV and mAs used in the acquisition. A transmission

Table 5. General guidelines for CT-based transmission imaging

CT parameter	General principle	Effect on patient dose
Slice collimation	Should approximate the slice thickness of PET (eg., 4–5 min.)	No effect
Gantry rotation speed	Slower rotation speed helps blur cardiac motion (eg., 1 sec/revolution or slower)	Slower gantry rotation increases radiation
Table feed per gantry rotation(pitch)	Relatively high pitch(eg., 1:1)	Inversely related to pitch
ECG gating	ECG gating is not recommended	Decreases without ECG gating
Tube potential	80–140 kVp, depending on manufacturer specification	Increases with higher kVp
Tube current	Because the scan is only acquired for AC, low tube current is preferred (10–20 mA)	Increases with higher mA
Breathing instructions	End-expiration breathhold or shallow free-breathing is preferred (see text)	No effect
Reconstructed slice thickness	Should approximate the slice thickness of PET (eg., 4–5 mm)	No effect

scan usually requires only a low CT current, as opposed to calcium scoring or CT angiography, which require higher CT currents.

2. Breathing protocols are not clearly settled. Recent data suggest that respiratory averaging may be a useful method of reducing breathing related artifacts. Other methods, such as free breathing with a slow CT scan or ultra-rapid CT acquisition (depending on the CT device available) have also been proposed. Current practice discourages breath-holding, particularly in end-inspiration because of the potential for it to cause uncorrectable misregistration. A transmission CT scan performed at the same speed as for whole-body PET/CT images frequently produces artifacts at the lung-liver interface and can sample parts of the heart and diaphragm in different positions, causing misregistration and an artifact where pieces of the diaphragm appear to be suspended in the lung. Although specifics vary among laboratories, the duration of the CT transmission scan is typically from 10-30 seconds. CT attenuation correction with 64 slice devices can achieve an ultra-rapid CT in 1.5 seconds, which appears to reduce such CT artifacts. Therefore, it is imperative to ensure proper registration between transmission and emission data for quality assurance and proper interpretation of PET images. Several approaches are currently being devised to reduce misregistration artifacts, such as reducing CT tube current and increasing the duration CT acquisition to better match the temporal resolution between the attenuation and emission maps.[18,19]
3. Metal artifacts[20] can present a challenge for the reconstruction algorithm and must be compensated for to produce accurate attenuation maps.[21,22]
4. Ideally, stress transmission images should be acquired during peak stress or vasodilation, which is not practical. As such, the technologist and physician must carefully inspect the transmission and emission data sets to ensure that they are properly registered in the transaxial, sagittal, and coronal planes. For patients undergoing PET/CT, a separate CT-based transmission scan for correction of the stress images is standard. For Rb-82, a post-stress transmission scan is preferred to minimize misregistration artifacts on the corrected Rb-82 images when misregistration compensation software is not available.

PET MYOCARDIAL PERFUSION IMAGING

The goal of evaluating myocardial perfusion with PET imaging is to detect physiologically significant coronary artery narrowing with a view towards aggressive risk factor modification in order to:

1. Delay or reverse the progression of atherosclerosis.
2. Alleviate symptoms of ischemia by medical or revascularization therapy.
3. Prevent future adverse events.
4. Improve patient survival.

Stress and rest paired myocardial perfusion studies are commonly performed to assess myocardial ischemia and/or infarction. Current Food and Drug Administration (FDA)-approved and Centers for Medicare & Medicaid Services (CMS)-reimbursable PET myocardial blood flow tracers are limited to Rb-82 and N-13 ammonia. Normal myocardial perfusion on stress imaging implies absence of physiologically significant coronary artery disease (CAD). Abnormal myocardial perfusion on stress imaging suggests the presence of significantly narrowed coronary arteries. If the stress-induced regional perfusion defect persists on the corresponding paired rest images, it suggests the presence of an irreversible myocardial injury. On the other hand, if the defect on the stress images resolves completely or partially on the rest images, it suggests the presence of stress induced myocardial ischemia. Imaging of myocardial perfusion can also be combined with myocardial metabolism imaging with F-18 FDG for the assessment of myocardial viability in areas of resting hypoperfusion and dysfunctional myocardium.

Patient Preparation

Patient preparation is similar to preparation for stress and rest myocardial SPECT imaging. This includes an overnight fast of 6 hours or more, with the exception of water intake. Patients should avoid caffeinated beverages for at least 12 hours, and avoid theophylline-containing medications for at least 48 hours.[23]

Cardiac Stress Testing

Details of pharmacologic or exercise stress testing are beyond the goals of this document. Nonetheless, stress protocols are, for the most part, generic for all perfusion agents.[23] The specific differences in acquisition protocols for Rb-82 and N-13 ammonia imaging are related to the duration of uptake and clearance of these radiopharmaceuticals and their physical half-lives. No data are available yet with PET and the newly approved A2A selective adenosine receptor agonist, Regadenoson.

Rb-82 Perfusion Imaging

Tracer properties. Rb-82 PET myocardial perfusion imaging is a well established and highly accurate

technique for detecting hemodynamically significant CAD.[14,24,25] Rb-82 is a monovalent cationic analog of potassium. It is produced in a commercially available generator by decay from strontium-82 (Sr-82) attached to an elution column. Sr-82 has a half-life of 25.5 days and decays to Rb-82 by electron capture. Rb-82 decays with a physical half-life of 75 seconds by emission of several possible positrons, predominantly of very high energy. The resulting long positron range slightly worsens image resolution compared to F-18 and N-13. The daughter product is krypton-82, which is stable. The Sr-82-containing generator is commercially available and is replaced every 4 weeks, thus obviating the need for a cyclotron.

Rb-82 is eluted from the generator with 10 to 50 mL normal saline by a computer-controlled elution pump, connected by intravenous (IV) tubing to the patient. While the generator is fully replenished every 10 minutes, experiments have shown that 90% of maximal available activity can be obtained within 5 minutes after the last elution. Thus, serial imaging can be performed every 5-6 minutes. While the short half-life of Rb-82 challenges the performance limits of PET scanners, it facilitates the rapid completion of a series of resting and stress myocardial perfusion studies.

Rb-82 is extracted from plasma with high efficiency by myocardial cells via the Na^+/K^+ adenosine triphosphatase pump. Its extraction is less than N-13 ammonia, and extraction decreases with increasing blood flow. Rb-82 extraction can be decreased by severe acidosis, hypoxia, and ischemia.[26-28] Thus, while uptake of Rb-82 predominantly depends on myocardial blood flow, it may be modulated by metabolism and cell integrity.

Dosimetry. The radiation dosimetry from Rb-82 in an adult may vary from 1.75 to 7.5 mSv total effective dose for a maximal allowable activity of 60 mCi at both rest and stress.[29] With current advances in PET instrumentation, diagnostic quality PET images can be acquired using only 20-40 mCi of Rb-82 for each of the rest and stress phases of the study. As a result, the effective dose of radiation exposure from Rb-82 PET can be halved.

Acquisition parameters. Acquisition parameters for different types of PET scanners are shown in Tables 6 and 7. The short half-life of Rb-82 poses a challenge for achieving optimal image quality. As such, optimal acquisition parameters differ among the several main types of PET scanners. Because of the short half-life of Rb-82 and the need for the patient to lie still in the camera during the study, stress imaging of this agent is primarily limited to pharmacologic stress, although

Table 6. Rb-82 rest/stress myocardial perfusion imaging guideline for BGO and LSO (LYSO) PET imaging systems

Feature	BGO Systems	LSO (LYSO) Systems	Technique
Stress testing	Pharmacologic agents		Standard
Tracer Dose			
2D Scanner	40–60 mCi (1480–2220 MBq)		Standard
3D Scanner	10–20 mCi (370–740 MBq)	30–40 mCi (1110–1480 MBq)	Standard
Injection rate	Bolus of ≤30 seconds		Standard
Imaging delay after injection	LVEF > 50%: 70–90 seconds		Acceptable
	LVEF < 50% or unknown: 90–130 seconds		
	List mode: acquire immediately		
Patient positioning			
PET	Use scout scan: 10–20 mCi Rb-82 (370–740 MBq)		Standard
	Use transmission scan		Optional
PET/CT	CT scout		Standard
Imaging mode	List mode: gated/dynamic (no delay after injection)		Preferred
	Gated acquisition (delay after injection)		Optional
Imaging duration	3–6 minutes		Standard
	3–10 minutes		Optional
Attenuation correction	Measured attenuation correction, before or after		Standard
Reconstruction method	FBP or iterative expectation maximization (e.g., OSEM)		Standard
Reconstruction filter	Sufficient to achieve desired resolution/smoothing, matched stress to rest		Standard
Reconstructed pixel size	2–3 mm		Preferred

Table 7. Rb-82 rest/stress myocardial perfusion imaging guideline for GSO PET imaging systems

Feature	GSO Systems	Technique
Stress testing	Pharmacologic agents	Standard
Tracer dose (3D)	20 mCi (740 MBq)	Standard
Injection rate	Bolus of $\leq$ 30 seconds	Standard
Imaging delay after injection	LVEF $>$ 50%: 70–90 seconds	Standard
	LVEF $<$ 50% or unknown: 90–130 seconds	
	List mode: acquire immediately	
	Longer delays than the above must be used if count rate at these times exceeds the maximum value specified by the manufacturer	
Patient positioning		
PET	Use scout scan: 10–20 mCi Rb-82 (370–740 MBq)	Standard
	Use transmission scan	Optional
PET/CT	CT scout	Standard
Imaging mode	List mode: gated/dynamic (no delay after injection)	Standard
Imaging duration	3–6 minutes	Standard
	3–10 minutes	Optional
Attenuation correction	Measured attenuation correction, before or after	Standard
Reconstruction method	Iterative (RAMLA)	Standard
Reconstruction filter	None	Standard
Reconstructed pixel size	4 mm	Standard

reasonable Rb-82 images have also been obtained with supine bicycle and treadmill exercise.[30,31]

Scout scanning. Scout scanning is recommended before each injection to ensure that the patient is correctly positioned and is not exposed to unnecessary radiation. This can be done with a fast transmission image or with a low-dose Rb-82 injection (10-20 mCi). Note that the low-dose Rb-82 scout scan is also used to estimate circulation times and cardiac blood pool clearance times, which assist in selection of the optimum injection to imaging delay time between Rb-82 injection and initiation of acquisition of myocardial Rb-82 images. With PET/CT systems, a low dose CT scout scan is routinely used for patient positioning.

Imaging parameters. Rest imaging should be performed before stress imaging to reduce the impact of residual stress effects (e.g., stunning and steal). For Rb-82, about 80% of the useful counts are acquired in the first 3 minutes, 95% of the useful counts are obtained in the first 5 minutes, and 97% are obtained in the first 6 minutes. The patient should be infused with Rb-82 for a maximum of 30 seconds. After the dose is delivered, patients with normal ventricular function, or left ventricular ejection fraction (LVEF) $>$ 50%, are typically imaged starting 70-90 seconds after the injection. For those with reduced ventricular function, or LVEF 30-50%, imaging usually is begun 90-110 seconds after termination of the infusion. Those with poor function, or LVEF $<$ 30%, are typically imaged at 110-130 seconds. Excessive blood pool counts can scatter into myocardial counts, impacting defect size and severity. Excessive blood pool counts can also make the left ventricular cavity appear smaller, especially at rest, leading to a false perception of LV cavity dilatation during stress. These delay times are applicable for both static and ECG gated acquired images.

N-13 Ammonia Perfusion Imaging

N-13 ammonia is a valuable agent for measuring either absolute or relative myocardial blood flow.[32,33] For measurements of absolute blood flow, dynamic acquisition from time of injection is required, followed by applying 2- and 3-compartment kinetic models that incorporate both extraction and retention rate constants. Absolute flow measurements with ammonia are

performed primarily in research settings, require a high level of expertise, and are not commercially available. In a clinical setting, ammonia PET images are assessed visually or semi-quantitatively for the evaluation of regional myocardial perfusion defects or for the determination of myocardial viability.[34-36]

N-13 ammonia is an extractable myocardial perfusion tracer that has been used extensively in scientific investigations with PET over the past two decades. At physiologic pH, ammonia is in its cationic form with a physical half-life of 10 minutes. Its relatively short half-life requires an on-site cyclotron and radiochemistry synthesis capability. The N-13 nitrogen decays by positron emission. The daughter product is C-13 carbon, which is stable. Myocardial uptake of N-13 ammonia depends on flow, extraction, and retention. First-pass myocardial extraction of N-13 ammonia is related inversely and nonlinearly to blood flow.[37] Following this initial extraction across the capillary membrane, ammonia may cross myocardial cell membranes by passive diffusion or as ammonium ion by the active sodium-potassium transport mechanism. Once in the myocyte, N-13 ammonia is either incorporated into the amino acid pool as N-13 glutamine or back-diffuses into the blood. The myocardial tissue retention of ammonia as N-13 glutamine is mediated by adenosine triphosphate and glutamine synthetase. Thus uptake and retention can both be altered by changes in the metabolic state of the myocardium although the magnitude of metabolic effects on the radiotracer retention appears to be small.

Dosimetry. The radiation dosimetry from N-13 ammonia in an adult is 1.48 mSv total effective dose from 20 mCi.[38] The critical organ is the urinary bladder, which receives 6 mSv from 20 mCi.[39] The dosimetry is relatively low, due to the short half-life of N-13 and the low energy of the emitted positrons.

Acquisition parameters. Table 8 summarizes the recommended guidelines for performing N-13 ammonia perfusion scans with dedicated, multicrystal PET or PET/CT cameras for rest and stress myocardial PET perfusion imaging for the diagnosis and evaluation of CAD, or as part of an assessment of myocardial viability.

Dose. Typically, 10-20 mCi of N-13 ammonia is injected. Large patients may benefit from higher, or 25-30 mCi, doses. In addition, the dose of radioactivity administered will also depend on whether images are obtained in 2D or 3D imaging mode.

PET METABOLIC IMAGING

PET Glucose Metabolism

For a given physiologic environment, the heart consumes the most efficient metabolic fuel as an adaptive response to meet its energy demands. Under fasting and aerobic conditions, long-chain fatty acids are the preferred fuel in the heart as they supply 65-70% of the energy for the working heart, and some 15-20% of the total energy supply comes from glucose.[40] However, the myocardium can use various other metabolic

Table 8. N-13 ammonia cardiac perfusion studies

Feature		Technique
Stress testing	Pharmacologic agents	Standard
Tracer dose (2D or 3D)	10–20 mCi (typical) (370–740 MBq)	Standard
Injection rate	Bolus or <30 seconds infusion	Preferred
Imaging delay after injection	1.5–3 minutes after end of infusion	Standard
Patient positioning		
PET	Use scout scan: 1–2 mCi (37–74 MBq)	Optional
	Use transmission scan	Standard
PET/CT	CT Scout Scan	Standard
Imaging mode	ECG gating of myocardium	Preferred
	Static or list mode	Optional
	Dynamic	Optional
Imaging duration	10–15 min	Standard
Attenuation correction	Measured attenuation correction, before or after	Standard
Reconstruction method	FBP or iterative expectation maximization (e.g., OSEM)	Standard
Reconstruction filter	Sufficient to achieve desired resolution/smoothing, matched stress to rest	Standard
Reconstructed pixel size	2–3 mm	Preferred
	4 mm	Optional

substrates depending on substrate availability, hormonal status, and other factors.[41,42]

Metabolic adaptation to changes in regional blood flow or other triggers is an essential component of maintaining normal cardiac function. Acute and chronic metabolic adaptation to a temporary or sustained reduction in coronary blood flow is in place to protect the structural and functional integrity of the myocardium. Reversible metabolic changes, as an adaptive measure to sustain myocardial viability, will occur in the setting of diminished, but not absent, regional myocardial blood flow. When myocardial blood flow is absent, irreversible metabolic changes will occur followed by myocardial infarction and cell death.

The breakdown of fatty acids in the mitochondria via beta-oxidation is exquisitely sensitive to oxygen deprivation. Therefore, in the setting of reduced oxygen supply, the myocytes compensate for the loss of oxidative potential by shifting toward greater utilization of glucose to generate high-energy phosphates. An acute switch from aerobic to anaerobic metabolism may be a necessary prerequisite for immediate cell survival following acute myocardial ischemia. Without these acute adaptive changes in metabolism, the resulting energy deficit leads to cell death.

Tracers of myocardial metabolism such as carbon-11 labeled fatty acids, acetate, or glucose, will not be covered in this document, due to their current investigational status and lack of FDA approval.

F-18 FDG Metabolism Imaging

Tracer properties. The principal radiopharmaceutical in clinical cardiac PET myocardial viability imaging is F-18 FDG, which is an analog of glucose and is used to image myocardial glucose utilization in vivo. CMS has approved reimbursement of FDG for the evaluation of myocardial viability.

The F-18 radiolabel is produced in a cyclotron through the (p,n) reaction, consisting of bombardment of O-18 enriched water.[43] F-18 decays by the emission of a positron with a half-life of $\sim$110 minutes. The low kinetic energy of the positron, 635 keV, allows the highest spatial resolution among all PET radionuclides. The 110-minute physical half-life of FDG allows sufficient time for synthesis and purification, its commercial distribution in a radius of several hours from the production site, its temporary storage at the user site, the absorption time after injection, and sufficient imaging time to yield images of high quality.

FDG enters myocardial cells by the same transport mechanism as glucose. Once in the cell, it is phosphorylated by hexokinase to FDG-6-phosphate. Once phosphorylated, subsequent metabolism of FDG is minimal. Because the dephosphorylation rate of FDG is slow, it becomes essentially trapped in the myocardium, allowing adequate time to image regional glucose uptake by PET. Following IV injection of 5-15 mCi of FDG, imaging can commence either immediately during the infusion of the radiotracer, if quantification of glucose metabolic rates is desired, or about 45-90 minutes after the injection of the radiotracer, if only qualitative assessment of the relative distribution of the radiotracer in the LV myocardium is needed.

Tracer dosimetry. The whole body dosimetry from a 10-mCi dose is 7 mSv.[44] For FDG, the critical organ is the urinary bladder, which receives 59 mSv.

Patient preparation. There are several approaches to stimulate myocardial glucose metabolism with either oral or IV glucose loading. Tables 9, 10, and 11 summarize the recommended guidelines for performing cardiac FDG scans with dedicated, multicrystal PET and PET/CT cameras, as part of an assessment of myocardial viability. Tables 10 and 11 summarize the patient preparation and method of FDG administration. Table 12 discusses the image acquisition.

Myocardial substrate utilization. For the evaluation of myocardial viability with FDG, the substrate and hormonal levels in the blood need to favor utilization of glucose over fatty acids by the myocardium.[40,42,45] This is usually accomplished by loading the patient with glucose after a fasting period of at least 6 hours to induce an endogenous insulin response. The temporary increase in plasma glucose levels stimulates pancreatic insulin production, which in turn reduces plasma fatty acid levels through its lipogeneic effects of adipocytes and also normalizes plasma glucose levels. The most common method of glucose loading is with an oral load of 25-100 g, but IV loading is also used. The IV route avoids potential problems due to variable gastrointestinal absorption times or inability to tolerate oral dosage. Because of its simplicity, most laboratories utilize the oral glucose-loading approach, with supplemental insulin administered as needed. The physician should take into account whether or not the patient is taking medications that may either antagonize or potentiate the effects of insulin.

Diabetic patients. Diabetic patients pose a challenge, either because they have limited ability to produce endogenous insulin or because their cells are less able to respond to insulin stimulation. For this reason, the simple fasting/oral glucose-loading paradigm is often not effective in diabetic patients. Use of insulin along with close monitoring of blood glucose (Table 10) yields satisfactory results. Improved FDG images can also be seen when image acquisition is delayed 2-3 hours after injection of the FDG dose. Of course, the latter comes at the expense of increased decay of the radiopharmaceutical. An alternative technique is the euglycemic hyperinsulinemic clamp, which is a rigorous and time-consuming

Table 9. FDG cardiac PET: patient preparation guidelines—an overview

Procedure		Technique
Fasting period	*Step 1*: Fast patient	
	6–12 hours	Preferred
	<6 hours	Suboptimal
	Step 2: Check blood glucose (BG) and then glucose load (choose one of the following 4 options)	
Oral glucose load	*Option 1*: Oral glucose loading	
	IF: fasting BG < ~250 mg/dL (13.9 mmol/L)	Standard
	THEN: (1) Oral glucose load: typically 25–100 g orally (see Table 10)	
	(2) Monitor BG (see Table 10)	
	IF: fasting BG > ~250 mg/dL (13.9 mmol/L)	Standard
	THEN: See Table 10	
	OR	
IV, protocol A	*Option 2*: Dextrose IV infusion	Optional
	For details, see sample protocol A (appendix 1)	
	OR	
IV, protocol B	*Option 3*: Dextrose IV infusion	Optional
	For details, see sample protocol B (appendix 2)	
	OR	
Acipimox	*Option 4*: Acipimox	
	Acipimox, 250 mg orally, not available in United States	
	Step 3: Administer FDG	
FDG injection	Time: Dependent on which option was selected	Standard
	Administer FDG intravenously; see Table 11, item 1, for details	
	Step 4: Begin imaging	
Begin PET imaging	Time 0–90 minutes post FDG injection: start imaging, see Table 11	

Table 10. Guidelines for blood glucose maintenance (e.g., after oral glucose administration) for optimal FDG cardiac uptake, blood glucose of approximately 100-140 mg/dL (5.55-7.77 mmol/L) at FDG injection time

BG at 45–60 min after administration	Possible restorative measure	Technique
130–140 mg/dL (7.22–7.78 mmol/L)	1 u regular insulin IV	Standard
140–160 mg/dL (7.78–8.89 mmol/L)	2 u regular insulin IV	
160–180 mg/dL (8.89–10 mmol/L)	3 u regular insulin IV	
180–200 mg/dL (10–11.11 mmol/L)	5 u regular insulin IV	
>200 mg/dL (>11.11 mmol/L)	Notify physician	

procedure.[46,47] However, it allows close titration of the metabolic substrates and insulin levels, which results in excellent image quality in most patients. Shorter IV glucose/insulin-loading procedures of 30 minutes have also been used with some success (see Protocol A, Appendix 1 and Protocol B, Appendix 2).[48]

While some have advocated performing FDG viability scans under fasting conditions, it is recommended that they be performed under glucose loaded conditions. This maximizes FDG uptake in the myocardium, results in superior image quality, and reduces the regional variations in FDG uptake

Table 11. FDG cardiac PET: acquisition guidelines for dedicated, multicrystal PET scanner

Feature		Technique
Tracer dose (2D or 3D)	5-15 mCi (185-555 MBq)	Standard
Injection rate	Not critical, bolus to 2 minutes	Standard
Image delay after injection	45-60 min after injection (keep constant for repeat studies)	Standard
Patient positioning		
PET	Use an FDG scout scan	Optional
	Use transmission scan	Standard
PET/CT	CT Scout Scan	Standard
Imaging mode	2D or 3D	Standard
	Static or list mode	Standard
	Dynamic	Optional
Image duration	10-30 min (depending on count rate and dose)	
Attenuation Correction	Measured attenuation correction: before or immediately after scan	Standard
Reconstruction method	FBP or iterative expectation maximization (e.g., OSEM)	Standard
Reconstruction filter	Sufficient to achieve desired resolution/smoothing, matched between consecutive studies	Standard
Reconstructed pixel size	2-3 mm	Preferred
	4-5 mm	Acceptable

Note: If metabolism imaging is combined with PET perfusion imaging, the same parameters for patient positioning, attenuation correction, and image reconstruction should be applied.

Table 12. Semiquantitative scoring system of defect severity and extent

Grade	Interpretation	Score
Normal counts	Normal perfusion	0
Mild reduction in counts	Mildly abnormal	1
Moderate reduction in counts	Definitely abnormal	2
Severe reduction in counts	Definitely abnormal	3
Absent counts	Definitely abnormal	4

that can occur when imaging under fasting conditions.[49]

Acipimox. Acipimox is a nicotinic acid derivative, which is not FDA approved in the United States. It has been used successfully in Europe instead of glucose loading. Acipimox inhibits peripheral lipolysis, reduces plasma free fatty acid levels, and stimulates myocardial glucose utilization.[48,50]

Acquisition parameters. Acquisition parameters for PET cardiac FDG imaging are itemized in Table 11 and its accompanying notes. If FDG PET metabolic images are being compared to perfusion images acquired by SPECT, the interpreter should be mindful that there will be differences in soft tissue attenuation, image resolution, and registration problems of images acquired on different instruments. It should be noted that if a Tl-201 or Tc-99m-labeled perfusion tracer is used to assess myocardial perfusion, there is no need to delay the FDG PET images, from an instrumentation point of view, if the 2D PET acquisition mode is applied. The relatively lower photons emitted from Tl-201 and Tc-99m will not interfere with the higher energy F-18 photons. However, with 3D PET imaging, the Tc-99m activity can increase dead time and thus decrease the ''true'' counts from the FDG. If FDG PET images are acquired first, then it is necessary to wait at least 15 or more half-lives, depending on the dose of F-18 administered, before a low-energy (e.g., Tl-201 or Tc-99m) SPECT study is performed. This is because the 511 keV photons from the PET tracers easily penetrate the collimators that are commonly used for Tl-201 or Tc-99m imaging.

Dose. Typically, 5-15 mCi is injected in a peripheral vein (see counts requirements below). Injection speed is not critical (i.e., bolus to 2 minutes). To reduce patient dose to the bladder, patients should be encouraged to void frequently for 3-4 hours after the study.

Scan start time and duration. Wait a minimum of 45 minutes before starting the static FDG scan acquisition. Myocardial uptake of FDG may continue to increase, and blood pool activity to decrease, even after 45 minutes. While waiting 90 minutes after the injection of FDG may give better blood pool clearance and myocardial uptake, especially in diabetics or subjects with high blood glucose levels, this comes at the expense of reduced count rate. Scan duration is typically 10-30 minutes. If acquired in 3D mode, compared with 2D mode with the same machine, a smaller dose is typically required to achieve the same total count rate, but the imaging time may or may not be reduced as a result of count rate limitations and increased scatter. In some PET cameras, beyond a certain dose, the 3D mode will actually produce poorer-quality images for the same dose and imaging time than 2D mode. For this reason, it is critical to have fully characterized the performance of the PET system.

IMAGE DISPLAY, NORMALIZATION, AND EVALUATION FOR TECHNICAL ERRORS

Recommendations for display of PET perfusion rest-stress and/or perfusion-metabolism images are consistent with those listed in previous guidelines for SPECT myocardial rest-stress perfusion imaging.[51] It is necessary to examine the transaxial, coronal, and sagittal views for assessing the alignment of the emission images acquired during stress, rest, and metabolism, as well as the transmission images. Fused transmission and emission images are preferred. Images that are not aligned (e.g., due to patient or cardiac motion) may cause serious image artifacts, especially when only one set of attenuation correction images has been applied to all emission images for attenuation correction. This is particularly a problem when CT is used for attenuation correction.[16] It is important that the fusion images be reviewed for potential misalignment problems and appropriate adjustments be made. Some vendors' systems now provide software that allows realignment of transmission CT and emission PET images before processing, and in other instances image data can be transferred to a stand-alone PC that has realignment software.

The reoriented images should be displayed as follows:

1. A short-axis view, by slicing perpendicular to the long axis of the LV from apex (left) to base (right).
2. A vertical long-axis view, by slicing vertically from septum (left) to lateral wall (right).
3. A horizontal long-axis view, by slicing from the inferior (left) to the anterior wall (right).

For interpretation and comparison of perfusion and metabolism images, slices of all data sets should be displayed aligned and adjacent to each other. In the absence of motion artifact, combined assessment of perfusion and metabolism within a single PET session offers the advantage of copying the ventricular long axis defined during image orientation from one image set to the second set, thereby optimizing the matching of the perfusion with the metabolism images. Normalization of the stress and rest perfusion image set is commonly performed by using the maximal myocardial pixel value in each of the two or three image sets; or, for example, the average pixel value with the highest 5% of activity of the perfusion images. Each perfusion study is then normalized to its own maximum.

The metabolism images are normalized to the counts in the same myocardial region on the resting perfusion images (e.g., with the highest count rates that were obtained on the perfusion study).[52,53] An important limitation of this approach, however, is that glucose metabolism may be enhanced or abnormally increased in regions with ''apparently'' normal resting myocardial perfusion, if such regions are subtended by significantly narrowed coronary arteries and are in fact ischemic on stress myocardial perfusion studies.[54] Moreover, visual assessment of resting myocardial uptake of the radiotracer reflects the distribution of myocardial blood flow in ''relative'' terms (i.e., relative to other regions of the LV myocardium) and not in ''absolute'' terms (i.e., mL/min/gm myocardial tissue). Thus, in some patients with multivessel CAD, it is possible that all myocardial regions are in fact hypoperfused at rest in ''absolute'' terms (i.e., termed balanced reduction in blood flow) yet appear normal in ''relative'' terms. If stress images of PET are available, it is recommended that the normal reference region on stress perfusion images be used for normalizing FDG PET images.[35] In the presence of left bundle-branch block (LBBB), where the septal FDG uptake is spuriously decreased, the septum should not be used as the site for normalization. Accordingly, the ECG should be reviewed in conjunction with perfusion/viability imaging.

Standard Segmentation and Polar Map Display

Standard segmentation model divides the LV into three major short-axis slices: apical, mid-cavity, and basal. The apical short-axis slice is divided into four

segments, whereas the mid-cavity and basal slices are divided into six segments. The apex is analyzed separately, usually from a vertical long-axis slice. Although the anatomy of coronary arteries may vary in individual patients, the anterior, septal, and apical segments are usually ascribed to the left anterior descending coronary artery, the inferior and basal septal segments to the right coronary artery, and the lateral segments to the left circumflex coronary artery. The apex can also be supplied by the right coronary and left circumflex artery. Data from the individual short-axis tomograms can be combined to create a polar map display, representing a 2D compilation of all the 3D short-axis perfusion data. Standard 17 segments in the polar map are displayed in Figure 1.[55] The 2D compilation of perfusion and metabolism data can then easily be assigned to specific vascular territories. These derivative polar maps should not be considered a substitute for the examination of the standard short-axis and long-axis cardiac tomographic slices.

3D Display

If suitable software is available, reconstructed myocardial perfusion and metabolism data sets can be displayed in a 3D static or cine mode, which may be convenient for morphologic correlation with angiographic correlation derived from CT, magnetic resonance, or conventional angiography. Some of the software may allow the overlay the coronary anatomy on the 3D reconstructed perfusion and metabolism images of the heart. Currently, an advantage of 3D over conventional 2D displays with regard to accuracy of PET image interpretation has not been demonstrated.

Recommended Medium for Display

It is strongly recommended for the interpreting physician to use the computer monitor rather than film hard copies for interpretation of myocardial perfusion and metabolism images. The latter would be especially important for gated PET images, where dynamic wall motion data is viewed for proper interpretation of regional abnormalities. A linear gray scale, monochromatic color scale, or multicolor scale can be used as the type of display, depending on user experience and preference.

Image Evaluation for Technical Sources of Errors

Patient motion. PET images are typically generated with nonmoving circular arrays of scintillation detectors that acquire all projection data simultaneously. In contrast to SPECT imaging with rotating gamma cameras, in which patient motion leads to a typical misalignment between adjacent projection images and can be identified by viewing a projection movie. Movement during static PET imaging affects all projections and is therefore more difficult to identify. Substantial patient motion can produce blurring of image contours. Therefore, attention to patient motion during image acquisition is essential to minimize motion artifacts.

Patient positioning before and immediately after image acquisition should be carefully evaluated (e.g., by checking the alignment of the camera's positioning laser beams with ink markers on the patient's skin). Acquisition of a brief scan or scout image after injection of a

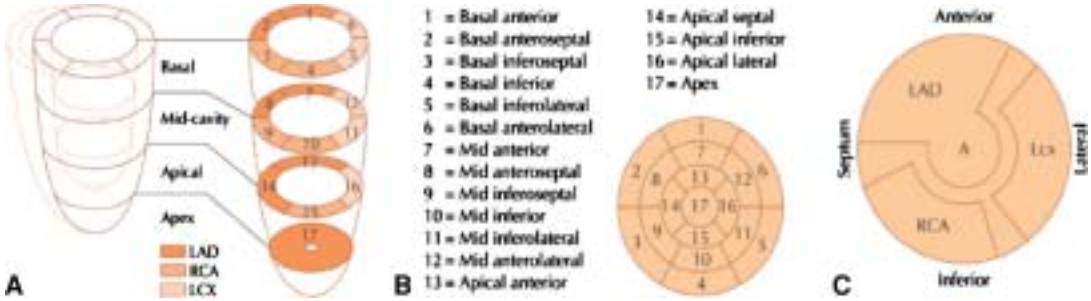

Figure 1. LV Myocardial segmentation, standard nomenclature, and vascular territories. PET images are interpreted on the basis of the presence, location, extent, and severity of myocardial perfusion and metabolic defects using a standard 17-segment model and visual scoring. **A** The standard segmentation model divides the LV into three major short-axis slices: apical, midcavity, and basal. The apical short-axis slice is divided into four segments, whereas the mid-cavity and basal slices are divided into six segments. The apex is analyzed separately, usually from a vertical long-axis slice. **B** Data from the individual short-axis tomograms can be combined to create a polar map plot, representing a 2D compilation of all the 3D short-axis perfusion data. Standard nomenclature for the 17 segments is outlined. **C** The 2D compilation of perfusion data can then easily be assigned to specific vascular territories. (*From* Dilsizian V.; *Reprinted with permission*)[55].

small dose, usually one-third of the standard dose of Rb-82, may facilitate accurate patient positioning. With PET/CT systems, a CT scout scan (10 mA) is routinely used for accurate patient positioning. In instances of patient discomfort and likely patient motion, especially during longer image acquisition times, one approach to reduce adverse effects of motion is to acquire a series of 3-4 sequential image frames instead of a single static image of longer duration. Dynamic imaging would also be effective for this purpose. If the quality of one of the serially acquired frames is compromised by motion, then that frame can be rejected and only frames that are of acceptable quality and are free of motion artifacts are summed for the final image analysis.

Attenuation correction. Correction of the emission images for photon attenuation is critical for cardiac PET imaging. Positron-emitting tracers are more sensitive to attenuation artifacts than single photons. Coincidence detection systems must detect both simultaneously emitted photons. As each of the two photons is susceptible to tissue attenuation, attenuation artifacts are generally greater. Therefore, only attenuation-corrected images should be used for clinical interpretation. Potential sources of errors include misalignment between emission and transmission data resulting from patient motion. Misalignments of 1.5-2 cm, for example, can lead to as much as a 30% change in the observed regional myocardial radioactivity.[10,16,17,56]

Vertical and transaxial displacement of the heart can occur even in the absence of movement of the chest. The latter is perhaps related to the change of breathing pattern, which may occur during pharmacologic stress. This could be thought as analogous to the ''upward creep'' phenomenon seen in SPECT imaging. As a result, under-correction artifacts due to the lower attenuation coefficient of the overlapping lung tissue may appear in the anterior or anterolateral regions, or over-correction artifacts due to the higher attenuation coefficients of the overlapping subdiaphragmatic tissues may appear in the inferior region as ''hot spots.'' Inspection of fused emission-transmission images for possible misalignment is essential because the resulting artifacts would greatly affect image interpretation. Fused images should be inspected in the axial (lateral displacement), coronal (vertical displacement) and sagittal (vertical displacement) slices. Alternatively, displacement can be detected on transaxial images by counting the number of pixels by which the cardiac image is displaced between resting and stress transaxial acquisitions. Identification of vertical and lateral displacements that result in misalignment between the emission and transmission images is relatively straightforward.

The degree of co-registration of transmission and emission images should be carefully examined using the fusion software available on integrated PET/CT systems to assess the reliability of images with attenuation correction. If there is patient motion and the cardiac silhouette does not superimpose perfectly on the transmission and emission images, the images without attenuation correction need to be examined as well. In general, vertical misalignment is easier to resolve by offsetting the alignment between the emission and transmission scans, but this option is not generally available.

When the transmission maps are acquired using CT, the incidental findings in the portion of the chest in the FOV should be reported, when relevant to patient care.

Reconstruction artifacts. Image artifacts may occur if extracardiac activity is present adjacent to the myocardium. For example, intense focal activity in the liver or the gastrointestinal tract may lead to spillover of residual activity from imperfect scatter compensation resulting in artificially elevated counts or cause a reconstruction (i.e., ramp-filter) artifact resulting in artifactually low count rates in adjacent myocardium. A method to correct for such artifacts is currently not available, but such artifacts, particularly the ramp-filter artifact, are less prominent when iterative reconstruction is used instead of the standard FBP techniques. Additional artifacts can result from problems with CT transmission images, such as streaks caused by insufficient x-ray tube intensity in obese individuals, truncations, beam hardening resulting from bone (e.g., arms down) or metal adjacent to the heart (e.g., pacemakers and internal defibrillators), and breathing leading to disconnected pieces of liver in the lungs or misalignment between CT and PET data. CT artifacts are propagated into the PET images through use of the CT image for attenuation and scatter corrections. These artifacts are less of a problem with Cs-137 attenuation correction.

Image count statistics. The final count density of PET images is influenced by additional factors such as body habitus and weight, radionuclide dose, scanner performance, acquisition time, and in the case of metabolic imaging, the dietary and hormonal state. Image count density directly affects the diagnostic quality and reliability of the study.

Image Analysis and Interpretation of PET Images

The rest and stress perfusion and/or metabolism images, should be interpreted initially without clinical information in order to minimize any bias in study interpretation. All relevant clinical data should be reviewed after a preliminary impression is formed.

LV and RV size. The reader should note whether there is an enlargement of the right ventricle (RV) or LV

at rest or whether there is transient stress-induced LV cavity dilation. Ventricular enlargement seen on the stress and rest perfusion or metabolic images generally indicates left, right, or bi-ventricular dysfunction. Transient stress-induced LV dilation usually reflects extensive CAD. LV and RV sizes as well as any changes associated with stress are typically described qualitatively. A number of commercially developed software packages originally developed for SPECT have the ability to quantify mean LV volumes and end-diastolic and end-systolic volumes for gated PET images, but not all such packages have been validated for all PET instruments, and they should be used with caution.

Lung uptake. Increased tracer activity in the lungs should be reported qualitatively. Increased lung uptake on the perfusion images, particularly when severe, may reflect severe LV dysfunction with increased LV end-diastolic and capillary wedge pressures. It can also reflect infiltrative diseases of the lungs, and can be seen in smokers.

RV uptake. Increased RV tracer uptake may be seen both on perfusion and metabolism images in the presence of pulmonary hypertension with or without significant RV hypertrophy. Assessment of increased RV uptake is usually assessed relative to the radiotracer uptake in the LV myocardium. Since the septum is shared by both ventricles, assessment of increased RV uptake should be made in relation to other regions of the LV myocardium. Abnormally increased RV tracer uptake is a qualitative assessment.

Blood pool activity. Visualization of persistent blood pool activity on either perfusion or metabolism images is usually a sign of relatively poor myocardial uptake of the radiotracer, insufficient time for uptake of the radiotracer into the myocardium, or diminished clearance of the radiotracer from blood. A major cause of increased blood pool activity, especially for perfusion imaging with Rb-82, is impairment of cardiac systolic function that prolongs the circulation time. This is especially relevant when only static images are acquired, because vasodilators typically increase cardiac output and shorten the circulation time. Increased blood pool activity may be seen if the acquisition of images begins prior to 70-170 seconds after Rb-82 administration, especially in patients with a history of congestive heart failure and poor LV function. If Rb-82 perfusion images are acquired serially, an appropriate starting point, after blood pool activity has cleared sufficiently, can be chosen after the acquisition for summing the myocardial tracer uptake images. Judicious adjustment of display threshold and contrast settings can help offset this problem. List mode acquisition allows for the re-processing of images with varying delay times and may be useful for optimizing the quality of reconstructed images.

Extra-cardiac findings. The tomographic images should be carefully examined for uptake of the radiotracer in organs other than the myocardium, particularly in the lungs and the mediastinum. Extra-cardiac uptake of a flow tracer may be of clinical significance, as it may be associated with malignancy and/or an inflammatory process. The 3D maximum intensity projection display, a method of displaying acquired PET images as a rotating 3D display, can be particularly helpful in this regard. When using PET/CT systems, review of the low-resolution CT-based transmission scans can be useful to delineate potentially important ancillary findings, such as pleural and pericardial effusion, coronary and/or aortic calcification, breast, mediastinal or lung mass, and others.

Interpretation of PET Perfusion Data

Perfusion defect location. Myocardial perfusion defects should be identified through careful visual analysis of the reoriented myocardial slices. Perfusion defects should be characterized by extent, severity and location relative to the specific myocardial territory, such as the anterior, lateral, inferior, septal, and/or apical walls. Standardized nomenclature should be used, according to previously published guidelines.[51] RV defects due to scarring and ischemia should be noted.

Perfusion defect severity and extent: Qualitative. Defect extent should be qualitatively estimated by describing the location of the abnormal segments involved (e.g., anterior, inferior, or lateral) as well as the extent in the LV (e.g., ''mid-to-distal'' or ''extending from base to the apex''). The extent of the defect may also be qualitatively described as small (5-10% of the LV), medium (10-20% of the LV), or large (>20% of the LV). A defect of more than 10% of the LV is associated with a higher risk of events. Defect severity is typically expressed qualitatively as mild, moderate, or severe. Severe defects may be considered as those having a tracer concentration equal or similar to background activity, and moderate defects are considered definitely abnormal but visually discernable activity above the background. Mild defects are those with a subtle but definite reduction in regional myocardial tracer.

Stress and rest myocardial perfusion image sets are compared in order to determine the presence, extent, and severity of stress-induced perfusion defects and to determine whether such defects represent regions of myocardial ischemia or infarction. Regions with stress-induced perfusion abnormalities, which have normal perfusion at rest, are termed reversible perfusion defects and represent ischemia. Perfusion abnormalities on stress, which remain unchanged on rest images, are

termed irreversible or fixed defects, and most often represent areas of prior myocardial infarction. When both ischemia and scar are present, the defect reversibility is incomplete, giving the appearance of partial reversibility.

Perfusion defect severity and extent: Semiquantitative scoring system. In addition to the qualitative assessment of perfusion defects, a semiquantitative approach based on a validated segmental scoring system has been developed Table 12). This approach standardizes the visual interpretation of scans, reduces the likelihood of overlooking clinically significant defects, and provides a semiquantitative index that is applicable to diagnostic and prognostic assessments.

A 17-segment model for semiquantitative visual analysis is usually employed.[51] The model is based on three short-axis slices (apical, mid, and basal) to represent most of the LV and one vertical long-axis slice to better represent the LV apex. The basal and mid short-axis slices are divided into six segments. The apical short-axis slice is divided into four segments. A single apical segment is taken from the vertical long-axis slice. Each segment has a specific name (Figure 1). The extent of stress and rest perfusion abnormalities, as well as an estimate of the extent of scarring and ischemia, can be performed by counting the number of segments. Myocardial segments may be assigned to coronary artery territories. Caution should be exercised because the coronary anatomy varies widely among patients. For example, it is not at all uncommon to find segments 9, 10, and 15 of the 17-segment model involved in left anterior descending artery disease. Similarly, segments 5 and 11 of the model may be affected by disease of the right coronary artery.

A well-accepted 5-point scale semi-quantitative visual scoring method is used in direct proportion to the observed count density of the segment, as follows: 0 = no defect, 1 = mildly reduced, 2 = moderately reduced, 3 = severely reduced; 4 = absent activity (Table 12). In addition to individual scores, calculation of summed scores is recommended, in which the summed stress score is the sum of the stress scores of all segments, the summed rest score is the sum of the resting scores of all segments, and the summed difference score is the difference between the summed stress and summed rest scores and serves as a measure of reversibility. The summed scores incorporate the global extent and severity of perfusion abnormality. For example, the summed stress score reflects the extent and severity of perfusion defects at stress and is affected by prior myocardial infarction as well as by stress-induced ischemia. On the other hand, the summed rest score reflects the amount of infarcted and/or hibernating myocardium. The summed difference score is a measure of the extent and severity of stress-induced ischemia.

Before scoring, it is necessary for the interpreting physician to be familiar with the normal regional variation in count distribution of myocardial perfusion PET. No regional variation in tracer uptake has been reported for Rb-82, except for a mild reduction in the apex and base of the LV, consistent with segmentation artifact and/or thinning of the LV myocardium in these locations. Regarding N-13 ammonia, unlike Rb-82 and other SPECT perfusion tracers, the lateral wall uptake may not necessarily be the region with the highest counts, serving as the reference region for normalization. This normal variation should be kept in mind when interpreting lateral perfusion defects with N-13 ammonia PET. Given the variability in the normal distribution of various radiotracers, the patient's polar map may be compared with a reference polar map derived from radiotracer and gender-specific normal database. Ideally, each camera system and acquisition protocol should have its own ''normal'' file but such normal databases are not widely available. The semi-quantitative analysis system provided by a specific vendor should be validated by appropriate studies published in peer-reviewed journals.

Absolute quantification of myocardial blood flow. Quantitative blood flow approaches offer an objective interpretation that is inherently more reproducible than visual analysis. Absolute quantification may aid in assessing the physiologic significance of known coronary artery stenosis, especially when of intermediate severity. Both relative and absolute quantification are particularly useful in describing changes between two studies in the same patient. In addition, quantitative measurements of myocardial blood flow may identify balanced reductions in myocardial blood flow due to multivessel CAD or diffuse, small-vessel disease.

Quantitative assessment of myocardial blood flow in absolute units (e.g., mL/min/gm tissue) has been well established in the literature with N-13 ammonia and O-15 water.[31-35,57-59] It requires the acquisition of images in dynamic mode. The use of list mode acquisition now enables flow quantification in conjunction with perfusion and gated LV and regional function. The added value in terms of diagnosis and prognosis is the subject of active investigation in several centers. ROIs are placed on the LV myocardium and the LV blood pool and are copied to all serially acquired images for generation of myocardial tissue and blood pool time-activity curves. The time-activity curves are corrected for activity spillover from the blood pool to the myocardium and for radioactive decay. They are then fitted with a validated tracer kinetic model, and estimates of myocardial blood flow in milliliters of blood per minute per

grams of myocardium are obtained. Software programs are also available for generating parametric polar maps that display regional myocardial blood flows in absolute units.

Oxygen-15-labeled water is often considered the ideal radiotracer for quantifying myocardial blood flow in absolute terms.[57-59] Because the capillary and sarcolemmal membranes do not exert a barrier effect to the exchange of water, the activity of O-15-labeled water observed in an ROI assigned to the myocardium on the serially acquired images can be described by a one-compartment tracer kinetic model. O-15 water is not FDA approved, and therefore, it is not used clinically in the United States. However, it is used in Europe for clinical imaging.

Quantification of myocardial blood flow with Rb-82 has been more challenging because of its 75 second half-life resulting in noisy myocardial and blood pool time activity curves.[60,61] The kinetic behavior of Rb-82 in tissue can be described by a one- or two-compartment model, that can be fitted using the arterial input function (i.e., obtain from the blood pool concentration of the LV cavity or left atrium) and myocardial time-activity curves at each segment, or even (with sufficient statistics) at each pixel.[60,62-65] The parameters of the model, which include flow, can be estimated using non-linear regression or other techniques. The large number of free parameters and the high noise levels frequently encountered in Rb-82 images mean that simultaneous estimation of all parameters cannot always be performed reliably.[66] The variability of flow estimates can be reduced by fixing certain parameters to physiologically realistic values, but the fact that the extraction fraction of Rb-82 is flow dependent remains a challenge for accurate quantification. Semi-quantitative indices of flow, such as dividing the mean tissue uptake over a certain period by the integral of the blood concentration, may prove more practical for routine use. Many of the error sources approximately cancel out when flow reserve is calculated and first-order corrections can be applied for the variable extraction fraction of Rb-82.[67]

Gated PET images. The ability to acquire cardiac PET images in conjunction with ECG gating is an important development that has not always been available, particularly on 3D scanners. Some systems support ECG gating via list-mode acquisition. In such a mode the positions of all coincidence pairs are recorded along with timing information and input from an ECG machine. These data can be retrospectively processed to produce ECG gated images, ungated images, and if necessary, dynamic images, which represent the activity distribution as a function of time. The flexibility of this mode of acquisition is particularly convenient for quantitative analysis.

ECG gating of the rest and peak stress myocardial perfusion images can provide additional information regarding changes in LV function and volumes that may be useful in identifying 3-vessel CAD with or without left main disease, which may be underestimated on the review of the perfusion images.[68] Unlike ECG gating of the post-stress SPECT images, PET acquisitions take place during peak pharmacologic vasodilation, especially when using ultra short-lived tracers like Rb-82 (acquisitions are shorter than those for N-13 ammonia and, thus, more likely to occur while the patient is at peak pharmacological stress).[69,70] ECG gating of FDG PET images can also provide additional information regarding regional and global LV function and volumes.

Assessment of Myocardial Viability

Detection of viable myocardium plays a central role in the management of patients with LV dysfunction due to CAD. It is based on the recognition that resting LV dysfunction may be reversible, attributable to myocardial hibernation/stunning, and not necessarily due to myocardial scar. As a consequence, its presence signifies a different prognosis and mandates a different treatment paradigm compared with the presence of predominantly non-viable or irreversible damaged tissue. Indeed, the importance of differentiating viable from non-viable tissue is highlighted by the plethora of techniques currently available to perform this task. Myocardial metabolism imaging with PET and FDG uses the preservation of myocardial glucose metabolism, particularly in the presence of resting hypoperfusion as a scintigraphic marker of viable myocardium. It is accomplished with FDG as a tracer of exogenous glucose utilization. The regional myocardial concentrations of this tracer are compared with the regional distribution of myocardial perfusion. Regional increases in FDG uptake relative to regional myocardial blood flow (i.e., perfusion-metabolism mismatch) signify myocardial viability. In contrast, a regional reduction in FDG uptake in proportion to regional reductions in myocardial perfusion (i.e., perfusion-metabolism match) signifies myocardial scar or nonviable tissue. Areas with maintained perfusion, but diminished FDG uptake, also likely reflect regions of jeopardized but viable myocardium since the perfusion tracers reflect active metabolic trapping.

Comparison of myocardial metabolism to perfusion. The comparison of perfusion and metabolism images obtained with PET is relatively straightforward because both image sets are attenuation-corrected. Thus, a relative increase in myocardial metabolism in regions of reduced perfusion by one grade or more, reflect the presence of perfusion-metabolism

mismatch, hence myocardial viability. In contrast, relative decrease in myocardial metabolism that is in proportion to reductions in regional perfusion reflects the presence of perfusion-metabolism match, hence myocardial scar or nonviable tissue.

Special considerations for combining SPECT perfusion with PET metabolism images. In current clinical practice, FDG PET images are often read in combination with SPECT myocardial perfusion images. The interpreting physician should be careful when comparing the non-attenuation-corrected SPECT images with attenuation-corrected FDG PET images. Myocardial regions showing an excessive reduction in tracer concentration as a result of attenuation artifacts, such as the inferior wall in men or the anterior wall in female subjects, may be interpreted as perfusion-metabolism mismatches, resulting in falsely positive perfusion-metabolism mismatches. Two approaches have proved useful for overcoming this limitation:

1. Because assessment of viability is relevant only in myocardium with regional contractile dysfunction, gated SPECT or PET images offer means for determining whether apparent perfusion defects are associated with abnormal regional wall motion.
2. Quantitative analysis with polar map displays that are compared with tracer- and gender-specific databases (for SPECT images) may be a useful aid to the visual interpretation. SPECT perfusion images with attenuation correction are helpful as well.[71,72] However, neither approach is infallible.

For myocardial FDG images acquired with ultra high-energy collimators or with SPECT-like coincidence detection systems, additional problems may be encountered, especially when the images are not corrected for photon attenuation.[73-75] Myocardial regions with severely reduced tracer activity concentrations due to attenuation artifacts on both perfusion and metabolism imaging, such as the inferior wall in men or the anterior wall in women, may be interpreted erroneously as perfusion-metabolism matches. Attenuation of the high-energy 511-keV photons is less than that for the 140-keV photons of Tc-99m or the 60- to 80-keV photons of Tl-201 so that attenuation artifacts are less prominent for FDG images and may result in an apparent mismatch. Furthermore, the lower spatial resolution of SPECT imaging systems for FDG imaging, especially when using high-energy photon collimation and then comparing with Tc-99m or Tl-201 images, causes apparent mismatches for small defects, at the base of the LV, or at the edges or borders of large perfusion defects. Such artifacts resulting from the use of different photon energies can be avoided by using dedicated PET systems for both perfusion and metabolism imaging. Again, use of ECG-gated imaging to demonstrate normal wall motion, quantitative analysis through polar map displays with comparison to radiotracer- and gender-specific databases of normal may aid in the visual interpretation.

Absolute myocardial glucose utilization. Quantitative estimates of myocardial glucose utilization in absolute units of micromoles of glucose per minute per grams of myocardium have not been found to aid in the assessment or characterization of myocardial viability due to the variability in substrate utilization by the myocardium, even when FDG images are acquired during a hyperinsulinemic-euglycemic clamp.[46,47,76] Methods for deriving quantitative estimates of myocardial metabolism require acquisition of serial images for 60 minutes that begin with tracer injection.[42,43] ROIs are placed on the myocardium and the LV blood pool and are copied to all serially acquired images in order to generate myocardial tissue and blood pool time-activity curves. The time-activity curves are corrected for spillover of activity from the blood pool into the myocardium and for radioactive decay. The time-activity curves are then fitted with a validated tracer kinetic model, and estimates of regional myocardial glucose utilization are obtained in micromoles of glucose per minute per grams of myocardium. Measurements of glucose metabolic rates further require determination of glucose concentrations in arterial or arterialized venous blood. Similar to myocardial perfusion, parametric images and polar maps are also available for display of rates of regional myocardial glucose utilization. Regional metabolic rates on such parametric images are coded by a color scale and can be determined noninvasively for any myocardial region through ROIs assigned to the polar map.[77]

Integration of perfusion and metabolism results. The combined evaluation of regional myocardial perfusion and FDG metabolism images allows identification of specific flow-metabolism patterns that are useful to differentiate viable from nonviable myocardium. It is useful to start with a functional assessment, ideally from gated PET or SPECT imaging, as dysfunctional segments are those suitable for evaluation of myocardial viability. If stress perfusion images as well as resting perfusion images are available, jeopardized myocardium can be distinguished from normal myocardium, and myocardium perfused normally at rest but dysfunctional as a result of repetitive stunning can be distinguished from myopathic or remodeled myocardium.

Differences in blood pool concentration of tracers can impact on the apparent match or mismatch of perfusion-FDG images. The separate adjustment of

threshold and contrast settings can help compensate for these discrepancies.

Four distinct resting perfusion-metabolism patterns may be observed in dysfunctional myocardium:[78-83]

1. Normal blood flow associated with normal FDG uptake.
2. Reduced blood flow associated with preserved or enhanced FDG uptake (perfusion-metabolism mismatch).
3. Normal or near-normal blood flow with reduced FDG uptake (reversed perfusion-metabolism mismatch).
4. Proportionally reduced blood flow and FDG uptake (perfusion-metabolism match).

The patterns 1-3 are all indicative of viable myocardium whereas pattern 4 represents nonviable tissue.

Some laboratories have added a fifth pattern, a mild perfusion-metabolism match in which the regional uptake of both the tracer of blood flow and of FDG is mildly to moderately reduced.[80,81,84] Because contractile function in such ''mild'' matches generally does not improve after revascularization, the pattern is subsequently included in the general category of perfusion-metabolism matches. If stress and rest perfusion imaging information is available, it is useful to add an estimate of the extent of stress-inducible ischemia in regions of normal resting perfusion and FDG uptake, in regions with matched resting perfusion-FDG defects, or in regions with resting perfusion FDG-metabolic mismatch. The simultaneous display of stress and rest perfusion and FDG metabolic images is most helpful but not available on all display workstations. In circumstances where only resting perfusion imaging is performed alongside FDG metabolic imaging, besides reporting on the extent of scar and extent of hibernating myocardium, it is useful to indicate that in the absence of corresponding stress myocardial perfusion images, one cannot rule out stress-induced myocardial ischemia.

In circumstances where only stress perfusion imaging is available in combination with FDG metabolic imaging, the following patterns can be found in segments with contractile dysfunction:

1. Stress perfusion defect with preserved FDG uptake indicates ischemic but viable myocardium. Revascularization is generally appropriate since myocardial ischemia is a very strong predictor for recovery of perfusion and function after a successful revascularization. With stress perfusion and FDG metabolic paired images, it is not possible to differentiate between myocardial ischemia, stunning, and hibernation.
2. Stress perfusion defects associated with proportionately decreased or lack of FDG uptake indicate scarred or nonviable myocardium, and revascularization is not recommended.

Qualitative or semiquantitative approaches can be applied to the interpretation of perfusion-metabolism patterns. When comparing FDG metabolism with perfusion images, it is important to first identify the normal reference region (the region with the highest tracer uptake), preferably on the stress myocardial perfusion images. The extent of mismatch or match defect may be small (5-10% of the LV), moderate (10-20% of the LV), or large (>20% of the LV). The severity of a match defect can be expressed as mild, moderate, or severe in order to differentiate between nontransmural and transmural myocardial infarction.

Interpretation of FDG images when perfusion images have not been obtained. Interpretation of FDG images without perfusion images and/or angiographic information and/or without information on regional wall motion is discouraged. The presence of relatively well-preserved FDG uptake in dysfunctional myocardium does not differentiate ischemic from non-ischemic cardiomyopathy. The degree of FDG accumulation over and above regional perfusion helps to assess the relative amount of scar and metabolically viable myocardium. The latter information may significantly influence the power of the test for predicting functional recovery. Therefore, it is recommended that FDG metabolic images be analyzed in conjunction with perfusion images, obtained either with SPECT or, preferably, with PET.

REPORTING OF MYOCARDIAL PERFUSION AND METABOLISM PET STUDIES

Patient Information

The report should start with the date of the study, patient's age, sex, height, and weight or body surface area, as well as the patient's medical identification number.

Indication for Study

Understanding the reason(s) why the study was requested, aids in focusing the study interpretation on the clinical question asked by the referring clinician. In addition, a clear statement for the indication of the study has become an important component of billing for services rendered.

History and Key Clinical Findings

A brief description of the patient's clinical history and findings can contribute to a more appropriate and

comprehensive interpretation of the rest (and stress) perfusion and of the metabolism images. This information may include past myocardial infarctions and their location, revascularization procedures, the patient's angina-related and congestive heart failure-related symptoms, presence of diabetes or hypertension, and other coronary risk factors. Information on regional and global LV function can similarly be important for the interpretation of regional perfusion and metabolism patterns.

A description of the ECG findings may serve as an aid in the study interpretation, such as the presence of Q waves and their location or conduction abnormalities (e.g., LBBB) for exploring septal perfusion and/or metabolic abnormalities.

Type of Study

The imaging protocols should be stated concisely. This should include the type of camera utilized for imaging myocardial perfusion and/or metabolism, for example, PET or PET/CT system, or SPECT perfusion and FDG PET metabolism. For stress myocardial perfusion PET studies, the type of stressor should be clearly indicated, such as treadmill, dipyridamole, adenosine, A2A adenosine receptor agonist, or dobutamine. Radiopharmaceuticals and their radioactivity doses used for the perfusion and the metabolism PET imaging studies should be identified. The acquisition modes and image sequences should be described, such as static or dynamic image acquisition, for stress and rest perfusion imaging, perfusion and metabolism imaging on different days, and the use of gating.

The main body of the report following this introductory descriptive information should then be tailored to the specific clinical question asked by the referring clinician and the procedural approach chosen for answering this question. For example, the report for a stress-rest myocardial PET perfusion study will be different from a report describing and interpreting a myocardial perfusion and myocardial metabolism study. Similarly, the report for a study that includes a stress and rest myocardial perfusion study along with a myocardial metabolism study should be different.

Summary of Stress Data

If myocardial perfusion has been evaluated during stress, the type of the stressor, the stress agent, the dose, route of administration, and time of infusion should be specified. Side effects and symptoms experienced during stress should be reported. If pharmacologic stress was discontinued prematurely, the reasons should be provided.

Hemodynamic and ECG responses during the stress study, including changes in heart rate, blood pressure, development of arrhythmias, conduction abnormalities, and ST-T wave changes and their location should be detailed. Symptoms such as chest pain, shortness of breath, and others during the administration of the stressor and in the recovery phase should be documented.

Summary of Clinical Laboratory Data and Dietary State

Information about the dietary state (e.g., fasting or post-prandial) and about interventions for manipulating plasma glucose levels through, for example, oral or IV administration of glucose or use of the euglycemic hyperinsulinemic clamp, should be given. If pharmacologic measures, such as nicotinic acid derivatives, have been used, this should be described. Furthermore, BG levels, if obtained at baseline or after intervention, should be listed, as they are useful for the interpretation of the metabolic images. If there is an expected abnormal response to a glucose load, this should also be reported.

Image Description and Interpretation: Perfusion

A statement regarding image quality is important. Reduced quality may affect the accuracy of the interpretation. If the cause of the reduced quality is known or suspected, then it should be stated accordingly. This information may prove useful when repeat images are obtained in the same patient.

The report should first describe the relative distribution of the perfusion tracer on the stress images and provide details on regions with decreased radiotracer uptake in terms of the location, extent, and severity of defects. The authors should then describe whether regional myocardial defects seen on stress images become reversible or persist on the corresponding paired rest images. Other findings, such as LV cavity dilatation at rest, transient (stress-induced) LV cavity dilation, lung uptake, concentric LV hypertrophy, asymmetric septal hypertrophy, pericardial photopenia, prominent RV cavity size and hypertrophy, and extra-cardiac abnormalities, should be included in the report. Regional and global LV function should be described from gated PET perfusion and/or metabolism images. The scintigraphic pattern on the stress/rest myocardial perfusion images should then be reported in clinical terms as:

1. Normal.
2. Ischemic.

3. Scarred with/without a history of prior myocardial infarction.
4. An admixture of scarred and ischemic but viable myocardium.
5. Non-ischemic cardiomyopathy.

Quantitative assessment of absolute regional myocardial blood flow is limited to only a few centers with extensive local expertise. Thus, reporting of myocardial blood flow in absolute terms should be made with caution, since FDA approved software for general clinical use is not available at the present time.

Image Description and Interpretation: Metabolism

The report should describe the relative distribution of myocardial perfusion at rest, and the location, extent, and severity of regional perfusion defects. The report should continue with a description of the FDG uptake in the myocardium and indicate the tracer activity concentrations in normally perfused and in hypoperfused myocardium. The adequacy of achieving a glucose-loaded state, as evident from the radiotracer uptake in normally perfused myocardium and also from blood pool activity, should then be reported and be related to the presence of insulin resistance, including impaired glucose tolerance and Type 2 diabetes. This should be related to the residual blood pool activity as additional evidence for inadequate clearance of FDG from blood into tissue and provide the information for low tracer uptake in normally perfused myocardium. Segments with regional dysfunction that exhibit patterns of viable myocardium (i.e., preserved perfusion or decreased perfusion with either preserved or increased FDG uptake) should be identified. Similar reporting should be performed for segments exhibiting a flow-metabolism matched pattern, that is, decreased regional FDG uptake in proportion to decreased regional myocardial perfusion. The presence of viable and non-viable tissue should be reported as a continuum (e.g., predominantly viable or admixture of viable and non-viable tissue).

Findings on semiquantitative or quantitative image analysis approaches may be added. Location and, in particular, extent of viable and non-viable tissue, expressed as a percentage of the LV, is important because it provides important prognostic information on future cardiac events and predictive information on potential outcomes in regional and global LV function, congestive heart failure-related symptoms, and long-term survival after revascularization. Finally, the description of the perfusion-metabolism findings may include a correlation to regional wall motion abnormalities and should indicate the potential for a post-revascularization improvement in the regional and global LV function. The potential for outcome benefit may also be reported.

Final Interpretation

Results should be succinctly summarized and first address whether the study is normal or abnormal. On rare occasions where a definitive conclusion cannot be made, the interpreter should aid the referring clinician by suggesting other tests that may provide further insight into the clinical dilemma. The report should always take into consideration the clinical question that is being asked: is the study requested for CAD detection or myocardial viability assessment? Any potential confounding artifacts or other quality concerns that significantly impact the clinical interpretation of the PET study should be mentioned.

A statement on the extent and severity of perfusion defects, reversibility and mismatch in relation to FDG metabolism, and their implication regarding ischemia, scar, or hibernating myocardium should be made. It may be useful to conclude the report with a summary of the extent and location of myocardial ischemia in relation to vascular territories, as well as the presence and extent of perfusion-metabolism mismatch in patients with chronic ischemic LV dysfunction. LV cavity size, function, and regional wall motion should be reported at rest and during stress with special note of transient ischemic cavity dilatation, if present. A statement as to the implication of the findings should be made.

Comparison should be made to prior studies, and interim changes regarding the presence and extent of myocardial ischemia, scar, or hibernation should be highlighted. On the basis of the scintigraphic findings (e.g., extent of perfusion-metabolism mismatch), the likelihood of recovery of function after revascularization can be estimated. The potential for a post-revascularization improvement in contractile function is low for perfusion-metabolism matched defects, even if the regional reductions in perfusion and in FDG uptake are only mild or moderate. Conversely, the potential for improvements in regional contractile dysfunction is high if perfusion is normal, if both perfusion and FDG uptake are normal, or if FDG uptake is significantly greater than regional perfusion (i.e., mismatch). Finally, the potential of a post-revascularization improvement in the LVEF by at least 5 or more EF units is high if the mismatch affects 20% or more of the LV myocardium.[83,85] Although lesser amounts of mismatch (5-20% of the LV myocardium) may also have potential outcome benefit, with or without improvement in the LVEF.[86,87] The latter may be included in the report at the reporting physician's discretion.

If additional diagnostic clarification seems needed, the physician may recommend an alternative modality. If a CT transmission scan was performed for attenuation correction, clinically relevant CT findings must be reported.

Acknowledgments

Dominique Delbeke, MD, PhD is a consultant for GE Healthcare and Spectrum Dynamics. Stephen L. Bacharach, PhD receives grant support from Siemens Medical Solutions and Philips Healthcare.

Publication and distribution of this document are made possible by corporate support from Bracco Diagnostics Inc.

APPENDIX 1. SAMPLE IV PROTOCOL: PROTOCOL A

A sample protocol for IV glucose loading is presented. This protocol is based on one in use at Vanderbilt University Medical Center, Nashville, TN, and is adapted from Martin et al[48]

1. IV glucose/insulin loading for nondiabetic patients with a BG level <110 mg/dL (<6.11 mmol/L) under fasting condition.
   a. Prepare dextrose/insulin solution: 15 U of regular insulin in 500 mL of 20% dextrose in a glass bottle. The initial 50 mL is discarded through the plastic IV tubing (no filter) to decrease adsorption of the insulin to the tubing.
   b. Prime the patient with 5 U of regular insulin and 50 mL of 20% dextrose (10 g) IV bolus.
   c. Infuse dextrose/insulin solution at a rate of 3 mL · kg^{-1} · h^{-1} for 60 minutes (corresponding to an insulin infusion of 1.5 mU · kg^{-1} · min^{-1} and a glucose infusion of 10 mg · kg^{-1} · min^{-1}). Monitor BG every 10 minutes (goal BG, 100-200 mg/dL [5.56-11.11 mmol/L]).
   d. If BG at 20 min is 100-200 mg/dL (5.56-11.11 mmol/L), preferably <150 mg/dL (8.33 mmol/L), administer FDG intravenously.
   e. If BG is >200 mg/dL (>11.11 mmol/L), administer small IV boluses of 4-8 U of regular insulin until BG decreases to <200 mg/dL (<11.11 mmol/L). Administer FDG intravenously.
   f. Stop dextrose/insulin infusion at 60 minutes and start 20% dextrose at 2-3 mL · kg^{-1} · h^{-1}.
   g. During image acquisition, continue infusion of 20% dextrose at 2-3 mL · kg^{-1} · h^{-1}.
   h. At completion of the acquisition of the images, discontinue infusion, give a snack to the patient, and advise him or her regarding the risk of late hypoglycemia.
   i. ALERT: (1) If BG is >400 mg/dL (>22.22 mmol/L), call the supervising physician immediately. (2) If BG is <55 mg/dL (<3.06 mmol/L) or if the patient develops symptoms of hypoglycemia with BG < 75 mg/dL (<4.17 mmol/L), discontinue dextrose/insulin infusion, administer one amp of 50% dextrose intravenously, and call the supervising physician.
2. IV glucose/insulin loading for diabetic patients or fasting BG is >110 mg/dL (>6.11 mmol/L):
   a. Prepare insulin solution: 100 U of regular insulin in 500 mL of normal saline solution in a glass bottle. The initial 50 mL is discarded through the plastic IV tubing (no filter) to decrease adsorption of the insulin to the tubing.
   b. Prime patient with regular insulin: If fasting BG is >140 mg/dL (>7.76 mmol/L), prime the patient with 10 U of regular insulin IV bolus. If fasting BG is <140 mg/dL (<7.76 mmol/L), prime the patient with 6 U of regular insulin IV bolus.
   c. Infuse insulin solution at a rate of 1.2 mL · kg^{-1} · h^{-1} for 60 minutes (corresponding to an insulin infusion of 4 mU · kg^{-1} · min^{-1}) or for the entire study (to calculate the regional glucose utilization rate).
   d. After 8-10 minutes or when BG is <140 mg/dL (<7.76 mmol/L), start 20% dextrose infusion at 1.8 mL · kg^{-1} · h^{-1} (corresponding to a dextrose infusion of 6 mg · kg^{-1} · min^{-1}).
   e. Monitor BG every 5-10 minutes and adjust dextrose infusion rate to maintain BG at 80-140 mg/dL (4.44-7.76 mmol/L).
   f. After 20-30 minutes of stable BG, administer FDG.
   g. Maintain the IV infusion of insulin plus 20% dextrose for 30-40 minutes after FDG injection or until the end of the scan (to calculate rMGU [rate of glucose utilization]). Some centers confirm FDG uptake particularly in patients with diabetes before discontinuing the clamp.
   h. At completion of the acquisition of the images, discontinue infusion, give a snack to the patient, and advise him or her regarding the risk of late hypoglycemia.
3. For lean patients with type 1 juvenile-onset diabetes mellitus, apply the following protocol:
   1. If fasting BG is <140 mg/dL (<7.76 mmol/L), inject 4 U of regular insulin and infuse insulin solution at 0.3 mL · kg^{-1} · h^{-1} (1 mU · kg^{-1} ·min^{-1}).
   2. After 8-10 minutes of infusion or when BG is <140 mg/dL (<7.76 mmol/L), start 20% dextrose at 2.4 mL · kg^{-1} · h^{-1} (8 mg · kg^{-1} · min^{-1}).

4. Some centers (Munich, Ottawa, and others) have also applied a front-loaded infusion.

    1. About 6 hours after a light breakfast and their usual dose of insulin or oral hypoglycemic, all diabetic patients have a catheter inserted in one arm for glucose and insulin infusion, as well as a catheter in the opposite arm for BG measurement.
    2. At time 0, the insulin infusion is started. Regular insulin is given at 4 times the final constant rate[88] for 4 minutes, then at 2 times the final constant rate for 3 minutes, then at a constant rate for the remainder of the study.
    3. If the BG is >200 mg/dL (>11.11 mmol/L), an additional bolus of insulin is given. An exogenous 20% glucose infusion is started at an initial rate of 0.25 mg $\cdot$ kg^{-1} $\cdot$ min^{-1} and adjusted until steady state is achieved. The BG concentrations are measured every 5 minutes during the insulin clamp. The glucose infusion is adjusted according to the plasma glucose over the preceding 5 minutes.

APPENDIX 2. SAMPLE IV PROTOCOL: PROTOCOL B

A sample protocol for IV glucose loading is presented. Protocol B is based on the protocol in use at the Emory University-Crawford Long Memorial Hospital (Atlanta, GA).[89] This protocol has been used in over 600 subjects (over one-third of whom were diabetic), resulting in good-quality images in over 98% of studies.

1. If fasting BG is <125 mg/dL (<6.94 mmol/L), give 50% dextrose in water (D-50-W), 25 g, intravenously. Hydrocortisone, 20 mg, should be added to the D-50-W to minimize the rather severe pain that can occur at the injection site with D-50-W. This is compatible and avoids the pain that limits patient cooperation. There is no negative effect on the quality of the FDG studies.
2. If fasting BG is between 125-225 mg/dL (6.94-12.5 mmol/L), give D-50-W, 13 g, intravenously.
3. If fasting BG is >225 mg/dL (>12.5 mmol/L), administer regular aqueous insulin as per the following formula: Regular aqueous insulin (dose units) = (BG − 50)/25.
4. After 30-60 minutes, if BG is less than 150 mg/dL (8.33 mmol/L), give FDG intravenously, but if BG is >150 mg/dL (>8.33 mmol/L), give more regular insulin, until BG is <150 mg/dL (<8.33 mmol/L), before giving FDG. Giving FDG when BG is 150-200 mg/dL (8.33-11.11 mmol/L) resulted in many poor-quality studies.

References

1. Zanzonico P. Positron emission tomography: A review of basic principles, scanner design and performance, and current systems. Semin Nucl Med 2004;34:87-111.
2. Machac J, Bacharach SL, Bateman TM, et al. Imaging guidelines for nuclear cardiology procedures: Positron emission tomography myocardial perfusion and glucose metabolism imaging. J Nucl Cardiol 2006;13:e121-51.
3. National Electrical Manufacturers Association. NEMA standards publication NU 2-1994: Performance measurements of positron emission tomographs. Washington, DC: National Electrical Manufacturers Association; 1994.
4. National Electrical Manufacturers Association. NEMA standards publication NU 2-2001: Performance measurements of positron emission tomographs. Washington, DC: National Electrical Manufacturers Association; 2001.
5. National Electrical Manufacturers Association. NEMA standards publication NU 2–2007: Performance measurements of positron emission tomographs. Rosslyn, VA: National Electrical Manufacturers Association; 2007.
6. deKemp RA, Yoshinaga K, Beanlands RS. Will 3D PET enable routine quantification of myocardial blood flow? J Nucl Cardiol 2007;14:380-97.
7. Ter-Pogossian MM, Ficke DC, Yamamoto M. PET I: A positron emission tomograph utilizing photon time-of-flight information. IEEE Trans Med Imaging 1982;1:179-87.
8. Yamamoto M, Ficke DC, Ter-Pogossian MM. Experimental assessment of the gain achieved by the utilization of time-of-flight information in a positron emission tomograph (Super PETT I). IEEE Trans Med Imaging 1982;1:187-92.
9. Lewellan TK. Time-of-flight PET. Semin Nucl Med 1998;28:268-75.
10. Le Meunier L, Maass-Moreno R, Carrasquillo JA, Dieckmann W, Bacharach SL. PET/CT imaging: Effect of respiratory motion on apparent myocardial uptake. J Nucl Cardiol 2006;13:821-30.
11. International Electrotechnical Commission. Radionuclide imaging devices–characteristics and test conditions. Part 1: Positron emission tomographs. Geneva; 1998.
12. American College of Radiology. ACR Web site. http://www.acr.org. Accessed 2 March 2009.
13. American Association of Physicists in Medicine. AAPM Web site. http://www.aapm.org. Accessed 2 March 2009.
14. Sampson UK, Dorbala S, Limaye A, et al. Diagnostic accuracy of rubidium-82 myocardial perfusion imaging with hybrid positron emission tomography/computed tomography in the detection of coronary artery disease. J Am Coll Cardiol 2007;49:1052-8.
15. Slomka PJ, LeMunier L, Hayes SW. Comparison of myocardial perfusion Rb-82 PET performed with CT- and transmission CT-based attenuation correction. J Nucl Med 2008;49:1992-8.
16. Gould KL, Pan T, Loughin C, Johnson NP, Guha A, Sdringola S. Frequent diagnostic errors in cardiac PET/CT due to misregistration of CT attenuation and emission PET images: A definitive analysis of causes, consequences and corrections. J Nucl Med 2007;48:1112-21.
17. Loghin C, Sdringola S, Gould K. Common artifacts in PET myocardial perfusion images due to attenuation-emission misregistration: Clinical significance, causes, and solution. J Nucl Med 2004;45:1029-39.
18. Alessio AM, Kohlmyer S, Branch K, et al. Cine CT for attenuation correction in cardiac PET/CT. J Nucl Med 2007;48:794-801.
19. Souvatzoglou M, Bengel F, Busch R, et al. Attenuation correction in cardiac PET/CT with three different CT protocols: A

comparison with conventional PET. Eur J Nucl Med Mol Imaging 2007;34:1991-2000.
20. DiFilippo FP, Brunken RC. Do implanted pacemaker leads and ICD leads cause metal-related artifact in cardiac PET/CT? J Nucl Med 2005;46:436-43.
21. Greenland P, Bonow RO, Brundage BH, et al. ACCF/AHA 2007 clinical expert consensus document on coronary artery calcium scoring by computed tomography in global cardiovascular risk assessment and in evaluation of patients with chest pain: A report of the American College of Cardiology Foundation Clinical Expert Consensus Task Force. J Am Coll Cardiol 2007;49:378-402.
22. Hamill JJ, Brunken RC, Bybel B, DiFilippo FP, Faul DD. A knowledge-based method for reducing attenuation artifacts caused by cardiac appliances in myocardial PET/CT. Phys Med Biol 2006;51:2901-18.
23. Henzlova MJ, Cerqueira MD, Hansen CL, Taillefer R, Yao S. Imaging guidelines for nuclear cardiology procedures: Stress protocols and tracers. J Nucl Cardiol 2009;16. doi: 10.1007/s12350-009-9062-4.
24. Beanlands RS, Chow BJW, Dick A, et al. CCS/CAR/CANM/CNCS/CanSCMR joint position statement on advanced noninvasive cardiac imaging using positron emission tomography, magnetic resonance imaging n multi-detector computed tomographic angiography in the diagnosis and evaluation of ischemic heart disease—executive summary. Can J Cardiol 2007;23:107-19.
25. Bateman TM, Friedman JD, Heller GV, et al. Diagnostic accuracy of rest/stress ECG-gated Rb-82 myocardial perfusion PET: Comparison with ECG-gated Tc-99m sestamibi SPECT. J Nucl Cardiol 2006;13:24-33.
26. Love WD, Burch GE. Influence of the rate of coronary plasma on the extraction of rubidium-86 from coronary blood. Circ Res 1959;7:24-30.
27. Selwyn AP, Allan RM, L'Abbate A, et al. Relation between regional myocardial uptake of rubidium-82 and perfusion: Absolute reduction of cation uptake in ischemia. Am J Cardiol 1982;50:112-21.
28. Goldstein RA, Mullani NA, Marani SK, et al. Myocardial perfusion with rubidium-82. II. Effects of metabolic and pharmacologic interventions. J Nucl Med 1983;24:907-15.
29. Stabin MG. Radiopharmaceuticals for nuclear cardiology: Radiation dosimetry, uncertainities and risk. J Nucl Med. 2008;49:1555–63.
30. Camici PG, Araujo LI, Spinks T, et al. Increased uptake of 18F-fluorodeoxyglucose in postischemic myocardium of patients with exercise-induced angina. Circulation 1986;74:81-8.
31. Chow BJW, Ananthasubramaniam K, deKemp RA, et al. Comparison of treadmill exercise versus dipyridamole stress with myocardial perfusion imaging using rubidium-82 positron emission tomography. J Am Coll Cardiol 2005;45:1227-34.
32. Hutchins GD, Schwaiger M, Rosenspire KC, et al. Noninvasive quantification of regional blood flow in the human heart using N-13 ammonia and dynamic positron emission tomographic imaging. J Am Coll Cardiol 1990;15:1032-42.
33. Krivokapich J, Smith GT, Huang SC, et al. 13 N ammonia myocardial imaging at rest and with exercise in normal volunteers. Quantification of absolute myocardial perfusion with dynamic positron emission tomography. Circulation 1989;80:1328-37.
34. Bergmann SR, Hack S, Tewson T, Welch MJ, Sobel BE. The dependence of accumulation of N-13 ammonia by myocardium on metabolic factors and its implications for quantitative assessment of perfusion. Circulation 1980;61:34-43.
35. Krivokapich J, Huang S-C, Phelps ME, MacDonald NS, Shine KI. Dependence of N-13 ammonia myocardial extraction and clearance on flow and metabolism. Am J Physiol: Heart Circ Physiol 1982;242:H536-42.
36. Kitsiou AN, Bacharach SL, Bartlett ML, et al. 13 N ammonia myocardial blood flow and uptake: Relation to functional outcome of asynergic regions after revascularization. J Am Coll Cardiol 1999;33:678-86.
37. Schelbert HR, Phelps ME, Huang SC, et al. N-13 ammonia as an indicator of myocardial blood flow. Circulation 1981;63:1259-72.
38. International Commission on Radiological Protection. Radiation dose to patients from radiopharmaceuticals. ICRP Publication 80. Ann ICRP 2000;28:113.
39. International Commission on Radiological Protection. Radiation dose to patients from radiopharmaceuticals. ICRP Publication 53. Ann ICRP 1988;18:62.
40. Neely JR, Rovetto MJ, Oram JF. Myocardial utilization of carbohydrate and lipids. Prog Cardiovasc Dis 1972;15:289-329.
41. Gallagher BM, Ansari A, Atkins H, et al. Radiopharmaceuticals XXVII. F-18-labeled 2-deoxy-2-fluoro-D-glucose as a radiopharmaceutical for measuring regional myocardial glucose metabolism in vivo: Tissue distribution and imaging studies in animals. J Nucl Med 1977;18:990-6.
42. Ratib O, Phelps ME, Huang SC, et al. Positron tomography with deoxyglucose for estimating local myocardial glucose metabolism. J Nucl Med 1982;23:577-86.
43. Hamacher K, Coenen HH, Stauocklin G. Efficient sterospecific synthesis of no-carrier-added 2-[F-18]-fluoro-2-deoxy-D-glucose using aminopolyether supported nucleophilic substitution. J Nucl Med 1986;27:235-8.
44. CDE Inc. Dosimetry Services. Dose estimates: Adult. http://www.internaldosimetry.com/freedosestimates/adult/index.html. Published 2001. Accessed 15 January 2009.
45. Ohtake T, Yokoyama I, Watanabe T, et al. Myocardial glucose-metabolism in noninsulin-dependent diabetes-mellitus patients evaluated by FDG-PET. J Nucl Med 1995;36:456-63.
46. Vitale GD, deKemp RA, Ruddy TD, Williams K, Beanlands RS. Myocardial glucose utilization and optimization of (18)F-FDG PET imaging in patients with non-insulin-dependent diabetes mellitus, coronary artery disease, and left ventricular dysfunction. J Nucl Med 2001;42:1730-6.
47. Knuuti MJ, Nuutila P, Ruotsalainen U, et al. Euglycemic hyperinsulinemic clamp and oral glucose load in stimulating myocardial glucose utilization during positron emission tomography. J Nucl Med 1992;33:1255-62.
48. Martin WH, Jones RC, Delbeke D, Sandler MP. A simplified intravenous glucose loading protocol for fluorine-18 fluorodeoxyglucose cardiac single-photon emission tomography. Eur J Nucl Med 1997;24:1291-7.
49. Gropler RJ, Siegel BA, Lee KJ, et al. Nonuniformity in myocardial accumulation of fluorine-18-fluorodeoxyglucose in normal fasted humans. J Nucl Med 1990;31:1749-56.
50. Bax JJ, Veening MA, Visser FC, et al. Optimal metabolic conditions during fluorine-18 fluorodeoxyglucose imaging; a comparative study using different protocols. Eur J Nucl Med 1997;24:35-41.
51. Cerqueira MD, Weissman NJ, Dilsizian V, et al. Standardized myocardial segmentation and nomenclature for tomographic imaging of the heart: A statement for healthcare professionals from the Cardiac Imaging Committee of the Council on Clinical Cardiology of the American Heart Association. J Nucl Cardiol 2002;9:240-5.
52. Porenta G, Kuhle W, Czernin J, et al. Semiquantitative assessment of myocardial blood flow and viability using polar map displays of cardiac PET images. J Nucl Med 1992;33:1628-36.

53. Nekolla SG, Miethaner C, Nguyen N, Ziegler SI, Schwaiger M. Reproducibility of polar map generation and assessment of defect severity and extent assessment in myocardial perfusion imaging using positron emission tomography. Eur J Nucl Med 1998;25: 1313-21.
54. Dou K, Yang M, Yang Y, Jain D, He Z. Myocardial 18F-FDG uptake after exercise-induced myocardial ischemia in patients with coronary artery disease. J Nucl Med 2008;49:1986-91.
55. Dilsizian V. SPECT and PET myocardial perfusion imaging: Tracers and techniques. In Dilsizian V, Narula J, editors. Atlas of Nuclear Cardiology, edition 3. Barunwald E (series editor), Philadelphia, Current Medicine, Inc. - Springer; 2009, p. 37-60.
56. McCord ME, Bacharach SL, Bonow RO, et al. Misalignment between PET transmission and emission scans: Its effect on myocardial imaging. J Nucl Med 1992;33:1209-14.
57. Bergmann SR, Fox KAA, Rand AL, et al. Quantification of regional myocardial blood flow in vivo with O-15 water. Circulation 1984;70:724-33.
58. Bergmann SR, Herrero P, Markham J, Weinheimer CJ, Walsh MN. Noninvasive quantitation of myocardial blood flow in human subjects with oxygen-15-labeled water and positron emission tomography. J Am Coll Cardiol 1989;14:639-52.
59. Iida H, Kanno I, Takahashi A, et al. Measurement of absolute myocardial blood flow with O-15 water and dynamic positron emission tomography. Circulation 1988;78:104-15.
60. Lortie M, Beanlands RS, Yoshinaga K, et al. Quantification of myocardial blood flow with 82Rb dynamic PET imaging. Eur J Nucl Med Mol Imaging 2007;34:1765-74.
61. Lin JW, Sciacca RR, Chou RL, Laine AF, Bergmann SR. Quantification of myocardial perfusion in human subjects using 82Rb and wavelet-based noise reduction. J Nucl Med 2001;42:201-8.
62. Herrero P, Markham J, Shelton ME, Weinheimer CJ, Bergmann SR. Noninvasive quantification of regional myocardial perfusion with rubidium-82 and positron emission tomography exploration of a mathematical model. Circulation 1990;82:1377-86.
63. Herrero P, Markham J, Shelton ME, Bergmann SR. Implementation and evaluation of a two-compartment model for quantification of myocardial perfusion with rubidium-82 and positron emission tomography. Circ Res 1992;70:496-507.
64. El Fakhri G, Sitek A, Guerin B, et al. Quantitative dynamic cardiac 82 Rb PET using generalized factor and compartment analyses. J Nucl Med 2005;46:1264–71.
65. El Fakhri G, Sitek A, Abi-Hatem N, et al (2009) Reproducibility and accuracy of quantitative myocardial blood flow: A PET study comparing 82 Rubidium and 13 N-Ammonia. J Nucl Med. in press
66. Coxson PG, Huesman RH, Borland L. Consequences of using a simplified kinetic model for dynamic PET data. J Nucl Med 1997;38:660-7.
67. Yoshida K, Mullani N, Gould KL. Coronary flow and flow reserve by PET simplified for clinical applications using rubidium-82 or nitrogen-13 ammonia. J Nucl Med 1996;37:1701-12.
68. Lertsburapa K, Ahlberg A, Bateman T, et al. Independent and incremental prognostic value of left ventricle ejection fraction determined by stress gated rubidium 82 PET imaging in patients with known or suspected coronary artery disease. J Nucl Cardiol 2008;15:745-53.
69. Dorbala S, Vangala D, Sampson U, et al. Value of vasodilator left ventricular ejection fraction reserve in evaluating the magnitude of myocardium at risk and the extent of angiographic coronary artery disease: A 82Rb PET/CT study. J Nucl Med. 2007;48:349–58.
70. Dorbala S, Hachamovitch R, Curillova Z, et al (2009) Incremental prognostic value of gated Rb-82 positron emission tomography over clinical variables and rest LVEF. J Am Coll Cardiol Img 2009 2:846-854.
71. Heller GV, Links J, Bateman TM, et al. American Society of Nuclear Cardiology and Society of Nuclear Medicine joint position statement: Attenuation correction of myocardial perfusion SPECT scintiography. J Nucl Cardiol 2004;11:229-30.
72. Malkerneker D, Brenner R, Martin WH, et al. CT-based attenuation correction versus prone imaging to decrease equivocal interpretations of rest/stress 99mTc-tetrafosmin SPECT MPI. J Nucl Cardiol 2007;14:314-23.
73. Sandler MP, Videlefsky S, Delbeke D, et al. Evaluation of myocardial ischemia using a rest metabolism/stress perfusion protocol with fluorine-18-fluorodeoxyglucose/technitium-99m-MIBI and dual-isotope simultaneous-acquisition single-photon emission computed tomography. J Am Coll Cardiol 1995;26:870-6.
74. Bax JJ, Visser FC, Blanksma PK, et al. Comparison of myocardial uptake of fluorine-18-fluorodeoxyglucose imaged with PET and SPECT in dyssynergic myocardium. J Nucl Med 1996;37:1631-6.
75. Dilsizian V, Bacharach SL, Muang KM, Smith MF. Fluorine-18-deoxyglucose SPECT and coincidence imaging for myocardial viability: Clinical and technological issues. J Nucl Cardiol 2001;8:75-88.
76. Choi Y, Brunken RC, Hawkins RA, et al. Factors affecting myocardial 2-[F-18] fluoro-2-deoxy-D-glucose uptake in positron emission tomography studies of normal humans. Eur J Nucl Med 1993;20:308-18.
77. Choi Y, Hawkins RA, Huang SC, et al. Parametric images of myocardial metabolic rate of glucose generated from dynamic cardiac PET and 2-[18F]fluoro-2-deoxy-D-glucose studies. J Nucl Med 1991;32:733-8.
78. Marshall RC, Tillisch JH, Phelps ME, et al. Identification and differentiation of resting myocardial ischemia and infarction in man with positron emission tomography, F-18 labeled fluorodeoxyglucose and N-13 ammonia. Circulation 1983;67:766-8.
79. Tillisch J, Brunken RC, Marshall R, et al. Reversibility of cardiac wall-motion abnormalities predicted by positron tomography. N Engl J Med 1986;314:884-8.
80. Schwartz E, Schaper J, vom Dahl J, et al. Myocardial hibernation is not sufficient to prevent morphological disarrangements with ischemic cell alterations and increased fibrosis. Circulation 1994;90:I-378.
81. vom Dahl J, Altehoefer C, Sheehan F, et al. Recovery of regional left ventricular dysfunction after coronary revascularization: Impact of myocardial viability assessed by nuclear imaging and vessel patency at follow-up angiography. J Am Coll Cardiol 1996;28:948-58.
82. Beanlands RS, Hendry PJ, Masters RG, et al. Delay in revascularization is associated with increased mortality rate in patients with severe left ventricular dysfunction and viable myocardium on fluorine 18-fluorodeoxyglucose positron emission tomography imaging. Circulation 1998;98:II51-6.
83. Gerber BL, Ordoubadi FF, Wijns W, et al. Positron emission tomography using (18)F-fluoro-deoxyglucose and euglycaemic hyperinsulinaemic glucose clamp: Optimal criteria for the prediction of recovery of post-ischaemic left ventricular dysfunction. Results from the European Community Concerted Action Multicenter study on the use of (18)F-fluoro-deoxyglucose positron emission tomography for the detection of myocardial viability. Eur Heart J 2001;22:1691-701.
84. Bonow RO, Dilsizian V, Cuocolo A, Bacharach SL. Identification of viable myocardium in patients with coronary artery disease and left ventricular dysfunction: Comparison of thallium scintigraphy with reinjection and PET imaging with 18F-fluorodeoxyglucose. Circulation 1991;83:26-37.
85. Pagano D, Townend JN, Littler WA, et al. Coronary artery bypass surgery as treatment for ischemic heart failure: The predictive

value of viability assessment with quantitative positron emission tomography for symptomatic and functional outcome. J Thorac Cardiovasc Surg 1998;115:791-9.
86. Di Carli MF, Davidson M, Little R, et al. Value of metabolic imaging with positron emission tomography for evaluating prognosis in patients with coronary artery disease and left ventricular dysfunction. Am J Cardiol 1994;73:527-33.
87. Beanlands RS, Nichol G, Huszti E, et al. F-18-fluorodeoxyglucose positron emission tomography imaging-assisted management of patients with severe left ventricular dysfunction and suspected coronary artery disease: A randomized, controlled trial (PARR-2). J Am Coll Cardiol 2007;50:2002-12.
88. DeFronzo RA, Tobin JD, Andres R. Glucose clamping technique: A method for quantifying insulin secretion and resistance. Am J Physiol 1979;237:E214-23.
89. Streeter J, Churchwell K, Sigman S, et al. Clinical glucose loading protocol for F-18 FDG myocardial viability imaging [abstract]. Mol Imaging Biol 2002;4:192.

ASNC IMAGING GUIDELINES FOR NUCLEAR CARDIOLOGY PROCEDURES

PET myocardial perfusion and metabolism clinical imaging

Vasken Dilsizian, MD,[a] Stephen L. Bacharach, PhD,[b] Robert S. Beanlands, MD,[c] Steven R. Bergmann, MD, PhD,[d] Dominique Delbeke, MD,[e] Robert J. Gropler, MD,[f] Juhani Knuuti, MD, PhD,[g] Heinrich R. Schelbert, MD, PhD,[h] and Mark I. Travin, MD[i]

INTRODUCTION

Positron emission tomography (PET) utilizes radionuclide tracer techniques that produce images of in vivo radionuclide distribution using measurements made with an external detector system. Similar to computed tomography (CT), the images acquired with PET represent cross-sectional slices through the heart. However, with PET, the image intensity reflects organ function as opposed to anatomy. The functional information that is illustrated in PET images depends upon the radiopharmaceutical employed for that particular study. PET allows noninvasive evaluation of myocardial blood flow, function, and metabolism, using physiological substrates prepared with positron-emitting radionuclies, such as carbon, oxygen, nitrogen, and fluorine. These radionuclides have half-lives that are considerably shorter than those used in single photon emission CT (SPECT). Positron emitting radionuclides are produced using a cyclotron, such as fluoro-2-deoxyglucose (F-18 FDG) with a 110 minute half-life or a generator such as rubidium-82 (Rb-82) with a 75 second half-life.

PET radionuclides reach a more stable configuration by the emission of a positron. Positrons are positively charged particles with the same rest mass as electrons. When a positron collides with an electron, two 511 keV gamma rays are emitted. These emitted photons are nearly collinear, travelling in opposite directions, almost exactly 180° apart.[1]

The PET detectors are configured to register only photon pairs that strike opposing detectors at approximately the same time, termed coincidence detection. Over the course of a typical scan, millions of coincidence events are recorded and projections of the activity distribution are measured at all angles around the patient. These projections are subsequently used to reconstruct an image of the in vivo radionuclide distribution using the same algorithms as those used in x-ray CT. The resulting PET images have improved spatial and temporal resolution when compared to SPECT.

Recent advances in the instrumentation of multichannel spiral CT allow detailed visualization of the coronary arteries, noninvasively, as an adjunct to PET imaging. Whereas multichannel CT angiography provides information on the presence and extent of anatomical luminal narrowing of epicardial coronary arteries, stress myocardial perfusion PET provides information on the downstream functional consequences of such anatomic lesions. Thus, with hybrid PET/CT systems, such complementary information of anatomy and physiology can be obtained during the same imaging session. The ability to determine coronary artery disease, myocardial perfusion, viability, and ventricular function from a hybrid PET/CT system has the potential to be an important tool in the clinical practice of cardiology.

The current document is an update of an earlier version of PET guidelines that was developed by the American Society of Nuclear Cardiology.[2] The publication is designed to provide imaging guidelines for physicians and technologists who are qualified to practice nuclear cardiology. While the information supplied in this document has been carefully reviewed by experts in the field, the document should not be considered

From the University of Maryland Medical Center,[a] Baltimore, MD; UCSF,[b] San Francisco, CA; University of Ottawa Heart Institute,[c] Ottawa, Ontario, Canada; Beth Israel Medical Center,[d] New York, NY; Vanderbilt University Medical Center,[e] Nashville, TN; Washington University,[f] St. Louis, MO; Turku University Hospital,[g] Turku, Finland; UCLA School of Medicine,[h] Los Angeles, CA; Montefiore Medical Center,[i] Pleasantville, NY.

Unless reaffirmed, retired or amended by express action of the Board of Directors of the American Society of Nuclear Cardiology, this Imaging Guideline shall expire as of May 2014.

Reprint requests: Vasken Dilsizian, MD, University of Maryland Medical Center, Baltimore, MD.

1071-3581/$34.00

doi:10.1007/s12350-009-9094-9

medical advice or a professional service. We are cognizant that PET and PET/CT technology is evolving rapidly and that these recommendations may need further revision in the near future. Hence, the imaging guidelines described in this publication should not be used in clinical studies until they have been reviewed and approved by qualified physicians and technologists from their own particular institutions.

PET AND PET/CT INSTRUMENTATION

PET Imaging Systems (2D and 3D)

The majority of dedicated PET cameras consist of rings of small detectors that are typically a few millimeters on a side, and tens of millimeters deep. Coincidences between detectors in a single ring produce one tomographic slice of data. Usually one or more adjacent rings may also contribute to counts in that slice. In a 2-dimensional (2D) or ''septa-in'' PET scanner, there is a septum (e.g., lead or tungsten) between adjacent rings. This septum partially shields coincidences from occurring between detectors in one ring and detectors in a non-adjacent or more distant ring. By minimizing coincidences between a ring and its more distant neighboring rings, the septa greatly reduce scattered events.

A scanner with no septa in place is referred to as a three-dimensional (3D) or ''septa-out'' scanner. This permits coincidences between all possible pairs of detectors, greatly increasing sensitivity but also greatly increasing scatter. The increased sensitivity is the greatest for the central slice and falls rapidly, and usually linearly, for slices more distant from the central slice. The slices near the edge have the sensitivity of about the same as in a 2D scanner but with greater scatter. Scatter is measured with standards given by the National Electrical Manufacturers Association (NEMA)[3-5] and is typically in the order of 10-15% for 2D scanners and 30-40% or more for 3D scanners. In chest slices encompassing the heart, as opposed to the relatively small NEMA phantom, there is an even larger increase in scattered counts for 3D imaging. For cardiac applications, scatter tends to increase the counts in cold areas surrounded by higher-activity regions (e.g., a defect surrounded by normal uptake).

Some manufacturers have scanners that have retractable septa, permitting the user to choose between 2D and 3D operation. Many PET/CT manufacturers have opted for scanners that operate only in 3D mode, since these are preferred for oncology studies. Situations in which 3D mode may be advantageous include those in which:

1. Whole-body patient throughput is important (e.g., a busy oncology practice).
2. Radiation exposure is critical, so that reductions in injected activity are desired.
3. Special (i.e., usually research) radiopharmaceuticals are being used, which can only be produced in low radioactivity quantities.

As noted above, although 3D acquisition is in principle many times more sensitive than 2D, random events (termed randoms), dead time, and scatter can greatly reduce the effective sensitivity of images acquired in 3D, especially at high doses. Thus, in order to prevent poor quality images, lower doses are administered. When using 3D imaging with a bismuth germanate (BGO) crystal camera, for example, 3D imaging had often been used when the dose had to be minimized (e.g., in normal volunteers, in children, or when multiple studies are planned) or when scatter was minimal (e.g., brain imaging). The advent of lutetium oxyothosilicate (LSO)- and gadolinium oxyorthosilicate (GSO)-based PET scanners, and even BGO scanners with new-generation optimized photo multiplier/crystal coupling schemes and high-speed electronics, has made 3D imaging more practical. Improvements in software, coupled with improvements in electronics and crystal technology can, in part, compensate for the increase in randoms, dead time, and scattered events.[6] The use of 3D cardiac imaging with new-generation machines continues to be evaluated. The degree to which any of these improvements is achieved in practice for cardiac imaging may vary between manufacturers.

PET Imaging-Crystal Types

Four different crystal types are commonly employed—BGO, GSO, LSO, and lutetium yttrium orthosilicate (LYSO)—although other crystal types have also been used. Each of them can be used successfully for cardiac imaging. BGO has the highest stopping power, but relatively poor energy resolution (i.e., limiting energy-based scatter reduction) and timing resolution (i.e., limiting its ability to reduce randoms). GSO, LSO, and LYSO have better timing resolution and, in theory, better energy resolution. For 2D imaging, GSO, LSO, and LYSO may not offer significant advantage over BGO, given the inherently high sensitivity of BGO. The main advantage of the newer crystals is their much reduced dead time, which enables them to acquire data at the much higher count rates associated with operating in 3D mode, and to better minimize the effects of randoms. One minor disadvantage of LSO and LYSO is their intrinsic radioactivity, which contributes to a small increase to the random event rate.

The better energy resolution of GSO, LSO, or LYSO, and consequent reduction of scatter in 3D mode, would make these detector types advantageous. At present, the theoretical energy resolution for these detectors does not seem to have been fully realized in practice, leaving all three crystal types with similar energy-based scatter rejection (i.e., GSO, LSO, and LYSO giving only slight potential improvement over BGO) and making 2D imaging still the method of choice if scatter rejection is critical. Modern image reconstruction algorithms incorporate improved models for scatter correction, and as a result, the impact of scatter for state-of-the-art scanners operating in 3D mode is usually acceptable for clinical imaging. The suitability of 3D mode for cardiac PET imaging should be evaluated by the user.

PET TOF Imaging

Machines that incorporate time-of-flight (TOF) information in the acquisition process have recently been commercially introduced. TOF refers to the time difference between the two 511 keV annihilation photons reaching their respective detectors, 180° apart. For example, if the positron annihilation occurred at the center of the machine, the two photons would reach their respective detectors at exactly the same time, while if the annihilation occurred closer to one detector than the other, the photon would reach the closer detector first. Adding TOF capability improves the statistical quality of the data (i.e., the noise).[7-9] If one could measure the time accurately enough, it would be possible to determine exactly where the photon originated. Unfortunately, current detector and instrumentation technology is not nearly good enough to achieve this level of accuracy. As machines with TOF ability have only recently been introduced, no quality control (QC) or other aspects of such machines are described here.

PET/CT Imaging

The latest trend in PET instrumentation is the addition of a CT system to the PET scanner. In all cases, the manufacturer starts with a state-of-the-art PET scanner, whose characteristics have been described in the section above. The manufacturer then adds a CT system, consisting of a 2-, 4-, 6-, 8-, 16-, 32-, 64-, or greater slice scanner. These combined systems, in practice, demonstrate a range of integration. At one end of the spectrum, the hardware and software of the CT systems are completely integrated within the PET scanner. In this approach, a common, unified gantry is used and a single, unified software system with an integrated PET/CT interface is provided. At the other end of the spectrum, the hardware and software of the CT system are less integrated. In some machines, a separate CT gantry is carefully placed in front of or behind the PET gantry, and a separate workstation is used to control the CT system.

PET Imaging-Attenuation Correction

For dedicated PET scanners, rotating rod sources of germanium-68 (Ge-68)/gallium-68 (Ga-68) or Cesium-137 (Cs-137) are used to acquire a transmission scan for attenuation correction. Typical transmission scans with a rotating rod add about 3-6 minutes to the overall imaging time. This is acceptable for cardiac imaging, but a significant drawback for multi-bed position oncology scans. Since oncology applications have been the driving force behind recent sales of PET scanners, manufacturers looked for a way to reduce this transmission scan time. For this reason, and because of other advantages of CT, nearly all current commercially available PET scanners are hybrid PET/CT systems. These scanners, in general, have eliminated the rotating rod source and instead rely on CT scans for attenuation correction.

CT-based attenuation correction typically adds less than 20 seconds to the scan time of a cardiac scan. The use of either CT or the rotating rod for attenuation correction requires precise alignment between the transmission image and the emission image. An advantage of CT over transmission sources is a much reduced scan time, which helps reduce overall patient motion. The high speed of CT scans, however, freezes the heart at one phase of the respiratory cycle, causing potential misalignment between the CT-based transmission image and the emission data. The latter, of course, are averaged over many respiratory cycles. The respiratory misalignment between the CT image and emission data can produce significant artifacts and errors in apparent uptake at the myocardial segments adjacent to lung tissue.[10] Errors in attenuation correction from misregistration are typically worse if the CT is acquired at full inspiration. At present, software realignment, usually manual, must be performed to minimize this misalignment. Other techniques (e.g., slow CT, respiratory gating, and 4D-CT) are under development for compensating for respiratory motion, but are still in the research phase and are not further described here.

PET AND PET/CT IMAGING QC

PET QC Procedures

The procedures below should be suitable for ensuring overall proper basic operation of a PET scanner. Table 1 lists recommended PET imaging QC

Table 1. Suggested QC procedures: dedicated PET imaging devices

Procedure	Frequency
Acceptance testing (NU 2-2007)	Once upon delivery and upon major hardware upgrades
Daily QC, as recommended by vendor (attenuation blank scan, phantom scan, etc.)	Daily
Sensitivity and overall system performance	Weekly (or at least monthly)
Accuracy (corrections for count losses and randoms)	At least annually
Scatter Fraction	At least annually
Accuracy of attenuation correction	At least annually
Image quality	At least annually
Measurements specified by the manufacturer	As per the manufacturer

schedules. Note that, unlike planar and SPECT imaging, there are no widely accepted, published QC procedures for PET. Some additional procedures may be required by particular manufacturers.

Acceptance testing. It is recommended that the NEMA performance measurements, as defined by NU 2-2007,[5] be made before accepting the PET scanner. Many of these tests can be performed by the company supplying the PET scanner. If so, it is recommended that the purchaser's representative work with the manufacturer's representatives during these tests. The NU 2-2007 recommendations have superseded the NU 2-2001 recommendations.[4] In scope, the tests are nearly equivalent between NU 2-2007 and NU 2-2001, the primary difference being NU 2-2007 addresses the intrinsic radioactivity in LSO and LYSO crystals. For cardiac imaging, these standards should be used rather than NU 2-1994 recommendations,[3] as they better reflect the imaging of objects of the size of a typical adult thorax region by incorporating measurements of the International Electrotechnical Commission (IEC) body phantoms.[11]

There are two reasons for making these performance measurements:

1. To ensure that the new PET scanner meets specifications published by the manufacturer.
2. To provide a standard set of measurements that allows the user to document the limitations of the scanner, and to provide a standard against which to track changes that may occur over time.

Daily QC scan. Each day the PET detectors should be evaluated to ensure proper operation before commencing with patient injections or scans. The daily quality procedure varies according to the design of the scanner and recommendations of the vendor. For example, some scanners utilize an attenuation blank scan to evaluate detector constancy, and others may use a scan of a standard phantom. In addition to numerical output of the scanners software (chi-square, uniformity, etc.), the raw sinogram data also should be inspected to evaluate detector constancy.

Sensitivity. NEMA NU 2-2007 provides recommended procedures for measuring system sensitivity. Subtle changes in PET system sensitivity may occur slowly over time. More dramatic changes in sensitivity may reflect hardware or software malfunction. There are simple tests designed to monitor such changes in sensitivity. Ideally, these tests should be performed weekly, but no less than monthly. For many systems, the daily QC scan also provides a measure useful for tracking changes in sensitivity.

Spatial resolution. Spatial resolution is measured using a point source as specified in the NEMA NU 2-2007 or NEMA NU 2-2001.

Scatter fraction. Intrinsic scatter fraction is measured according to either NEMA NU 2-2007 or NEMA NU 2-2001 specifications.

Accuracy of attenuation correction and overall clinical image quality. Attenuation correction should be assessed using the IEC phantom, as specified in the NU 2-2007 recommendations.[11] If this phantom is not readily available, it is suggested that similar measurements be performed with a phantom approximating a typical human body shape and size (e.g., a 20 by 30-cm elliptical phantom or anthropomorphic phantom). It should have at least one cold sphere or cylinder and one hot sphere or cylinder, as well as at least some material simulating lung tissue to ensure proper performance in the presence of non-uniform attenuating substances.

Variations among manufacturers. The above recommendations regarding PET scanner quality assurance are general guidelines. In addition, each manufacturer has its own periodic QC recommendations for parameters such as ''singles'' sensitivity, coincidence timing, energy calibration, and overall system

performance. These, by necessity, require different measurement protocols that may vary even between models for the same manufacturer. These measurements must be performed as detailed by the manufacturer. However, the measurements specified above are not intended to replace these basic system-specific QC measurements.

CT QC Procedures

The procedures below should be suitable for ensuring overall proper basic operation of a CT scanner. Table 2 lists recommended CT imaging QC schedules. Some additional procedures may be required by particular manufacturers.

Calibration. The reconstructed CT image must exhibit accurate, absolute CT numbers in Hounsfield Units (HU). This is critical for the use of CT images for PET attenuation correction, because the quantitative CT values are transformed, usually via a bilinear or trilinear function with one hinge at or near the CT value for water, to attenuation coefficients at 511 keV. Any errors in CT numbers will be propagated as errors in estimated 511 keV attenuation coefficients, which in turn will adversely affect the attenuation-corrected PET values. CT system calibration is performed with a special calibration phantom that includes inserts of known CT numbers. This calibration is done by the manufacturer's field service engineers. The CT calibration is then checked daily with a water-filled cylinder, usually 24 cm in diameter provided by the manufacturer. In practice, if the error is greater than 5 HU (i.e., different than the anticipated value of 0 HU), the CT system is considered to be out of calibration. The technologist will usually then do an air calibration, to determine if this corrects the overall calibration (i.e., brings the CT number for water back to within 5 HU of 0). If it does not, the manufacturer's field service engineer must be called. On an annual basis, or after any major repair or calibration, calibration is checked by the manufacturer's service engineer.

Field uniformity. The reconstructed CT image must exhibit uniform response throughout the field of view (FOV). In practice, this means that a reconstructed image of a uniform water-filled cylinder must itself demonstrate low variation in CT number throughout this image. In practice, small circular regions of interest (ROIs) are placed at the four corners of the cylinder image, and the mean CT number is compared to that from a region in the center of the phantom; the difference in mean region CT number should not exceed 5 HU. Non-uniformities greater than this may produce sufficient quantitative inaccuracies so as to affect PET attenuation correction based on the CT image.

Table 3 lists recommended CT QC schedules for combined PET/CT Units. Users should consult the manufacturer regarding the specific manner and frequency with which tests should be performed for the CT component of their PET/CT device. Both the American College of Radiology (ACR) and American Association of Physicists in Medicine (AAPM) have published CT testing procedural guidelines.[12,13]

Table 2. CT QC procedures

Test	Requirement	Frequency
Calibration	Mandatory	Monthly*
Field Uniformity	Mandatory	Monthly*

*Or as recommended by the manufacturer.

Combined PET/CT QC Procedures

The PET and CT portion of the combined system should be assessed as described for the dedicated PET and CT imaging devices. In addition to the independent QC tests for the PET and CT portions of the combined system, it is necessary to perform additional tests that assess the combined use of PET and CT. Table 4 lists recommended QC procedures for combined PET/CT units.

Registration. The reconstructed PET and CT images must accurately reflect the same 3D locations (i.e., the two images must be in registration). Such registration is often difficult because the PET and CT portions of all commercial combined PET/CT systems are not coincident (i.e., the PET and CT ''slices'' are not in the same plane) and because the PET and CT gantries are contiguous. In practice, this means that the PET and CT acquisitions do not simultaneously image the same

Table 3. Schedule of CT QC for PET/CT units

Test	Frequency
Water phantom QA	Daily
Tube warm-up	Daily
Air calibration ("fast QA")	Daily
Water phantom checks: slice thickness, accuracy, positioning	Monthly

Table 4. Combined PET/CT QC procedures

Test	Requirement
Registration	Mandatory
Attenuation correction accuracy	Mandatory

slice. In fact, because the bed must travel different distances into the gantry to image the same slice in the patient for PET versus CT, there is ample opportunity for misregistration via x, y, z misalignment of bed motion—or, of perhaps even greater concern, because of differential ''bed sag'' for the PET and CT portions, depending on the table design.

In addition, electronic drift can influence the ''position'' of each image, so that calibrations for mechanical registration can become inaccurate over time. Thus, it is imperative to check PET-to-CT registration on an ongoing basis. This is usually performed with a specific phantom or jig containing an array of point sources visible in both PET and CT.

Errors in co-location in the fused PET-CT images are assessed, such as by means of count profiles generated across transaxial slices. Such errors, after software registration corrections, should be less than 1 mm. It is important to image this registration jig in a number of positions along the bed. It may also be helpful to place a weight on the end of the bed to produce some bed sag and repeat the assessment.

Note: The above considerations are in addition to the patient-specific alignment QC clinically necessary to assess possible patient or respiratory motion (not described here).

Attenuation correction accuracy. The use of the CT image for PET attenuation correction requires a transformation of the observed CT numbers in HU to attenuation coefficients at 511 keV. This transformation is usually accomplished with a bilinear or trilinear calibration curve, with one ''hinge'' at a CT value of 0 (i.e., hinged at the CT value for water).

At a minimum, it is important to image a water-filled cylinder to assess PET field uniformity and PET activity concentrations after CT-based PET attenuation correction. Errors in CT-to-PET attenuation transformations are usually manifest as a corrected PET image without a ''flat'' profile from edge to center (i.e., the activity at the edge is either too high or too low relative to that at the center of the phantom) and with resulting attenuation-corrected absolute PET values that are incorrect (although these values depend on absolute PET scanner calibration as well as accurate CT-based PET attenuation correction).

If possible, the CT-based attenuation-corrected PET values should be compared with those from the rotating rod source-based attenuation-corrected PET values in the same phantom. Moreover, if available, more sophisticated phantoms with variable attenuation and variable activity distributions can be used to more comprehensively assess any errors in CT-based PET attenuation correction.

The accuracy of CT attenuation-corrected PET images is still under investigation.[14] Recent work has reported that even after correcting for potential PET/CT misalignment, tracer uptake maps derived from CT-based attenuation correction differ from those derived using transmission source correction.[10,15,16]

PET ACQUISITION AND PROCESSING PARAMETERS

The acquisition and processing parameters defined in this section apply to both the perfusion and metabolic PET tracers in the sections that follow.

Patient Positioning

Ideally, the patient should be placed in the supine position, with the arms out of the camera FOV. This can be tolerated by nearly all patients, provided that some care is given to a method to support the arms. Alternatively, an overhead bar has often been used as a handhold for arm support. In patients with severe arthritis, whose arms cannot be positioned outside the camera's FOV, cardiac images should be obtained with the patient's arms resting on his/her side. In the latter case, the transmission scan time may have to be increased, and it is of critical importance that the arms do not move between transmission and emission, or artifacts will result. Note that when performing perfusion/metabolism PET studies, it is best to keep the patient positioned similarly for both studies. In patients undergoing PET/CT imaging, arms resting inside the FOV will result in beam-hardening artifacts on the CT-based transmission scan, which usually lead to streak artifact of the corrected emission scans.

Dose Considerations

In determining appropriate patient doses, the following issues should be considered:

1. Staff exposure could be high because of the limited effectiveness of shielding and the potential for large doses (e.g., Rb-82 PET). Thus, standing in close proximity to an Rb-82 generator or the patient during injection should be avoided.
2. Large patients may benefit from higher doses.
3. 3D imaging requires less dosage than 2D imaging due to the improved sensitivity of the system.

Total Counts

The counts per slice necessary to yield adequate quality images will vary from camera to camera depending, in part, on scatter and randoms corrections, as well as the amount of smoothing that is performed. If

one tries to achieve on the order of 7 mm full width at half maximum (FWHM) in-plane resolution and has 10-15% scatter (NEMA), then a typical good-quality study in 2D mode might have on the order of 50,000 true counts per millimeter of transaxial distance over the region of the heart (e.g., for a 4.25-mm slice separation, the counts would be $50{,}000 \times 4.25 = 250{,}000$ counts per slice). These numbers are very approximate and may differ from one scanner to the next. If one is willing to accept a lower resolution (e.g., more smoothing) or more noise, imaging time can be reduced. Since 3D scanners have greater scatter, they usually require more counts than a 2D scanner to achieve the same noise level.

Pixel Size

It is recommended that 2-3 mm per pixel be used. A ''rule of thumb'' in nuclear medicine physics is that one needs at least 3 pixels for every FWHM of resolution in the image. For example, if the data are reconstructed to 8 mm FWHM, then one needs roughly $8 \text{ mm}/3 = 2.7$ mm/pixel. Many institutions achieve a 3 mm sampling rate or better with a 256×256 array over the entire FOV of the camera. Other institutions choose to use a 128×128 array over a limited FOV (e.g., 25-35 cm diameter) centered over the heart, in which case, 2-3 mm/pixel is easy to achieve, cutting out extraneous structures in the FOV, even with a 128×128 array. Either method is acceptable to achieve the desired 2-3 mm/pixel. Greater than 3 mm/pixel may be acceptable for older PET cameras with resolution worse than 1 cm.

Imaging Mode (Static, Gated or Dynamic)

Static PET acquisition produces images that allow relative assessment of tracer uptake on a regional basis. Comparison of regional tracer uptake in relation to the normal tracer distribution is the current standard for the identification regional abnormalities.

Usually, PET tracer counts are sufficiently high to yield good quality ventricular function study. Electrocardiographic (ECG)-gated images are acquired in 8-16 time frames per R to R interval, in a manner similar to SPECT gated perfusion studies but at higher spatial resolution. Given that ventricular contraction and thickening are often clinically useful for assessing viability, gating should be performed when possible. It is important that the gating software does not adversely affect the ungated images (e.g., by loss of counts as a result of beat length rejection). Monitoring the length and number of the accepted beats is critical to assure the accuracy of the gated data. Arrhythmias such as atrial fibrillation, frequent premature ventricular contractions (PVCs), or other abnormal rythms can lead to highly erroneous gated information.

For a dynamic acquisition, PET data are acquired in multiple time sequenced frames. A potential advantage of the dynamic over static acquisition is in the case of patient motion artifact. For example, if a patient should move at the end of the study, one can select and utilize only those dynamic frames with no motion (i.e., summing them together to make one static image). This is easily implemented and takes almost no additional operator time. A more elaborate dynamic acquisition beginning with tracer injection may optionally be used when kinetic analysis over the entire uptake period is to be performed (e.g., compartmental analysis or Patlak analysis). Kinetic analysis permits absolute quantification of the tracer's kinetic properties (e.g., blood flow for Rb-82 and N-13 ammonia, rate of FDG utilization). Performing and interpreting such kinetic analyses can be complex and require expertise.

List mode acquisitions are now available with many new cameras, which enable simultaneous dynamic and ECG-gated acquisitions. This is considered an optional acquisition mode, although it is routinely used by some vendors' processing software.

Image Reconstruction

Several corrections are required for creating data sets that can be used for reconstruction. PET data must be corrected for randoms, scatter, dead time, attenuation, and decay before reconstruction can begin. Once these corrections are applied, the data can be reconstructed with either filtered backprojection (FBP) or iterative algorithms. FBP is the standard method used for reconstruction on older PET systems. FBP images are subject to streak artifacts, especially when the subject is obese or large. This can affect visual analysis but usually does not adversely affect quantitative analysis with regions of interest (i.e., the streaks tend to average out properly over typical volumes of interest). Newer PET/CT systems employ iterative reconstruction methods (e.g., the method of ordered-subsets expectation maximization [OSEM]) yielding images with better noise properties. Although high uptake structures, such as the heart, may not improve their noise characteristics with OSEM, the surrounding lower uptake structures do improve, and streak artifacts are nearly eliminated, thus greatly improving the visual appearance of the image. However, low uptake areas, such as myocardial defects and the left ventricular (LV) cavity at late times, may have slightly or artificially elevated activity levels unless sufficient iterations are performed. It is recommended that one thoroughly characterizes the PET machine and its reconstruction algorithm's behavior with a realistic cardiac phantom.

For rest/stress comparisons, the rest/stress images must have matched resolution. Filtering is usually necessary to achieve adequate noise properties. Care must be taken to match reconstructed resolution when making pixel-by-pixel comparisons of paired myocardial perfusion and metabolism data.

For GSO systems, the images are reconstructed using a row action maximum likelihood algorithm (RAMLA) reconstruction technique, which includes a texture/filter factor. Thus, an additional reconstruction filter should not be performed.

Attenuation Correction

PET cardiac imaging should only be performed with attenuation correction. Attenuation correction can be accomplished with a rotating line source in a dedicated PET system or with CT in a PET/CT system.

For dedicated PET systems, two techniques are typically used for creating the patient-specific transmission maps: direct measurement of patient attenuation with a rotating line source of either Ge-68 or Cs-137 or segmentation of patient-specific attenuation maps. The former are very sensitive to the choice of reconstruction algorithm and, depending on reconstruction algorithm used, could require 60-600 seconds' acquisition time to produce a reasonable attenuation map. Segmentation algorithms are relatively insensitive to noise but are very dependent on the quality of the program used for performing the transmission scan segmentation and are influenced by lung attenuation inhomogeneities (e.g., partial-volume effects from the liver).

Transmission data are typically acquired sequentially, so it is essential that the patient remain still between transmission and emission images. Either pre- or post-scan transmission imaging is satisfactory, providing that the system's software can adequately correct for residual emission activity. Transmission imaging simultaneous with emission imaging is not recommended unless the high count rate and rapidly changing distribution of the emission tracer can be assured to not adversely affect the transmission scan. If the transmission scan is performed at the beginning of the study, attention should be made for potential misregistration with the emission images, possibly due to gradual upward creep of the diaphragm, due to pressure from visceral fat.[17]

For PET/CT systems, x-ray CT can be used for acquiring a transmission map for attenuation correction. An advantage of this approach is the rather rapid (15-30 seconds) acquisition of the transmission map, which can be repeated for each imaging session, rest and stress perfusion studies as well as for subsequent metabolic imaging, if necessary. The CT scan can be reviewed for additional, independent diagnostic information, such as coronary calcium visualization and other extra-cardiac anatomic information. To acquire a CT-based transmission scan, it is necessary to first acquire a planar scout CT acquisition. This scan is used to measure the axial limits of the CT acquisition. Following this acquisition, the CT transmission scan is acquired. The best approach for CT transmission imaging is still evolving, and therefore this guideline can only suggest some considerations. Some of the considerations for CT scanning are as follows (Table 5):

1. If CT is used for either attenuation correction or anatomical evaluation, this will have an effect on the kV and mAs used in the acquisition. A transmission

Table 5. General guidelines for CT-based transmission imaging

CT parameter	General principle	Effect on patient dose
Slice collimation	Should approximate the slice thickness of PET (eg., 4–5 min.)	No effect
Gantry rotation speed	Slower rotation speed helps blur cardiac motion (eg., 1 sec/revolution or slower)	Slower gantry rotation increases radiation
Table feed per gantry rotation(pitch)	Relatively high pitch(eg., 1:1)	Inversely related to pitch
ECG gating	ECG gating is not recommended	Decreases without ECG gating
Tube potential	80–140 kVp, depending on manufacturer specification	Increases with higher kVp
Tube current	Because the scan is only acquired for AC, low tube current is preferred (10–20 mA)	Increases with higher mA
Breathing instructions	End-expiration breathhold or shallow free-breathing is preferred (see text)	No effect
Reconstructed slice thickness	Should approximate the slice thickness of PET (eg., 4–5 mm)	No effect

scan usually requires only a low CT current, as opposed to calcium scoring or CT angiography, which require higher CT currents.

2. Breathing protocols are not clearly settled. Recent data suggest that respiratory averaging may be a useful method of reducing breathing related artifacts. Other methods, such as free breathing with a slow CT scan or ultra-rapid CT acquisition (depending on the CT device available) have also been proposed. Current practice discourages breath-holding, particularly in end-inspiration because of the potential for it to cause uncorrectable misregistration. A transmission CT scan performed at the same speed as for whole-body PET/CT images frequently produces artifacts at the lung-liver interface and can sample parts of the heart and diaphragm in different positions, causing misregistration and an artifact where pieces of the diaphragm appear to be suspended in the lung. Although specifics vary among laboratories, the duration of the CT transmission scan is typically from 10-30 seconds. CT attenuation correction with 64 slice devices can achieve an ultra-rapid CT in 1.5 seconds, which appears to reduce such CT artifacts. Therefore, it is imperative to ensure proper registration between transmission and emission data for quality assurance and proper interpretation of PET images. Several approaches are currently being devised to reduce misregistration artifacts, such as reducing CT tube current and increasing the duration CT acquisition to better match the temporal resolution between the attenuation and emission maps.[18,19]
3. Metal artifacts[20] can present a challenge for the reconstruction algorithm and must be compensated for to produce accurate attenuation maps.[21,22]
4. Ideally, stress transmission images should be acquired during peak stress or vasodilation, which is not practical. As such, the technologist and physician must carefully inspect the transmission and emission data sets to ensure that they are properly registered in the transaxial, sagittal, and coronal planes. For patients undergoing PET/CT, a separate CT-based transmission scan for correction of the stress images is standard. For Rb-82, a post-stress transmission scan is preferred to minimize misregistration artifacts on the corrected Rb-82 images when misregistration compensation software is not available.

PET MYOCARDIAL PERFUSION IMAGING

The goal of evaluating myocardial perfusion with PET imaging is to detect physiologically significant coronary artery narrowing with a view towards aggressive risk factor modification in order to:

1. Delay or reverse the progression of atherosclerosis.
2. Alleviate symptoms of ischemia by medical or revascularization therapy.
3. Prevent future adverse events.
4. Improve patient survival.

Stress and rest paired myocardial perfusion studies are commonly performed to assess myocardial ischemia and/or infarction. Current Food and Drug Administration (FDA)-approved and Centers for Medicare & Medicaid Services (CMS)-reimbursable PET myocardial blood flow tracers are limited to Rb-82 and N-13 ammonia. Normal myocardial perfusion on stress imaging implies absence of physiologically significant coronary artery disease (CAD). Abnormal myocardial perfusion on stress imaging suggests the presence of significantly narrowed coronary arteries. If the stress-induced regional perfusion defect persists on the corresponding paired rest images, it suggests the presence of an irreversible myocardial injury. On the other hand, if the defect on the stress images resolves completely or partially on the rest images, it suggests the presence of stress induced myocardial ischemia. Imaging of myocardial perfusion can also be combined with myocardial metabolism imaging with F-18 FDG for the assessment of myocardial viability in areas of resting hypoperfusion and dysfunctional myocardium.

Patient Preparation

Patient preparation is similar to preparation for stress and rest myocardial SPECT imaging. This includes an overnight fast of 6 hours or more, with the exception of water intake. Patients should avoid caffeinated beverages for at least 12 hours, and avoid theophylline-containing medications for at least 48 hours.[23]

Cardiac Stress Testing

Details of pharmacologic or exercise stress testing are beyond the goals of this document. Nonetheless, stress protocols are, for the most part, generic for all perfusion agents.[23] The specific differences in acquisition protocols for Rb-82 and N-13 ammonia imaging are related to the duration of uptake and clearance of these radiopharmaceuticals and their physical half-lives. No data are available yet with PET and the newly approved A2A selective adenosine receptor agonist, Regadenoson.

Rb-82 Perfusion Imaging

Tracer properties. Rb-82 PET myocardial perfusion imaging is a well established and highly accurate

technique for detecting hemodynamically significant CAD.[14,24,25] Rb-82 is a monovalent cationic analog of potassium. It is produced in a commercially available generator by decay from strontium-82 (Sr-82) attached to an elution column. Sr-82 has a half-life of 25.5 days and decays to Rb-82 by electron capture. Rb-82 decays with a physical half-life of 75 seconds by emission of several possible positrons, predominantly of very high energy. The resulting long positron range slightly worsens image resolution compared to F-18 and N-13. The daughter product is krypton-82, which is stable. The Sr-82-containing generator is commercially available and is replaced every 4 weeks, thus obviating the need for a cyclotron.

Rb-82 is eluted from the generator with 10 to 50 mL normal saline by a computer-controlled elution pump, connected by intravenous (IV) tubing to the patient. While the generator is fully replenished every 10 minutes, experiments have shown that 90% of maximal available activity can be obtained within 5 minutes after the last elution. Thus, serial imaging can be performed every 5-6 minutes. While the short half-life of Rb-82 challenges the performance limits of PET scanners, it facilitates the rapid completion of a series of resting and stress myocardial perfusion studies.

Rb-82 is extracted from plasma with high efficiency by myocardial cells via the Na^+/K^+ adenosine triphosphatase pump. Its extraction is less than N-13 ammonia, and extraction decreases with increasing blood flow. Rb-82 extraction can be decreased by severe acidosis, hypoxia, and ischemia.[26-28] Thus, while uptake of Rb-82 predominantly depends on myocardial blood flow, it may be modulated by metabolism and cell integrity.

Dosimetry. The radiation dosimetry from Rb-82 in an adult may vary from 1.75 to 7.5 mSv total effective dose for a maximal allowable activity of 60 mCi at both rest and stress.[29] With current advances in PET instrumentation, diagnostic quality PET images can be acquired using only 20-40 mCi of Rb-82 for each of the rest and stress phases of the study. As a result, the effective dose of radiation exposure from Rb-82 PET can be halved.

Acquisition parameters. Acquisition parameters for different types of PET scanners are shown in Tables 6 and 7. The short half-life of Rb-82 poses a challenge for achieving optimal image quality. As such, optimal acquisition parameters differ among the several main types of PET scanners. Because of the short half-life of Rb-82 and the need for the patient to lie still in the camera during the study, stress imaging of this agent is primarily limited to pharmacologic stress, although

Table 6. Rb-82 rest/stress myocardial perfusion imaging guideline for BGO and LSO (LYSO) PET imaging systems

Feature	BGO Systems	LSO (LYSO) Systems	Technique
Stress testing	Pharmacologic agents		Standard
Tracer Dose			
2D Scanner	40–60 mCi (1480–2220 MBq)		Standard
3D Scanner	10–20 mCi (370–740 MBq)	30–40 mCi (1110–1480 MBq)	Standard
Injection rate	Bolus of ≤30 seconds		Standard
Imaging delay after injection	LVEF > 50%: 70–90 seconds		Acceptable
	LVEF < 50% or unknown: 90–130 seconds		
	List mode: acquire immediately		
Patient positioning			
PET	Use scout scan: 10–20 mCi Rb-82 (370–740 MBq)		Standard
	Use transmission scan		Optional
PET/CT	CT scout		Standard
Imaging mode	List mode: gated/dynamic (no delay after injection)		Preferred
	Gated acquisition (delay after injection)		Optional
Imaging duration	3–6 minutes		Standard
	3–10 minutes		Optional
Attenuation correction	Measured attenuation correction, before or after		Standard
Reconstruction method	FBP or iterative expectation maximization (e.g., OSEM)		Standard
Reconstruction filter	Sufficient to achieve desired resolution/smoothing, matched stress to rest		Standard
Reconstructed pixel size	2–3 mm		Preferred

Table 7. Rb-82 rest/stress myocardial perfusion imaging guideline for GSO PET imaging systems

Feature	GSO Systems	Technique
Stress testing	Pharmacologic agents	Standard
Tracer dose (3D)	20 mCi (740 MBq)	Standard
Injection rate	Bolus of $\leq$ 30 seconds	Standard
Imaging delay after injection	LVEF $>$ 50%: 70–90 seconds	Standard
	LVEF $<$ 50% or unknown: 90–130 seconds	
	List mode: acquire immediately	
	Longer delays than the above must be used if count rate at these times exceeds the maximum value specified by the manufacturer	
Patient positioning		
PET	Use scout scan: 10–20 mCi Rb-82 (370–740 MBq)	Standard
	Use transmission scan	Optional
PET/CT	CT scout	Standard
Imaging mode	List mode: gated/dynamic (no delay after injection)	Standard
Imaging duration	3–6 minutes	Standard
	3–10 minutes	Optional
Attenuation correction	Measured attenuation correction, before or after	Standard
Reconstruction method	Iterative (RAMLA)	Standard
Reconstruction filter	None	Standard
Reconstructed pixel size	4 mm	Standard

reasonable Rb-82 images have also been obtained with supine bicycle and treadmill exercise.[30,31]

Scout scanning. Scout scanning is recommended before each injection to ensure that the patient is correctly positioned and is not exposed to unnecessary radiation. This can be done with a fast transmission image or with a low-dose Rb-82 injection (10-20 mCi). Note that the low-dose Rb-82 scout scan is also used to estimate circulation times and cardiac blood pool clearance times, which assist in selection of the optimum injection to imaging delay time between Rb-82 injection and initiation of acquisition of myocardial Rb-82 images. With PET/CT systems, a low dose CT scout scan is routinely used for patient positioning.

Imaging parameters. Rest imaging should be performed before stress imaging to reduce the impact of residual stress effects (e.g., stunning and steal). For Rb-82, about 80% of the useful counts are acquired in the first 3 minutes, 95% of the useful counts are obtained in the first 5 minutes, and 97% are obtained in the first 6 minutes. The patient should be infused with Rb-82 for a maximum of 30 seconds. After the dose is delivered, patients with normal ventricular function, or left ventricular ejection fraction (LVEF) $>$ 50%, are typically imaged starting 70-90 seconds after the injection. For those with reduced ventricular function, or LVEF 30-50%, imaging usually is begun 90-110 seconds after termination of the infusion. Those with poor function, or LVEF $<$ 30%, are typically imaged at 110-130 seconds. Excessive blood pool counts can scatter into myocardial counts, impacting defect size and severity. Excessive blood pool counts can also make the left ventricular cavity appear smaller, especially at rest, leading to a false perception of LV cavity dilatation during stress. These delay times are applicable for both static and ECG gated acquired images.

N-13 Ammonia Perfusion Imaging

N-13 ammonia is a valuable agent for measuring either absolute or relative myocardial blood flow.[32,33] For measurements of absolute blood flow, dynamic acquisition from time of injection is required, followed by applying 2- and 3-compartment kinetic models that incorporate both extraction and retention rate constants. Absolute flow measurements with ammonia are

performed primarily in research settings, require a high level of expertise, and are not commercially available. In a clinical setting, ammonia PET images are assessed visually or semi-quantitatively for the evaluation of regional myocardial perfusion defects or for the determination of myocardial viability.[34-36]

N-13 ammonia is an extractable myocardial perfusion tracer that has been used extensively in scientific investigations with PET over the past two decades. At physiologic pH, ammonia is in its cationic form with a physical half-life of 10 minutes. Its relatively short half-life requires an on-site cyclotron and radiochemistry synthesis capability. The N-13 nitrogen decays by positron emission. The daughter product is C-13 carbon, which is stable. Myocardial uptake of N-13 ammonia depends on flow, extraction, and retention. First-pass myocardial extraction of N-13 ammonia is related inversely and nonlinearly to blood flow.[37] Following this initial extraction across the capillary membrane, ammonia may cross myocardial cell membranes by passive diffusion or as ammonium ion by the active sodium-potassium transport mechanism. Once in the myocyte, N-13 ammonia is either incorporated into the amino acid pool as N-13 glutamine or back-diffuses into the blood. The myocardial tissue retention of ammonia as N-13 glutamine is mediated by adenosine triphosphate and glutamine synthetase. Thus uptake and retention can both be altered by changes in the metabolic state of the myocardium although the magnitude of metabolic effects on the radiotracer retention appears to be small.

Dosimetry. The radiation dosimetry from N-13 ammonia in an adult is 1.48 mSv total effective dose from 20 mCi.[38] The critical organ is the urinary bladder, which receives 6 mSv from 20 mCi.[39] The dosimetry is relatively low, due to the short half-life of N-13 and the low energy of the emitted positrons.

Acquisition parameters. Table 8 summarizes the recommended guidelines for performing N-13 ammonia perfusion scans with dedicated, multicrystal PET or PET/CT cameras for rest and stress myocardial PET perfusion imaging for the diagnosis and evaluation of CAD, or as part of an assessment of myocardial viability.

Dose. Typically, 10-20 mCi of N-13 ammonia is injected. Large patients may benefit from higher, or 25-30 mCi, doses. In addition, the dose of radioactivity administered will also depend on whether images are obtained in 2D or 3D imaging mode.

PET METABOLIC IMAGING

PET Glucose Metabolism

For a given physiologic environment, the heart consumes the most efficient metabolic fuel as an adaptive response to meet its energy demands. Under fasting and aerobic conditions, long-chain fatty acids are the preferred fuel in the heart as they supply 65-70% of the energy for the working heart, and some 15-20% of the total energy supply comes from glucose.[40] However, the myocardium can use various other metabolic

Table 8. N-13 ammonia cardiac perfusion studies

Feature		Technique
Stress testing	Pharmacologic agents	Standard
Tracer dose (2D or 3D)	10–20 mCi (typical) (370–740 MBq)	Standard
Injection rate	Bolus or <30 seconds infusion	Preferred
Imaging delay after injection	1.5–3 minutes after end of infusion	Standard
Patient positioning		
PET	Use scout scan: 1–2 mCi (37–74 MBq)	Optional
	Use transmission scan	Standard
PET/CT	CT Scout Scan	Standard
Imaging mode	ECG gating of myocardium	Preferred
	Static or list mode	Optional
	Dynamic	Optional
Imaging duration	10–15 min	Standard
Attenuation correction	Measured attenuation correction, before or after	Standard
Reconstruction method	FBP or iterative expectation maximization (e.g., OSEM)	Standard
Reconstruction filter	Sufficient to achieve desired resolution/smoothing, matched stress to rest	Standard
Reconstructed pixel size	2–3 mm	Preferred
	4 mm	Optional

substrates depending on substrate availability, hormonal status, and other factors.[41,42]

Metabolic adaptation to changes in regional blood flow or other triggers is an essential component of maintaining normal cardiac function. Acute and chronic metabolic adaptation to a temporary or sustained reduction in coronary blood flow is in place to protect the structural and functional integrity of the myocardium. Reversible metabolic changes, as an adaptive measure to sustain myocardial viability, will occur in the setting of diminished, but not absent, regional myocardial blood flow. When myocardial blood flow is absent, irreversible metabolic changes will occur followed by myocardial infarction and cell death.

The breakdown of fatty acids in the mitochondria via beta-oxidation is exquisitely sensitive to oxygen deprivation. Therefore, in the setting of reduced oxygen supply, the myocytes compensate for the loss of oxidative potential by shifting toward greater utilization of glucose to generate high-energy phosphates. An acute switch from aerobic to anaerobic metabolism may be a necessary prerequisite for immediate cell survival following acute myocardial ischemia. Without these acute adaptive changes in metabolism, the resulting energy deficit leads to cell death.

Tracers of myocardial metabolism such as carbon-11 labeled fatty acids, acetate, or glucose, will not be covered in this document, due to their current investigational status and lack of FDA approval.

F-18 FDG Metabolism Imaging

Tracer properties. The principal radiopharmaceutical in clinical cardiac PET myocardial viability imaging is F-18 FDG, which is an analog of glucose and is used to image myocardial glucose utilization in vivo. CMS has approved reimbursement of FDG for the evaluation of myocardial viability.

The F-18 radiolabel is produced in a cyclotron through the (p,n) reaction, consisting of bombardment of O-18 enriched water.[43] F-18 decays by the emission of a positron with a half-life of $\sim$110 minutes. The low kinetic energy of the positron, 635 keV, allows the highest spatial resolution among all PET radionuclides. The 110-minute physical half-life of FDG allows sufficient time for synthesis and purification, its commercial distribution in a radius of several hours from the production site, its temporary storage at the user site, the absorption time after injection, and sufficient imaging time to yield images of high quality.

FDG enters myocardial cells by the same transport mechanism as glucose. Once in the cell, it is phosphorylated by hexokinase to FDG-6-phosphate. Once phosphorylated, subsequent metabolism of FDG is minimal. Because the dephosphorylation rate of FDG is slow, it becomes essentially trapped in the myocardium, allowing adequate time to image regional glucose uptake by PET. Following IV injection of 5-15 mCi of FDG, imaging can commence either immediately during the infusion of the radiotracer, if quantification of glucose metabolic rates is desired, or about 45-90 minutes after the injection of the radiotracer, if only qualitative assessment of the relative distribution of the radiotracer in the LV myocardium is needed.

Tracer dosimetry. The whole body dosimetry from a 10-mCi dose is 7 mSv.[44] For FDG, the critical organ is the urinary bladder, which receives 59 mSv.

Patient preparation. There are several approaches to stimulate myocardial glucose metabolism with either oral or IV glucose loading. Tables 9, 10, and 11 summarize the recommended guidelines for performing cardiac FDG scans with dedicated, multicrystal PET and PET/CT cameras, as part of an assessment of myocardial viability. Tables 10 and 11 summarize the patient preparation and method of FDG administration. Table 12 discusses the image acquisition.

Myocardial substrate utilization. For the evaluation of myocardial viability with FDG, the substrate and hormonal levels in the blood need to favor utilization of glucose over fatty acids by the myocardium.[40,42,45] This is usually accomplished by loading the patient with glucose after a fasting period of at least 6 hours to induce an endogenous insulin response. The temporary increase in plasma glucose levels stimulates pancreatic insulin production, which in turn reduces plasma fatty acid levels through its lipogeneic effects of adipocytes and also normalizes plasma glucose levels. The most common method of glucose loading is with an oral load of 25-100 g, but IV loading is also used. The IV route avoids potential problems due to variable gastrointestinal absorption times or inability to tolerate oral dosage. Because of its simplicity, most laboratories utilize the oral glucose-loading approach, with supplemental insulin administered as needed. The physician should take into account whether or not the patient is taking medications that may either antagonize or potentiate the effects of insulin.

Diabetic patients. Diabetic patients pose a challenge, either because they have limited ability to produce endogenous insulin or because their cells are less able to respond to insulin stimulation. For this reason, the simple fasting/oral glucose-loading paradigm is often not effective in diabetic patients. Use of insulin along with close monitoring of blood glucose (Table 10) yields satisfactory results. Improved FDG images can also be seen when image acquisition is delayed 2-3 hours after injection of the FDG dose. Of course, the latter comes at the expense of increased decay of the radiopharmaceutical. An alternative technique is the euglycemic hyperinsulinemic clamp, which is a rigorous and time-consuming

Table 9. FDG cardiac PET: patient preparation guidelines—an overview

Procedure		Technique
Fasting period	*Step 1*: Fast patient	
	6–12 hours	Preferred
	<6 hours	Suboptimal
	Step 2: Check blood glucose (BG) and then glucose load (choose one of the following 4 options)	
Oral glucose load	*Option 1*: Oral glucose loading	
	IF: fasting BG < ~250 mg/dL (13.9 mmol/L)	Standard
	THEN: (1) Oral glucose load: typically 25–100 g orally (see Table 10)	
	(2) Monitor BG (see Table 10)	
	IF: fasting BG > ~250 mg/dL (13.9 mmol/L)	Standard
	THEN: See Table 10	
	OR	
IV, protocol A	*Option 2*: Dextrose IV infusion	Optional
	For details, see sample protocol A (appendix 1)	
	OR	
IV, protocol B	*Option 3*: Dextrose IV infusion	Optional
	For details, see sample protocol B (appendix 2)	
	OR	
Acipimox	*Option 4*: Acipimox	
	Acipimox, 250 mg orally, not available in United States	
	Step 3: Administer FDG	
FDG injection	Time: Dependent on which option was selected	Standard
	Administer FDG intravenously; see Table 11, item 1, for details	
	Step 4: Begin imaging	
Begin PET imaging	Time 0–90 minutes post FDG injection: start imaging, see Table 11	

Table 10. Guidelines for blood glucose maintenance (e.g., after oral glucose administration) for optimal FDG cardiac uptake, blood glucose of approximately 100-140 mg/dL (5.55-7.77 mmol/L) at FDG injection time

BG at 45–60 min after administration	Possible restorative measure	Technique
130–140 mg/dL (7.22–7.78 mmol/L)	1 u regular insulin IV	Standard
140–160 mg/dL (7.78–8.89 mmol/L)	2 u regular insulin IV	
160–180 mg/dL (8.89–10 mmol/L)	3 u regular insulin IV	
180–200 mg/dL (10–11.11 mmol/L)	5 u regular insulin IV	
>200 mg/dL (>11.11 mmol/L)	Notify physician	

procedure.[46,47] However, it allows close titration of the metabolic substrates and insulin levels, which results in excellent image quality in most patients. Shorter IV glucose/insulin-loading procedures of 30 minutes have also been used with some success (see Protocol A, Appendix 1 and Protocol B, Appendix 2).[48]

While some have advocated performing FDG viability scans under fasting conditions, it is recommended that they be performed under glucose loaded conditions. This maximizes FDG uptake in the myocardium, results in superior image quality, and reduces the regional variations in FDG uptake

Table 11. FDG cardiac PET: acquisition guidelines for dedicated, multicrystal PET scanner

Feature		Technique
Tracer dose (2D or 3D)	5-15 mCi (185-555 MBq)	Standard
Injection rate	Not critical, bolus to 2 minutes	Standard
Image delay after injection	45-60 min after injection (keep constant for repeat studies)	Standard
Patient positioning		
PET	Use an FDG scout scan	Optional
	Use transmission scan	Standard
PET/CT	CT Scout Scan	Standard
Imaging mode	2D or 3D	Standard
	Static or list mode	Standard
	Dynamic	Optional
Image duration	10-30 min (depending on count rate and dose)	
Attenuation Correction	Measured attenuation correction: before or immediately after scan	Standard
Reconstruction method	FBP or iterative expectation maximization (e.g., OSEM)	Standard
Reconstruction filter	Sufficient to achieve desired resolution/smoothing, matched between consecutive studies	Standard
Reconstructed pixel size	2-3 mm	Preferred
	4-5 mm	Acceptable

Note: If metabolism imaging is combined with PET perfusion imaging, the same parameters for patient positioning, attenuation correction, and image reconstruction should be applied.

Table 12. Semiquantitative scoring system of defect severity and extent

Grade	Interpretation	Score
Normal counts	Normal perfusion	0
Mild reduction in counts	Mildly abnormal	1
Moderate reduction in counts	Definitely abnormal	2
Severe reduction in counts	Definitely abnormal	3
Absent counts	Definitely abnormal	4

that can occur when imaging under fasting conditions.[49]

Acipimox. Acipimox is a nicotinic acid derivative, which is not FDA approved in the United States. It has been used successfully in Europe instead of glucose loading. Acipimox inhibits peripheral lipolysis, reduces plasma free fatty acid levels, and stimulates myocardial glucose utilization.[48,50]

Acquisition parameters. Acquisition parameters for PET cardiac FDG imaging are itemized in Table 11 and its accompanying notes. If FDG PET metabolic images are being compared to perfusion images acquired by SPECT, the interpreter should be mindful that there will be differences in soft tissue attenuation, image resolution, and registration problems of images acquired on different instruments. It should be noted that if a Tl-201 or Tc-99m-labeled perfusion tracer is used to assess myocardial perfusion, there is no need to delay the FDG PET images, from an instrumentation point of view, if the 2D PET acquisition mode is applied. The relatively lower photons emitted from Tl-201 and Tc-99m will not interfere with the higher energy F-18 photons. However, with 3D PET imaging, the Tc-99m activity can increase dead time and thus decrease the ''true'' counts from the FDG. If FDG PET images are acquired first, then it is necessary to wait at least 15 or more half-lives, depending on the dose of F-18 administered, before a low-energy (e.g., Tl-201 or Tc-99m) SPECT study is performed. This is because the 511 keV photons from the PET tracers easily penetrate the collimators that are commonly used for Tl-201 or Tc-99m imaging.

Dose. Typically, 5-15 mCi is injected in a peripheral vein (see counts requirements below). Injection speed is not critical (i.e., bolus to 2 minutes). To reduce patient dose to the bladder, patients should be encouraged to void frequently for 3-4 hours after the study.

Scan start time and duration. Wait a minimum of 45 minutes before starting the static FDG scan acquisition. Myocardial uptake of FDG may continue to increase, and blood pool activity to decrease, even after 45 minutes. While waiting 90 minutes after the injection of FDG may give better blood pool clearance and myocardial uptake, especially in diabetics or subjects with high blood glucose levels, this comes at the expense of reduced count rate. Scan duration is typically 10-30 minutes. If acquired in 3D mode, compared with 2D mode with the same machine, a smaller dose is typically required to achieve the same total count rate, but the imaging time may or may not be reduced as a result of count rate limitations and increased scatter. In some PET cameras, beyond a certain dose, the 3D mode will actually produce poorer-quality images for the same dose and imaging time than 2D mode. For this reason, it is critical to have fully characterized the performance of the PET system.

IMAGE DISPLAY, NORMALIZATION, AND EVALUATION FOR TECHNICAL ERRORS

Recommendations for display of PET perfusion rest-stress and/or perfusion-metabolism images are consistent with those listed in previous guidelines for SPECT myocardial rest-stress perfusion imaging.[51] It is necessary to examine the transaxial, coronal, and sagittal views for assessing the alignment of the emission images acquired during stress, rest, and metabolism, as well as the transmission images. Fused transmission and emission images are preferred. Images that are not aligned (e.g., due to patient or cardiac motion) may cause serious image artifacts, especially when only one set of attenuation correction images has been applied to all emission images for attenuation correction. This is particularly a problem when CT is used for attenuation correction.[16] It is important that the fusion images be reviewed for potential misalignment problems and appropriate adjustments be made. Some vendors' systems now provide software that allows realignment of transmission CT and emission PET images before processing, and in other instances image data can be transferred to a stand-alone PC that has realignment software.

The reoriented images should be displayed as follows:

1. A short-axis view, by slicing perpendicular to the long axis of the LV from apex (left) to base (right).
2. A vertical long-axis view, by slicing vertically from septum (left) to lateral wall (right).
3. A horizontal long-axis view, by slicing from the inferior (left) to the anterior wall (right).

For interpretation and comparison of perfusion and metabolism images, slices of all data sets should be displayed aligned and adjacent to each other. In the absence of motion artifact, combined assessment of perfusion and metabolism within a single PET session offers the advantage of copying the ventricular long axis defined during image orientation from one image set to the second set, thereby optimizing the matching of the perfusion with the metabolism images. Normalization of the stress and rest perfusion image set is commonly performed by using the maximal myocardial pixel value in each of the two or three image sets; or, for example, the average pixel value with the highest 5% of activity of the perfusion images. Each perfusion study is then normalized to its own maximum.

The metabolism images are normalized to the counts in the same myocardial region on the resting perfusion images (e.g., with the highest count rates that were obtained on the perfusion study).[52,53] An important limitation of this approach, however, is that glucose metabolism may be enhanced or abnormally increased in regions with ''apparently'' normal resting myocardial perfusion, if such regions are subtended by significantly narrowed coronary arteries and are in fact ischemic on stress myocardial perfusion studies.[54] Moreover, visual assessment of resting myocardial uptake of the radiotracer reflects the distribution of myocardial blood flow in ''relative'' terms (i.e., relative to other regions of the LV myocardium) and not in ''absolute'' terms (i.e., mL/min/gm myocardial tissue). Thus, in some patients with multivessel CAD, it is possible that all myocardial regions are in fact hypoperfused at rest in ''absolute'' terms (i.e., termed balanced reduction in blood flow) yet appear normal in ''relative'' terms. If stress images of PET are available, it is recommended that the normal reference region on stress perfusion images be used for normalizing FDG PET images.[35] In the presence of left bundle-branch block (LBBB), where the septal FDG uptake is spuriously decreased, the septum should not be used as the site for normalization. Accordingly, the ECG should be reviewed in conjunction with perfusion/viability imaging.

Standard Segmentation and Polar Map Display

Standard segmentation model divides the LV into three major short-axis slices: apical, mid-cavity, and basal. The apical short-axis slice is divided into four

segments, whereas the mid-cavity and basal slices are divided into six segments. The apex is analyzed separately, usually from a vertical long-axis slice. Although the anatomy of coronary arteries may vary in individual patients, the anterior, septal, and apical segments are usually ascribed to the left anterior descending coronary artery, the inferior and basal septal segments to the right coronary artery, and the lateral segments to the left circumflex coronary artery. The apex can also be supplied by the right coronary and left circumflex artery. Data from the individual short-axis tomograms can be combined to create a polar map display, representing a 2D compilation of all the 3D short-axis perfusion data. Standard 17 segments in the polar map are displayed in Figure 1.[55] The 2D compilation of perfusion and metabolism data can then easily be assigned to specific vascular territories. These derivative polar maps should not be considered a substitute for the examination of the standard short-axis and long-axis cardiac tomographic slices.

3D Display

If suitable software is available, reconstructed myocardial perfusion and metabolism data sets can be displayed in a 3D static or cine mode, which may be convenient for morphologic correlation with angiographic correlation derived from CT, magnetic resonance, or conventional angiography. Some of the software may allow the overlay the coronary anatomy on the 3D reconstructed perfusion and metabolism images of the heart. Currently, an advantage of 3D over conventional 2D displays with regard to accuracy of PET image interpretation has not been demonstrated.

Recommended Medium for Display

It is strongly recommended for the interpreting physician to use the computer monitor rather than film hard copies for interpretation of myocardial perfusion and metabolism images. The latter would be especially important for gated PET images, where dynamic wall motion data is viewed for proper interpretation of regional abnormalities. A linear gray scale, monochromatic color scale, or multicolor scale can be used as the type of display, depending on user experience and preference.

Image Evaluation for Technical Sources of Errors

Patient motion. PET images are typically generated with nonmoving circular arrays of scintillation detectors that acquire all projection data simultaneously. In contrast to SPECT imaging with rotating gamma cameras, in which patient motion leads to a typical misalignment between adjacent projection images and can be identified by viewing a projection movie. Movement during static PET imaging affects all projections and is therefore more difficult to identify. Substantial patient motion can produce blurring of image contours. Therefore, attention to patient motion during image acquisition is essential to minimize motion artifacts.

Patient positioning before and immediately after image acquisition should be carefully evaluated (e.g., by checking the alignment of the camera's positioning laser beams with ink markers on the patient's skin). Acquisition of a brief scan or scout image after injection of a

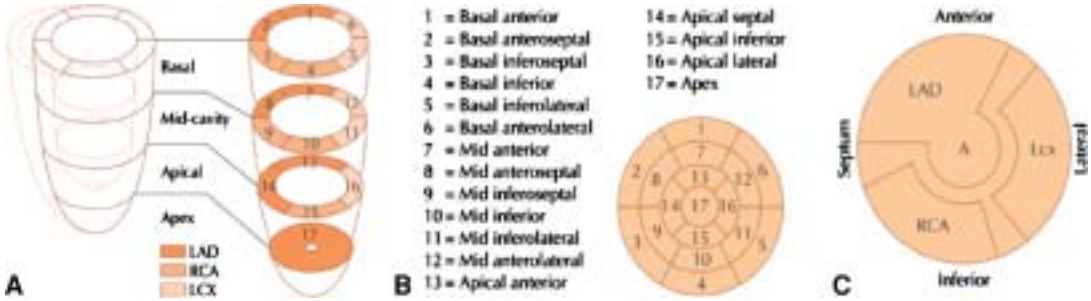

Figure 1. LV Myocardial segmentation, standard nomenclature, and vascular territories. PET images are interpreted on the basis of the presence, location, extent, and severity of myocardial perfusion and metabolic defects using a standard 17-segment model and visual scoring. **A** The standard segmentation model divides the LV into three major short-axis slices: apical, midcavity, and basal. The apical short-axis slice is divided into four segments, whereas the mid-cavity and basal slices are divided into six segments. The apex is analyzed separately, usually from a vertical long-axis slice. **B** Data from the individual short-axis tomograms can be combined to create a polar map plot, representing a 2D compilation of all the 3D short-axis perfusion data. Standard nomenclature for the 17 segments is outlined. **C** The 2D compilation of perfusion data can then easily be assigned to specific vascular territories. (*From* Dilsizian V.; *Reprinted with permission*)[55].

small dose, usually one-third of the standard dose of Rb-82, may facilitate accurate patient positioning. With PET/CT systems, a CT scout scan (10 mA) is routinely used for accurate patient positioning. In instances of patient discomfort and likely patient motion, especially during longer image acquisition times, one approach to reduce adverse effects of motion is to acquire a series of 3-4 sequential image frames instead of a single static image of longer duration. Dynamic imaging would also be effective for this purpose. If the quality of one of the serially acquired frames is compromised by motion, then that frame can be rejected and only frames that are of acceptable quality and are free of motion artifacts are summed for the final image analysis.

Attenuation correction. Correction of the emission images for photon attenuation is critical for cardiac PET imaging. Positron-emitting tracers are more sensitive to attenuation artifacts than single photons. Coincidence detection systems must detect both simultaneously emitted photons. As each of the two photons is susceptible to tissue attenuation, attenuation artifacts are generally greater. Therefore, only attenuation-corrected images should be used for clinical interpretation. Potential sources of errors include misalignment between emission and transmission data resulting from patient motion. Misalignments of 1.5-2 cm, for example, can lead to as much as a 30% change in the observed regional myocardial radioactivity.[10,16,17,56]

Vertical and transaxial displacement of the heart can occur even in the absence of movement of the chest. The latter is perhaps related to the change of breathing pattern, which may occur during pharmacologic stress. This could be thought as analogous to the ''upward creep'' phenomenon seen in SPECT imaging. As a result, under-correction artifacts due to the lower attenuation coefficient of the overlapping lung tissue may appear in the anterior or anterolateral regions, or over-correction artifacts due to the higher attenuation coefficients of the overlapping subdiaphragmatic tissues may appear in the inferior region as ''hot spots.'' Inspection of fused emission-transmission images for possible misalignment is essential because the resulting artifacts would greatly affect image interpretation. Fused images should be inspected in the axial (lateral displacement), coronal (vertical displacement) and sagittal (vertical displacement) slices. Alternatively, displacement can be detected on transaxial images by counting the number of pixels by which the cardiac image is displaced between resting and stress transaxial acquisitions. Identification of vertical and lateral displacements that result in misalignment between the emission and transmission images is relatively straightforward.

The degree of co-registration of transmission and emission images should be carefully examined using the fusion software available on integrated PET/CT systems to assess the reliability of images with attenuation correction. If there is patient motion and the cardiac silhouette does not superimpose perfectly on the transmission and emission images, the images without attenuation correction need to be examined as well. In general, vertical misalignment is easier to resolve by offsetting the alignment between the emission and transmission scans, but this option is not generally available.

When the transmission maps are acquired using CT, the incidental findings in the portion of the chest in the FOV should be reported, when relevant to patient care.

Reconstruction artifacts. Image artifacts may occur if extracardiac activity is present adjacent to the myocardium. For example, intense focal activity in the liver or the gastrointestinal tract may lead to spillover of residual activity from imperfect scatter compensation resulting in artificially elevated counts or cause a reconstruction (i.e., ramp-filter) artifact resulting in artifactually low count rates in adjacent myocardium. A method to correct for such artifacts is currently not available, but such artifacts, particularly the ramp-filter artifact, are less prominent when iterative reconstruction is used instead of the standard FBP techniques. Additional artifacts can result from problems with CT transmission images, such as streaks caused by insufficient x-ray tube intensity in obese individuals, truncations, beam hardening resulting from bone (e.g., arms down) or metal adjacent to the heart (e.g., pacemakers and internal defibrillators), and breathing leading to disconnected pieces of liver in the lungs or misalignment between CT and PET data. CT artifacts are propagated into the PET images through use of the CT image for attenuation and scatter corrections. These artifacts are less of a problem with Cs-137 attenuation correction.

Image count statistics. The final count density of PET images is influenced by additional factors such as body habitus and weight, radionuclide dose, scanner performance, acquisition time, and in the case of metabolic imaging, the dietary and hormonal state. Image count density directly affects the diagnostic quality and reliability of the study.

Image Analysis and Interpretation of PET Images

The rest and stress perfusion and/or metabolism images, should be interpreted initially without clinical information in order to minimize any bias in study interpretation. All relevant clinical data should be reviewed after a preliminary impression is formed.

LV and RV size. The reader should note whether there is an enlargement of the right ventricle (RV) or LV

at rest or whether there is transient stress-induced LV cavity dilation. Ventricular enlargement seen on the stress and rest perfusion or metabolic images generally indicates left, right, or bi-ventricular dysfunction. Transient stress-induced LV dilation usually reflects extensive CAD. LV and RV sizes as well as any changes associated with stress are typically described qualitatively. A number of commercially developed software packages originally developed for SPECT have the ability to quantify mean LV volumes and end-diastolic and end-systolic volumes for gated PET images, but not all such packages have been validated for all PET instruments, and they should be used with caution.

Lung uptake. Increased tracer activity in the lungs should be reported qualitatively. Increased lung uptake on the perfusion images, particularly when severe, may reflect severe LV dysfunction with increased LV end-diastolic and capillary wedge pressures. It can also reflect infiltrative diseases of the lungs, and can be seen in smokers.

RV uptake. Increased RV tracer uptake may be seen both on perfusion and metabolism images in the presence of pulmonary hypertension with or without significant RV hypertrophy. Assessment of increased RV uptake is usually assessed relative to the radiotracer uptake in the LV myocardium. Since the septum is shared by both ventricles, assessment of increased RV uptake should be made in relation to other regions of the LV myocardium. Abnormally increased RV tracer uptake is a qualitative assessment.

Blood pool activity. Visualization of persistent blood pool activity on either perfusion or metabolism images is usually a sign of relatively poor myocardial uptake of the radiotracer, insufficient time for uptake of the radiotracer into the myocardium, or diminished clearance of the radiotracer from blood. A major cause of increased blood pool activity, especially for perfusion imaging with Rb-82, is impairment of cardiac systolic function that prolongs the circulation time. This is especially relevant when only static images are acquired, because vasodilators typically increase cardiac output and shorten the circulation time. Increased blood pool activity may be seen if the acquisition of images begins prior to 70-170 seconds after Rb-82 administration, especially in patients with a history of congestive heart failure and poor LV function. If Rb-82 perfusion images are acquired serially, an appropriate starting point, after blood pool activity has cleared sufficiently, can be chosen after the acquisition for summing the myocardial tracer uptake images. Judicious adjustment of display threshold and contrast settings can help offset this problem. List mode acquisition allows for the re-processing of images with varying delay times and may be useful for optimizing the quality of reconstructed images.

Extra-cardiac findings. The tomographic images should be carefully examined for uptake of the radiotracer in organs other than the myocardium, particularly in the lungs and the mediastinum. Extra-cardiac uptake of a flow tracer may be of clinical significance, as it may be associated with malignancy and/or an inflammatory process. The 3D maximum intensity projection display, a method of displaying acquired PET images as a rotating 3D display, can be particularly helpful in this regard. When using PET/CT systems, review of the low-resolution CT-based transmission scans can be useful to delineate potentially important ancillary findings, such as pleural and pericardial effusion, coronary and/or aortic calcification, breast, mediastinal or lung mass, and others.

Interpretation of PET Perfusion Data

Perfusion defect location. Myocardial perfusion defects should be identified through careful visual analysis of the reoriented myocardial slices. Perfusion defects should be characterized by extent, severity and location relative to the specific myocardial territory, such as the anterior, lateral, inferior, septal, and/or apical walls. Standardized nomenclature should be used, according to previously published guidelines.[51] RV defects due to scarring and ischemia should be noted.

Perfusion defect severity and extent: Qualitative. Defect extent should be qualitatively estimated by describing the location of the abnormal segments involved (e.g., anterior, inferior, or lateral) as well as the extent in the LV (e.g., ''mid-to-distal'' or ''extending from base to the apex''). The extent of the defect may also be qualitatively described as small (5-10% of the LV), medium (10-20% of the LV), or large (>20% of the LV). A defect of more than 10% of the LV is associated with a higher risk of events. Defect severity is typically expressed qualitatively as mild, moderate, or severe. Severe defects may be considered as those having a tracer concentration equal or similar to background activity, and moderate defects are considered definitely abnormal but visually discernable activity above the background. Mild defects are those with a subtle but definite reduction in regional myocardial tracer.

Stress and rest myocardial perfusion image sets are compared in order to determine the presence, extent, and severity of stress-induced perfusion defects and to determine whether such defects represent regions of myocardial ischemia or infarction. Regions with stress-induced perfusion abnormalities, which have normal perfusion at rest, are termed reversible perfusion defects and represent ischemia. Perfusion abnormalities on stress, which remain unchanged on rest images, are

termed irreversible or fixed defects, and most often represent areas of prior myocardial infarction. When both ischemia and scar are present, the defect reversibility is incomplete, giving the appearance of partial reversibility.

Perfusion defect severity and extent: Semiquantitative scoring system. In addition to the qualitative assessment of perfusion defects, a semiquantitative approach based on a validated segmental scoring system has been developed Table 12). This approach standardizes the visual interpretation of scans, reduces the likelihood of overlooking clinically significant defects, and provides a semiquantitative index that is applicable to diagnostic and prognostic assessments.

A 17-segment model for semiquantitative visual analysis is usually employed.[51] The model is based on three short-axis slices (apical, mid, and basal) to represent most of the LV and one vertical long-axis slice to better represent the LV apex. The basal and mid short-axis slices are divided into six segments. The apical short-axis slice is divided into four segments. A single apical segment is taken from the vertical long-axis slice. Each segment has a specific name (Figure 1). The extent of stress and rest perfusion abnormalities, as well as an estimate of the extent of scarring and ischemia, can be performed by counting the number of segments. Myocardial segments may be assigned to coronary artery territories. Caution should be exercised because the coronary anatomy varies widely among patients. For example, it is not at all uncommon to find segments 9, 10, and 15 of the 17-segment model involved in left anterior descending artery disease. Similarly, segments 5 and 11 of the model may be affected by disease of the right coronary artery.

A well-accepted 5-point scale semi-quantitative visual scoring method is used in direct proportion to the observed count density of the segment, as follows: 0 = no defect, 1 = mildly reduced, 2 = moderately reduced, 3 = severely reduced; 4 = absent activity (Table 12). In addition to individual scores, calculation of summed scores is recommended, in which the summed stress score is the sum of the stress scores of all segments, the summed rest score is the sum of the resting scores of all segments, and the summed difference score is the difference between the summed stress and summed rest scores and serves as a measure of reversibility. The summed scores incorporate the global extent and severity of perfusion abnormality. For example, the summed stress score reflects the extent and severity of perfusion defects at stress and is affected by prior myocardial infarction as well as by stress-induced ischemia. On the other hand, the summed rest score reflects the amount of infarcted and/or hibernating myocardium. The summed difference score is a measure of the extent and severity of stress-induced ischemia.

Before scoring, it is necessary for the interpreting physician to be familiar with the normal regional variation in count distribution of myocardial perfusion PET. No regional variation in tracer uptake has been reported for Rb-82, except for a mild reduction in the apex and base of the LV, consistent with segmentation artifact and/or thinning of the LV myocardium in these locations. Regarding N-13 ammonia, unlike Rb-82 and other SPECT perfusion tracers, the lateral wall uptake may not necessarily be the region with the highest counts, serving as the reference region for normalization. This normal variation should be kept in mind when interpreting lateral perfusion defects with N-13 ammonia PET. Given the variability in the normal distribution of various radiotracers, the patient's polar map may be compared with a reference polar map derived from radiotracer and gender-specific normal database. Ideally, each camera system and acquisition protocol should have its own ''normal'' file but such normal databases are not widely available. The semi-quantitative analysis system provided by a specific vendor should be validated by appropriate studies published in peer-reviewed journals.

Absolute quantification of myocardial blood flow. Quantitative blood flow approaches offer an objective interpretation that is inherently more reproducible than visual analysis. Absolute quantification may aid in assessing the physiologic significance of known coronary artery stenosis, especially when of intermediate severity. Both relative and absolute quantification are particularly useful in describing changes between two studies in the same patient. In addition, quantitative measurements of myocardial blood flow may identify balanced reductions in myocardial blood flow due to multivessel CAD or diffuse, small-vessel disease.

Quantitative assessment of myocardial blood flow in absolute units (e.g., mL/min/gm tissue) has been well established in the literature with N-13 ammonia and O-15 water.[31-35,57-59] It requires the acquisition of images in dynamic mode. The use of list mode acquisition now enables flow quantification in conjunction with perfusion and gated LV and regional function. The added value in terms of diagnosis and prognosis is the subject of active investigation in several centers. ROIs are placed on the LV myocardium and the LV blood pool and are copied to all serially acquired images for generation of myocardial tissue and blood pool time-activity curves. The time-activity curves are corrected for activity spillover from the blood pool to the myocardium and for radioactive decay. They are then fitted with a validated tracer kinetic model, and estimates of myocardial blood flow in milliliters of blood per minute per

grams of myocardium are obtained. Software programs are also available for generating parametric polar maps that display regional myocardial blood flows in absolute units.

Oxygen-15-labeled water is often considered the ideal radiotracer for quantifying myocardial blood flow in absolute terms.[57-59] Because the capillary and sarcolemmal membranes do not exert a barrier effect to the exchange of water, the activity of O-15-labeled water observed in an ROI assigned to the myocardium on the serially acquired images can be described by a one-compartment tracer kinetic model. O-15 water is not FDA approved, and therefore, it is not used clinically in the United States. However, it is used in Europe for clinical imaging.

Quantification of myocardial blood flow with Rb-82 has been more challenging because of its 75 second half-life resulting in noisy myocardial and blood pool time activity curves.[60,61] The kinetic behavior of Rb-82 in tissue can be described by a one- or two-compartment model, that can be fitted using the arterial input function (i.e., obtain from the blood pool concentration of the LV cavity or left atrium) and myocardial time-activity curves at each segment, or even (with sufficient statistics) at each pixel.[60,62-65] The parameters of the model, which include flow, can be estimated using non-linear regression or other techniques. The large number of free parameters and the high noise levels frequently encountered in Rb-82 images mean that simultaneous estimation of all parameters cannot always be performed reliably.[66] The variability of flow estimates can be reduced by fixing certain parameters to physiologically realistic values, but the fact that the extraction fraction of Rb-82 is flow dependent remains a challenge for accurate quantification. Semi-quantitative indices of flow, such as dividing the mean tissue uptake over a certain period by the integral of the blood concentration, may prove more practical for routine use. Many of the error sources approximately cancel out when flow reserve is calculated and first-order corrections can be applied for the variable extraction fraction of Rb-82.[67]

Gated PET images. The ability to acquire cardiac PET images in conjunction with ECG gating is an important development that has not always been available, particularly on 3D scanners. Some systems support ECG gating via list-mode acquisition. In such a mode the positions of all coincidence pairs are recorded along with timing information and input from an ECG machine. These data can be retrospectively processed to produce ECG gated images, ungated images, and if necessary, dynamic images, which represent the activity distribution as a function of time. The flexibility of this mode of acquisition is particularly convenient for quantitative analysis.

ECG gating of the rest and peak stress myocardial perfusion images can provide additional information regarding changes in LV function and volumes that may be useful in identifying 3-vessel CAD with or without left main disease, which may be underestimated on the review of the perfusion images.[68] Unlike ECG gating of the post-stress SPECT images, PET acquisitions take place during peak pharmacologic vasodilation, especially when using ultra short-lived tracers like Rb-82 (acquisitions are shorter than those for N-13 ammonia and, thus, more likely to occur while the patient is at peak pharmacological stress).[69,70] ECG gating of FDG PET images can also provide additional information regarding regional and global LV function and volumes.

Assessment of Myocardial Viability

Detection of viable myocardium plays a central role in the management of patients with LV dysfunction due to CAD. It is based on the recognition that resting LV dysfunction may be reversible, attributable to myocardial hibernation/stunning, and not necessarily due to myocardial scar. As a consequence, its presence signifies a different prognosis and mandates a different treatment paradigm compared with the presence of predominantly non-viable or irreversible damaged tissue. Indeed, the importance of differentiating viable from non-viable tissue is highlighted by the plethora of techniques currently available to perform this task. Myocardial metabolism imaging with PET and FDG uses the preservation of myocardial glucose metabolism, particularly in the presence of resting hypoperfusion as a scintigraphic marker of viable myocardium. It is accomplished with FDG as a tracer of exogenous glucose utilization. The regional myocardial concentrations of this tracer are compared with the regional distribution of myocardial perfusion. Regional increases in FDG uptake relative to regional myocardial blood flow (i.e., perfusion-metabolism mismatch) signify myocardial viability. In contrast, a regional reduction in FDG uptake in proportion to regional reductions in myocardial perfusion (i.e., perfusion-metabolism match) signifies myocardial scar or nonviable tissue. Areas with maintained perfusion, but diminished FDG uptake, also likely reflect regions of jeopardized but viable myocardium since the perfusion tracers reflect active metabolic trapping.

Comparison of myocardial metabolism to perfusion. The comparison of perfusion and metabolism images obtained with PET is relatively straightforward because both image sets are attenuation-corrected. Thus, a relative increase in myocardial metabolism in regions of reduced perfusion by one grade or more, reflect the presence of perfusion-metabolism

mismatch, hence myocardial viability. In contrast, relative decrease in myocardial metabolism that is in proportion to reductions in regional perfusion reflects the presence of perfusion-metabolism match, hence myocardial scar or nonviable tissue.

Special considerations for combining SPECT perfusion with PET metabolism images. In current clinical practice, FDG PET images are often read in combination with SPECT myocardial perfusion images. The interpreting physician should be careful when comparing the non-attenuation-corrected SPECT images with attenuation-corrected FDG PET images. Myocardial regions showing an excessive reduction in tracer concentration as a result of attenuation artifacts, such as the inferior wall in men or the anterior wall in female subjects, may be interpreted as perfusion-metabolism mismatches, resulting in falsely positive perfusion-metabolism mismatches. Two approaches have proved useful for overcoming this limitation:

1. Because assessment of viability is relevant only in myocardium with regional contractile dysfunction, gated SPECT or PET images offer means for determining whether apparent perfusion defects are associated with abnormal regional wall motion.
2. Quantitative analysis with polar map displays that are compared with tracer- and gender-specific databases (for SPECT images) may be a useful aid to the visual interpretation. SPECT perfusion images with attenuation correction are helpful as well.[71,72] However, neither approach is infallible.

For myocardial FDG images acquired with ultra high-energy collimators or with SPECT-like coincidence detection systems, additional problems may be encountered, especially when the images are not corrected for photon attenuation.[73-75] Myocardial regions with severely reduced tracer activity concentrations due to attenuation artifacts on both perfusion and metabolism imaging, such as the inferior wall in men or the anterior wall in women, may be interpreted erroneously as perfusion-metabolism matches. Attenuation of the high-energy 511-keV photons is less than that for the 140-keV photons of Tc-99m or the 60- to 80-keV photons of Tl-201 so that attenuation artifacts are less prominent for FDG images and may result in an apparent mismatch. Furthermore, the lower spatial resolution of SPECT imaging systems for FDG imaging, especially when using high-energy photon collimation and then comparing with Tc-99m or Tl-201 images, causes apparent mismatches for small defects, at the base of the LV, or at the edges or borders of large perfusion defects. Such artifacts resulting from the use of different photon energies can be avoided by using dedicated PET systems for both perfusion and metabolism imaging. Again, use of ECG-gated imaging to demonstrate normal wall motion, quantitative analysis through polar map displays with comparison to radiotracer- and gender-specific databases of normal may aid in the visual interpretation.

Absolute myocardial glucose utilization. Quantitative estimates of myocardial glucose utilization in absolute units of micromoles of glucose per minute per grams of myocardium have not been found to aid in the assessment or characterization of myocardial viability due to the variability in substrate utilization by the myocardium, even when FDG images are acquired during a hyperinsulinemic-euglycemic clamp.[46,47,76] Methods for deriving quantitative estimates of myocardial metabolism require acquisition of serial images for 60 minutes that begin with tracer injection.[42,43] ROIs are placed on the myocardium and the LV blood pool and are copied to all serially acquired images in order to generate myocardial tissue and blood pool time-activity curves. The time-activity curves are corrected for spillover of activity from the blood pool into the myocardium and for radioactive decay. The time-activity curves are then fitted with a validated tracer kinetic model, and estimates of regional myocardial glucose utilization are obtained in micromoles of glucose per minute per grams of myocardium. Measurements of glucose metabolic rates further require determination of glucose concentrations in arterial or arterialized venous blood. Similar to myocardial perfusion, parametric images and polar maps are also available for display of rates of regional myocardial glucose utilization. Regional metabolic rates on such parametric images are coded by a color scale and can be determined noninvasively for any myocardial region through ROIs assigned to the polar map.[77]

Integration of perfusion and metabolism results. The combined evaluation of regional myocardial perfusion and FDG metabolism images allows identification of specific flow-metabolism patterns that are useful to differentiate viable from nonviable myocardium. It is useful to start with a functional assessment, ideally from gated PET or SPECT imaging, as dysfunctional segments are those suitable for evaluation of myocardial viability. If stress perfusion images as well as resting perfusion images are available, jeopardized myocardium can be distinguished from normal myocardium, and myocardium perfused normally at rest but dysfunctional as a result of repetitive stunning can be distinguished from myopathic or remodeled myocardium.

Differences in blood pool concentration of tracers can impact on the apparent match or mismatch of perfusion-FDG images. The separate adjustment of

threshold and contrast settings can help compensate for these discrepancies.

Four distinct resting perfusion-metabolism patterns may be observed in dysfunctional myocardium:[78-83]

1. Normal blood flow associated with normal FDG uptake.
2. Reduced blood flow associated with preserved or enhanced FDG uptake (perfusion-metabolism mismatch).
3. Normal or near-normal blood flow with reduced FDG uptake (reversed perfusion-metabolism mismatch).
4. Proportionally reduced blood flow and FDG uptake (perfusion-metabolism match).

The patterns 1-3 are all indicative of viable myocardium whereas pattern 4 represents nonviable tissue.

Some laboratories have added a fifth pattern, a mild perfusion-metabolism match in which the regional uptake of both the tracer of blood flow and of FDG is mildly to moderately reduced.[80,81,84] Because contractile function in such ''mild'' matches generally does not improve after revascularization, the pattern is subsequently included in the general category of perfusion-metabolism matches. If stress and rest perfusion imaging information is available, it is useful to add an estimate of the extent of stress-inducible ischemia in regions of normal resting perfusion and FDG uptake, in regions with matched resting perfusion-FDG defects, or in regions with resting perfusion FDG-metabolic mismatch. The simultaneous display of stress and rest perfusion and FDG metabolic images is most helpful but not available on all display workstations. In circumstances where only resting perfusion imaging is performed alongside FDG metabolic imaging, besides reporting on the extent of scar and extent of hibernating myocardium, it is useful to indicate that in the absence of corresponding stress myocardial perfusion images, one cannot rule out stress-induced myocardial ischemia.

In circumstances where only stress perfusion imaging is available in combination with FDG metabolic imaging, the following patterns can be found in segments with contractile dysfunction:

1. Stress perfusion defect with preserved FDG uptake indicates ischemic but viable myocardium. Revascularization is generally appropriate since myocardial ischemia is a very strong predictor for recovery of perfusion and function after a successful revascularization. With stress perfusion and FDG metabolic paired images, it is not possible to differentiate between myocardial ischemia, stunning, and hibernation.
2. Stress perfusion defects associated with proportionately decreased or lack of FDG uptake indicate scarred or nonviable myocardium, and revascularization is not recommended.

Qualitative or semiquantitative approaches can be applied to the interpretation of perfusion-metabolism patterns. When comparing FDG metabolism with perfusion images, it is important to first identify the normal reference region (the region with the highest tracer uptake), preferably on the stress myocardial perfusion images. The extent of mismatch or match defect may be small (5-10% of the LV), moderate (10-20% of the LV), or large (>20% of the LV). The severity of a match defect can be expressed as mild, moderate, or severe in order to differentiate between nontransmural and transmural myocardial infarction.

Interpretation of FDG images when perfusion images have not been obtained. Interpretation of FDG images without perfusion images and/or angiographic information and/or without information on regional wall motion is discouraged. The presence of relatively well-preserved FDG uptake in dysfunctional myocardium does not differentiate ischemic from non-ischemic cardiomyopathy. The degree of FDG accumulation over and above regional perfusion helps to assess the relative amount of scar and metabolically viable myocardium. The latter information may significantly influence the power of the test for predicting functional recovery. Therefore, it is recommended that FDG metabolic images be analyzed in conjunction with perfusion images, obtained either with SPECT or, preferably, with PET.

REPORTING OF MYOCARDIAL PERFUSION AND METABOLISM PET STUDIES

Patient Information

The report should start with the date of the study, patient's age, sex, height, and weight or body surface area, as well as the patient's medical identification number.

Indication for Study

Understanding the reason(s) why the study was requested, aids in focusing the study interpretation on the clinical question asked by the referring clinician. In addition, a clear statement for the indication of the study has become an important component of billing for services rendered.

History and Key Clinical Findings

A brief description of the patient's clinical history and findings can contribute to a more appropriate and

comprehensive interpretation of the rest (and stress) perfusion and of the metabolism images. This information may include past myocardial infarctions and their location, revascularization procedures, the patient's angina-related and congestive heart failure-related symptoms, presence of diabetes or hypertension, and other coronary risk factors. Information on regional and global LV function can similarly be important for the interpretation of regional perfusion and metabolism patterns.

A description of the ECG findings may serve as an aid in the study interpretation, such as the presence of Q waves and their location or conduction abnormalities (e.g., LBBB) for exploring septal perfusion and/or metabolic abnormalities.

Type of Study

The imaging protocols should be stated concisely. This should include the type of camera utilized for imaging myocardial perfusion and/or metabolism, for example, PET or PET/CT system, or SPECT perfusion and FDG PET metabolism. For stress myocardial perfusion PET studies, the type of stressor should be clearly indicated, such as treadmill, dipyridamole, adenosine, A2A adenosine receptor agonist, or dobutamine. Radiopharmaceuticals and their radioactivity doses used for the perfusion and the metabolism PET imaging studies should be identified. The acquisition modes and image sequences should be described, such as static or dynamic image acquisition, for stress and rest perfusion imaging, perfusion and metabolism imaging on different days, and the use of gating.

The main body of the report following this introductory descriptive information should then be tailored to the specific clinical question asked by the referring clinician and the procedural approach chosen for answering this question. For example, the report for a stress-rest myocardial PET perfusion study will be different from a report describing and interpreting a myocardial perfusion and myocardial metabolism study. Similarly, the report for a study that includes a stress and rest myocardial perfusion study along with a myocardial metabolism study should be different.

Summary of Stress Data

If myocardial perfusion has been evaluated during stress, the type of the stressor, the stress agent, the dose, route of administration, and time of infusion should be specified. Side effects and symptoms experienced during stress should be reported. If pharmacologic stress was discontinued prematurely, the reasons should be provided.

Hemodynamic and ECG responses during the stress study, including changes in heart rate, blood pressure, development of arrhythmias, conduction abnormalities, and ST-T wave changes and their location should be detailed. Symptoms such as chest pain, shortness of breath, and others during the administration of the stressor and in the recovery phase should be documented.

Summary of Clinical Laboratory Data and Dietary State

Information about the dietary state (e.g., fasting or post-prandial) and about interventions for manipulating plasma glucose levels through, for example, oral or IV administration of glucose or use of the euglycemic hyperinsulinemic clamp, should be given. If pharmacologic measures, such as nicotinic acid derivatives, have been used, this should be described. Furthermore, BG levels, if obtained at baseline or after intervention, should be listed, as they are useful for the interpretation of the metabolic images. If there is an expected abnormal response to a glucose load, this should also be reported.

Image Description and Interpretation: Perfusion

A statement regarding image quality is important. Reduced quality may affect the accuracy of the interpretation. If the cause of the reduced quality is known or suspected, then it should be stated accordingly. This information may prove useful when repeat images are obtained in the same patient.

The report should first describe the relative distribution of the perfusion tracer on the stress images and provide details on regions with decreased radiotracer uptake in terms of the location, extent, and severity of defects. The authors should then describe whether regional myocardial defects seen on stress images become reversible or persist on the corresponding paired rest images. Other findings, such as LV cavity dilatation at rest, transient (stress-induced) LV cavity dilation, lung uptake, concentric LV hypertrophy, asymmetric septal hypertrophy, pericardial photopenia, prominent RV cavity size and hypertrophy, and extra-cardiac abnormalities, should be included in the report. Regional and global LV function should be described from gated PET perfusion and/or metabolism images. The scintigraphic pattern on the stress/rest myocardial perfusion images should then be reported in clinical terms as:

1. Normal.
2. Ischemic.

3. Scarred with/without a history of prior myocardial infarction.
4. An admixture of scarred and ischemic but viable myocardium.
5. Non-ischemic cardiomyopathy.

Quantitative assessment of absolute regional myocardial blood flow is limited to only a few centers with extensive local expertise. Thus, reporting of myocardial blood flow in absolute terms should be made with caution, since FDA approved software for general clinical use is not available at the present time.

Image Description and Interpretation: Metabolism

The report should describe the relative distribution of myocardial perfusion at rest, and the location, extent, and severity of regional perfusion defects. The report should continue with a description of the FDG uptake in the myocardium and indicate the tracer activity concentrations in normally perfused and in hypoperfused myocardium. The adequacy of achieving a glucose-loaded state, as evident from the radiotracer uptake in normally perfused myocardium and also from blood pool activity, should then be reported and be related to the presence of insulin resistance, including impaired glucose tolerance and Type 2 diabetes. This should be related to the residual blood pool activity as additional evidence for inadequate clearance of FDG from blood into tissue and provide the information for low tracer uptake in normally perfused myocardium. Segments with regional dysfunction that exhibit patterns of viable myocardium (i.e., preserved perfusion or decreased perfusion with either preserved or increased FDG uptake) should be identified. Similar reporting should be performed for segments exhibiting a flow-metabolism matched pattern, that is, decreased regional FDG uptake in proportion to decreased regional myocardial perfusion. The presence of viable and non-viable tissue should be reported as a continuum (e.g., predominantly viable or admixture of viable and non-viable tissue).

Findings on semiquantitative or quantitative image analysis approaches may be added. Location and, in particular, extent of viable and non-viable tissue, expressed as a percentage of the LV, is important because it provides important prognostic information on future cardiac events and predictive information on potential outcomes in regional and global LV function, congestive heart failure-related symptoms, and long-term survival after revascularization. Finally, the description of the perfusion-metabolism findings may include a correlation to regional wall motion abnormalities and should indicate the potential for a post-revascularization improvement in the regional and global LV function. The potential for outcome benefit may also be reported.

Final Interpretation

Results should be succinctly summarized and first address whether the study is normal or abnormal. On rare occasions where a definitive conclusion cannot be made, the interpreter should aid the referring clinician by suggesting other tests that may provide further insight into the clinical dilemma. The report should always take into consideration the clinical question that is being asked: is the study requested for CAD detection or myocardial viability assessment? Any potential confounding artifacts or other quality concerns that significantly impact the clinical interpretation of the PET study should be mentioned.

A statement on the extent and severity of perfusion defects, reversibility and mismatch in relation to FDG metabolism, and their implication regarding ischemia, scar, or hibernating myocardium should be made. It may be useful to conclude the report with a summary of the extent and location of myocardial ischemia in relation to vascular territories, as well as the presence and extent of perfusion-metabolism mismatch in patients with chronic ischemic LV dysfunction. LV cavity size, function, and regional wall motion should be reported at rest and during stress with special note of transient ischemic cavity dilatation, if present. A statement as to the implication of the findings should be made.

Comparison should be made to prior studies, and interim changes regarding the presence and extent of myocardial ischemia, scar, or hibernation should be highlighted. On the basis of the scintigraphic findings (e.g., extent of perfusion-metabolism mismatch), the likelihood of recovery of function after revascularization can be estimated. The potential for a post-revascularization improvement in contractile function is low for perfusion-metabolism matched defects, even if the regional reductions in perfusion and in FDG uptake are only mild or moderate. Conversely, the potential for improvements in regional contractile dysfunction is high if perfusion is normal, if both perfusion and FDG uptake are normal, or if FDG uptake is significantly greater than regional perfusion (i.e., mismatch). Finally, the potential of a post-revascularization improvement in the LVEF by at least 5 or more EF units is high if the mismatch affects 20% or more of the LV myocardium.[83,85] Although lesser amounts of mismatch (5-20% of the LV myocardium) may also have potential outcome benefit, with or without improvement in the LVEF.[86,87] The latter may be included in the report at the reporting physician's discretion.

If additional diagnostic clarification seems needed, the physician may recommend an alternative modality. If a CT transmission scan was performed for attenuation correction, clinically relevant CT findings must be reported.

Acknowledgments

Dominique Delbeke, MD, PhD is a consultant for GE Healthcare and Spectrum Dynamics. Stephen L. Bacharach, PhD receives grant support from Siemens Medical Solutions and Philips Healthcare.

Publication and distribution of this document are made possible by corporate support from Bracco Diagnostics Inc.

APPENDIX 1. SAMPLE IV PROTOCOL: PROTOCOL A

A sample protocol for IV glucose loading is presented. This protocol is based on one in use at Vanderbilt University Medical Center, Nashville, TN, and is adapted from Martin et al[48]

1. IV glucose/insulin loading for nondiabetic patients with a BG level <110 mg/dL (<6.11 mmol/L) under fasting condition.
   a. Prepare dextrose/insulin solution: 15 U of regular insulin in 500 mL of 20% dextrose in a glass bottle. The initial 50 mL is discarded through the plastic IV tubing (no filter) to decrease adsorption of the insulin to the tubing.
   b. Prime the patient with 5 U of regular insulin and 50 mL of 20% dextrose (10 g) IV bolus.
   c. Infuse dextrose/insulin solution at a rate of 3 mL · kg^{-1} · h^{-1} for 60 minutes (corresponding to an insulin infusion of 1.5 mU · kg^{-1} · min^{-1} and a glucose infusion of 10 mg · kg^{-1} · min^{-1}). Monitor BG every 10 minutes (goal BG, 100-200 mg/dL [5.56-11.11 mmol/L]).
   d. If BG at 20 min is 100-200 mg/dL (5.56-11.11 mmol/L), preferably <150 mg/dL (8.33 mmol/L), administer FDG intravenously.
   e. If BG is >200 mg/dL (>11.11 mmol/L), administer small IV boluses of 4-8 U of regular insulin until BG decreases to <200 mg/dL (<11.11 mmol/L). Administer FDG intravenously.
   f. Stop dextrose/insulin infusion at 60 minutes and start 20% dextrose at 2-3 mL · kg^{-1} · h^{-1}.
   g. During image acquisition, continue infusion of 20% dextrose at 2-3 mL · kg^{-1} · h^{-1}.
   h. At completion of the acquisition of the images, discontinue infusion, give a snack to the patient, and advise him or her regarding the risk of late hypoglycemia.
   i. ALERT: (1) If BG is >400 mg/dL (>22.22 mmol/L), call the supervising physician immediately. (2) If BG is <55 mg/dL (<3.06 mmol/L) or if the patient develops symptoms of hypoglycemia with BG < 75 mg/dL (<4.17 mmol/L), discontinue dextrose/insulin infusion, administer one amp of 50% dextrose intravenously, and call the supervising physician.
2. IV glucose/insulin loading for diabetic patients or fasting BG is >110 mg/dL (>6.11 mmol/L):
   a. Prepare insulin solution: 100 U of regular insulin in 500 mL of normal saline solution in a glass bottle. The initial 50 mL is discarded through the plastic IV tubing (no filter) to decrease adsorption of the insulin to the tubing.
   b. Prime patient with regular insulin: If fasting BG is >140 mg/dL (>7.76 mmol/L), prime the patient with 10 U of regular insulin IV bolus. If fasting BG is <140 mg/dL (<7.76 mmol/L), prime the patient with 6 U of regular insulin IV bolus.
   c. Infuse insulin solution at a rate of 1.2 mL · kg^{-1} · h^{-1} for 60 minutes (corresponding to an insulin infusion of 4 mU · kg^{-1} · min^{-1}) or for the entire study (to calculate the regional glucose utilization rate).
   d. After 8-10 minutes or when BG is <140 mg/dL (<7.76 mmol/L), start 20% dextrose infusion at 1.8 mL · kg^{-1} · h^{-1} (corresponding to a dextrose infusion of 6 mg · kg^{-1} · min^{-1}).
   e. Monitor BG every 5-10 minutes and adjust dextrose infusion rate to maintain BG at 80-140 mg/dL (4.44-7.76 mmol/L).
   f. After 20-30 minutes of stable BG, administer FDG.
   g. Maintain the IV infusion of insulin plus 20% dextrose for 30-40 minutes after FDG injection or until the end of the scan (to calculate rMGU [rate of glucose utilization]). Some centers confirm FDG uptake particularly in patients with diabetes before discontinuing the clamp.
   h. At completion of the acquisition of the images, discontinue infusion, give a snack to the patient, and advise him or her regarding the risk of late hypoglycemia.
3. For lean patients with type 1 juvenile-onset diabetes mellitus, apply the following protocol:
   1. If fasting BG is <140 mg/dL (<7.76 mmol/L), inject 4 U of regular insulin and infuse insulin solution at 0.3 mL · kg^{-1} · h^{-1} (1 mU · kg^{-1} ·min^{-1}).
   2. After 8-10 minutes of infusion or when BG is <140 mg/dL (<7.76 mmol/L), start 20% dextrose at 2.4 mL · kg^{-1} · h^{-1} (8 mg · kg^{-1} · min^{-1}).

4. Some centers (Munich, Ottawa, and others) have also applied a front-loaded infusion.

    1. About 6 hours after a light breakfast and their usual dose of insulin or oral hypoglycemic, all diabetic patients have a catheter inserted in one arm for glucose and insulin infusion, as well as a catheter in the opposite arm for BG measurement.
    2. At time 0, the insulin infusion is started. Regular insulin is given at 4 times the final constant rate[88] for 4 minutes, then at 2 times the final constant rate for 3 minutes, then at a constant rate for the remainder of the study.
    3. If the BG is >200 mg/dL (>11.11 mmol/L), an additional bolus of insulin is given. An exogenous 20% glucose infusion is started at an initial rate of 0.25 mg $\cdot$ kg^{-1} $\cdot$ min^{-1} and adjusted until steady state is achieved. The BG concentrations are measured every 5 minutes during the insulin clamp. The glucose infusion is adjusted according to the plasma glucose over the preceding 5 minutes.

APPENDIX 2. SAMPLE IV PROTOCOL: PROTOCOL B

A sample protocol for IV glucose loading is presented. Protocol B is based on the protocol in use at the Emory University-Crawford Long Memorial Hospital (Atlanta, GA).[89] This protocol has been used in over 600 subjects (over one-third of whom were diabetic), resulting in good-quality images in over 98% of studies.

1. If fasting BG is <125 mg/dL (<6.94 mmol/L), give 50% dextrose in water (D-50-W), 25 g, intravenously. Hydrocortisone, 20 mg, should be added to the D-50-W to minimize the rather severe pain that can occur at the injection site with D-50-W. This is compatible and avoids the pain that limits patient cooperation. There is no negative effect on the quality of the FDG studies.
2. If fasting BG is between 125-225 mg/dL (6.94-12.5 mmol/L), give D-50-W, 13 g, intravenously.
3. If fasting BG is >225 mg/dL (>12.5 mmol/L), administer regular aqueous insulin as per the following formula: Regular aqueous insulin (dose units) = (BG − 50)/25.
4. After 30-60 minutes, if BG is less than 150 mg/dL (8.33 mmol/L), give FDG intravenously, but if BG is >150 mg/dL (>8.33 mmol/L), give more regular insulin, until BG is <150 mg/dL (<8.33 mmol/L), before giving FDG. Giving FDG when BG is 150-200 mg/dL (8.33-11.11 mmol/L) resulted in many poor-quality studies.

References

1. Zanzonico P. Positron emission tomography: A review of basic principles, scanner design and performance, and current systems. Semin Nucl Med 2004;34:87-111.
2. Machac J, Bacharach SL, Bateman TM, et al. Imaging guidelines for nuclear cardiology procedures: Positron emission tomography myocardial perfusion and glucose metabolism imaging. J Nucl Cardiol 2006;13:e121-51.
3. National Electrical Manufacturers Association. NEMA standards publication NU 2-1994: Performance measurements of positron emission tomographs. Washington, DC: National Electrical Manufacturers Association; 1994.
4. National Electrical Manufacturers Association. NEMA standards publication NU 2-2001: Performance measurements of positron emission tomographs. Washington, DC: National Electrical Manufacturers Association; 2001.
5. National Electrical Manufacturers Association. NEMA standards publication NU 2–2007: Performance measurements of positron emission tomographs. Rosslyn, VA: National Electrical Manufacturers Association; 2007.
6. deKemp RA, Yoshinaga K, Beanlands RS. Will 3D PET enable routine quantification of myocardial blood flow? J Nucl Cardiol 2007;14:380-97.
7. Ter-Pogossian MM, Ficke DC, Yamamoto M. PET I: A positron emission tomograph utilizing photon time-of-flight information. IEEE Trans Med Imaging 1982;1:179-87.
8. Yamamoto M, Ficke DC, Ter-Pogossian MM. Experimental assessment of the gain achieved by the utilization of time-of-flight information in a positron emission tomograph (Super PETT I). IEEE Trans Med Imaging 1982;1:187-92.
9. Lewellan TK. Time-of-flight PET. Semin Nucl Med 1998;28:268-75.
10. Le Meunier L, Maass-Moreno R, Carrasquillo JA, Dieckmann W, Bacharach SL. PET/CT imaging: Effect of respiratory motion on apparent myocardial uptake. J Nucl Cardiol 2006;13:821-30.
11. International Electrotechnical Commission. Radionuclide imaging devices–characteristics and test conditions. Part 1: Positron emission tomographs. Geneva; 1998.
12. American College of Radiology. ACR Web site. http://www.acr.org. Accessed 2 March 2009.
13. American Association of Physicists in Medicine. AAPM Web site. http://www.aapm.org. Accessed 2 March 2009.
14. Sampson UK, Dorbala S, Limaye A, et al. Diagnostic accuracy of rubidium-82 myocardial perfusion imaging with hybrid positron emission tomography/computed tomography in the detection of coronary artery disease. J Am Coll Cardiol 2007;49:1052-8.
15. Slomka PJ, LeMunier L, Hayes SW. Comparison of myocardial perfusion Rb-82 PET performed with CT- and transmission CT-based attenuation correction. J Nucl Med 2008;49:1992-8.
16. Gould KL, Pan T, Loughin C, Johnson NP, Guha A, Sdringola S. Frequent diagnostic errors in cardiac PET/CT due to misregistration of CT attenuation and emission PET images: A definitive analysis of causes, consequences and corrections. J Nucl Med 2007;48:1112-21.
17. Loghin C, Sdringola S, Gould K. Common artifacts in PET myocardial perfusion images due to attenuation-emission misregistration: Clinical significance, causes, and solution. J Nucl Med 2004;45:1029-39.
18. Alessio AM, Kohlmyer S, Branch K, et al. Cine CT for attenuation correction in cardiac PET/CT. J Nucl Med 2007;48:794-801.
19. Souvatzoglou M, Bengel F, Busch R, et al. Attenuation correction in cardiac PET/CT with three different CT protocols: A

comparison with conventional PET. Eur J Nucl Med Mol Imaging 2007;34:1991-2000.
20. DiFilippo FP, Brunken RC. Do implanted pacemaker leads and ICD leads cause metal-related artifact in cardiac PET/CT? J Nucl Med 2005;46:436-43.
21. Greenland P, Bonow RO, Brundage BH, et al. ACCF/AHA 2007 clinical expert consensus document on coronary artery calcium scoring by computed tomography in global cardiovascular risk assessment and in evaluation of patients with chest pain: A report of the American College of Cardiology Foundation Clinical Expert Consensus Task Force. J Am Coll Cardiol 2007;49:378-402.
22. Hamill JJ, Brunken RC, Bybel B, DiFilippo FP, Faul DD. A knowledge-based method for reducing attenuation artifacts caused by cardiac appliances in myocardial PET/CT. Phys Med Biol 2006;51:2901-18.
23. Henzlova MJ, Cerqueira MD, Hansen CL, Taillefer R, Yao S. Imaging guidelines for nuclear cardiology procedures: Stress protocols and tracers. J Nucl Cardiol 2009;16. doi: 10.1007/s12350-009-9062-4.
24. Beanlands RS, Chow BJW, Dick A, et al. CCS/CAR/CANM/CNCS/CanSCMR joint position statement on advanced noninvasive cardiac imaging using positron emission tomography, magnetic resonance imaging n multi-detector computed tomographic angiography in the diagnosis and evaluation of ischemic heart disease—executive summary. Can J Cardiol 2007;23:107-19.
25. Bateman TM, Friedman JD, Heller GV, et al. Diagnostic accuracy of rest/stress ECG-gated Rb-82 myocardial perfusion PET: Comparison with ECG-gated Tc-99m sestamibi SPECT. J Nucl Cardiol 2006;13:24-33.
26. Love WD, Burch GE. Influence of the rate of coronary plasma on the extraction of rubidium-86 from coronary blood. Circ Res 1959;7:24-30.
27. Selwyn AP, Allan RM, L'Abbate A, et al. Relation between regional myocardial uptake of rubidium-82 and perfusion: Absolute reduction of cation uptake in ischemia. Am J Cardiol 1982;50:112-21.
28. Goldstein RA, Mullani NA, Marani SK, et al. Myocardial perfusion with rubidium-82. II. Effects of metabolic and pharmacologic interventions. J Nucl Med 1983;24:907-15.
29. Stabin MG. Radiopharmaceuticals for nuclear cardiology: Radiation dosimetry, uncertainities and risk. J Nucl Med. 2008;49:1555–63.
30. Camici PG, Araujo LI, Spinks T, et al. Increased uptake of 18F-fluorodeoxyglucose in postischemic myocardium of patients with exercise-induced angina. Circulation 1986;74:81-8.
31. Chow BJW, Ananthasubramaniam K, deKemp RA, et al. Comparison of treadmill exercise versus dipyridamole stress with myocardial perfusion imaging using rubidium-82 positron emission tomography. J Am Coll Cardiol 2005;45:1227-34.
32. Hutchins GD, Schwaiger M, Rosenspire KC, et al. Noninvasive quantification of regional blood flow in the human heart using N-13 ammonia and dynamic positron emission tomographic imaging. J Am Coll Cardiol 1990;15:1032-42.
33. Krivokapich J, Smith GT, Huang SC, et al. 13 N ammonia myocardial imaging at rest and with exercise in normal volunteers. Quantification of absolute myocardial perfusion with dynamic positron emission tomography. Circulation 1989;80:1328-37.
34. Bergmann SR, Hack S, Tewson T, Welch MJ, Sobel BE. The dependence of accumulation of N-13 ammonia by myocardium on metabolic factors and its implications for quantitative assessment of perfusion. Circulation 1980;61:34-43.
35. Krivokapich J, Huang S-C, Phelps ME, MacDonald NS, Shine KI. Dependence of N-13 ammonia myocardial extraction and clearance on flow and metabolism. Am J Physiol: Heart Circ Physiol 1982;242:H536-42.
36. Kitsiou AN, Bacharach SL, Bartlett ML, et al. 13 N ammonia myocardial blood flow and uptake: Relation to functional outcome of asynergic regions after revascularization. J Am Coll Cardiol 1999;33:678-86.
37. Schelbert HR, Phelps ME, Huang SC, et al. N-13 ammonia as an indicator of myocardial blood flow. Circulation 1981;63:1259-72.
38. International Commission on Radiological Protection. Radiation dose to patients from radiopharmaceuticals. ICRP Publication 80. Ann ICRP 2000;28:113.
39. International Commission on Radiological Protection. Radiation dose to patients from radiopharmaceuticals. ICRP Publication 53. Ann ICRP 1988;18:62.
40. Neely JR, Rovetto MJ, Oram JF. Myocardial utilization of carbohydrate and lipids. Prog Cardiovasc Dis 1972;15:289-329.
41. Gallagher BM, Ansari A, Atkins H, et al. Radiopharmaceuticals XXVII. F-18-labeled 2-deoxy-2-fluoro-D-glucose as a radiopharmaceutical for measuring regional myocardial glucose metabolism in vivo: Tissue distribution and imaging studies in animals. J Nucl Med 1977;18:990-6.
42. Ratib O, Phelps ME, Huang SC, et al. Positron tomography with deoxyglucose for estimating local myocardial glucose metabolism. J Nucl Med 1982;23:577-86.
43. Hamacher K, Coenen HH, Stauocklin G. Efficient sterospecific synthesis of no-carrier-added 2-[F-18]-fluoro-2-deoxy-D-glucose using aminopolyether supported nucleophilic substitution. J Nucl Med 1986;27:235-8.
44. CDE Inc. Dosimetry Services. Dose estimates: Adult. http://www.internaldosimetry.com/freedosestimates/adult/index.html. Published 2001. Accessed 15 January 2009.
45. Ohtake T, Yokoyama I, Watanabe T, et al. Myocardial glucose-metabolism in noninsulin-dependent diabetes-mellitus patients evaluated by FDG-PET. J Nucl Med 1995;36:456-63.
46. Vitale GD, deKemp RA, Ruddy TD, Williams K, Beanlands RS. Myocardial glucose utilization and optimization of (18)F-FDG PET imaging in patients with non-insulin-dependent diabetes mellitus, coronary artery disease, and left ventricular dysfunction. J Nucl Med 2001;42:1730-6.
47. Knuuti MJ, Nuutila P, Ruotsalainen U, et al. Euglycemic hyperinsulinemic clamp and oral glucose load in stimulating myocardial glucose utilization during positron emission tomography. J Nucl Med 1992;33:1255-62.
48. Martin WH, Jones RC, Delbeke D, Sandler MP. A simplified intravenous glucose loading protocol for fluorine-18 fluorodeoxyglucose cardiac single-photon emission tomography. Eur J Nucl Med 1997;24:1291-7.
49. Gropler RJ, Siegel BA, Lee KJ, et al. Nonuniformity in myocardial accumulation of fluorine-18-fluorodeoxyglucose in normal fasted humans. J Nucl Med 1990;31:1749-56.
50. Bax JJ, Veening MA, Visser FC, et al. Optimal metabolic conditions during fluorine-18 fluorodeoxyglucose imaging; a comparative study using different protocols. Eur J Nucl Med 1997;24:35-41.
51. Cerqueira MD, Weissman NJ, Dilsizian V, et al. Standardized myocardial segmentation and nomenclature for tomographic imaging of the heart: A statement for healthcare professionals from the Cardiac Imaging Committee of the Council on Clinical Cardiology of the American Heart Association. J Nucl Cardiol 2002;9:240-5.
52. Porenta G, Kuhle W, Czernin J, et al. Semiquantitative assessment of myocardial blood flow and viability using polar map displays of cardiac PET images. J Nucl Med 1992;33:1628-36.

53. Nekolla SG, Miethaner C, Nguyen N, Ziegler SI, Schwaiger M. Reproducibility of polar map generation and assessment of defect severity and extent assessment in myocardial perfusion imaging using positron emission tomography. Eur J Nucl Med 1998;25: 1313-21.
54. Dou K, Yang M, Yang Y, Jain D, He Z. Myocardial 18F-FDG uptake after exercise-induced myocardial ischemia in patients with coronary artery disease. J Nucl Med 2008;49:1986-91.
55. Dilsizian V. SPECT and PET myocardial perfusion imaging: Tracers and techniques. In Dilsizian V, Narula J, editors. Atlas of Nuclear Cardiology, edition 3. Barunwald E (series editor), Philadelphia, Current Medicine, Inc. - Springer; 2009, p. 37-60.
56. McCord ME, Bacharach SL, Bonow RO, et al. Misalignment between PET transmission and emission scans: Its effect on myocardial imaging. J Nucl Med 1992;33:1209-14.
57. Bergmann SR, Fox KAA, Rand AL, et al. Quantification of regional myocardial blood flow in vivo with O-15 water. Circulation 1984;70:724-33.
58. Bergmann SR, Herrero P, Markham J, Weinheimer CJ, Walsh MN. Noninvasive quantitation of myocardial blood flow in human subjects with oxygen-15-labeled water and positron emission tomography. J Am Coll Cardiol 1989;14:639-52.
59. Iida H, Kanno I, Takahashi A, et al. Measurement of absolute myocardial blood flow with O-15 water and dynamic positron emission tomography. Circulation 1988;78:104-15.
60. Lortie M, Beanlands RS, Yoshinaga K, et al. Quantification of myocardial blood flow with 82Rb dynamic PET imaging. Eur J Nucl Med Mol Imaging 2007;34:1765-74.
61. Lin JW, Sciacca RR, Chou RL, Laine AF, Bergmann SR. Quantification of myocardial perfusion in human subjects using 82Rb and wavelet-based noise reduction. J Nucl Med 2001;42:201-8.
62. Herrero P, Markham J, Shelton ME, Weinheimer CJ, Bergmann SR. Noninvasive quantification of regional myocardial perfusion with rubidium-82 and positron emission tomography exploration of a mathematical model. Circulation 1990;82:1377-86.
63. Herrero P, Markham J, Shelton ME, Bergmann SR. Implementation and evaluation of a two-compartment model for quantification of myocardial perfusion with rubidium-82 and positron emission tomography. Circ Res 1992;70:496-507.
64. El Fakhri G, Sitek A, Guerin B, et al. Quantitative dynamic cardiac 82 Rb PET using generalized factor and compartment analyses. J Nucl Med 2005;46:1264–71.
65. El Fakhri G, Sitek A, Abi-Hatem N, et al (2009) Reproducibility and accuracy of quantitative myocardial blood flow: A PET study comparing 82 Rubidium and 13 N-Ammonia. J Nucl Med. in press
66. Coxson PG, Huesman RH, Borland L. Consequences of using a simplified kinetic model for dynamic PET data. J Nucl Med 1997;38:660-7.
67. Yoshida K, Mullani N, Gould KL. Coronary flow and flow reserve by PET simplified for clinical applications using rubidium-82 or nitrogen-13 ammonia. J Nucl Med 1996;37:1701-12.
68. Lertsburapa K, Ahlberg A, Bateman T, et al. Independent and incremental prognostic value of left ventricle ejection fraction determined by stress gated rubidium 82 PET imaging in patients with known or suspected coronary artery disease. J Nucl Cardiol 2008;15:745-53.
69. Dorbala S, Vangala D, Sampson U, et al. Value of vasodilator left ventricular ejection fraction reserve in evaluating the magnitude of myocardium at risk and the extent of angiographic coronary artery disease: A 82Rb PET/CT study. J Nucl Med. 2007;48:349–58.
70. Dorbala S, Hachamovitch R, Curillova Z, et al (2009) Incremental prognostic value of myocardial perfusion imaging with positron emission tomography: A Rubidium-82 PET/CT study. J AM Coll Cardiol Imaging. in press
71. Heller GV, Links J, Bateman TM, et al. American Society of Nuclear Cardiology and Society of Nuclear Medicine joint position statement: Attenuation correction of myocardial perfusion SPECT scintiography. J Nucl Cardiol 2004;11:229-30.
72. Malkerneker D, Brenner R, Martin WH, et al. CT-based attenuation correction versus prone imaging to decrease equivocal interpretations of rest/stress 99mTc-tetrafosmin SPECT MPI. J Nucl Cardiol 2007;14:314-23.
73. Sandler MP, Videlefsky S, Delbeke D, et al. Evaluation of myocardial ischemia using a rest metabolism/stress perfusion protocol with fluorine-18-fluorodeoxyglucose/technitium-99m-MIBI and dual-isotope simultaneous-acquisition single-photon emission computed tomography. J Am Coll Cardiol 1995;26:870-6.
74. Bax JJ, Visser FC, Blanksma PK, et al. Comparison of myocardial uptake of fluorine-18-fluorodeoxyglucose imaged with PET and SPECT in dyssynergic myocardium. J Nucl Med 1996;37:1631-6.
75. Dilsizian V, Bacharach SL, Muang KM, Smith MF. Fluorine-18-deoxyglucose SPECT and coincidence imaging for myocardial viability: Clinical and technological issues. J Nucl Cardiol 2001;8:75-88.
76. Choi Y, Brunken RC, Hawkins RA, et al. Factors affecting myocardial 2-[F-18] fluoro-2-deoxy-D-glucose uptake in positron emission tomography studies of normal humans. Eur J Nucl Med 1993;20:308-18.
77. Choi Y, Hawkins RA, Huang SC, et al. Parametric images of myocardial metabolic rate of glucose generated from dynamic cardiac PET and 2-[18F]fluoro-2-deoxy-D-glucose studies. J Nucl Med 1991;32:733-8.
78. Marshall RC, Tillisch JH, Phelps ME, et al. Identification and differentiation of resting myocardial ischemia and infarction in man with positron emission tomography, F-18 labeled fluorodeoxyglucose and N-13 ammonia. Circulation 1983;67:766-8.
79. Tillisch J, Brunken RC, Marshall R, et al. Reversibility of cardiac wall-motion abnormalities predicted by positron tomography. N Engl J Med 1986;314:884-8.
80. Schwartz E, Schaper J, vom Dahl J, et al. Myocardial hibernation is not sufficient to prevent morphological disarrangements with ischemic cell alterations and increased fibrosis. Circulation 1994;90:I-378.
81. vom Dahl J, Altehoefer C, Sheehan F, et al. Recovery of regional left ventricular dysfunction after coronary revascularization: Impact of myocardial viability assessed by nuclear imaging and vessel patency at follow-up angiography. J Am Coll Cardiol 1996;28:948-58.
82. Beanlands RS, Hendry PJ, Masters RG, et al. Delay in revascularization is associated with increased mortality rate in patients with severe left ventricular dysfunction and viable myocardium on fluorine 18-fluorodeoxyglucose positron emission tomography imaging. Circulation 1998;98:II51-6.
83. Gerber BL, Ordoubadi FF, Wijns W, et al. Positron emission tomography using (18)F-fluoro-deoxyglucose and euglycaemic hyperinsulinaemic glucose clamp: Optimal criteria for the prediction of recovery of post-ischaemic left ventricular dysfunction. Results from the European Community Concerted Action Multicenter study on the use of (18)F-fluoro-deoxyglucose positron emission tomography for the detection of myocardial viability. Eur Heart J 2001;22:1691-701.
84. Bonow RO, Dilsizian V, Cuocolo A, Bacharach SL. Identification of viable myocardium in patients with coronary artery disease and left ventricular dysfunction: Comparison of thallium scintigraphy with reinjection and PET imaging with 18F-fluorodeoxyglucose. Circulation 1991;83:26-37.
85. Pagano D, Townend JN, Littler WA, et al. Coronary artery bypass surgery as treatment for ischemic heart failure: The predictive

value of viability assessment with quantitative positron emission tomography for symptomatic and functional outcome. J Thorac Cardiovasc Surg 1998;115:791-9.
86. Di Carli MF, Davidson M, Little R, et al. Value of metabolic imaging with positron emission tomography for evaluating prognosis in patients with coronary artery disease and left ventricular dysfunction. Am J Cardiol 1994;73:527-33.
87. Beanlands RS, Nichol G, Huszti E, et al. F-18-fluorodeoxyglucose positron emission tomography imaging-assisted management of patients with severe left ventricular dysfunction and suspected coronary artery disease: A randomized, controlled trial (PARR-2). J Am Coll Cardiol 2007;50:2002-12.
88. DeFronzo RA, Tobin JD, Andres R. Glucose clamping technique: A method for quantifying insulin secretion and resistance. Am J Physiol 1979;237:E214-23.
89. Streeter J, Churchwell K, Sigman S, et al. Clinical glucose loading protocol for F-18 FDG myocardial viability imaging [abstract]. Mol Imaging Biol 2002;4:192.